CENTRAL RESEARCH LIBRARY
DOCUMENT COLLECTION

165

MARTIN MARIETTA ENERGY SYSTEMS LIBRARIES
3 4456 0361344 5

ORNL-2653
Reactors – Power
TID-4500 (14th ed.)

THE HGCR-1,
A DESIGN STUDY OF A NUCLEAR POWER STATION EMPLOYING A HIGH-TEMPERATURE GAS-COOLED REACTOR WITH GRAPHITE-UO_2 FUEL ELEMENTS

W. B. Cottrell
C. M. Copenhaver
H. N. Culver
M. H. Fontana
V. J. Kelleghan
G. Samuels

CENTRAL RESEARCH LIBRARY
DOCUMENT COLLECTION
LIBRARY LOAN COPY
DO NOT TRANSFER TO ANOTHER PERSON
If you wish someone else to see this document, send in name with document and the library will arrange a loan.

OAK RIDGE NATIONAL LABORATORY
operated by
UNION CARBIDE CORPORATION
for the
U.S. ATOMIC ENERGY COMMISSION

Printed in USA. Price $3.50. Available from the

Office of Technical Services
Department of Commerce
Washington 25, D.C.

LEGAL NOTICE

This report was prepared as an account of Government sponsored work. Neither the United States, nor the Commission, nor any person acting on behalf of the Commission:

A. Makes any warranty or representation, expressed or implied, with respect to the accuracy, completeness, or usefulness of the information contained in this report, or that the use of any information, apparatus, method, or process disclosed in this report may not infringe privately owned rights; or

B. Assumes any liabilities with respect to the use of, or for damages resulting from the use of any information, apparatus, method, or process disclosed in this report.

As used in the above, "person acting on behalf of the Commission" includes any employee or contractor of the Commission, or employee of such contractor, to the extent that such employee or contractor of the Commission, or employee of such contractor prepares, disseminates, or provides access to, any information pursuant to his employment or contract with the Commission, or his employment with such contractor.

ORNL-2653
Reactors – Power
TID-4500 (14th ed.)

Contract No. W-7405-eng-26

REACTOR PROJECTS DIVISION

THE HGCR-1, A DESIGN STUDY OF A NUCLEAR POWER STATION EMPLOYING A HIGH-TEMPERATURE GAS-COOLED REACTOR WITH GRAPHITE-UO_2 FUEL ELEMENTS

W. B. Cottrell
C. M. Copenhaver
H. N. Culver
M. H. Fontana
V. J. Kelleghan
G. Samuels

DATE ISSUED

JUN 14 1959

OAK RIDGE NATIONAL LABORATORY
Oak Ridge, Tennessee
operated by
UNION CARBIDE CORPORATION
for the
U. S. ATOMIC ENERGY COMMISSION

MARTIN MARIETTA ENERGY SYSTEMS LIBRARIES

3 4456 0361344 5

ABSTRACT

The preliminary design of a 3095-Mw(thermal), helium-cooled, graphite-moderated reactor employing graphite-UO_2 fuel elements has been investigated. At design conditions, 1500°F reactor outlet gas would be circulated to eight steam generators to produce 1050°F, 1450-psi steam which would be converted to electrical power in eight 157-Mw(electrical) turbine-generators. The over-all efficiency of this nuclear power station is 36.5%. The significant activities released from the unclad graphite-UO_2 fuel appear to be less than 0.2% of those produced and would be equivalent to 0.002 curie/cm^3 in the primary helium circuit. The maintenance problems associated with this contamination level are discussed. A cost analysis indicates that the capital cost of this nuclear station per electrical kilowatt would be around $220, and that the production cost of electrical power would be 7.8 mills/kwhr.

CONTENTS

1. INTRODUCTION AND SUMMARY 1

2. PROPOSED PLANT DESIGN 5

Containment Provisions 7
Shielding 11
Fuel Storage 11
Auxiliary Equipment 12
Contamination Control 12

3. PHYSICS 14

Multiplication Factor 15
Neutron Yield 16
Fast Effect 16
Resonance-Escape Probability 16
Thermal Utilization 18
Cross Sections 19
Neutron Leakage 20
Lattice Calculations 21

4. FUEL ELEMENT 31

Materials and Design Limitations 31
Fuel Element Characteristics 31
Material 32
UO_2 Particle Size 32
UO_2 Volume Fraction 33
UO_2-Graphite Reaction 33
Fuel Element Corrosion 34
Heat Transfer Calculations 34
Surface Temperature 35
Nuclear Considerations 36
Core Heat Transfer Studies 36
Reactor Output vs Pumping Power 39
Thermal Stress in Fuel Plates 40
Fuel Element Configuration 43
Alternate Configurations 43

5. REACTOR AND GAS SYSTEMS 45

Leak-Tightness 45
Reactor Pressure Vessel 47
Fuel Loading 47
Blowers, Motors, and Valves 48
Piping and Expansion Joints 48
Helium Purification System 49
Helium Storage System 50

6. POWER RECOVERY SYSTEM 52

Design Philosophy 52
Description of Steam Generators 52
Steam Plant Performance 53
Calculation of Steam Generators and Steam Cycle 54
Afterheat Removal 60

7. ACTIVITY RELEASE 62

Fission-Product Release from UO_2-Graphite Fuel 63
Release of Fission Products from UO_2 63
Release of Fission Products from Graphite 65
Total Activity Release from UO_2-Graphite Fuel 67
Disposition of Activity in Primary System 70
Shielding Requirements for the HGCR-1 71
Shutdown Dose Calculations 71
Containment Requirements 71

8. INSTRUMENTATION, CONTROLS, AND OPERATION 73

9. MAINTENANCE 74

Maintenance Techniques and Problems 75
Contact Servicing Without Decontamination 75
Contact Servicing After Decontamination 75
Remote Servicing in Place 76
Remote Replacement 77
Built-In Spare Equipment 77
Maintenance of Specific Components 78
Maintenance Philosophy 78
Fuel Element Failure 78
Steam Generator 79
Blower and Blower Motor 80
Valves 80
Piping System 81
Helium Purification System 81
Helium Storage and Vent System 81
Fuel Storage Heat Removal Equipment 82

10. COST ANALYSIS 83

Capital Costs 83
Steam Generator 83
Valves 84
Expansion Joints 84
Piping 85
Neutron Curtain and Shield Cooling 85
Reactor Pressure Vessel, Including Supports 86
Fuel-Handling Costs 86
Helium Gas System 86
Helium Blowers and Motors 86
Instruments and Controls 87
Miscellaneous Laboratory Equipment 87
Remote Maintenance Equipment 87
Containment Vessel 88
Steam Plant Equipment 89
Turbine and Electrical Equipment 89
Moderator and Reflector 89
Summary of Capital Costs 90

Operating Costs 92
General 92
Wages 92
Supplies 93
Maintenance 93
Fuel Element Fabrication 94
Fuel Reprocessing 96
Fuel Burnup 96
Fuel in Process 97
Total Power Costs 97
Fuel Inventory Costs 97
Power Costs 99
Comparison of HGCR-1 and GCR-2 Power Costs 99

11. DISCUSSION AND RECOMMENDATIONS 103

APPENDICES

A. RELEASE OF FISSION PRODUCTS FROM UO_2 107
Diffusion of Fission Products Out of UO_2 107
Recoil of Fission Products from UO_2 111

B. RELEASE OF FISSION PRODUCTS FROM THE GRAPHITE 119

C. ACTIVITY IN THE PRIMARY GAS SYSTEM 133

D. DOSE RATE AT STEAM GENERATORS 151

E. STEAM SYSTEM CALCULATIONS 168
Nomenclature 168
Heat Transfer in Steam Generator Sections 170
Log Mean Temperature Differences in Steam Generator Sections 171
Superheater 171
Boiler 172
Economizer 173
Procedure for Scaling GCR-2 Steam Generators 173
Power Output per Heat Exchanger 173
Temperature Rise Due to Pumping Power 173
Feedwater Temperature 174
Heat Removed by Each Section 174
The Over-All Heat Transfer Coefficient 175
Calculation of Tube Area, Length, and Matrix Height 177
Determination of Annulus Size 179
Temperature Rise Through Annulus 180
Gas-Side Pressure Drop 182
Water-Side Pressure Drop 185
Calculation of Pumping Power and Over-All Efficiency 185
Calculation of Steam Cycle Efficiency 186

F. RELEASE OF RADIOACTIVITY 187

THE HGCR-1, A DESIGN STUDY OF A NUCLEAR POWER STATION EMPLOYING A HIGH-TEMPERATURE GAS-COOLED REACTOR WITH GRAPHITE-UO_2 FUEL ELEMENTS

W. B. Cottrell
C. M. Copenhaver
H. N. Culver[1]
M. H. Fontana
V. J. Kelleghan
G. Samuels

1. INTRODUCTION AND SUMMARY

In the spring of 1958, ORNL completed a design study of an enriched-uranium-fueled helium-cooled reactor, designated GCR-2, for the production of electrical power.[2] The reactor employed UO_2 slugs in stainless steel capsules from which circulating helium carried the nuclear heat to four steam generators. The reactor was designed to utilize existing technology, with the expectation that a reactor of this type could be built in the near future. The cost of power from a single 700-Mw (thermal) reactor station was estimated to be ~11.2 mills/kwhr.

While this design study was being made, it became obvious that there were numerous areas in which improved performance could be realized, either by a change in the design or as a consequence of equipment and materials developments. A report presenting a general discussion of these advanced concepts[3] was subsequently issued by ORNL as a guide to both analytical and experimental work on gas-cooled reactors. Of the many concepts which may potentially reduce nuclear power costs in comparison with those estimated for the GCR-2, the most important is the development of a fuel element capable of operating at surface temperatures of 1800°F or above. Such a fuel element would attain high heat fluxes and high power densities and would lead to both low capital charges and low fuel costs. The high coolant temperature may be used either in a direct power-recovery cycle or to reduce steam generator size and to improve steam cycle efficiency.

The metal-clad fuel elements of the type proposed for the GCR-2 or of the type employed in nuclear power stations in Great Britain are capable of containing virtually all the fission products. Comparable metal-clad fuel elements for high ($\geq$ 1800°F) temperatures do not exist; ceramic materials must be used at the desired temperatures. Unfortunately, the ceramic materials currently available will not completely retain fission-product gases. It thus becomes apparent that the high-temperature gas-cooled reactor system which can be based on existing materials will be contaminated with fission products which will have escaped from the fuel elements.

---

[1] On assignment from Tennessee Valley Authority.

[2] *The ORNL Gas-Cooled Reactor*, ORNL-2500, pts 1–4, and *The ORNL Gas-Cooled Reactor. Materials and Hazards*, ORNL-2505 (April 1, 1958).

[3] *The ORNL Gas-Cooled Reactor. Advanced Concepts*, ORNL-2510 (Oct. 2, 1958).

The incentive for higher temperatures arises more from economies in the reactor and steam generator than in the turbine portion of the plant. Nevertheless, most recent economic analyses, as typified by an ORNL study of turbine plants,[4] show that turbine costs are not optimized at operating temperatures below 1000°F, regardless of fuel costs. In any event, the higher temperatures will significantly increase the power density and specific power in the reactor, decrease the size of the steam generator, and reduce the capital cost (per kilowatt) of both these items. Indeed, these economies plus those from the fuel cycle should, and apparently can, compensate for the costs associated with the contaminated primary coolant, which requires more shielding, additional containment, and remote maintenance.

The concept of a gas-cooled reactor in which the coolant is highly contaminated is not new,[5,6] and in recent years there has been increasing interest in such systems.[7–10] The interest is undoubtedly related to an increasing appreciation of the temperature limitations of the uncontaminated coolant system. This should not be interpreted as implying that adequate additional information is now available to evaluate fully the difficulties, as well as the potentialities, inherent in a contaminated gas-cooled reactor system. An appreciation of the incentives for a contaminated-coolant system suggested the feasibility study and economic evaluation described in this report. This study was initiated in June 1958 on a part-time basis. It was originally planned as a three-month study, but the pressure of other commitments prolonged the study over a period of five months. The results of preliminary calculations on the release of activity from graphite-UO_2 fuel elements were presented at the Information Meeting on Gas-Cooled Power Reactors at ORNL, October 21–22, 1958.[11]

The reactor described here does not represent an optimized (lowest power cost) design. Indeed, the uncertainties which exist in many of the cost figures that must be used in this type of study are so great as to render such an undertaking questionable.

---

[4] J. D. Maloney, Jr., *Cost Estimates for Seven 200-Mw Turbine Plants for Operation with Nuclear Reactors at Various Steam Conditions*, ORNL-1387 (Jan. 22, 1953).

[5] F. Daniels, *Suggestions for an Experimental Reactor*, AECD-4095 (April 1950).

[6] F. Daniels, *Suggestions for a High-Temperature Pebble Pile*, N-1668b (Oct. 25, 1944).

[7] L. R. Shepherd *et al.*, *The Possibilities of Achieving High Temperatures in a Gas-Cooled Reactor*, 1958 Geneva Conference Paper No. 314.

[8] R. Schulten, *The Pebble-Bed High-Temperature Reactor for West Germany*, 1958 Geneva Conference Paper No. 1054.

[9] R. P. Hammond *et al.*, *Turret: A High-Temperature Gas Cycle Reactor Proposal*, LA-2198 (Jan. 23, 1958).

[10] Staffs of Sanderson & Porter and Alco Products, Inc., *Design and Feasibility Study of a Pebble Bed Reactor—Steam Power Plant*, S&P 1963, Sanderson & Porter, New York, May 1, 1958.

[11] W. B. Cottrell, "Release of Activity from Various GCR Systems," from *Information Meeting on Gas-Cooled Power Reactors, Oct. 21–22, 1958*, TID-7564 (Dec. 1958).

In this study, the recently completed GCR-2 design was modified as required to accommodate the high-temperature fuel elements and the resulting contaminated coolant. Although this decision arbitrarily eliminated homogeneous-graphite and pebble-bed reactors from specific consideration, the results of the analyses of fission-product release and contamination, as well as the meager information on maintenance, will be applicable to any contaminated system. Further, since any potential cost advantage of the contaminated system in comparison with a clean system is singularly dependent upon such analyses, the conclusions reached in this report are in general applicable to other contaminated-gas-cooled reactor systems.

The emphasis throughout this study has been to develop the features of the contaminated system as completely as possible from the data available. This approach has been quite successful in some areas, in particular, in analyzing the release of activity from unclad fuel elements. Although the disposition of this activity throughout the primary system is uncertain, this study provided a reasonable upper limit from which shielding, maintenance, and containment criteria could be established. Costs of shielding and containment may be estimated with some confidence on the basis of the established criteria, but maintenance costs remain unresolved, since they must be considered in terms of a specific system and operating goals.

The study of any reactor system is, of course, of greatest significance if its cost is based on a specific reference system. The GCR-2 design was used as the reference system because detailed cost analyses of that design had recently been derived; and, since manpower was not available for a completely independent optimization, the reactor described here is simply a modification of the GCR-2.

It was soon realized in this study that the power to be derived from a contaminated-coolant system that was of the same physical core size as the GCR-2 and was operated at the same pressure would be much greater than the 700 Mw (thermal) of the GCR-2. The difference in power levels presented a significant problem in comparing the power costs, since, with all other factors equal, the larger plant would be expected to produce lower cost power. In order to resolve this problem an attempt was made to extrapolate the GCR-2 cost to that expected from a plant of the same output as the contaminated-coolant system.

The contaminated-gas-cooled reactor system considered here is helium cooled and graphite moderated, with the fuel elements positioned in vertical cooling holes in the graphite. The fission products released from the fuel elements are circulated with the helium coolant throughout the primary system. It is obvious that such a plant requires, in comparison with the GCR-2, additional containment, additional shielding, decontamination facilities, and special facilities for maintenance. The costs of these added features must be evaluated against improved reactor and system performance, including

better neutron economy and higher gas and steam temperatures, and the lower fuel and capital costs that follow from these improvements.

The results of this study indicate that lower power costs can be realized from the contaminated-coolant system. The cheaper power results from a small reduction in operating costs and a large reduction in the capital costs associated with the reactor portion of the plant. The lower reactor cost is attributable principally to a factor of 7 increase in specific power. It was estimated that the capital cost would be $220 per kilowatt of installed capacity and that the plant would produce electrical power at a cost of 7.8 mills/kwhr, that is, at a cost less than the extrapolated GCR-2 power cost. These estimates are, of course, only as accurate as the GCR-2 costs from which these are largely derived. A conservative approach was used in the cost evaluation, however, and there is reason to believe that the relative position of the contaminated-coolant plant will improve as a consequence of the development of equipment and additional studies of fuel fabrication, fuel lifetime, and fission-product release rates for which conservative values were taken in lieu of demonstrable data.

Significant parts of this analysis were design and heat transfer studies of the unclad fuel element (Chap. 4), steam cycle analyses (Chap. 6 and App. E), the calculation of activity released from the proposed graphite-UO_2 fuel element (Chap. 7 and Apps. A, B, C, and D), and physics calculations (Chap. 3). The results of each of these studies place the contaminated-coolant system in a more favorable light than is generally assumed.

The plant layout and reactor system are described in Chaps. 2 and 5, respectively. The study of plant maintenance is presented in Chap. 9, and, finally, the analysis of power costs is given in Chap. 10. Although the cost of most items may be predicted with the accuracy inherent in the GCR-2 cost estimates, little progress was made in developing costs for remote maintenance and servicing equipment. In all probability these costs will remain indefinite until the system contamination is better defined and much more development work has been done on remote-servicing equipment.

Tabulations of the design data and power costs may be found in Chaps. 2 and 10, respectively. The plant is designated HGCR-1, for the first design of a Hot Gas-Cooled Reactor. Hot in this instance describes both the thermal and radioactive characteristics of the coolant.

2. PROPOSED PLANT DESIGN

Preliminary plant layouts were prepared to facilitate the study of the advantages and disadvantages of a helium-cooled, graphite-moderated reactor fueled with unclad ceramic fuel elements. Plan and elevation sections of the reactor portion of the plant are shown in Figs. 1 and 2, respectively. Although these layouts were developed from information subsequently described in this report, the information is presented here to give a general concept of the plant as a basis for detailed analyses of specific problems.

A major objective of the study was to determine what advantage could be obtained by higher fuel element surface temperatures and what disadvantages would be associated with any resulting contamination of the coolant stream. The study was to be carried out with a minimum of deviation from equipment sizes employed in the GCR-2 design in order to permit the use of much of the cost data assembled during the course of the GCR-2 plant study.

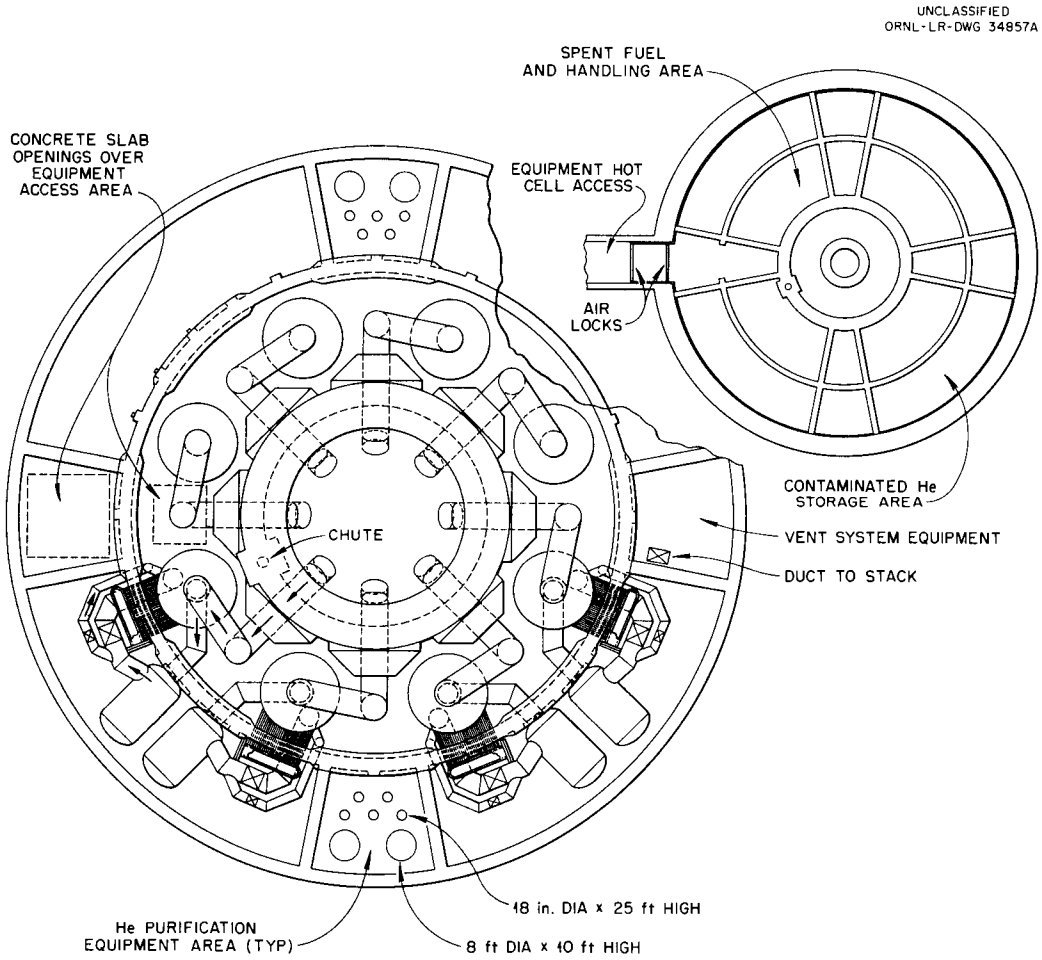

Fig. 1. Plan Section of HGCR-1 Plant.

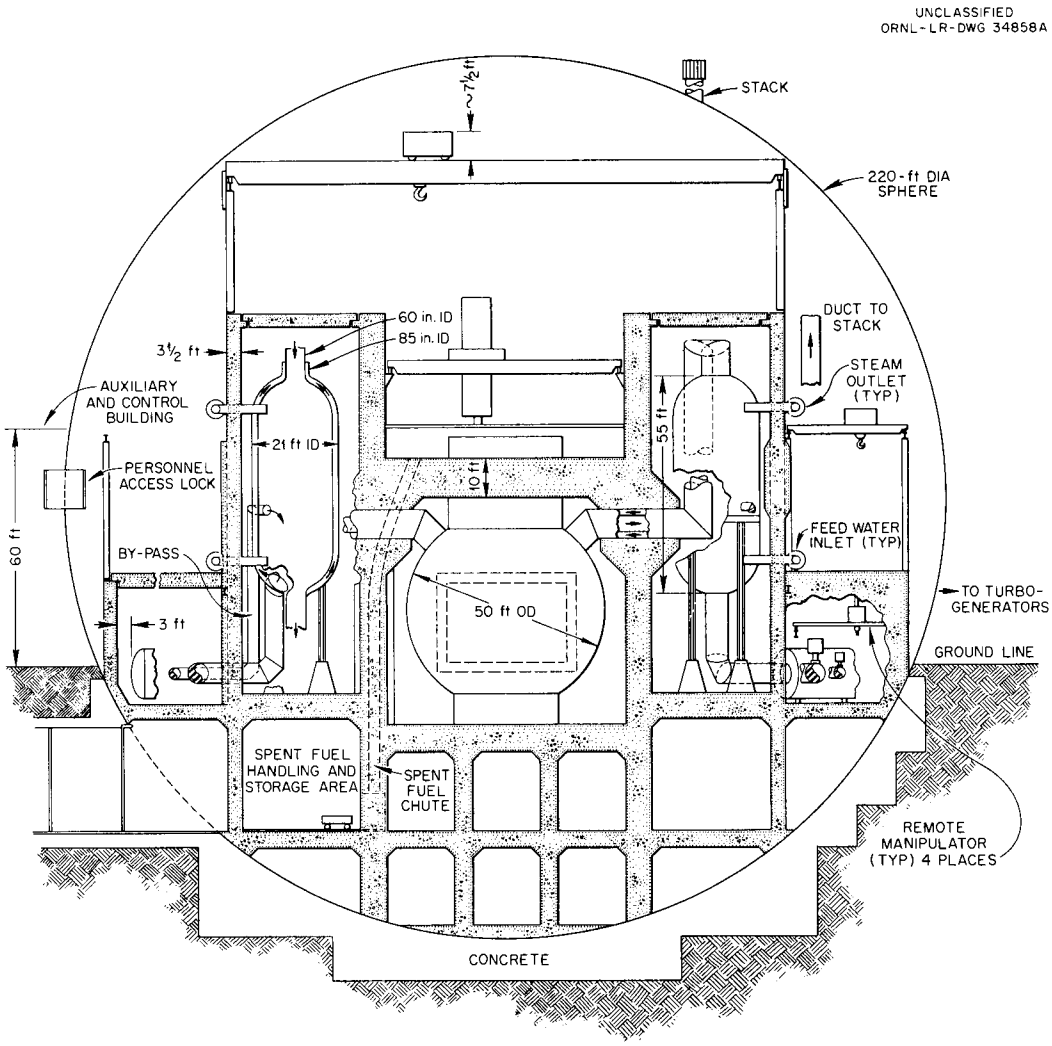

Fig. 2. Elevation Section of HGCR-1 Plant.

The reactor vessel and core designed for the HGCR-1 are the same as for the GCR-2. The reactor vessel is 50 ft in diameter and is fabricated from type SA-212 stainless steel, grade B; the 30-ft-dia, 20-ft-long reactor core is mounted within the spherical vessel. For a core of this size and a maximum fuel element surface temperature of 2000°F, calculations (Chap. 4) indicated that the power level of the core could be increased in comparison with that of the GCR-2 by a factor of 4.5, that is, to 3095 Mw (thermal). The core heat would be removed from the gas stream in eight steam generators, each 54 ft long and 21.5 ft in diameter, as compared with the four, 60-ft-long, 20-ft-dia steam generators used in GCR-2. Twice the number of steam generators, each about the same size as those in the GCR-2, would be capable of transferring 4.5 times as much heat because of the improved heat transfer performance associated with the higher temperature differences and gas velocities. The number of steam generators for the HGCR-1 was not optimized with reference to the cost of helium piping, steam piping,

turbines, etc., but rather was selected so that the size of the required blower motors would not be too great an extrapolation from existing technology. At the time, the resulting steam generators were sufficiently similar to those of the GCR-2 to permit cost estimation by extrapolation of GCR-2 costs.

A plant arrangement in which the steam generators were symmetrically placed about the reactor pressure vessel, as shown in Fig. 1, was selected to minimize the shield size and the plant containment vessel size. Layouts were not prepared for the portions of the plant outside the containment vessel. It was assumed that the cost of the turbine generators and their building structures and auxiliary equipment would vary directly with the plant power level, as has been indicated by other studies.[1]

Design data for HGCR-1 are presented in Table 1, together with comparable data for GCR-2. Some of the unique features of the plant not covered in detail elsewhere are described below.

CONTAINMENT PROVISIONS

The high activity level in the helium as a consequence of the use of unclad fuel elements would be such a potential hazard if an expansion bellows or other system component failed that it was deemed necessary to contain the entire helium system within a second pressure-tight container. For the HGCR-1, a spherical containment shell 220 ft in diameter would be required, that is, a shell comparable in size to the containers for the Dresden[2] and the West Milton[3] plants. Within the containment shell would be the reactor, steam generators, helium piping, and all primary and auxiliary equipment which might become contaminated during service. Adequate biological shielding would be provided to permit occasional entry into the containment vessel for inspection and maintenance while the reactor was operating, but all protracted operations and all control manipulations would be accomplished from outside the containment cell. Servicing areas for contaminated equipment would be provided within the containment shell as well as outside it.

Even with the water available in one steam loop, in addition to the helium in the primary system, taken into account, the pressure within the containment shell in the event of the maximum credible accident would be only a few pounds per square inch. The 220-ft-dia containment sphere would have to be approximately $\frac{7}{8}$ in. thick to withstand the "dead" weight loads and thus would be more than thick enough to withstand

---

[1] M. Bender and R. D. Stulting, *Cost Comparisons of Capital Investment in Various Nuclear Power Plants for Central Station Application*, ORNL CF-58-10-49 (Oct. 14, 1958).

[2] G. Sege, *Containment-Vessel Design Basis for the Dresden Nuclear Power Station*, Paper No. 121 presented at the Nuclear Engineering and Science Conference, March 17–21, 1958.

[3] H. S. Isbin, "Nuclear Reactor Catalog," *Proc. Intern. Conf. Peaceful Uses Atomic Energy, Geneva, 1955* 3, 387 (1955).

Table 1. Comparison of HGCR-1 and GCR-2 Design Data

Plant Characteristics	GCR-2	HGCR-1
General		
Reactor heat rating, Mw	687	3095
Electrical output to grid, Mw	225	1130
Over-all net efficiency, %	32.8	36.5
Core power density, w/cm^2	1.76	7.9
Fuel		
Total uranium inventory, kg	136,800	85,390
Specific power, w/g	4.95	36.2
Number of channels	1597	1415
Channel dimensions, in.	3.05 to 3.45 dia (cylinder)	4.5×4.5 (square)
Fuel configuration	Bundle of seven pins	Box containing four plates
Fuel composition	UO_2 slugs	UO_2 particles in graphite
Fuel enrichment, % U^{235}	2	2
Fuel cladding	Type 304 stainless steel	None
Length of element, in.	40	24
Number of elements per channel	6	10
Dimensions of fuel pin or plate, in.	0.75 dia	0.372×4.5
Density of UO_2, g/cm^3	10.4	10.4
Maximum fuel element heat flux, $Btu/ft^2 \cdot hr$	110,000	245,000
Maximum fuel element surface temperature, °F	1200	2000
Maximum temperature rise in fuel, °F	900	95
Physics and Control		
Burnup, Mwd/tonne	7350	10,000
Fuel temperature coefficient per °C	-4.7×10^{-5}	-5.5×10^{-5} (initial)
Lattice pitch, in.	8×8	8.5×8.5
Average thermal flux (at 2200 m/sec), $neutrons/cm^2 \cdot sec$	5×10^{12}	4×10^{13}
Average fast flux (at > 100 ev), $neutrons/cm^2 \cdot sec$	2×10^{13}	9×10^{13}
Conversion ratio	0.735	0.816
Number of control rods	61	61
Control rod material	Silver	Silver

Table 1 (continued)

Plant Characteristics	GCR-2	HGCR-1
Moderator and Reflector		
Material	TSF graphite	TSF graphite
Core size		
Height, ft	20	20
Diameter, ft	30	30
Reflector thickness, ft	2.5	2.5
Weight of graphite, tons	1122	990
Density, g/cm^3	1.65	1.65
Maximum temperature, °F	750	1100 (est.)
Shielding		
Thermal shield material	Boron-containing glass	Boron-containing glass
Thickness, in.	0.5	0.5
Biological shield material	Concrete	Concrete
Thickness around reactor, ft	9	6.5
Thickness around primary system, ft	None	3.5
Density, lb/ft^3	145	145
Coolant		
Gas	Helium	Helium
Working pressure, psia	300	300
Flow, normal (lb/sec)	972	2400
Blower inlet temperature, °F	450	506
Reactor inlet temperature, °F	460	525
Reactor outlet temperature, °F	1000	1500
Number of primary loops	4	8
Duct configuration	5-ft-dia cylinder	5- and 7-ft-dia coaxial cylinders
Primary system volume, ft^3	107,000	190,000
Blower		
Type	Axial	Axial
Number per loop	1	1
Number per plant	4	8
Mass flow, lb/sec	972	2400
Blower power, hp	5700	9000
Speed control	Constant	Constant
Reactor flow control	Bypass flow	Bypass flow

Table 1 (continued)

Plant Characteristics	GCR-2	HGCR-1
Pressure Vessel		
Configuration	Sphere	Sphere
Diameter, ft	50	50
Material	Type SA-212 stainless steel, grade B	Type SA-212 stainless steel, grade B
Thickness, in.	3.25	3.25
Pressure, psia	300	300
Heat Exchangers		
Type	Once through	Once through
Diameter, ft	20	21.5
Height, ft	60	54
Number	4	8
Steam temperature, °F	950	1050
Steam pressure, psia	950	1450
Gas flow per unit, lb/sec	243	300
Water flow per unit, lb/sec	142	340
Turbogenerators		
Number of sets	2	8
Maximum constant rating, Mw (electrical)	125	157
Speed, rpm	3600	3600
Gross thermal efficiency, %	36	40
Hazards		
Gamma activity in primary system, curies		
From materials activation	18	~0
From fission-product release	~18 (per defective capsule)	10^7
Specific activity in primary system, $\mu c/cm^3$	3×10^{-3} (for one defective capsule)	2000
Dose rate adjacent to steam generator during operation (due to contamination in the gas stream only), mr/hr		
With no shielding	2.5	~30,000
With 3.5 ft of concrete	~0	~2.5
Special containment provisions	None required	220-ft-dia containment vessel
Estimated failure rate of fuel capsules due to cladding defects, failures/year	5	0

the maximum internal pressures. The shell would be thicker in areas of nozzle penetrations and support attachments where there would be additional loads. Some precaution would have to be taken, however, to prevent application of collapsing loads to this relatively thin shell, since uniform external loads of the order of 0.5 psi would be hazardous.

A second method of arranging the equipment was studied from the standpoint of maintenance operations, safety considerations, and cost estimates. The reactor vessel and fuel-charging equipment were located within one containment cell, while a second containment cell housed the steam generators. A connection was made between these cells to take full advantage of the cell volume available for minimizing the cell pressure in the event of system failure. Although this layout permitted closer grouping of the steam generators and consequently some savings in steam piping runs, it did not appear obviously better than the first layout; therefore, the first layout was chosen to permit completion of the study.

SHIELDING

Preliminary calculations have indicated that 3.5 ft of concrete would be required for shielding the primary gas system external to the shielded reactor compartment (Chap. 7). The reactor pressure vessel would require 6.5 ft of concrete shielding in addition to that afforded by the primary system shielding. Since the blowers and the valves would be expected to require periodic checking and, possibly, repair, they would be enclosed in a separate cell where remote viewing and handling equipment would be available. Removable roof plugs would provide access for replacement of this equipment through the use of the cell crane and remotely operated cutting tools.

Repairs might also be required at the steam and water headers of the steam generators. The steam generators would be once-through monotube boilers with water-containing tubes penetrating the boiler shells and connecting to external headers. Shielding could be interposed between the headers and the steam generator shell to permit contact maintenance work so that locating and plugging off a leaking tube should be a relatively simple matter.

FUEL STORAGE

Upon removal from the reactor, the fuel would be transferred to a fuel storage area within the containment shell, where it would be held for a suitable cooling-off period. It would then be placed in a shielded transfer cask and removed from the containment shell. The cask would be removed through an air-lock arrangement that would prevent escape of fission products from the containment cell in the event of a reactor failure.

The dry storage area provided for spent fuel elements within the containment shell could also be used for storage of partially spent fuel elements in the event that they

had to be temporarily removed from the reactor core. Such dry storage would avoid the special drying problems associated with wet storage. Residual moisture in porous graphite fuel elements that had been stored in water would become steam when the elements increased in temperature, and, if the temperature increase were rapid, there might be mechanical damage of the elements. Further, the moisture would subsequently have to be removed from the helium stream by the helium purification system.

Cooling of the dry storage area would be accomplished by blowing cell air through the storage racks, thence through filters, and up the stack. Since the stack would discharge outside the containment shell, equipment would have to be provided to prevent accidental discharge of fission products in the event of a sudden reactor failure. The fuel elements would not be placed in the dry storage area until they had been cooled to a surface temperature of approximately 150°F, and therefore diffusion of any fission products existing within the graphite fuel element would not be significant. Only a minor amount of active material would be expected to diffuse into the air stream and hence be discharged through the stack.

AUXILIARY EQUIPMENT

In addition to the main items of equipment mentioned above, much auxiliary equipment is located within the containment shell. This equipment includes items such as a vacuum pump for testing and evacuating the helium system, helium purification equipment, helium transfer equipment, contaminated helium storage cylinders, shield cooling air blowers, air filters, contaminated equipment maintenance areas, a decontamination control station, and fuel-handling area.

An auxiliary equipment and control building would adjoin the cell, and the turbine-generator building would be connected to the auxiliary equipment and control building. The turbine-generator building would be 115 ft wide, 420 ft long, and 60 ft high. The auxiliary equipment and control building would be 50 ft wide, 70 ft long, and 60 ft high. All steam plant auxiliary equipment would be located either in the basement of the turbine-generator building or in the auxiliary equipment and control building. This layout is essentially the same as that proposed for GCR-2, with an appropriate increase in size.

CONTAMINATION CONTROL

In the HGCR-1 system, the shield cooling air would become activated as it flowed through the reactor compartment. A small amount of the activity would be due to the activation of the argon in the air, but the principal source of activity would be leakage from the primary system. Based on the activities of the various isotopes in the gas stream of the primary system (see Chap. 7), a leakage rate of 0.1% per day could be

tolerated without exceeding the maximum exposure downstream from the plant stack exhaust (see App. F).

The shield cooling air would be exhausted directly to the stack, since the activity leaking into the containment vessel at the 0.1% per day primary system leakage rate would be too high to permit access to the containment vessel. The air would circulate from the areas of least contamination (outside the secondary shield) to areas of high contamination (adjacent to the reactor and primary cooling system), and would reduce the background activity inside the containment vessel by preventing the buildup of long-lived nuclides. It would, of course, be necessary to have a valve in the stack that would close when activity levels were detected that exceeded those associated with the normal allowable leakage.

By maintaining air flow in the direction described it would be possible for personnel to enter the containment vessel to perform minor maintenance while the reactor was at operating pressure. Since the persons who entered the containment vessel would always be external to the secondary shield, the possibility of inhaling large amounts of activity would be small.

If higher than normal activity levels were recorded while personnel were inside the containment vessel, there would be sufficient time to evacuate the vessel before the valve in the stack was closed and the contaminated air was directed into the containment vessel. The level of activity of all the nuclides would be maintained at an equilibrium level by the cleanup system. However, xenon and krypton would continue to build up and would reach an activity level which would be determined by the leakage rate from the primary system and the length of time the activity was allowed to accumulate inside the containment vessel. The leakage of activity into the containment vessel in this situation would continue until the system pressure was reduced and the primary system gas was transferred to the storage system. The activity inside the containment vessel would then be vented to the atmosphere at a rate which would not cause excessive exposures downstream. This could be done by controlling the activity release or by waiting for satisfactory atmospheric conditions.

The activity of the air inside the containment vessel would be reduced to the allowable concentrations before maintenance personnel were permitted inside. In emergencies, personnel could be allowed into the containment vessel.

3. PHYSICS

Studies of various fuel element configurations and compositions were made to obtain the information needed for economic optimizations of gas-cooled reactor plants utilizing fuel elements having nonmetallic cladding or no cladding. Before such studies could be made it was necessary that the moderator, coolant system temperature, and other major core parameters be specified, since the fuel element composition and configuration must be chosen on the basis of a proper balance between reactor physics considerations, heat transfer properties, fission-product retention capabilities, and general fuel costs that will result in a minimum power cost for a given plant net electrical rating. The major nuclear parameters required for optimization are the effective multiplication factor and reactivity lifetime of the fuel as functions of fuel element composition and configuration.

There are at least two significant advantages to be realized by the elimination of the cladding from the fuel element: (1) a reduction in the amount of fissionable material required because of the reduced poison in the core and (2) an increase in fuel lifetime because of the removal of metallurgical restrictions imposed by the cladding. Of these advantages only the first has been examined in any detail. While the fuel lifetime has not been calculated for the HGCR-1, a value of 10,000 Mwd/tonne was used for the cost estimates in this study. This is believed to be conservative, since calculations indicated that the nuclear lifetime of the GCR-2 fuel element was approximately 15,000 Mwd/ton.

Another area of concern which has not been fully explored is the effect of reactor temperatures on reactivity. The mixture of graphite and fuel and the graphite sleeve would tend to make the temperature coefficient of reactivity of the HGCR-1 less negative than that of the GCR-2. However, preliminary calculations indicate that the prompt fuel temperature coefficient, that is, the Doppler coefficient, would be negative, although it would become less negative as Pu^{239} built up in the fuel.

In order to reduce the number of computations required in this preliminary study of unclad fuel element systems from an economic optimization point of view, the restrictive assumptions listed below were made.

1. The fuel plates were assumed to be homogeneous mixtures of 25 vol % UO_2 and 75 vol % graphite. The UO_2 content selected was the maximum UO_2 volume fraction permitted by metallurgical considerations.

2. The fuel element configuration assumed was a rectangular box having a square cross-sectional area, as shown in Fig. 3. Since the physics calculations are rather insensitive to the number of fuel plates used to provide a fixed volume fraction of fuel and the heat transfer calculations indicated four to be a reasonable number, the fuel element was assumed throughout this study to be made up of four plates. Thus, the only variable parameters of the fuel element were the lattice pitch, the plate thickness, the cooling gap size, and the channel width.

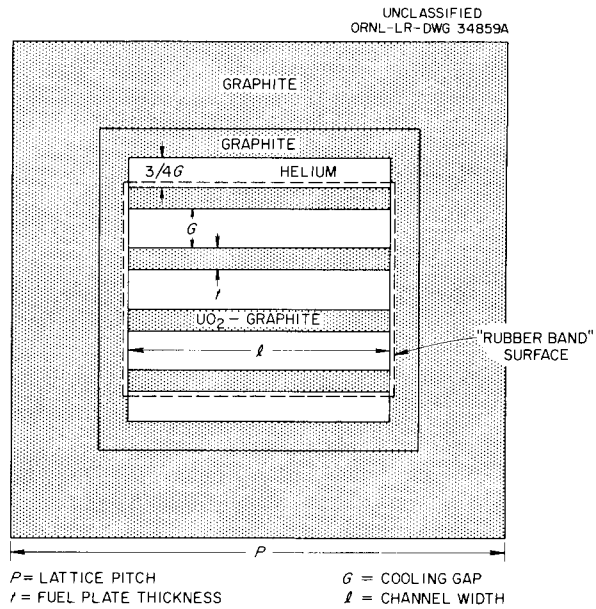

Fig. 3. Cross-Sectional Configuration of Fuel Element.

3. The fuel enrichment was assumed to be limited to the range 2 to 4%, and the graphite and UO_2 densities were assumed to be 1.65 and 10.4 g/cm^3, respectively.

The calculational methods described in the report on the GCR-2 study[1] were followed in this evaluation wherever practical.

MULTIPLICATION FACTOR

The effective multiplication factor of the reactor system is expressed by

$$k_{\text{eff}} = \eta \epsilon p f \, e^{-B^2 \tau} (1 + L^2 B^2)^{-1} \quad ,$$

where L is the diffusion length, B is the buckling factor, and τ is the age. This equation is equivalent to that used in the design of the GCR-2, but for this study the factors η, ϵ, p, and f, which comprise the infinite multiplication factor, are defined somewhat differently. The changes in the definitions of the four factors are negligible, however, and the calculated values can be compared directly with corresponding values obtained in the GCR-2 design. The four factors and their definitions are discussed in the following sections.

[1] *The ORNL Gas-Cooled Reactor*, ORNL-2500 (April 1, 1958).

Neutron Yield

The neutron yield, η, is defined here as the number of neutrons produced per neutron (with energy below 0.1 Mev) absorbed in uranium; resonance absorptions in U^{238} are not included. The neutron yield values were obtained from effective cross sections, as described in a subsequent section.

Fast Effect

The fast fission factor, ϵ, is defined here as the number of neutrons that slow down to energies below 0.1 Mev or escape from the fuel element per primary fission neutron. Primary fission neutrons result from fissions of U^{235} caused by neutrons with energies below 0.1 Mev. The equation for ϵ is essentially that given by Carlvik and Pershagen,[2] who evaluate ϵ by a two-group calculation with the group 1 neutrons having zero fission cross section and energies ranging from 0.1 to 1.49 Mev and the group 2 neutrons having a constant fission cross section and energies above 1.49 Mev. This method was modified to permit fissioning in group 1 and thus take fast fission of U^{235} into account in the proper manner; however, for small fuel enrichments, the effect of the modification is insignificant. The principal advantage of the two-group method relative to the one-group method used in the GCR-2 study is that the choice of average cross sections and collision probabilities is simplified, particularly for the highly moderating fuel elements being studied. The collision probabilities for groups 1 and 2 are obtained by computing the probabilities of escape from an equivalent homogeneized cylinder having a surface equal to the "rubber band" surface of the fuel element (see Fig. 3). For the lattice spacings considered here, the coupling effect, or the probability that a neutron emitted from a fuel element will collide with another fuel element before colliding with the moderator, is small. Also, the probability of rescattering of the escaping fission neutrons back into the fuel with energies above 0.1 Mev is negligible.

Resonance-Escape Probability

The resonance-escape probability, p, is defined here as the probability that neutrons slowing down to energies below 0.1 Mev will slow down below the lowest resonance of U^{238} without captures in U^{238} resonances. Epithermal captures in U^{238} attributable to the $1/v$ portion of the epithermal cross section and all epithermal captures in U^{235} are taken into account in calculating the thermal utilization and thus are not included in the resonance-escape probability.

---

[2] I. Carlvik and B. Pershagen, *The Fast Fission Effect in a Cylindrical Fuel Element*, AEF-70, AB Atomenergi, Stockholm, Nov. 1956.

The resonance-escape probability is expressed by

$$p = \exp - \left[\frac{\sigma_{r,28}}{\frac{N_m}{N_{28}} (\xi\sigma_s)_m + \frac{N_O}{N_{28}} (\xi\sigma_s)_O + \frac{N_u}{N_{28}} (\xi\sigma_s)_u} \right] ,$$

where

$\sigma_{r,28}$ = effective resonance integral for U^{238} in the energy interval 0.1 Mev to approximately 5 ev,

σ_s = scattering cross section of material indicated by subscript,

N = atom concentration in lattice cell of material indicated by subscript,

ξ = average lethargy decrement per elastic collision.

The subscripts m, O, u, 28 refer to moderator, oxygen, uranium, and U^{238}, respectively. This equation assumes no moderator disadvantage factor for the epithermal flux.

Dresner[3] has shown that in heterogeneous media the effective resonance integral can be expressed in terms of the homogeneous case for the "narrow resonance" approximation. The effective resonance integral for the heterogeneous case is obtained by using homogeneous experimental data where the potential scattering cross section per absorbing atom, σ_p, for the fuel plate is replaced by $b\sigma_p$. The reduction parameter is

$$b = 1 + \frac{1}{\Sigma_p \bar{s}} ,$$

where

Σ_p = macroscopic potential scattering cross section of the fuel plate,

$\bar{s}$ = average chord length.

For the particular fuel element configuration studied,

$$\bar{s} = \frac{8tl}{l + 4t + 3G\gamma} ,$$

where

γ = the absorptions on the internal surfaces of the fuel element relative to the total neutron current entering the gap,

and, for isotropic neutron source distribution in the external moderator,

$$\gamma \cong 1 - \frac{G}{2l} .$$

The terms appearing in γ and $\bar{s}$ are defined by Fig. 3.

---

[3] L. Dresner, ORNL, to C. Copenhaver, private communication, Dec. 1958.

The values of $\sigma_{r,28}$ were obtained from a U^{238} resonance integral curve[4] for the homogeneous case by using the computed values of $b\sigma_p$.

The effective resonance integral at the operating temperature is expressed by

$$\sigma_r(T) = \sigma_r(\text{at } 20°\text{C}) \exp\left[1.56 \times 10^{-4} (\bar{T} - 20)\right] ,$$

where the value of $\bar{T}$ used is 1110°C.

Thermal Utilization

The thermal utilization factor, f, is defined here as the ratio of the thermal and epithermal absorptions in the uranium, excluding the resonance absorption in U^{238}, to the total thermal and epithermal absorptions, again excluding the U^{238} resonance absorptions for a lattice cell. The effective cross sections defined below were used.

The inverse of the thermal utilization factor for the particular fuel element configuration being studied is

$$f^{-1} = 1 + \frac{\Sigma_{a,m}}{\Sigma_{a,u}} \left(3 + \frac{V_{m,e} F_{m,e}}{F_f}\right) ,$$

where

Σ_a = effective macroscopic absorption cross section of material indicated by subscript,

V = lattice cell volume fraction,

F = flux disadvantage factor,

and the subscripts u, m, e, and f refer to uranium, moderator, external, and fuel (UO_2), respectively.

The external moderator disadvantage factor, $F_{m,e}$ (see Fig. 4), was obtained by the P_3 spherical harmonics approximation method. The particular P_3 program used was the I_2 program[5] developed

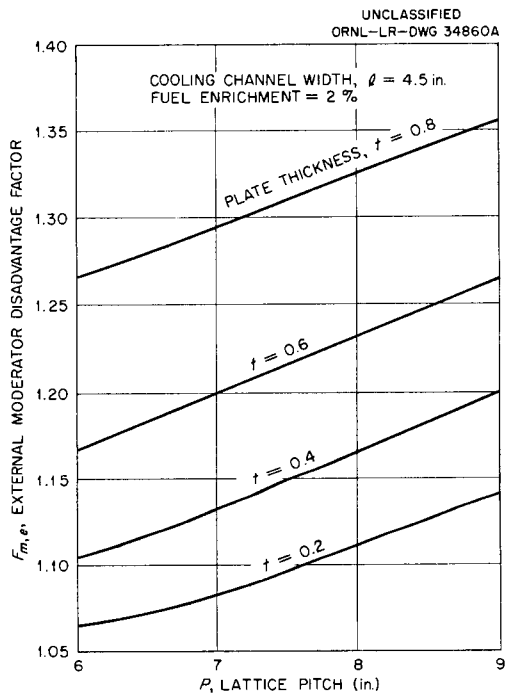

Fig. 4. Effect of Fuel Plate Thickness and Lattice Pitch on External Moderator Disadvantage Factor.

---

[4] R. L. Macklin and H. S. Pomerance, "Resonance Capture Integrals," *Proc. Intern. Conf. Peaceful Uses Atomic Energy, Geneva, 1955* 5, 99, Fig. 1 (1955).

[5] R. C. McCready and D. B. Vollenweider, *A 704 Program for the Solution of the Neutron Transport Equation in Fifty Concentric Annuli by the Weil Method (Program I_2)*, DC-58-1-158, GE-ANP (Jan. 1958).

for the IBM 704 computer. The fuel element was homogeneized with the void, and equivalent cylindrical geometry was used. The extremely good interpolation possible from the external moderator disadvantage factor over the limited range of fuel enrichments considered made it unnecessary to do calculations for every change in configuration parameters.

Cross Sections

In the formulation of the multiplication factor, effective cross sections are required that should be defined in terms of the reaction rate per target nucleus at energies below 0.1 Mev, excluding U^{238} resonance reactions. Since the $1/v$ portion of the cross section above 0.1 Mev represents a negligible contribution to the total reaction rate, effective cross sections were used:

$$\hat{\sigma} = (g + rs)\,\sigma_0 \quad ,$$

where g, r, and s are as defined by Westcott.[6] The subscript 0 refers to a neutron velocity of 2200 m/sec. This effective cross section is equivalent to the one used in the GCR-2 study. Thus the flux spectrum is assumed to consist of a Maxwellian component at a neutron temperature T_n plus a dE/E tail cut off at a lower limit of $5kT_n$, where k is the Boltzmann constant.

The choice of an effective moderator temperature, T_m, is complicated, since a considerable portion of the neutron moderation occurs in the fuel element graphite. The approach used here was to volume-weight the moderator temperature with the slowing-down density below the U^{238} resonances. The neutron temperature was then obtained, in the manner suggested by Coveyou *et al.*,[7] as

$$T_n \sim T_m \left\{ 1 + \left[1.08 \times 12 \left(\frac{2}{3} \right)^{1/2} \frac{\Sigma_a(T_m)}{\Sigma_s} \right] \right\}$$

for graphite moderators, where Σ_a and Σ_s refer to the flux-weighted absorption and scattering cross sections of the lattice cell, respectively. The results of the neutron temperature calculations are given in Table 2.

The neutron temperature chosen for the HGCR-1 calculations was 980°K. For the fuel element configurations studied here, neutron moderation in the fuel element raises the effective moderator temperature about 100°F above the external moderator temperature. A mean value of 0.17 was chosen for the r factor for all calculations, since r generally ranged between 0.16 and 0.18 for the cases considered.

---

[6] C. H. Westcott, *The Specification of Neutron Flux and Effective Cross Sections in Reactor Calculations*, CRRP-662 (Aug. 15, 1956).

[7] R. R. Coveyou, R. R. Bate, and R. K. Osborn, *J. Nuclear Energy* **2**, 153 (1956).

Table 2. Calculated Neutron Temperatures of the Fuel Element Described in Fig. 3 as a Function of Fuel Enrichment

Fuel plate thickness: 0.3 in.
Cooling channel width: 4.5 in.
Lattice pitch: 8 in.
Moderator temperature: 1130°F

Fuel Enrichment (at. % U^{235})	Ratio of Neutron Temperature to Moderator Temperature	Neutron Temperature (°K)
2	1.100	971
3	1.136	1003
4	1.168	1031

The external moderator disadvantage factors required for evaluating the thermal utilization were obtained by using effective cross sections defined as

$$\sigma_{\text{eff}} = \hat{\sigma}\left(\frac{\pi T_0}{4T_n}\right)^{1/2} ,$$

where T_0 is the temperature at which $kT = 0.0252$ ev. This formula, which implies that the preponderance of absorptions, excluding U^{238} resonance absorptions, results from the Maxwellian portion of the neutron spectrum, is a good approximation for the cases considered.

Neutron Leakage

The neutron leakage is given by

$$M^2B^2 \cong M_0^2\,(B_1^2 g_1 + B_2^2 g_2) ,$$

where

M_0^2 = migration area in the absence of voids = $L_0^2 + \tau_0$,

B_1^2, B_2^2 = geometric buckling in axial and radial directions, respectively,

g_1, g_2 = geometric void correction factors for axial and radial directions, respectively.

This reduced form of the neutron leakage equations results from the similarity of the fast- and thermal-neutron mean paths for the cases considered. The geometric void correction factors used are

$$g_1 = 1 + 2\phi + \frac{3}{2}\frac{Qr\phi}{\lambda}$$

and

$$g_2 = 1 + 2\phi + \frac{3}{4}\frac{Qr\phi}{\lambda} ,$$

as derived by Behrens,[8] where

ϕ = void ratio, that is, voids per unit of solid material,

r = hydraulic radius of the voids, $r^{-1} \sim l^{-1} + 5\,(l - 4t)^{-1}$,

λ = mean free path = 1.06 cm,

Q = ratio of the mean square passage length through the holes to the square of the mean free path, that is,

$$Q \sim \frac{3(G^2 + l^2)}{G^2 + 2lG + l^2} \; .$$

The age in the absence of voids, τ_0, for the cases considered is 300 ± 20 cm^2. This value includes the age to thermal energies of fission neutrons elastically and inelastically scattered at energies below 0.1 Mev. The square of the diffusion length in the absence of voids is

$$L_0^2 \cong f_m L_m^2 = (1 - f)\, L_m^2 \; ,$$

where

L_m = the diffusion length of the moderator, 23.5 cm.

The reflector saving used was 65 cm.

LATTICE CALCULATIONS

Lattice calculations were performed for 160 lattices, and the results for 145 are reported here. The reported cases adhere to the restrictive assumptions mentioned previously. A description of the lattice and the values of η, ϵ, p, f, M^2B^2, k_{eff}, and the initial conversion ratio, R_c, are given for the 145 cases in Table 3, with HGCR-1 being the first case listed. The results are also presented graphically in Figs. 5 through 9.

Optimization of the fuel element composition and configuration on the basis of minimum power cost is required before the significance of the results can be made apparent. The system appears economically interesting even in the unoptimized form, however, and conclusions can be drawn.

It may be seen that the elimination of all cladding material permits a substantially higher conversion ratio for a given k_{eff}. This reduction in nonproductive absorption also increases the attractiveness of low fuel enrichment. Thus, it would seem desirable to look closely at the range of enrichment between natural and 2%.

---

[8] D. J. Behrens, *The Migration Length of Neutrons in an Infinite Lattice*, AERE-TR-239 (1958).

Table 3. Results of Lattice Calculations

Moderator temperature: 1130°F
Neutron temperature: 980°K
Number of fuel plates: 4
Volumetric composition of fuel plate: 25% UO_2 and 75% graphite
Width of gap between fuel plates: G (in.) = $(l - 4t)/4.5$

Case Number	Fuel Enrichment (at. % U^{235})	Channel Width, l (in.)	Plate Thickness, t (in.)	Lattice Pitch, P (in.)	η	ϵ	p	f	M^2B^2	k_{eff}	R_c
HGCR-1	2.0	4.5	0.372	8.5	1.663	1.024	0.7023	0.9651	0.0226	1.129	0.805
1		3.5	0.2	6.0	1.663	1.014	0.6931	0.9663	0.0269	1.100	0.823
2				7.0	1.663	1.014	0.7829	0.9493	0.0227	1.225	0.643
3				8.0	1.663	1.014	0.8379	0.9292	0.0207	1.286	0.532
4				9.0	1.663	1.014	0.8741	0.9066	0.0196	1.311	0.460
5			0.4	6.0	1.663	1.022	0.5508	0.9806	0.0210	0.8991	1.109
6				7.0	1.663	1.022	0.6641	0.9708	0.0186	1.076	0.881
7				8.0	1.663	1.022	0.7404	0.9597	0.0172	1.187	0.728
8				9.0	1.663	1.022	0.7937	0.9467	0.0165	1.256	0.621
9			0.6	6.0	1.663	1.032	0.4525	0.9850	0.0169	0.7522	1.306
10				7.0	1.663	1.032	0.5725	0.9780	0.0156	0.9462	1.065
11				8.0	1.663	1.032	0.6599	0.9697	0.0150	1.082	0.890
12				9.0	1.663	1.032	0.7244	0.9602	0.0146	1.177	0.760
13			0.8	6.0	1.663	1.040	0.3889	0.9868	0.0139	0.6546	1.434
14				7.0	1.663	1.040	0.5072	0.9808	0.0135	0.8489	1.196
15				8.0	1.663	1.040	0.5991	0.9737	0.0133	0.9957	1.012
16				9.0	1.663	1.040	0.6696	0.9654	0.0133	1.103	0.870
17		4.5	0.2	6.0	1.663	1.013	0.5203	0.9806	0.0508	0.8180	1.170
18				7.0	1.663	1.013	0.6796	0.9667	0.0357	1.069	0.850
19				8.0	1.663	1.013	0.7692	0.9503	0.0290	1.197	0.670
20				9.0	1.663	1.013	0.8248	0.9315	0.0254	1.262	0.559

Table 3 (continued)

Case Number	Fuel Enrichment (at. % U^{235})	Channel Width, l (in.)	Plate Thickness, t (in.)	Lattice Pitch, P (in.)	η	ϵ	p	f	M^2B^2	k_{eff}	R_c
21	2.0	4.5	0.4	6.0	1.663	1.021	0.3691	0.9885	0.0370	0.5974	1.474
22				7.0	1.663	1.021	0.5354	0.9811	0.0278	0.8678	1.140
23				8.0	1.663	1.021	0.6462	0.9720	0.0234	1.042	0.917
24				9.0	1.663	1.021	0.7221	0.9616	0.0210	1.155	0.765
25			0.6	6.0	1.663	1.031	0.2848	0.9911	0.0274	0.4711	1.643
26				7.0	1.663	1.031	0.4383	0.9857	0.0222	0.7247	1.335
27				8.0	1.663	1.031	0.5538	0.9793	0.0194	0.9122	1.103
28				9.0	1.663	1.031	0.6395	0.9719	0.0179	1.047	0.931
29			0.8	6.0	1.663	1.048	0.2380	0.9923	0.0205	0.4003	1.737
30				7.0	1.663	1.048	0.3757	0.9879	0.0178	0.6307	1.460
31				8.0	1.663	1.048	0.4884	0.9828	0.0164	0.8168	1.234
32				9.0	1.663	1.048	0.5774	0.9768	0.0155	0.9606	1.055
33		5.5	0.2	6.0	1.663	1.010	0.2067	0.9921	0.1433	0.3013	1.799
34				7.0	1.663	1.010	0.5147	0.9804	0.0672	0.7942	1.181
35				8.0	1.663	1.010	0.6714	0.9666	0.0460	1.042	0.867
36				9.0	1.663	1.010	0.7603	0.9509	0.0365	1.172	0.688
37			0.4	6.0	1.663	1.021	0.1338	0.9946	0.0885	0.2076	1.946
38				7.0	1.663	1.021	0.3631	0.9884	0.0497	0.5805	1.486
39				8.0	1.663	1.021	0.5252	0.9811	0.0362	0.8443	1.160
40				9.0	1.663	1.021	0.6340	0.9724	0.0295	1.017	0.942
41			0.6	6.0	1.663	1.031	0.1066	0.9954	0.0580	0.1720	2.000
42				7.0	1.663	1.031	0.2823	0.9911	0.0373	0.4625	1.648
43				8.0	1.663	1.031	0.4308	0.9859	0.0289	0.7078	1.350
44				9.0	1.663	1.031	0.5428	0.9799	0.0244	0.8902	1.125
45			0.8	6.0	1.663	1.043	0.0944	0.9958	0.0391	0.1569	2.025
46				7.0	1.663	1.043	0.2352	0.9924	0.0282	0.3938	1.742
47				8.0	1.663	1.043	0.3678	0.9883	0.0245	0.6154	1.476

Table 3 (continued)

Case Number	Fuel Enrichment (at. % U^{235})	Channel Width, l (in.)	Plate Thickness, t (in.)	Lattice Pitch, P (in.)	η	ϵ	p	f	M^2B^2	k_{eff}	R_c
48	2.0	5.5	0.8	9.0	1.663	1.043	0.4764	0.9835	0.0204	0.7964	1.258
49	3.0	3.5	0.2	6.0	1.766	1.014	0.6956	0.9753	0.0265	1.183	0.748
50				7.0	1.766	1.014	0.7848	0.9626	0.0222	1.323	0.569
51				8.0	1.766	1.014	0.8394	0.9477	0.0200	1.397	0.459
52				9.0	1.766	1.014	0.8752	0.9308	0.0188	1.432	0.387
53			0.4	6.0	1.766	1.022	0.5540	0.9856	0.0209	0.9653	1.032
54				7.0	1.766	1.022	0.6670	0.9783	0.0183	1.157	0.805
55				8.0	1.766	1.022	0.7428	0.9696	0.0169	1.278	0.653
56				9.0	1.766	1.022	0.7956	0.9592	0.0162	1.355	0.547
57			0.6	6.0	1.766	1.032	0.4562	0.9887	0.0168	0.8085	1.228
58				7.0	1.766	1.032	0.5757	0.9832	0.0155	1.016	0.988
59				8.0	1.766	1.032	0.6627	0.9766	0.0148	1.162	0.814
60				9.0	1.766	1.032	0.7268	0.9689	0.0144	1.265	0.685
61			0.8	6.0	1.766	1.040	0.3925	0.9904	0.0138	0.7042	1.356
62				7.0	1.766	1.040	0.5107	0.9585	0.0134	0.9124	1.119
63				8.0	1.766	1.040	0.6022	0.9803	0.0132	1.070	0.935
64				9.0	1.766	1.040	0.6723	0.9739	0.0131	1.187	0.794
65		4.5	0.2	6.0	1.766	1.013	0.5238	0.9860	0.0504	0.8796	1.092
66				7.0	1.766	1.013	0.6822	0.9758	0.0351	1.151	0.775
67				8.0	1.766	1.013	0.7713	0.9639	0.0283	1.293	0.596
68				9.0	1.766	1.013	0.8265	0.9506	0.0246	1.372	0.485
69			0.4	6.0	1.766	1.021	0.3728	0.9917	0.0368	0.6430	1.396
70				7.0	1.766	1.021	0.5388	0.9860	0.0276	0.9322	1.062
71				8.0	1.766	1.021	0.6490	0.9792	0.0231	1.120	0.841
72				9.0	1.766	1.021	0.7245	0.9713	0.0206	1.243	0.690
73			0.6	6.0	1.766	1.031	0.2885	0.9934	0.0273	0.5080	1.565
74				7.0	1.766	1.031	0.4420	0.9893	0.0220	0.7790	1.257

Table 3 (continued)

Case Number	Fuel Enrichment (at. % U^{235})	Channel Width, l (in.)	Plate Thickness, t (in.)	Lattice Pitch, P (in.)	η	ϵ	p	f	M^2B^2	k_{eff}	R_c
75	3.0	4.5	0.6	8.0	1.766	1.031	0.5570	0.9843	0.0193	0.9793	1.026
76				9.0	1.766	1.031	0.6423	0.9785	0.0177	1.124	0.855
77			0.8	6.0	1.766	1.040	0.2417	0.9942	0.0205	0.4325	1.659
78				7.0	1.766	1.040	0.3795	0.9909	0.0178	0.6786	1.382
79				8.0	1.766	1.040	0.4922	0.9868	0.0163	0.8778	1.156
80				9.0	1.766	1.040	0.5805	0.9820	0.0154	1.031	0.989
81		5.5	0.2	6.0	1.766	1.010	0.2100	0.9943	0.1428	0.3259	1.722
82				7.0	1.766	1.010	0.5180	0.9858	0.0666	0.8539	1.104
83				8.0	1.766	1.010	0.6740	0.9759	0.0453	1.122	0.791
84				9.0	1.766	1.010	0.7623	0.9646	0.0356	1.266	0.614
85			0.4	6.0	1.766	1.021	0.1366	0.9961	0.0883	0.2254	1.870
86				7.0	1.766	1.021	0.3670	0.9916	0.0495	0.6252	1.407
87				8.0	1.766	1.021	0.5288	0.9861	0.0359	0.9076	1.082
88				9.0	1.766	1.021	0.6370	0.9297	0.0291	1.093	0.865
89			0.6	6.0	1.766	1.031	0.1092	0.9967	0.0579	0.1873	1.925
90				7.0	1.766	1.031	0.2860	0.9934	0.0372	0.4987	1.570
91				8.0	1.766	1.031	0.4345	0.9895	0.0287	0.7610	1.272
92				9.0	1.766	1.031	0.5462	0.9848	0.0242	0.9562	1.048
93			0.8	6.0	1.766	1.043	0.0968	0.9969	0.0391	0.1711	1.950
94				7.0	1.766	1.043	0.2385	0.9443	0.0281	0.4249	1.665
95				8.0	1.766	1.043	0.3715	0.9912	0.0244	0.6621	1.398
96				9.0	1.766	1.043	0.4800	0.9874	0.0202	0.8557	1.180
97	4.0	3.5	0.2	6.0	1.823	1.014	0.6982	0.9806	0.0262	1.233	0.707
98				7.0	1.823	1.014	0.7868	0.9701	0.0219	1.381	0.529
99				8.0	1.823	1.014	0.8408	0.9579	0.0197	1.460	0.421
100				9.0	1.823	1.014	0.8763	0.9435	0.0185	1.501	0.350
101			0.4	6.0	1.823	1.022	0.5580	0.9884	0.0208	1.007	0.989

Table 3 (continued)

Case Number	Fuel Enrichment (at. % U^{235})	Channel Width, l (in.)	Plate Thickness, t (in.)	Lattice Pitch, P (in.)	η	ϵ	p	f	M^2B^2	k_{eff}	R_c
102	4.0	3.5	0.4	7.0	1.823	1.022	0.6698	0.9823	0.0182	1.204	0.764
103				8.0	1.823	1.022	0.7450	0.9748	0.0168	1.331	0.613
104				9.0	1.823	1.022	0.7973	0.9663	0.0160	1.413	0.508
105			0.6	6.0	1.823	1.032	0.4600	0.9908	0.0167	0.8434	1.185
106				7.0	1.823	1.032	0.5790	0.9861	0.0154	1.058	0.946
107				8.0	1.823	1.032	0.6655	0.9805	0.0147	1.210	0.773
108				9.0	1.823	1.032	0.7292	0.9737	0.0143	1.317	0.645
109			0.8	6.0	1.823	1.040	0.3965	0.9920	0.0138	0.7356	1.313
110				7.0	1.823	1.040	0.5142	0.9879	0.0134	0.9504	1.077
111				8.0	1.823	1.040	0.6052	0.9831	0.0131	1.113	0.894
112				9.0	1.823	1.040	0.6750	0.9773	0.0130	1.235	0.754
113		4.5	0.2	6.0	1.823	1.013	0.5272	0.9889	0.0501	0.9168	1.050
114				7.0	1.823	1.013	0.6850	0.9808	0.0348	1.199	0.734
115				8.0	1.823	1.013	0.7733	0.9711	0.0280	1.349	0.556
116				9.0	1.823	1.013	0.8282	0.9598	0.0243	1.433	0.446
117			0.4	6.0	1.823	1.021	0.3770	0.9933	0.0367	0.6723	1.352
118				7.0	1.823	1.021	0.5425	0.9887	0.0275	0.9716	1.020
119				8.0	1.823	1.021	0.6520	0.9831	0.0230	1.166	0.800
120				9.0	1.823	1.021	0.7270	0.9764	0.0204	1.295	0.649
121			0.6	6.0	1.823	1.031	0.2920	0.9947	0.0272	0.5315	1.523
122				7.0	1.823	1.031	0.4460	0.9913	0.0220	0.8131	1.213
123				8.0	1.823	1.031	0.5605	0.9871	0.0192	1.020	0.984
124				9.0	1.823	1.031	0.6455	0.9821	0.0176	1.171	0.813
125			0.8	6.0	1.823	1.040	0.2450	0.9953	0.0204	0.4433	1.617
126				7.0	1.823	1.040	0.3835	0.9925	0.0177	0.7091	1.339
127				8.0	1.823	1.040	0.4957	0.9890	0.0162	0.9147	1.114
128				9.0	1.823	1.040	0.5840	0.9848	0.0153	1.074	0.936

Table 3 (continued)

Case Number	Fuel Enrichment (at. % U^{235})	Channel Width, l (in.)	Plate Thickness, t (in.)	Lattice Pitch, P (in.)	η	ϵ	p	f	M^2B^2	k_{eff}	R_c
129	4.0	5.5	0.2	6.0	1.823	1.010	0.2133	0.9956	0.1425	0.3422	1.681
130				7.0	1.823	1.010	0.5220	0.9888	0.0663	0.8913	1.061
131				8.0	1.823	1.010	0.6770	0.9807	0.0449	1.170	0.750
132				9.0	1.823	1.010	0.7645	0.9717	0.0352	1.321	0.574
133			0.4	6.0	1.823	1.021	0.1395	0.9969	0.0882	0.2379	1.829
134				7.0	1.823	1.021	0.3710	0.9933	0.0493	0.6537	1.364
135				8.0	1.823	1.021	0.5323	0.9888	0.0357	0.9459	1.040
136				9.0	1.823	1.021	0.6400	0.9836	0.0289	1.139	0.824
137			0.6	6.0	1.823	1.031	0.1117	0.9974	0.0578	0.1980	1.884
138				7.0	1.823	1.031	0.2863	0.9947	0.0371	0.5161	1.534
139				8.0	1.823	1.031	0.4382	0.9915	0.0286	0.7939	1.229
140				9.0	1.823	1.031	0.5498	0.9876	0.0241	0.9965	1.005
141			0.8	6.0	1.823	1.043	0.0990	0.9976	0.0390	0.1807	1.910
142				7.0	1.823	1.043	0.2422	0.9954	0.0281	0.4459	1.623
143				8.0	1.823	1.043	0.3753	0.9928	0.2343	0.6916	1.355
144				9.0	1.823	1.043	0.4837	0.9895	0.0202	0.8923	1.138

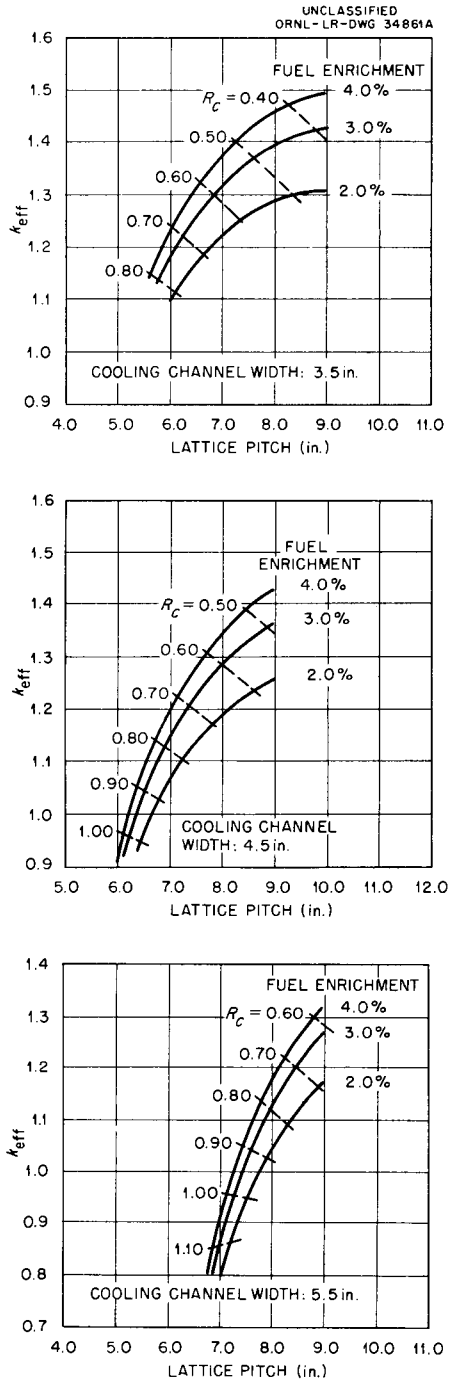

Fig. 5. Multiplication Factor vs Lattice Pitch and Enrichment at a Neutron Temperature of 980°K for the Fuel Element Configuration Shown in Fig. 3 with Fuel Plates 0.20 in. Thick and Cooling Channel Widths of 3.5, 4.5, and 5.5 in.

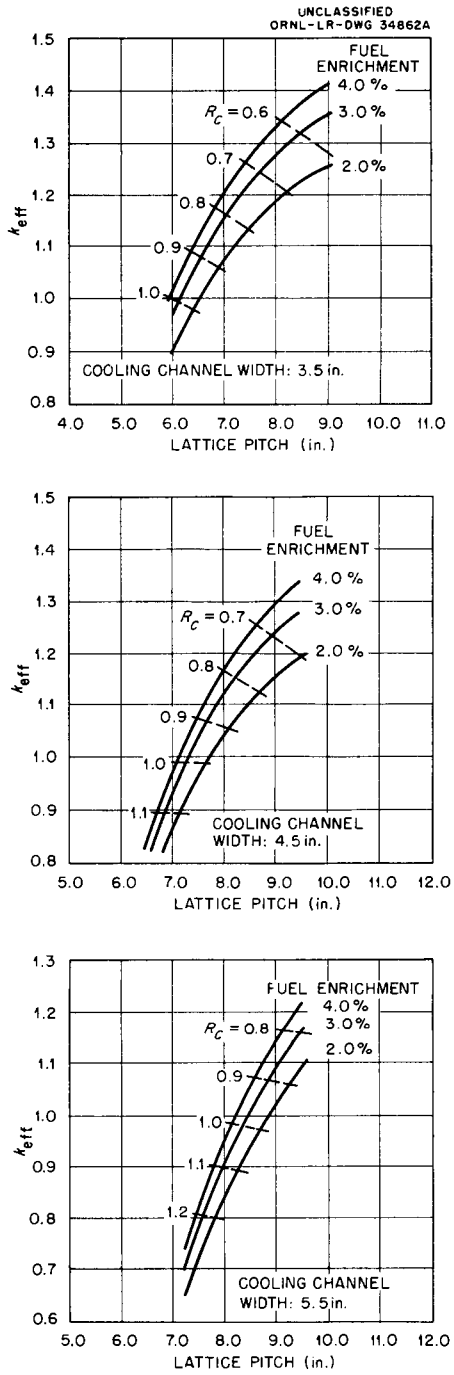

Fig. 6. Multiplication Factor vs Lattice Pitch and Enrichment at a Neutron Temperature of 980°K for the Fuel Element Configuration Shown in Fig. 3 with Fuel Plates 0.40 in. Thick and Cooling Channel Widths of 3.5, 4.5, and 5.5 in.

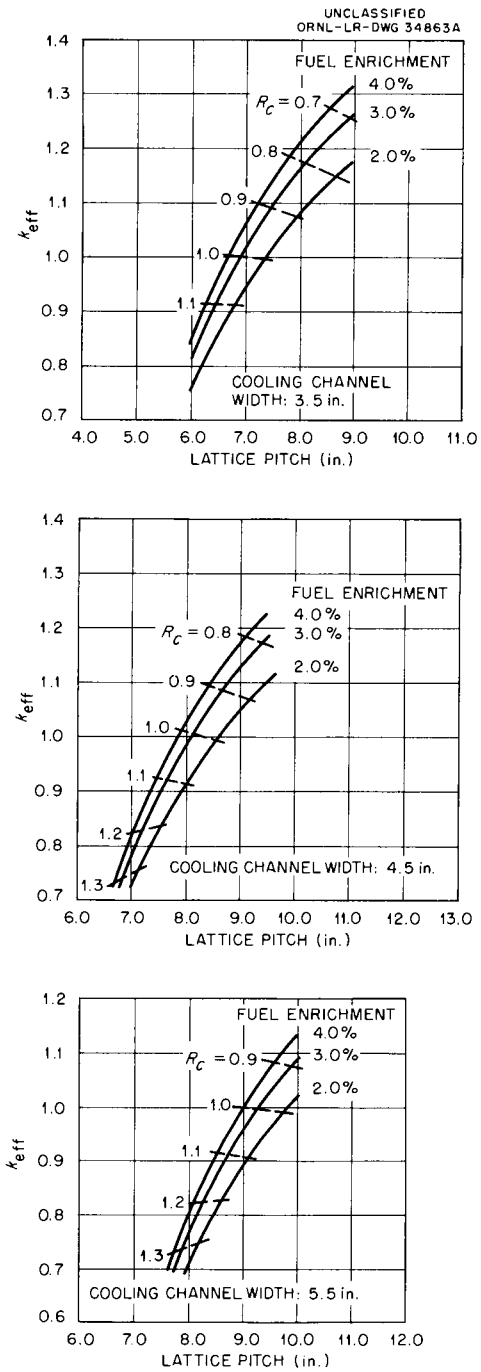

Fig. 7. Multiplication Factor vs Lattice Pitch and Enrichment at a Neutron Temperature of 980°K for the Fuel Element Configuration Shown in Fig. 3 with Fuel Plates 0.60 in. Thick and Cooling Channel Widths of 3.5, 4.5, and 5.5 in.

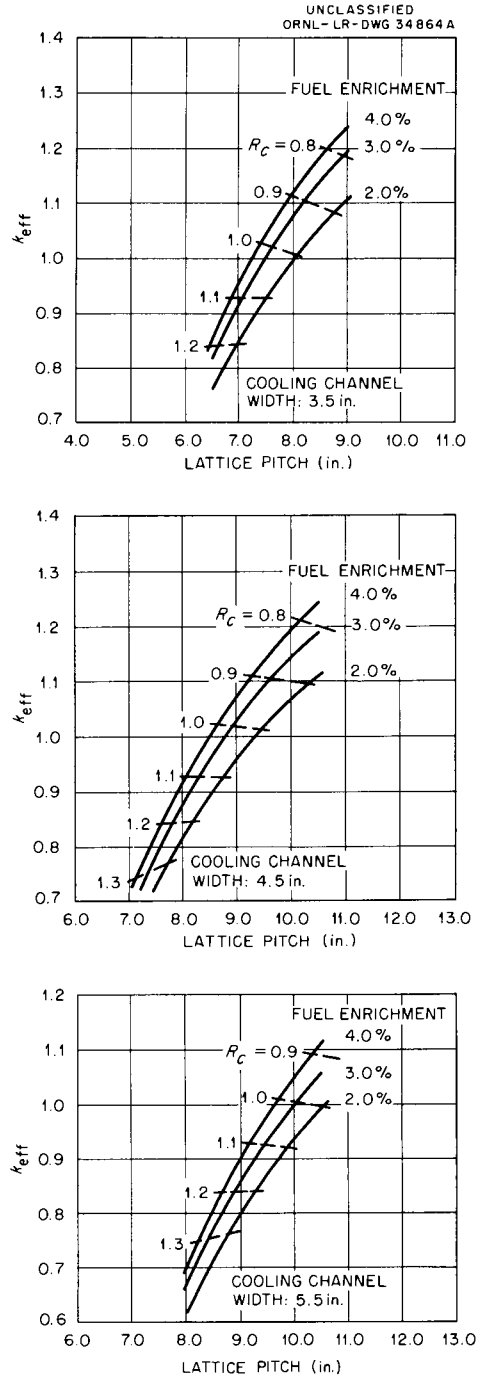

Fig. 8. Multiplication Factor vs Lattice Pitch and Enrichment at a Neutron Temperature of 980°K for the Fuel Element Configuration Shown in Fig. 3 with Fuel Plates 0.80 in. Thick and Cooling Channel Widths of 3.5, 4.5, and 5.5 in.

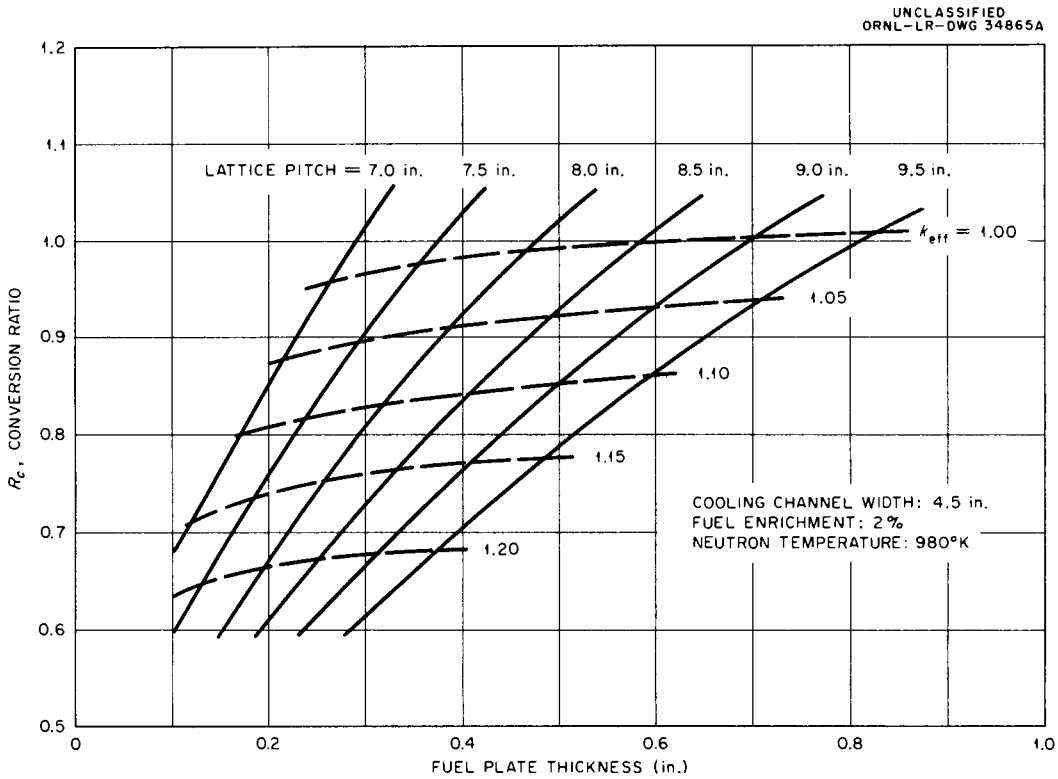

Fig. 9. Conversion Ratio vs Multiplication Factor, Plate Thickness, and Lattice Pitch for Reactors of the HGCR-1 Type.

4. FUEL ELEMENT

MATERIALS AND DESIGN LIMITATIONS

The association of unclad fuel elements with high temperatures ($\geq$2000°F) in gas-cooled reactors appears to be inherent. Even if there were metal fuel claddings which would possess the required neutron cross section, fabricability, availability, and structural strength, it is reasonably certain that the diffusion of uranium and fission products through the metal would be significant.[1] The inevitable hot spot problem, which is especially serious with clad elements, further limits the use of clad materials, since hot spots might increase the diffusion losses. The known ceramic materials (including graphite) which offer promise as a matrix material for high-temperature fuel elements are vastly more permeable than metals, and thus it appears inevitable that higher temperatures will be associated with higher contamination levels in the primary coolant.

The use of high temperatures implies a contaminated system, but it does not necessarily follow that low-temperature systems will not be contaminated. However, for a system to be both contaminated and not capable of realizing the improved performance which is associated with high temperatures is to impose an economic burden on the plant which it is difficult to offset through other economies. Perfectly leak-tight containers for the fission products from high-temperature fuel elements do not currently exist, but it is reasonable to anticipate that the materials development research now under way will reduce, though probably not eliminate, fission-product escape from the fuel.

Fuel Element Characteristics

As a basis for the selection of a fuel element the characteristics which are necessary for the intended application are as follows:[2]

1. The fuel element material must have a high melting point and only one crystal structure so that it may be used in bulk form rather than as a dispersion.

2. The constituent of the uranium compound must have a low neutron absorption cross section.

3. The fuel material must be chemically and metallurgically inert with respect to the reactor coolant and the matrix material in which the compound might be dispersed.

4. The uranium compound must have a broad range of homogeneity such that it is stable over a range of composition so that the structure will not be affected by non-stoichiometry caused by poor preparation or uranium depletion by fission.

---

[1] W. B. Cottrell and H. N. Culver, *Contamination in the Gas Stream of the Gas-Cooled Reactor*, ORNL CF-58-1-119 (Jan. 2, 1958).

[2] E. Epremian, *Uranium Compounds for New High-Temperature Fuels*, paper presented at Fuel Elements Conference, Paris, Nov. 18–23, 1957, TID-7546 (March 1958).

5. It must have good stability in high-temperature irradiation.

6. The thermal conductivity of the bulk uranium compound fuel must be high to facilitate a high heat flux and to prevent melting at the core of the fuel element.

7. The density of uranium atoms in the compound must be high to keep the fuel volume low.

8. The bulk fuel must have good mechanical strength and resistance to thermal shock to prevent fracture during reactor operation.

Material

A large number of uranium compounds are currently being considered for use in high-temperature fuels. The materials include uranium carbides, silicides, nitrides, oxides, sulfides, beryllides,[2] and some others. However, of all these potential fuel materials, information upon which to base a reactor design exists for only UO_2-graphite fuel elements. Although the UO_2 lacks structural strength and has poor thermal conductivity, it fulfills the other requirements satisfactorily and appears to be the best high-temperature fuel available at this time. Furthermore, the use of UO_2 in a graphite matrix results in a high-temperature material with good structural strength and thermal conductivity.

UO_2 Particle Size

The use of UO_2 in a graphite matrix has been considered for some time, and much experimental work has been done on the physical properties of such a fuel element.[3-7] These studies have included fabrication and chemical processing, as well as irradiation effects on the physical properties of the graphite-UO_2 matrix. Aside from the type of graphite, which can have an important bearing on the characteristics of the fuel element, the parameters of particular concern have been the volume fraction and the size of the UO_2 particles. The various studies have considered matrices ranging from a homogeneous dispersion of UO_2 in graphite to admixtures of UO_2 particles of several hundred microns in graphite and in concentrations up to 60 wt % UO_2. These studies indicate that the radiation damage to the graphite decreases with increasing particle size because of the

---

[3] L. D. Loch, J. A. Slyh, and W. H. Duckworth, *Studies of Graphite for Fuel Elements*, TID-10001 (Oct. 13, 1954).

[4] F. E. Faris, *Reactor Sci. Technol.*, vol 2, No. 4, TID-2004 (Dec. 1952).

[5] *Ceramic Information Meeting Held at Oak Ridge National Laboratory on October 1–3, 1956*, TID-7530, pt I (April 1957).

[6] W. P. Eatherly *et al.*, *Physical Properties of Graphite Materials for Special Nuclear Applications*, 1958 Geneva Conference Paper No. 708.

[7] R. H. Kernohan, *Effect of Fissionable Particle Size on Fission Damage in Graphite*, ORNL-1722 (April 21, 1954).

decreasing fraction of recoil fission products which enter the graphite. Although several sources[3,7,8] indicate that the knee of the curve of damage vs particle size is approximately 100 μ, there is some additional reduction with still larger particles. A particle size of 200 μ was selected for the current study, with the realization that some additional decrease in damage effects and fission-product escape (see Chap. 7) might be realized from the use of even larger UO_2 particles.

UO_2 Volume Fraction

The volume fraction of UO_2 in the graphite matrix was, somewhat arbitrarily, taken as 0.25. Although literature data indicate that UO_2-graphite matrices with up to 60 wt % UO_2 ($\sim$18 vol %) have been fabricated, it is not expected[9] that the physical properties of the graphite would be significantly impaired if the volume fraction of UO_2 were increased to 0.25. The validity of this opinion can only be proved (or disproved) by irradiation tests, but the proposed reactor and fuel element are not uniquely dependent upon this condition. Two schemes for reducing the volume fraction are conveniently available: (1) with the same size fuel element the uranium enrichment may be increased, and (2) the size of the fuel element (and fuel channel) may be increased so that the same amount of fuel is dispersed in a greater volume of graphite.

UO_2-Graphite Reaction

At some high temperature the UO_2 in contact with graphite will tend to become converted to UC_2 by the reaction

$$UO_2 + 4C = UC_2 + 2CO$$

The threshold temperature for this reaction has been reported to be around 2500°F or above.[3,6,7] It is clear that the highest temperature that can be employed with uranium-bearing graphite without an appreciable reduction of the oxide will depend upon such factors as time at temperature, the UO_2 particle size and density, and the surrounding atmosphere. Mixtures of UO_2 and powdered graphite have been heated for ½ hr at 1750°C ($\sim$3180°F) with only slight reduction of the oxide. On the other hand, the maximum fuel element temperature will be sustained for long periods of time, and in order to avoid conversion to the carbide the maximum operating temperature should be considerably less than 3180°F. This is a somewhat arbitrary restriction, since the relative activity escape from UC_2 as compared with UO_2 is not known, but, since the diffusion of activity from the fuel may be comparable to the recoil escape (see Chap. 7), it seemed desirable to stay within existing knowledge where possible.

---

[8] R. J. Harrison, *Effect of Particle Size on Fission-Fragment Damage for Particles of Fissionable Material Dispersed in a Matrix*, BMI-846 (June 30, 1953).

[9] Personal communication from A. J. Taylor, Metallurgy Division, ORNL, to W. B. Cottrell, Reactor Projects Division, ORNL, Aug. 1, 1958.

Fuel Element Corrosion

Another problem of concern would be the direct loss of uranium to the gas stream by diffusion, corrosion, or erosion. The limited existing data[10,11] pertinent to the diffusion of uranium in graphite imply that at temperatures below approximately 2600°F the amount would be negligible. On the other hand, the corrosion (and/or erosion) of the graphite by the impurities in the helium coolant may not be negligible at the gas pressures and fuel element temperatures of interest. Data on the processes are not available in the literature, but it is known that the release of uranium to the coolant stream may be minimized by coating the outside surfaces of the UO_2-graphite matrix with a layer of graphite. It is not anticipated that this would be difficult to do or expensive.[12] Accordingly such a coating was assumed for the HGCR-1 fuel elements. A much greater improvement in the ability of graphite to retain fission products may be anticipated from various attempts to decrease the graphite porosity,[6] and/or to develop impregnable coatings for the graphite[13] (or the UO_2 in the graphite[14]). These developments remain to be proved.

At the temperatures that would exist within the reactor, the oxidation of both the fuel element and the moderator by impurities in the helium is of concern. Extrapolation of limited existing data suggests that, inasmuch as the moderator graphite surface temperature would be less than 1500°F (820°C) and the fuel lifetime would be relatively short even though the reactor would be operated with a maximum fuel element surface temperature of 2000°F (1100°C), the loss of graphite from the reactor and fuel elements need not be of concern if excessive fouling of the heat exchanger surfaces does not ensue. For the purpose of this study it was assumed that the gas cleanup system would be capable of removing the graphite corrosion products, and thus excessive fouling of heat exchanger surfaces would be prevented.

HEAT TRANSFER CALCULATIONS

In the heat transfer analyses no attempt was made to obtain the optimum reactor output for an unclad-fuel-element system. As previously noted the heat transfer components were sized to facilitate a cost comparison with the clad-element systems already studied. The time available for this study did not permit an evaluation of different fuel

---

[10] J. G. Malm and G. W. Mason, *Volatilization of Uranium from Uranium-Impregnated Graphite*, ANL-4153 (July 23, 1948).

[11] R. L. Loftness, *Diffusion of Uranium Carbide in Graphite*, NAA-SR-64 (Aug. 2, 1950).

[12] Personal communication from H. G. MacPherson, ORNL, to W. B. Cottrell, ORNL, Sept. 1958.

[13] L. M. Daney, *Refractory Materials Meeting*, ORNL CF-58-6-107 (June 27, 1958).

[14] W. C. Riley, "Improved Fueled Graphite," from *Progress Relating to Military Applications During August, 1958*, BMI-1287 (Sept. 1, 1958).

elements and channel geometries. For the present study the fuel elements were assumed to be flat plates in order to obtain the desired heat transfer surface, and the channels were assumed to be square. Four fuel plates per channel were selected to give a reasonable void fraction for the coolant and at the same time a plate dimension of fabricable size. The fuel choice was UO_2 because of the lack of data on uranium compounds more suitable for use at high temperatures. In order to utilize the advantages of unclad elements, the heat flux must be so large that a pure UO_2 plate would crack from the resulting thermal stress. As discussed in the preceding chapter, the fuel plates were assumed to be a homogeneous mixture of UO_2 and graphite.

The reactor was assumed to have an active core diameter of 30 ft; the active length was fixed at 20 ft; and the pressure was taken to be 300 psia to match that of the GCR-2 case. The square coolant channels were varied from 4 to 6 in. on a side. In all the calculations the peak-to-average power ratio was assumed to be 1.32 axially and 1.5 radially. The heat transfer coefficient was determined from the Dittus-Boelter equation; the core friction pressure drop was obtained from the Fanning equation; and the friction factor was held constant at a value of 0.006. The total pressure drop was assumed to be 1.5 times the core pressure drop. The calculations for the blower horsepower were based on the average core temperature rather than the pump suction temperature. This method gave a pumping power which was approximately 50% too high, and as a result the calculated over-all pumping power was about 2.25 times that required to overcome the core friction loss. This factor should give pumping power sufficient for the external circuit losses and also the expansion and contraction losses through the core.

Surface Temperature

One of the principal advantages of the unclad fuel element is the much higher allowable surface temperature. The higher surface temperature results in a higher heat flux for a given gas velocity and required pumping power. There are, however, several factors other than the physical properties of the fuel element that limit the surface temperature. If the heat flux from a given fuel element is increased by increasing the element temperature, the gas flow and therefore the void volume of the reactor or the gas exit temperature from the reactor must be increased. The exit gas temperature is limited by the piping system external to the core. Increasing the void volume leads to either excessive neutron leakage or to an increase in the lattice pitch, which results in fewer channels and therefore less output per volume of reactor. The higher fuel element temperature also lowers the value of k_∞, and increases the number of fission products escaping from the fuel elements (see Chap. 7). On the basis of preliminary heat transfer and void volume calculations the maximum surface temperature was set at 2000°F.

Nuclear Considerations

Nuclear considerations imposed several restrictions on the final size of the channels. For the 30-ft-dia core the ratio of void volume to fuel plate volume was limited to a maximum of 3 to 1. The lattice pitch was equal to the channel dimension plus 4 in., that is, for a 4-in. by 4-in. channel, the lattice pitch would be 8 in. For the case where the lattice pitch was directly related to the channel size, it was possible to calculate the optimum channel size in order to obtain the maximum heat transfer surface. For plate-type elements the heat transfer surface is

$$A_s = 2N_p DL \ ,$$

where N_p is the number of plates per channel, D is the dimension of the square channel, and L is the length of the fuel element. The reactor core volume per channel is

$$V_c = (D + t)^2 L \ ,$$

where t is the thickness of graphite between channels and $(D + t)$ is the lattice pitch. The ratio of the heat transfer surface to the core volume per channel is thus

$$\frac{A_s}{V_c} = \frac{2N_p DL}{(D + t)^2 L} \ .$$

If the above expression is differentiated with respect to D and equated to 0, it may be seen that $D = t$ and thus that the optimum channel dimension is equal to the thickness of graphite required between each channel. As will be seen later, the void volume limitations may force an increase in the channel dimensions.

Core Heat Transfer Studies

The effect of channel size, heat flux, and gas temperatures on the reactor output and required pumping power for the 30-ft-dia core is illustrated in Fig. 10. The effect of the same parameters on the spacing between fuel plates is shown in Fig. 11. It should be noted that a large part of Fig. 11 is geometrically impossible, since the clearance between the plates exceeds the total width of the channel. The results presented in Fig. 11 when correlated with the void-to-plate volume ratio limit of 3 to 1 indicate that the 1250°F exit gas temperature cases can be eliminated.

The reactor output used in the calculations was the output of the center channel. The total reactor output is equal to the center channel output multiplied by the number of channels and divided by the radial peak-to-average power ratio. The GCR-2 studies showed that a mixed mean exit gas temperature for the whole reactor could be maintained as high as that of the center channel by the use of orifices to restrict gas flow through the lower output channels.

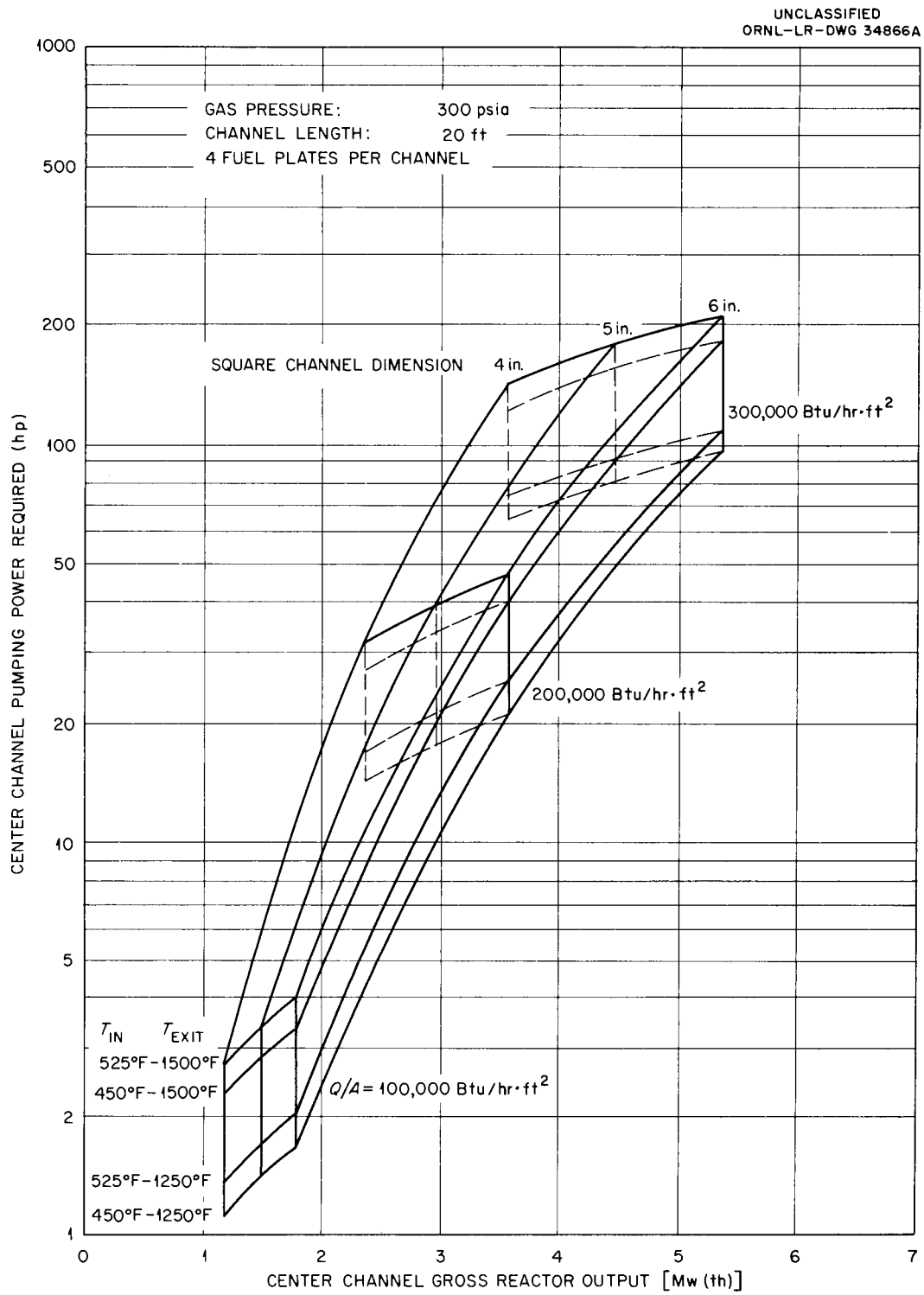

Fig. 10. Required Pumping Power vs Gross Reactor Output for Center Channel.

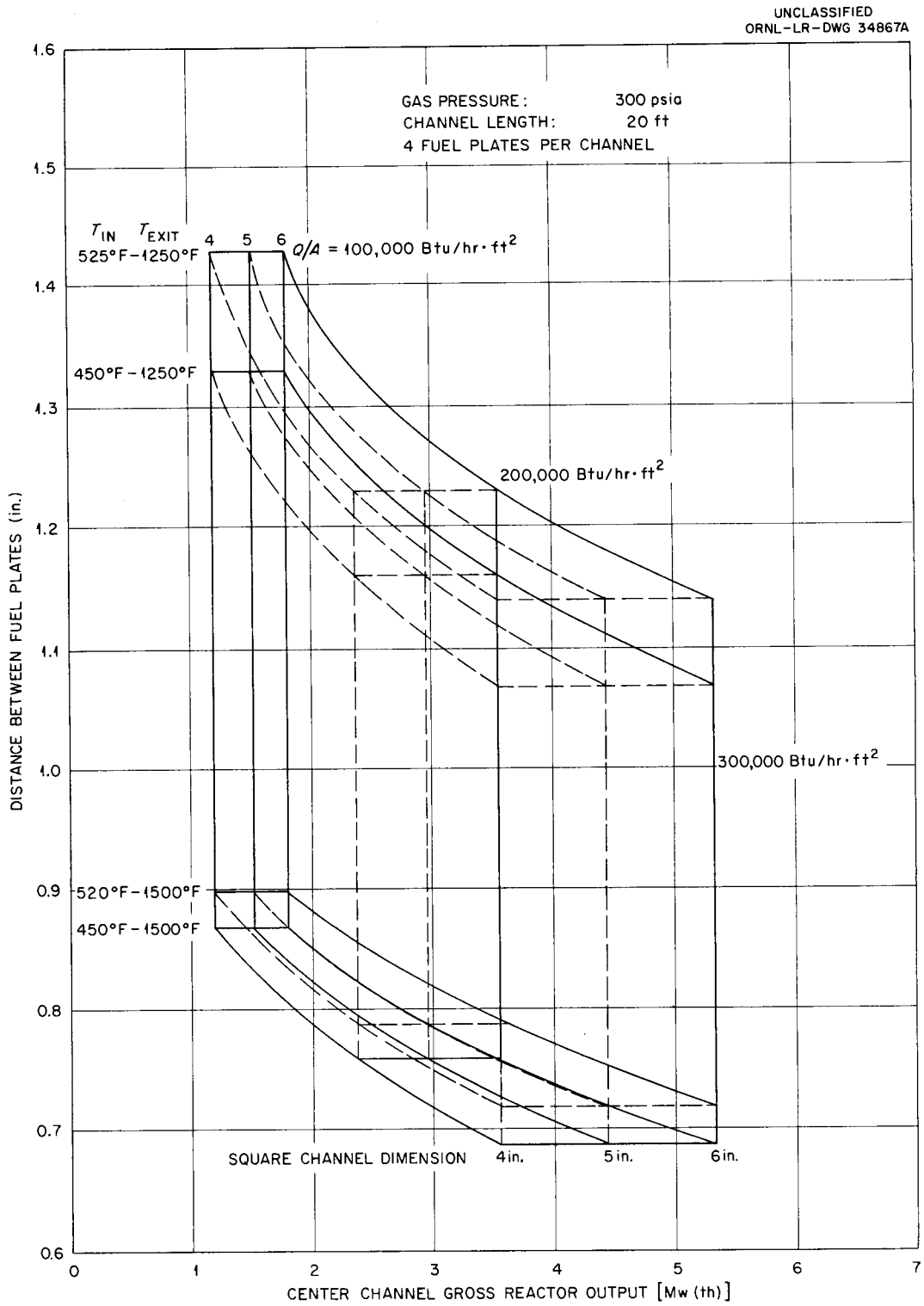

Fig. 11. Clearance Between Fuel Plates vs Gross Reactor Output for Center Channel.

The final reactor inlet and exit gas temperatures were 525°F and 1500°F. The 525°F inlet temperature was a compromise between the higher pumping power required and a higher feedwater temperature, while the choice of the 1500°F exit temperature was largely influenced by the void-to-plate volume ratio and the size of the steam generators required to remove the heat from the gas.

Reactor Output vs Pumping Power

The total reactor output as a function of the pumping power is shown in Fig. 12. In this case the factor limiting the reactor output is the availability of large electric motors. The reactor requirements are such that the motors must start up under load. The largest motors of this type being built today have a rating of about 6000 hp. By the addition of small starting motors it is believed that this size can be increased to 9000 hp. In the present study it was assumed that each gas circuit would contain one motor-blower combination with a maximum rating of 9000 hp. Thus, for the HGCR-1 with eight circuits, the maximum horsepower was 72,000. In Fig. 12 the net output was found by assuming a cycle thermal efficiency of 39%, with a feedback to auxiliaries other than the blowers of 3.6%.[15] The final design values chosen are listed below:

Thermal rating, Mw	3095
Net electrical rating, Mw	1130
Active core diameter, ft	30
Active core length, ft	20
Number of channels	1415
Channel dimensions, in.	$4\frac{1}{2} \times 4\frac{1}{2}$
Lattice pitch, in.	$8\frac{1}{2} \times 8\frac{1}{2}$
Plate thickness, in.	0.372
Gas coolant	Helium
Number of gas circuits	8
Gas pressure, psia	300
Inlet gas temperature, °F	525
Exit gas temperature, °F	1500
Maximum fuel element surface temperature, °F	2000
Maximum heat flux, Btu/hr·ft^2	245,000
Blower power required, hp	72,000
Temperature rise in fuel plate, °F	95

[15]The actual thermal efficiency turned out to be 40% and the net efficiency (i.e., thermal less gas and water pumping power and auxiliaries) is 36.5%.

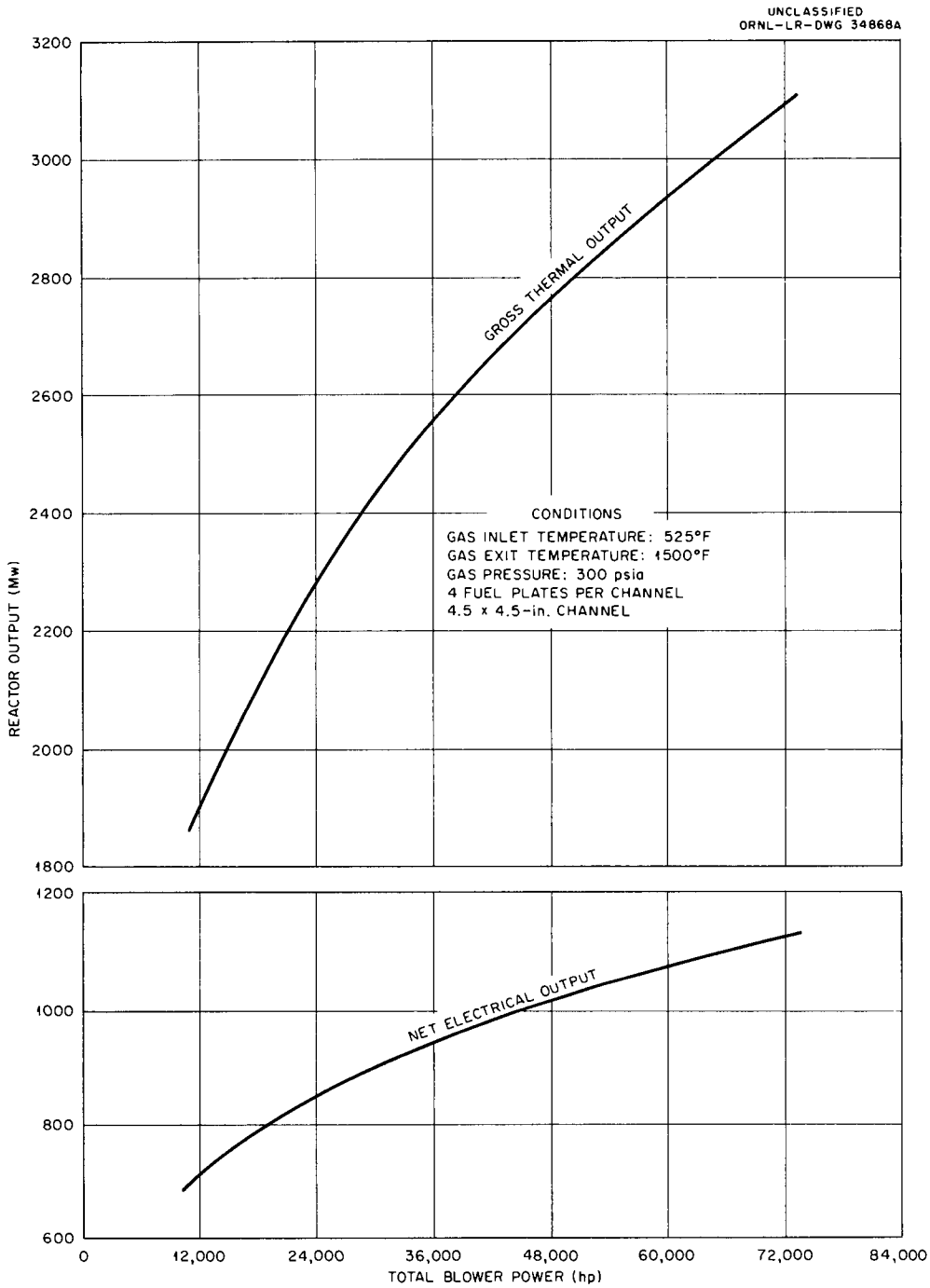

Fig. 12. Reactor Output vs Pumping Power.

Thermal Stress in Fuel Plates

The effects of heat flux and plate thickness on the temperature rise and thermal stress in both UO_2 and UO_2-graphite elements are shown in Figs. 13 and 14, respectively. It may be seen from Fig. 13 that the thermal stress in the UO_2 for even very thin plates far exceeds the maximum stress of about 10,000 psi that the UO_2 can withstand without

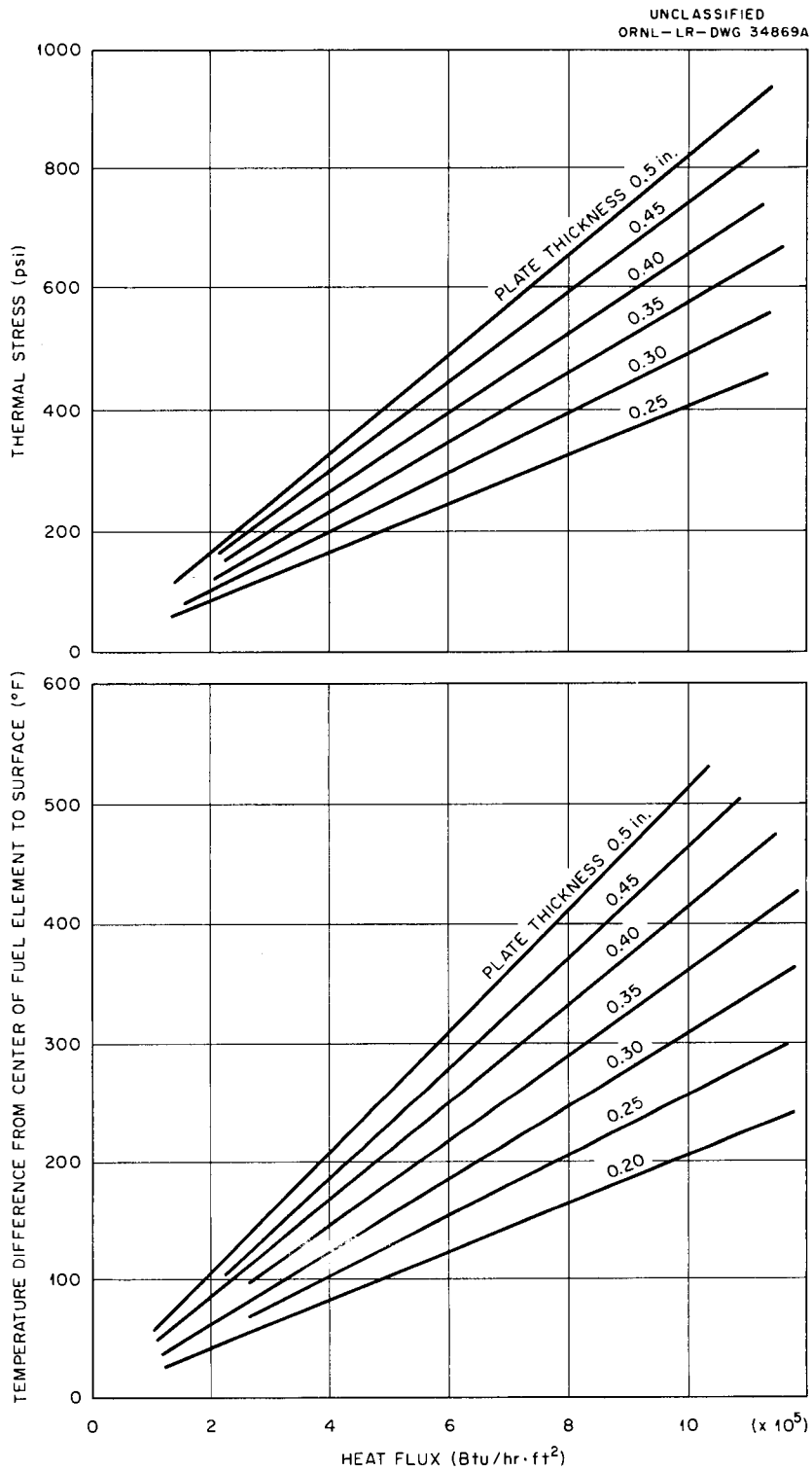

Fig. 13. Thermal Stress and Temperature Rise in a Graphite-UO_2 Fuel Plate vs Heat Flux.

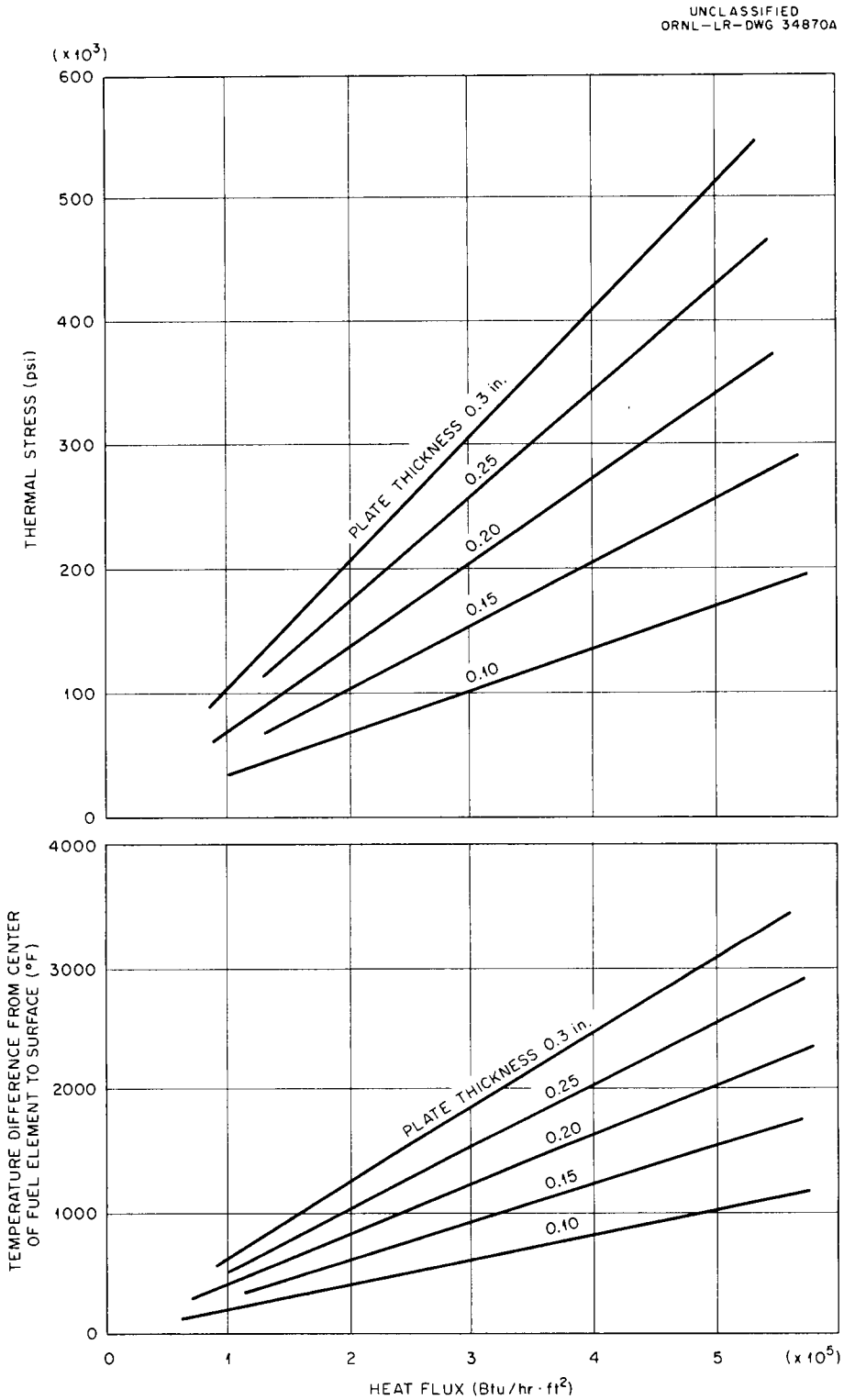

Fig. 14. Thermal Stress and Temperature Rise in a UO_2 Fuel Plate vs Heat Flux.

cracking. The stress in the UO_2-graphite plates, using the properties of graphite, does not exceed about 1000 psi for any cases under consideration. This is well below the 3000- to 4000-psi limit for graphite at the reactor operating temperature.

FUEL ELEMENT CONFIGURATION

A sketch of the fuel element is shown in Fig. 15. The four fuel plates are held in a box made of four ½-in.-thick graphite plates. The graphite boxes containing the fuel plates are stacked in the moderator structure. The clearance between the boxes and the moderator must be large enough to allow for changing or relocating the elements. The gas leakage through this clearance should amount to only a few per cent of that through the fuel elements so that the mixed mean exit gas temperature will not be adversely affected. This allowance for side clearance makes it impossible to obtain perfect vertical alignment of the fuel elements. In order to minimize the effect of the misalignment on the gas flow to the passages between the outer fuel plates and the graphite side plates, the orientation of the fuel elements would be alternated, as shown in Fig. 15.

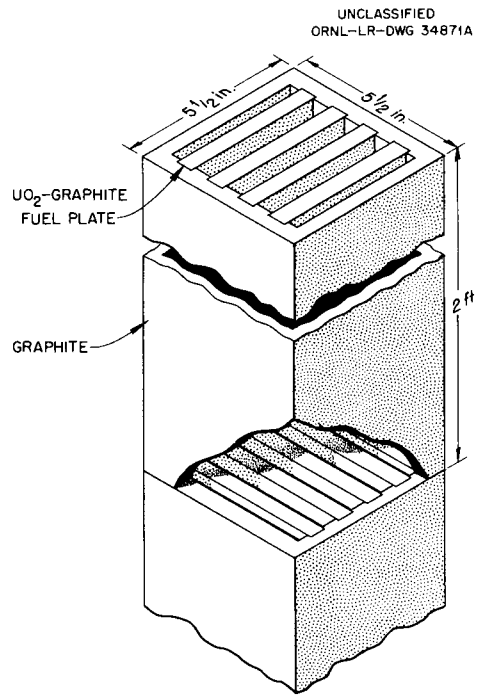

Fig. 15. Fuel Element.

There are several methods by which the fuel elements could be made. One method would be to bond one side of each fuel plate to one side of the graphite box and to leave the other end free to expand. An expansion allowance of about 10 mils or less would be required. Another method would be to taper the ends of the fuel plates and the matching slots in the side plate so that when the four sides of the graphite box were joined the plates would be locked into place. Both of the above methods would necessitate heating the final assembly to a high temperature to join the pieces.

Alternate Configurations

Within the limitations discussed above, many fuel element shapes are admissible, and it is not possible, in view of the lack of basic data, to eliminate all alternative fuel element

configurations on the basis of analytical studies. Thus, several radically different fuel element configurations are conceivable. However, the fuel element selected as the basis for this study is believed to possess the essential characteristics of a good fuel element, while staying closest to existing technology and experimental data. One alternative fuel element configuration is illustrated in Fig. 16. This element does have the advantage associated with a single axial rod. It has the same volume fraction of UO_2 but only 75% of the surface area of the reference design. The fraction of activity escaping by recoil would be reduced, but the reduction might be more than offset by the higher temperature which would exist in the UO_2.

UNCLASSIFIED
ORNL-LR-DWG 34872A

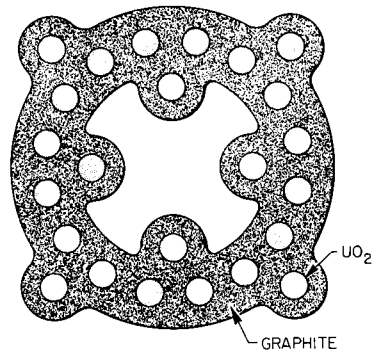

Fig. 16. Alternate Fuel Element Consisting of UO_2 Pellets in Graphite.

5. REACTOR AND GAS SYSTEMS

The layout of the gas system for the HGCR-1 is shown in Fig. 17. The plant consists of a single reactor and eight steam generator–blower combinations. (Each steam generator, in turn, is paired with a separate turbine-generator unit.) The hot gas leaving the reactor core is divided into eight parallel circuits, each going to one steam generator. The cooled gas from the steam generators is directed to the blowers, from which it is returned to the reactor via the annuli for cooling the steam generator shells, the hot gas duct to the steam generator, and the reactor pressure vessel. A valve is located in the blower discharge line, and a bypass equipped with another valve permits control of the flow through the reactor without varying blower conditions. Helium purification systems and helium storage systems – integral parts of the gas system – are provided. An all-welded gas system is specified to reduce leakage to an absolute minimum, and the entire helium-containing system is shielded with $3\frac{1}{2}$ ft of concrete.

LEAK-TIGHTNESS

The activity of the gas inside the primary system would, of course, determine how much gas leakage could be tolerated from the primary system under normal operating conditions. An analysis of the release of activity (see App. F) indicated that the maximum allowable leakage from the system based on allowable exposure levels would be $\sim$0.2% per day. This leakage rate would therefore be an upper limit on the leakage from such a system for the specified purification rate, fuel temperature, stack height, and power level, all of which influence the exposure downstream from the stack.

The choice of a leakage rate is influenced by the cost of the helium lost due to leakage and the cost of maintaining a specified leakage rate. The total free volume of the primary gas system is about 190,000 ft^3 at an average temperature of 1012°F and pressure of 300 psia. Therefore the helium inventory for the plant is about 1,368,000 scf. If helium is assumed to cost \$44.50 per 1000 ft^3, the cost of this volume of helium is about \$61,000. Although the current price of helium is about one-half this price, the \$44.50 per 1000 ft^3 is used because it represents the cost if the national helium conservation policy is put into effect.[1]

If 0.1% of the helium were lost per day, the total leakage-loss cost per year would be 0.365 times the initial charge, or \$22,250, and the leakage-loss cost per kilowatt-hour would be negligible (0.003 mill/kwhr). Therefore, from the standpoint of cost, a leakage rate of 0.1% per day would be satisfactory, and somewhat greater leakage could be tolerated.

---

[1] O. H. Chilson, *The Cost and Implementation of a National Helium Conservation Policy*, report presented at Helium Symposium, Bureau of Mines, Oct. 14–15, 1958 (Jan. 24, 1959).

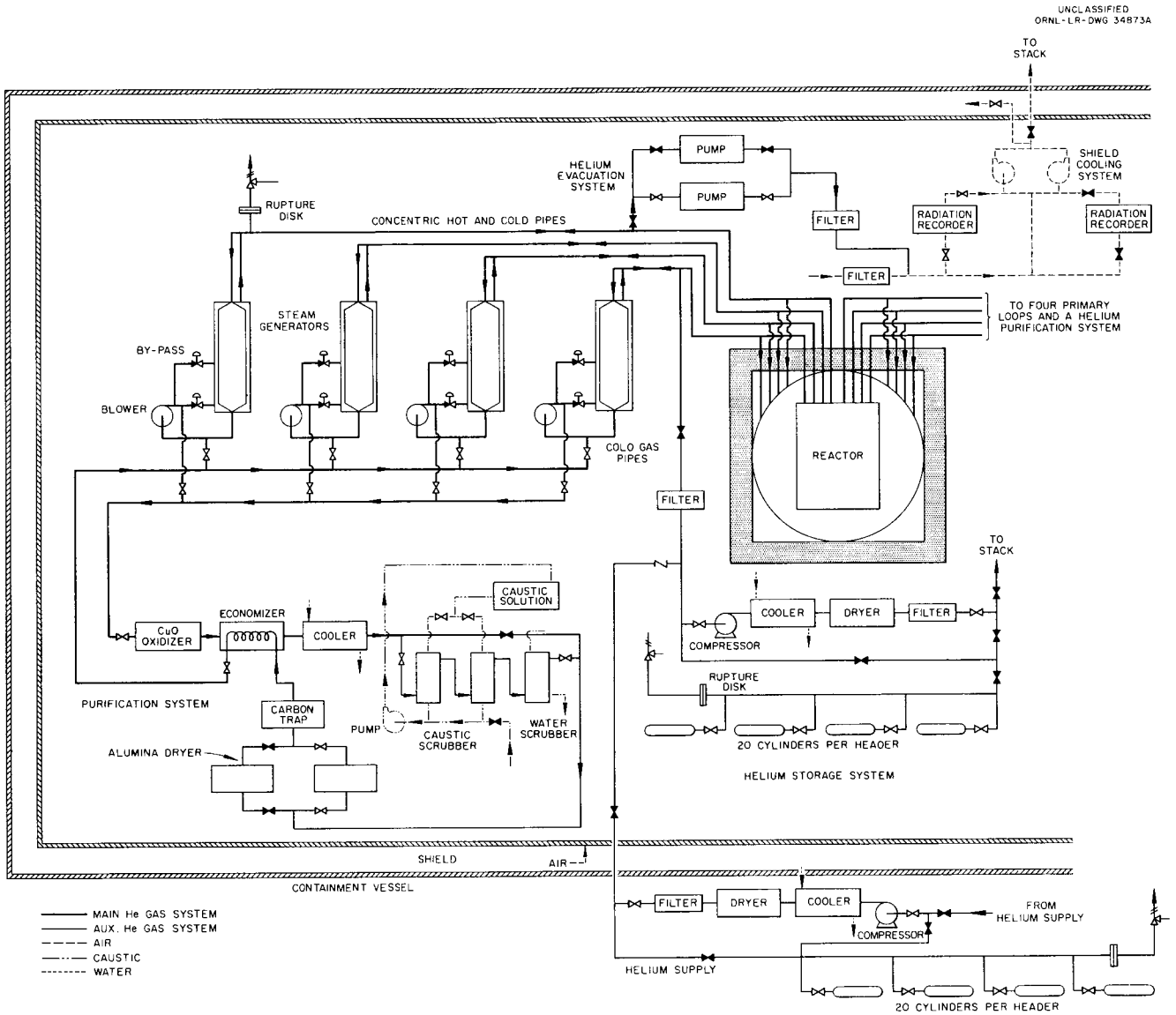

Fig. 17. Flow Diagram of Gas System for HGCR-1.

The leakage rate for the HGCR-1 has been established at 0.1% per day. Experience at Oak Ridge[2] indicates that a leakage rate of 0.03% per day is practical for properly designed large-volume systems. The basic position taken in the GCR-2 study with respect to leak-testing time and costs is applicable to the HGCR-1, and the necessary cost and time factors are present in HGCR-1 cost estimates.

REACTOR PRESSURE VESSEL

The reactor pressure vessel is a 50-ft-dia sphere fabricated from type SA-212 steel, grade B. The basic shell thickness is $3\frac{1}{4}$ in., with sufficient reinforcement added at nozzles and support points to prevent overstressing. The design stress is 15,000 psi, with a maximum metal temperature of 650°F. The vessel temperature is controlled by returning cool helium from the outlet of the steam generator to the reactor vessel in such a way that the helium flows over the vessel shell to maintain the temperature at less than 650°F. Since there are eight steam generators, the reactor pressure vessel has eight helium outlet nozzles and eight helium inlet nozzles. The inlet nozzles are 60 in. in diameter, and the outlet nozzles are 84 in. in diameter. Because the core matrix has been changed to an $8\frac{1}{2}$-in. square pitch and the fuel channels have been changed from round to square, the location and number of control rods and fuel-charging nozzles have been modified accordingly.

Although the reactor outlet temperature has been increased from 1200 to 1500°F, the vessel shell thickness has not been changed from that used for the GCR-2 because the vessel shell temperature is maintained at less than 650°F by the cold helium. Additional insulation will be required on the thermal barrier between the pressure vessel shell and the top of the reactor core to minimize bypass heat loss.

FUEL LOADING

Although the fuel element configuration and materials have been changed, the basic scheme for loading the reactor has been retained, with the additional provision that on-stream loading be possible. Fuel would be charged and discharged by the fuel-loading machine operating from above the reactor. Changes to the fuel-loading machine would involve modifications to permit on-stream loading and modifications of the details of the handling and grab mechanisms used to contact the fuel elements. The grab mechanism would be designed to make positive contact with the graphite side plate of the element and with the fuel plates. This would ensure removal of a fuel element as an integral unit. The grab mechanism would be designed so that the lifting force would be exerted on the side plates and not the fuel plates unless there were relative motion between

[2] *The ORNL Gas-Cooled Reactor*, ORNL-2500, pt 3 (April 1, 1958).

the two. If trouble were experienced in removing an element, a suitably designed fuel-removal tool could be employed to grind or cut the fuel element free. Such a procedure can be resorted to in a reactor of this type in which the coolant gas is already highly contaminated with fission products.

After removal of the fuel element from the reactor core, the fuel-loading machine would withdraw the element into a shielded and cooled chamber, index to a new chamber, and charge a new fuel element to the tube from which one had just been removed. After accomplishing this procedure a prescribed number of times the fuel-handling machine would then be positioned above the fuel discharge chute. Fuel elements would be discharged from the fuel-loading machine and would be conveyed through the chute to the dry spent-fuel cooling area.

BLOWERS, MOTORS, AND VALVES

The helium coolant would be circulated through the eight steam generator circuits by eight blowers (one blower to a circuit). As in the GCR-2 design, the motors for these blowers would be 3600-rpm induction motors. To handle the required gas flow, 9000-hp motors would be required. Each blower would handle 300 lb/sec of helium at a head of 16,500 ft-lb/lb and a temperature of approximately 515°F. The suction volume of each blower would be approximately 180,000 cfm. The motor and blower would be located in an all-welded pressure vessel connected to the main helium stream by 60-in.-dia pipes. The motor would be isolated from the blower portion of the pressure vessel by a heat barrier. Helium in the motor portion of the pressure vessel would be maintained at a maximum temperature of 104°F through the use of a water cooler. This canned-motor arrangement would eliminate the possibility of helium leakage at the blower, since no shaft seal would be required.

Helium flow control would be accomplished by means of a bypass valve and a control valve. As the control valve closed to reduce the gas flow to the reactor, the bypass valve would open to permit some gas flow to go to a point within the steam generator. This point would be located so that any heat of compression would be removed before the gas reached the suction of the blower for the second time. In this manner the flow to the reactor would be varied without changing the operating conditions for the blower.

PIPING AND EXPANSION JOINTS

Hot gas leaving the reactor core would be ducted to the top of the steam generator. The gas would then pass down through the steam generator and be cooled in transit. The cool gas would leave the steam generator and pass to the blower, where the pressure would be increased sufficiently to offset system losses. From the blower the gas would pass back to the steam generator where baffles would cause it to cool the steam

generator shell as it rose from the bottom to the top. The gas would then leave the top of the steam generator shell through a pipe concentric with the hot pipe and return to the reactor pressure vessel. At the reactor pressure vessel the gas would cool the pressure vessel shell before passing to the bottom of the core. The inner pipe of the concentric piping would be fabricated from chromium-molybdenum steel. Stainless steel could be used but was not considered in this study because cost data were not available. Type SA-212 steel, grade B, would be used for the outer pipe. Thermal expansion would be taken care of in this pipe line through the introduction of expansion bellows. The number of expansion joints required in the concentric piping has not been determined; however, it has been presumed that three expansion joints would be adequate for this application. All the expansion joints would have to be specially designed. The expansion joint for the inner hot line would be especially difficult to design because it would operate with 1500°F gas on one side and 525°F gas on the other. It is felt that insulation would probably be required on the hot side, and therefore an internal gas sleeve would be needed. Two-ply stainless steel bellows are envisioned for the hot lines. The cost for these joints in the outer 84-in.-dia line has been extrapolated from the GCR-2 costs for 60-in.-dia joints. A piping analysis has not been completed to determine the number and placement of expansion joints, and therefore none are shown in Figs. 1 and 2. In estimating it was assumed that the number of joints used in GCR-2 would be adequate for comparable HGCR-1 lines.

HELIUM PURIFICATION SYSTEM

The helium purification system for the HGCR-1 is expected to include the same types of equipment as specified for this service in the GCR-2 design (see Fig. 17). This equipment includes an oxidizer tower packed with pellets of copper oxide that includes provisions for maintaining the temperature of the bed and gas at 900 to 1000°F. In this tower, hydrogen and CO would be converted to H_2O and CO_2. A tower volume of 160 ft^3 containing about 20,000 lb of copper oxide would be required. Carbon dioxide would be removed from the helium stream by absorption in an aqueous sodium hydroxide solution. Two towers 15 in. in diameter and 12 ft high packed with 1-in. Berl saddles should suffice to remove CO_2 to less than 10 ppm. The gas leaving these towers would be saturated with water vapor, and therefore a drying system capable of producing helium under a pressure of 300 psia with a dew point of −21°F would be required. A system with two parallel towers 6 ft in diameter by 8 ft high containing alumina should be adequate. Means for regenerating each of these three systems would also be required. A final tower containing activated charcoal would be used to remove other trace gases. Because of the contamination in the gas stream, all this equipment would have to be shielded and operated remotely. Further, two complete systems would be required to

permit operation of one system while the other was on standby and thus provide uninterrupted purification of the helium stream during maintenance of one system. Because of the different equipment involved (blowers, towers, dryers, etc.), the plant would be compartmentalized to place the equipment expected to require the most maintenance work in a shielded cell where a manipulator and viewing window would be available to facilitate repair work. Special equipment would be required for the alumina dryers, including filters and piping to the vent stack to permit the dryers to be reactivated by applying heat and blowing ambient air through the alumina. Following reactivation the residual air would be purged with dry helium. Venting the dryers in this manner would be necessary to exclude the activity in the dryer from the containment-cell ambient air.

HELIUM STORAGE SYSTEM

Two helium storage systems would be required – one containing contaminated helium, the other clean helium. The clean helium would be required for initially charging the system and for introducing makeup helium which might be required during operations. The contaminated helium storage system would be used to store the helium which had been contaminated with fission products by passage through the core, and to balance minor pressure fluctuations in the system. The high activity level in this helium would prevent its being vented directly to the stack. The contaminated helium storage volume would be equal to the helium inventory of the plant and would require shielding. The storage of contaminated helium would be in 80 cylinders at a pressure of approximately 2500 psi. Since the cylinders would have to be shielded, provision would also be required for remote service of the helium compressor in this system.

No event is foreseen that would prevent scheduling of a complete replacement of the helium inventory, and therefore the helium inventory in the clean helium storage system would not have to equal the complete inventory of the plant. For replacement of the complete helium inventory, helium storage trucks or freight cars would be used.

Although pressure-relieving devices are commonly employed on pressure vessels, considerable hazard would accompany their use on the HGCR-1 primary system, because the highly active helium should not be discharged either to the stack or inside the containment vessel. Since there is no accident or excursion in which the pressure in the primary system is expected to rise very fast or very high, the primary helium would be pumped into the storage helium volume in the event the system pressure became too high. The action would be manual, initially, and then automatic at a somewhat higher pressure. A high pressure in the system at any time would be cause for evacuation of the containment vessel and securing of the vessel, including closing the stack valves.

Should the pressure in the primary system continue to rise for some reason, relief valves set for the highest feasible pressure could relieve the system to the area within the shield. The shield cooling system would hold up this gas for some slight additional period and filter it before discharging it to the cell ambient. The probability that the relief valves would be called upon to operate is small. In any event, the cell is designed to accommodate all the helium discharged during the maximum credible accident, and therefore it appears wiser to expect possible contamination of the containment cell rather than venting of a large quantity of fission products to the atmosphere.

6. POWER RECOVERY SYSTEM

DESIGN PHILOSOPHY

One of the aims of this investigation was to compare the performance of the contaminated-coolant reactor to that of the GCR-2 as directly as possible, but, in view of the high gas temperature that would be attained by this system, it was arbitrarily decided to consider a steam recovery system that would operate at the maximum widely used steam temperature of 1050°F. A simple, regenerative, single-pressure, nonreheat-cycle, straight-through GCR-2 type of boiler was selected not only to allow more direct comparison with the GCR-2, but also to eliminate the extra shell penetrations and the intermediate pressure piping that would be necessary with the reheat, dual-pressure, and other more complicated cycles. Simplicity was considered to be of prime importance because the radiation hazard would make any internal repairs very difficult at best. The pressure was limited to approximately 1450 psia by the initial temperature to allow for expansion in the turbine to approximately 10% moisture.

The eight steam generators would feed into eight turbines that would each produce about 157 Mw of electricity. Such a power rating is rather large for nonreheat turbines, but it is felt that this goal can be attained. If reheat were used, four 314-Mw turbines could be employed, with each turbine receiving steam from two steam generators. As mentioned above, it was felt that the added complexity and size of the steam generators did not warrant the use of the reheat cycle.

DESCRIPTION OF STEAM GENERATORS

The steam generators would have the same matrix and tube outside diameters as the GCR-2 boilers, but the proportions of the superheater, boiler, and economizer would be scaled to the new conditions. The combined height of the tube matrices would be 6 ft less than for the GCR-2 boilers; each would remove 2.25 times as much heat.

After being cooled in downflow outside the steam and water tubes, the full coolant flow would be pumped through the blowers and directed upward through an annular area just inside the pressure shell for cooling. It would then pass to the reactor through the outside of an annular pipe. Five inches of insulation between the hot gas region and the annular region would reduce heat losses to a negligible amount. This type of shell cooling is effective, but is not very conducive to natural convection in case of blower failures. Another scheme would be to cool the shell with water tubes. If the proposed amount of insulation were retained, the heat load would be small, and the resulting steam generators would be of approximately the same size and proportions as those for the annular cooling scheme. With the water cooling arrangement, the hot gas would enter the boiler from the bottom, pass to the top through the voids on each side of the tube bundle, and proceed downward through the tubes. It would then pass through the

blowers and return to the reactor through the outside of an annular pipe. Although this scheme would allow better natural convection in case of a blower failure, it was not considered for this design because of time limitations.

The temperature of the inlet gas would require that the hottest 22% of the superheater be made of type 321 stainless steel. The remainder could be built of T11 steel.[1] The placement of the steam and economizer headers would differ from GCR-2 placement in that they would be outside the shell and behind shielding material, as would be necessary for manual blanking of faulty tubes. In addition, removal of the steam drum from the hot ambient gas allows considerable savings in insulation and material cost. This arrangement poses some problems in joining the stainless steel tubes to the type SA-201 grade B steel shell at each penetration and to the boiler tubes.

STEAM PLANT PERFORMANCE

The high performance of the boiler would result in higher pressure drops on both the gas and steam sides than in the GCR-2. The gas-side drop would be within the limits imposed by reactor calculations, and the water-side drop, although numerically high, would not result in an appreciable loss in efficiency. The gross efficiency of the steam plant with six heaters would be about 40.6%. After deducting the power needed to pump water and gas and to operate auxiliary equipment, the efficiency would be about 36.5%.

The performance characteristics of the power recovery system and design details of the steam generator are presented below:

Performance Characteristics

Gas inlet temperature	1500°F
Gas temperature to reactor	525°F
Gas temperature out of economizer	506°F
Gas pressure	300 psia
Gas pressure drop through steam generator	0.694 psia 1207 lb-ft/lb_m
Gas flow per unit	10.83×10^5 lb/hr
Steam outlet temperature	1050°F
Steam outlet pressure	1450 psia
Water inlet temperature	445°F
Water inlet pressure	1688 psia
Steam flow per unit	1.225×10^6 lb/hr
Number of feedwater heaters	6

[1] The superheaters at the Widow's Creek Steam Plant of the Tennessee Valley Authority are constructed as proposed here.

Cycle efficiency (gross)	
Ideal	40.7%
With heater, mechanical, and heat losses	~40%
Approximate net efficiency (including power for auxiliary equipment and for pumping gas and water)	36.5%
Power per unit	393 Mw (th) 157 Mw (e)

Details of Steam Generator

Outside shell inside diameter	21.5 ft
Outside diameter of inner insulation	20 ft
Approximate maximum outside diameter of tube bundles	19.2 ft
Insulation thickness	5 in.
Approximate height of shell	54 ft

Tube matrix data for the economizer, boiler, and superheater are given in Table 4. The design calculations are summarized below, and detailed sample calculations are presented in Appendix E.

Table 4. Matrix Data

	Economizer	Boiler	Superheater
Length of tubing, ft	26,820	22,830	16,100
Total outside area of tubes, ft^2	130,000	90,000	10,000
Height of tube bundles, ft	9.5	9.42	9.03
Tube outside diameter, in.	1.5	1.75	2.375
Fin outside diameter, in.	2.5	2.5	None
Fins per foot	105.6	105.6	None
Transverse pitch, in.	4	4	4
Longitudinal pitch, in.	3	3.5	4.75

CALCULATION OF STEAM GENERATORS AND STEAM CYCLE

A steam outlet temperature of 1050°F and a pressure of 1450 psia were chosen that were based on materials limitations and the last-stage moisture content in the turbine; an expansion efficiency of 85% was assumed, since no reheat or moisture separation would be employed. A pinch temperature difference between the gas and the water was optimized at 80°F, as shown in Fig. 18. This optimum occurs at a higher pinch temperature than that of the GCR-2 because, as indicated by the high slope of the gas-temperature curve through the heat exchanger, there would otherwise be a prohibitively

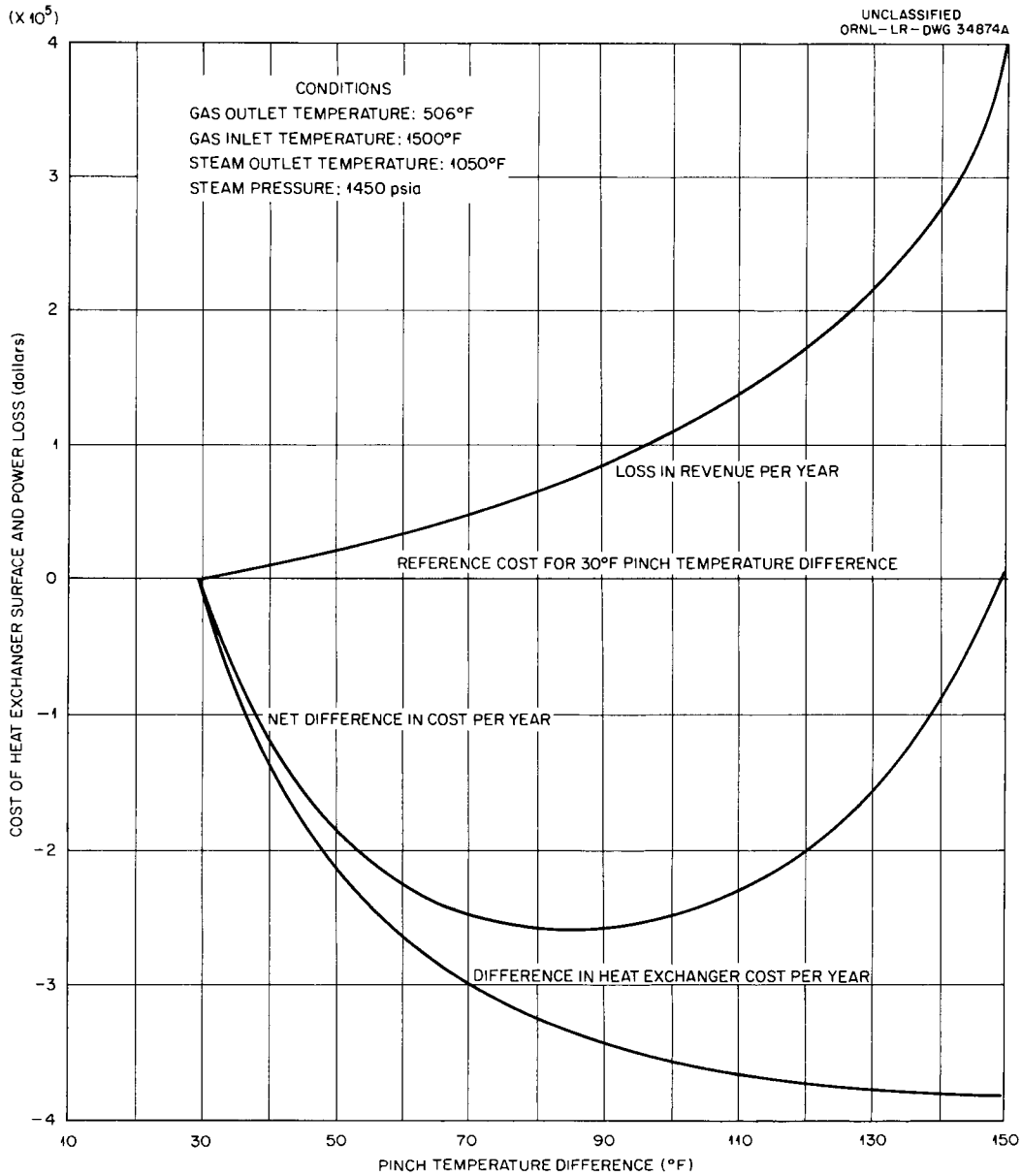

Fig. 18. Relative Cost of Heat Exchanger Surface and Power Loss vs Pinch Temperature Difference.

small temperature difference in the economizer section that would result in an exceedingly large economizer (see Fig. 19).

In passing through the blowers, the temperature of the gas would be raised 18.6°F before it was passed to the cold end of the reactor. In cooling the reactor shell the temperature would be raised another 0.4°F. Since the core was designed for inlet and outlet temperatures of 525 and 1500°F, respectively, it would therefore be necessary that the gas be cooled to 506°F in the steam generator. The relationship between the

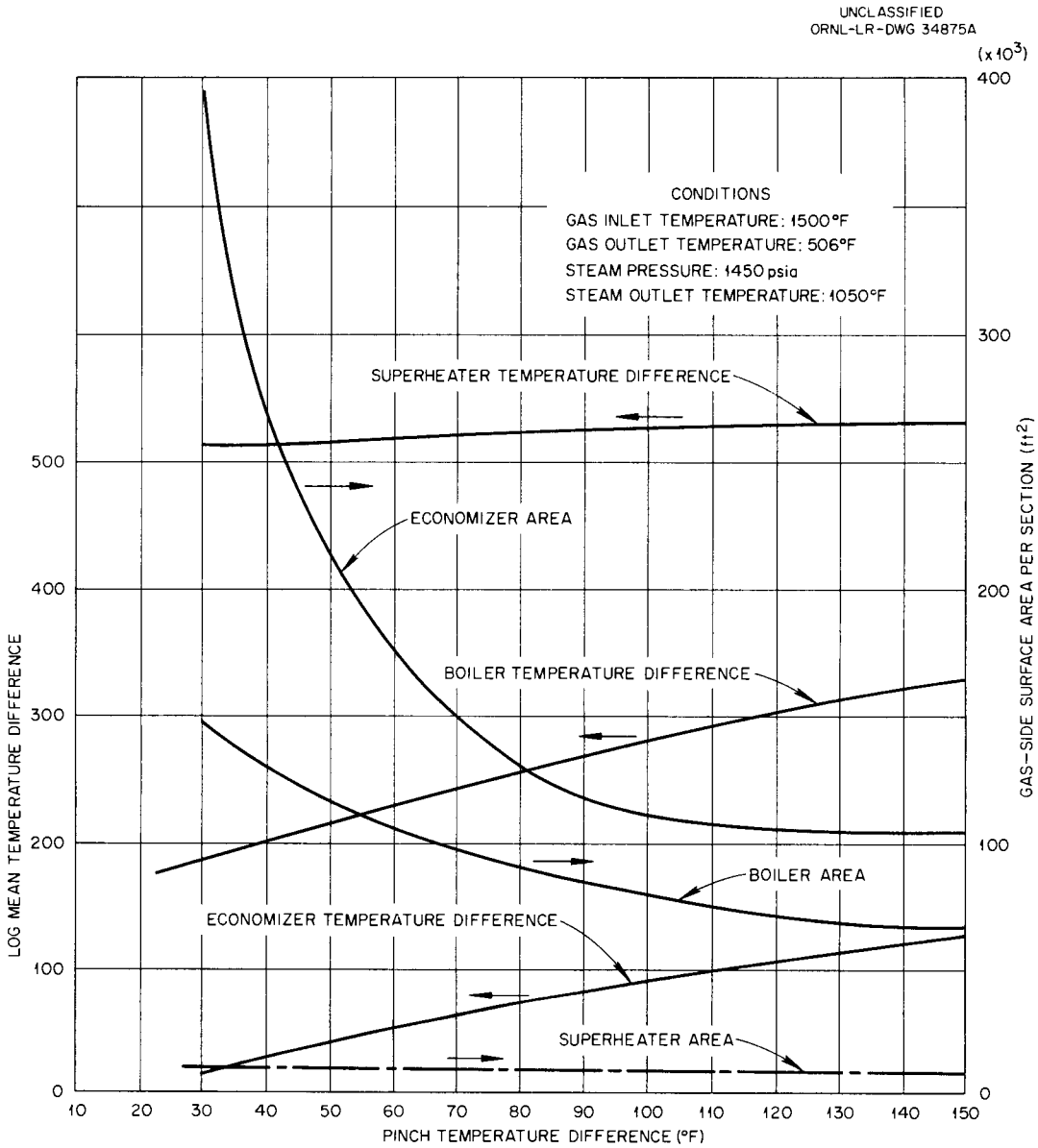

Fig. 19. Log Mean Temperature Difference and Surface Area vs Pinch Temperature Difference.

pinch temperature difference and the allowable feedwater temperature for fixed helium inlet and outlet temperatures is shown in Fig. 20. The curve shows that, for 80°F pinch temperature difference, a feedwater temperature of 445°F may be attained. In addition, Fig. 20 shows that for a feedwater temperature of 445°F the percentage of heat removed by each section is as follows: 16.6% in the economizer, 51.2% in the boiler, and 32.2% in the superheater. The required surface area was scaled directly from the GCR-2 calculations.

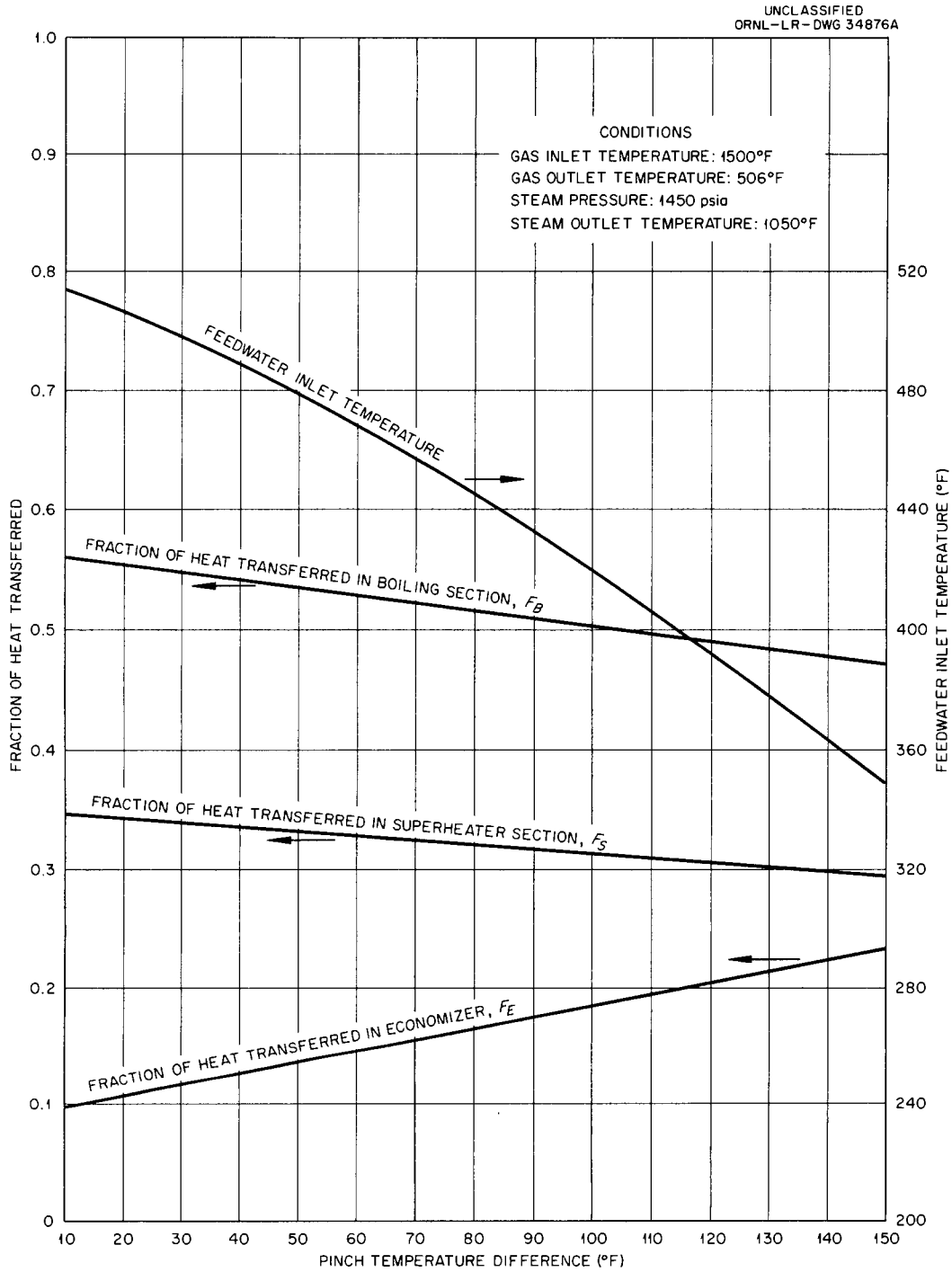

Fig. 20. Fraction of Heat Transferred in Each Section of Steam Generator and Feedwater Inlet Temperature vs Pinch Temperature Difference.

The cycle efficiency as a function of feedwater inlet temperature with various numbers of feedwater heaters is shown in Fig. 21. The data presented do not include arrangement losses and pressure drop losses in the heaters, but can be considered a good guide for the purposes of this study. An approximate correction for a heater

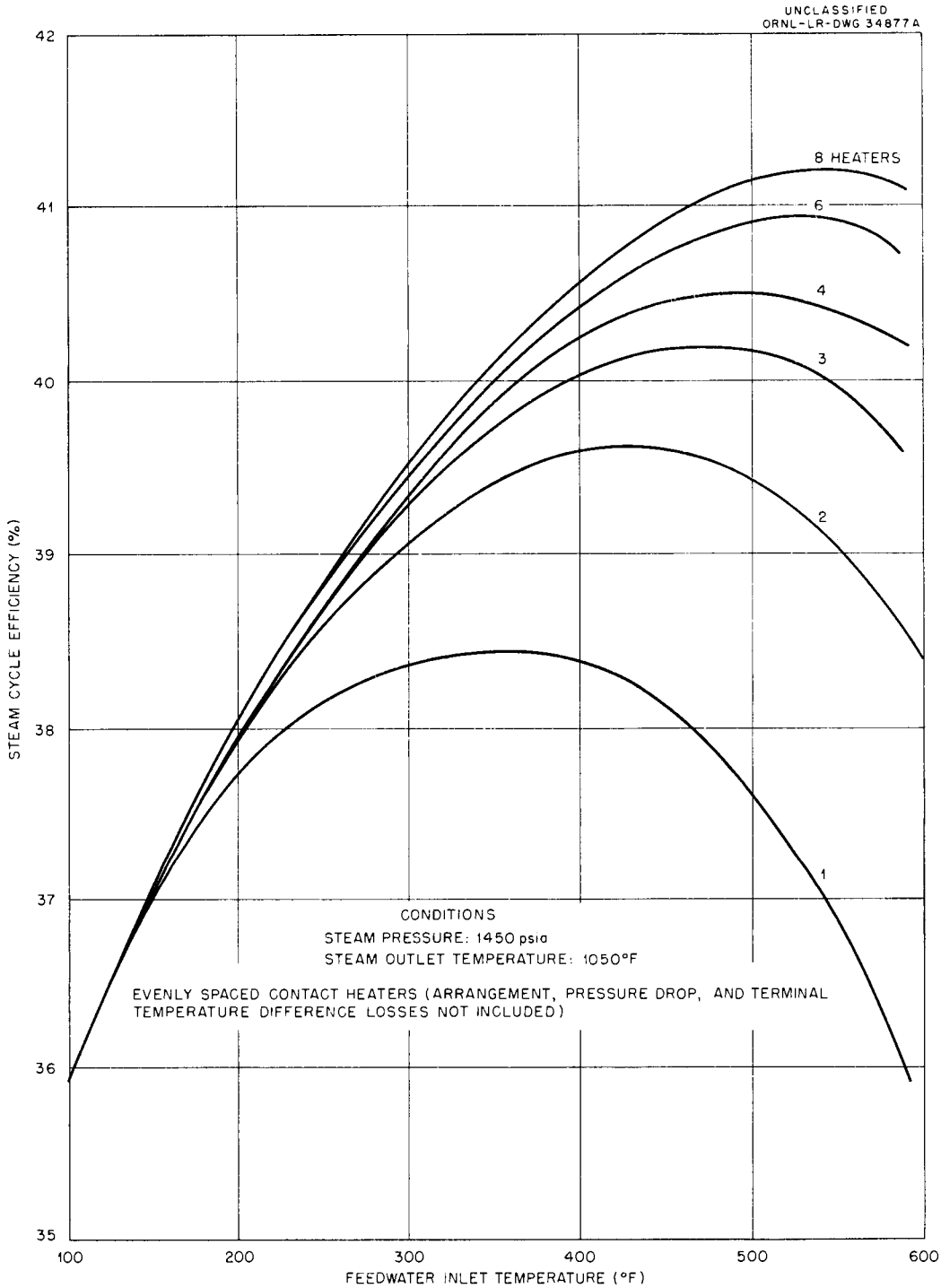

Fig. 21. Steam Cycle Efficiency vs Feedwater Temperature for Various Numbers of Heaters.

terminal temperature difference of 5°F and an extraction line pressure drop of 10% reduces the efficiency for the HGCR-1 system from 40.7 to 40.6%. It was assumed that mechanical and heat losses would further reduce this to approximately 40%.

At a feedwater temperature of 445°F, the incremental increase in efficiency for each additional heater decreases with larger numbers of heaters. In the absence of a precise cost optimization, it is felt that six heaters should be used.

The annulus size for the full-flow cooled-shell heat exchanger was optimized as shown in Fig. 22. The basis for the calculation was the net value of the power (10 mills/kwhr), a plant factor of 0.8, and a capital charge of 14% per year. The shell cost was based on the use of type SA-201, grade B, steel. The annulus inner diameter was held constant at 20 ft to accommodate the tube bundles and the insulation, and the optimum annulus outer diameter was found to be 21.5 ft. The temperatures throughout the steam generator for the fixed design conditions are shown in Fig. 23.

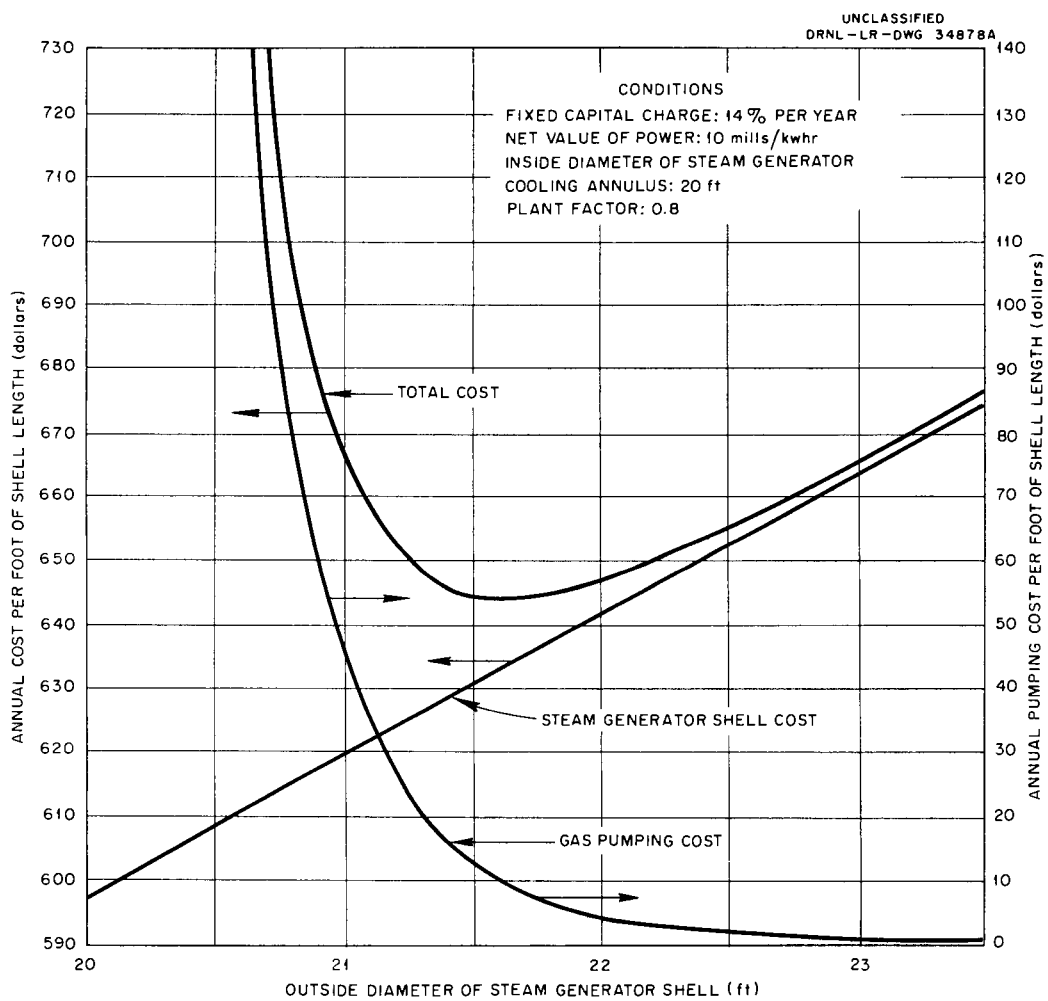

Fig. 22. Steam Generator Shell and Gas Pumping Power Costs vs Outside Diameter of Shell.

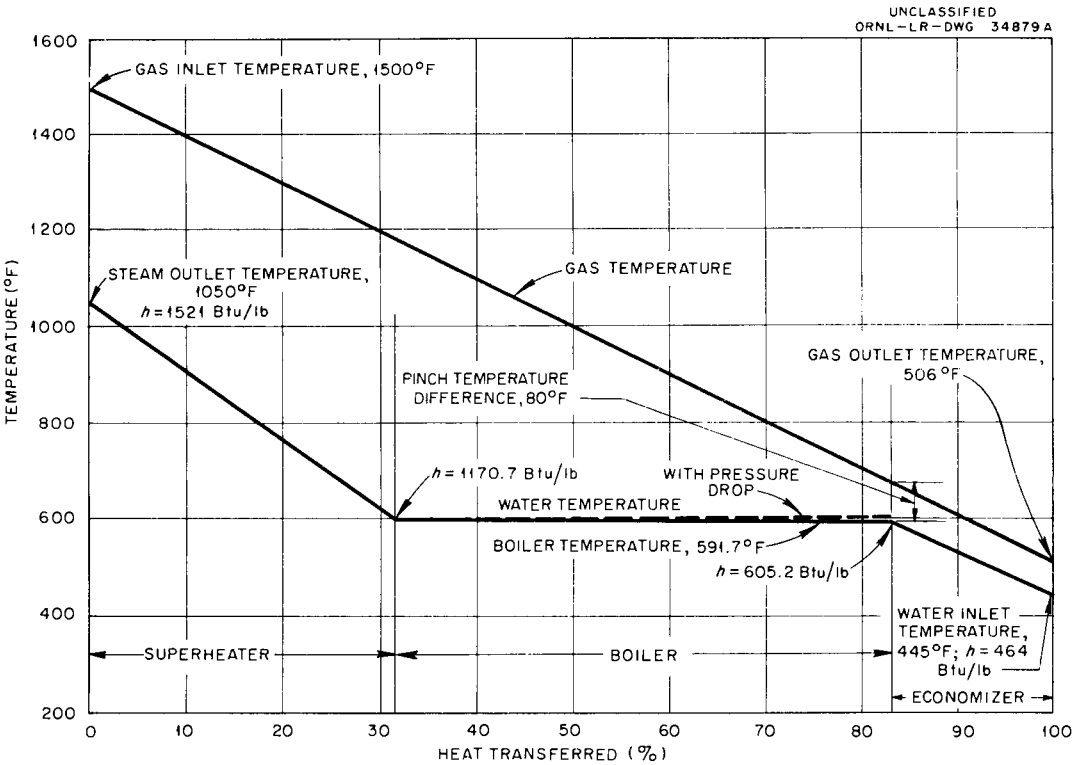

Fig. 23. Gas Temperature and Steam Conditions vs Percentage of Heat Removed in Steam Generator.

AFTERHEAT REMOVAL

The system layout, as shown in Figs. 1 and 2, is not an adequate arrangement for the removal of the afterheat by natural convection. Preliminary calculations show that in case of blower failure after operation at full power, natural convection of the helium at pressure can remove the afterheat at 3 min after shutdown with the gas at design inlet and outlet temperatures. This is quite acceptable, since in this time interval, excess heat in the fuel plates will radiate to the graphite moderator and raise the temperature only about 2°F.

If the system pressure must be reduced to atmospheric pressure, natural circulation of the helium would be completely inadequate to remove afterheat. On the other hand, if air at atmospheric pressure were allowed to circulate in the system, 11 to 12 days would have to elapse before the afterheat generation rate would be small enough for the air to remove the heat without attaining an excessive outlet temperature. If all the heat generated in this time interval were allowed to radiate to the graphite, its temperature would rise, on the average, 415°F. Further studies of graphite oxidation in air are necessary before a final decision can be made as to the acceptability of this condition.

However, it is felt that the hotter portions of the graphite would burn under these conditions.

In view of these considerations, it is thought that it would be necessary to supply emergency power to one of the blowers and to circulate helium at atmospheric pressure. In order to remove the heat generated 3 min after shutdown, only 0.6% of the full-load total power need be applied, that is, one motor would be supplied with 4.8% of its full load power of 432 hp.

7. ACTIVITY RELEASE

The operation of any nuclear power plant for extended periods of time results in the production of large amounts of radioactivity. Although the fission products produced directly in uranium fission are the main source of this activity, additional and significant amounts of activity may result from (1) activation of the coolant, (2) activation of corrosion products and corrosion of activated nuclides, (3) recoil of activated nuclides from in-pile material, and (4) activation of impurities in the coolant. In general, a reactor may be considered a "clean" system if the main source of activity (that due to fission products) is contained in the fuel and not allowed to circulate throughout the primary cooling system. Circulating-fuel reactors are contaminated systems in that all the fission products generated in the fission process are circulated throughout the primary coolant system. Reactors having stationary fuel with a cladding to retain the fission products do not become highly radioactive, but they do have activity in the primary system from the other activation processes. The degree of the contamination of the system depends strongly upon the choice of coolant and fuel cladding. Sodium-cooled reactors are highly radioactive during operation because of the activation of the coolant. Water-cooled reactors become radioactive because of corrosion-product activation and the activation of the water. Gas-cooled reactors with clad fuel become radioactive primarily because of recoil of activated nuclides from in-pile material. The relative intensity of activity in water-cooled and gas-cooled reactors is strongly dependent upon the materials used for the fuel element cladding. In general, gas-cooled reactors tend to have appreciably less activity than water-cooled reactors, and both have less activity than the sodium-cooled reactors.

In addition to determining the activity to be expected in the primary system under normal operating conditions, it is also necessary to evaluate various circumstances which may lead to the introduction of additional amounts of activity into the primary system. Hazards analyses of the so-called "clean" systems generally show that conditions may exist in a system that could introduce fission products into the primary coolant. The amount of activity that could be released generally determines whether the reactor must be contained in a manner similar to that required for a contaminated reactor. Of course, release of fission products into the cooling system leads to contaminated fluids, and the containment problem becomes similar to that of a circulating-fuel reactor.

The activity to be expected in a reactor system is important in establishing many of the major design features of the plant. The activity in the primary system would influence (1) the shielding of the equipment, (2) the containment provisions, (3) the instrumentation, (4) leakage criteria for equipment and piping, (5) the vent system inside the reactor building, (6) the exhaust stack design, (7) the coolant purification

system, and (8) the maintenance facilities. Further, the procedures for operation, decontamination, and maintenance would be affected substantially by the amount and location of activity in the primary system.

The use of an unclad fuel element of the type described for the HGCR-1 implies the release of large amounts of fission products into the primary coolant. In order to estimate the level of activity to be expected in the coolant, an extensive study was made of the release of fission products from a fuel matrix consisting of UO_2 and graphite. The main objective of the study was to understand the mechanism for release and to investigate the factors which would have the greatest influence on the release of the various fission products.

A general study of activity release in contaminated systems should, of course, include an analysis of the release of all the fission products (both beta- and gamma-ray emitters), but, in order to expedite the calculations, only those fission products of sufficient gamma-ray decay energy to influence the shielding requirements were studied. Thus, only nuclides with chain fission yields of 0.1% and with gamma-ray energies of 0.5 Mev or greater were studied. These nuclides are indicated in Table A.2 of App. A. It is estimated that the total system activity would be about ten times that calculated here if all gamma- and beta-emitting nuclides were included.

FISSION-PRODUCT RELEASE FROM UO_2-GRAPHITE FUEL

Release of Fission Products from UO_2

The structure of ceramic fuel materials is such that they will not retain fission products. Investigations carried out in connection with Pressurized-Water Reactor (PWR) fuel elements indicated that the release of fission products from the ceramic fuel material UO_2 is by solid-state diffusion.[1] The release of activity from the UO_2 of the HGCR-1 fuel elements by diffusion was estimated (App. A) by use of the Westinghouse method for predicting fission-gas release for the PWR. The Westinghouse model was obtained in the following manner:

1. A diffusion model was derived which predicted the fractional release of fission gas from a sphere of equivalent radius a [see Eq. (1) below].

2. Experiments were performed which related surface area to UO_2 density. From these data the radius a of an equivalent sphere with the same surface-area-to-volume ratio was calculated.

3. Diffusion coefficients were calculated based on experimental data on fission-gas release.

4. A comparison of experimental and calculated values of fractional release for the fission gas Kr^{85} was made. The results indicated that the diffusion mechanism adequately represented the process of fission-gas release.

[1] J. D. Eichenberg *et al.*, *Effects of Irradiation on Bulk UO_2*, WAPD-183 (Oct. 1957).

The diffusion model, which was derived by J. M. Markowitz, for predicting the fractional fission-gas release from a sphere of equivalent radius a is given by

$$F = 1 + \frac{6}{\pi^4 \gamma^2} \sum_{n=1}^{\infty} \frac{1}{n^4} (e^{-n^2 \pi^2 \gamma^2} - 1) \ , \tag{1}$$

where

F = fractional release,

$\gamma = Dt/a^2$,

t = time (sec),

D = diffusion coefficient (cm^2/sec),

a = radius of the equivalent sphere (cm).

This relationship does not take into account decay of the various fission products but is a satisfactory model for a stable or long-lived nuclide.

A similar expression for predicting the release of fission products by diffusion, which takes into account the half life of the diffusing nuclei, is given[1] by

$$N_i = 4\pi a^3 f Y R \ , \tag{2}$$

where

N_i = total number of atoms external to the equivalent sphere at time t,

f = fissioning rate per unit volume (fissions/sec·cm^3),

Y = fission yield (atoms/fission),

and R is defined by

$$R = \left\{ \left[\left(\frac{d}{\lambda} \right)^{1/2} \frac{\cosh (d/\lambda)^{1/2}}{\sinh (d/\lambda)^{1/2}} - \frac{d}{\lambda} \right] \frac{1 - e^{-\lambda t}}{\lambda} - \left[\frac{2}{\pi^2} e^{-\lambda t} \sum_{n=1}^{\infty} \frac{1 - e^{-n^2 \pi^2 d t}}{n^2 (n^2 \pi^2 d + \lambda)} \right] \right\} , \tag{3}$$

where

λ = radioactive decay constant (sec^{-1}),

$d = D/a^2$ (sec^{-1}).

The diffusion coefficients for xenon and krypton are given in the literature,[1,2] and are presented in Fig. A.1 of App. A. For this study the diffusion coefficients given by Westinghouse[1] were used. In order to predict the release of all the fission products which diffuse from UO_2, it is necessary to have values of the diffusion coefficients of the various elements in UO_2 as a function of temperature. Since values for rubidium, iodine, bromine, and cesium have not been measured experimentally and those for xenon are quite limited, it was assumed for this study that these elements have the same diffusion coefficient as that of krypton. The diffusion coefficients for xenon and krypton in UO_2 indicate that their mobility in UO_2 may be a function of atomic size.

---

[2] J. Belle, *Properties of Uranium Dioxide*, 1958 Geneva Conference Paper No. 2404.

The model used for predicting the release of fission products assumes that release from the equivalent sphere is the rate-controlling mechanism and that when the fission products have been released from the spheres the subsequent diffusion out of the UO_2 pores is very rapid.

A decision was made to limit this study to the diffusion of the fission products xenon, krypton, bromine, iodine, rubidium, and cesium because the measured escape rate data indicate that only these elements tended to diffuse out of UO_2 in significant quantities. However, the daughters of these elements would also contribute activity to the primary system of an HGCR-1, even though they did not escape directly from the UO_2.

The results of the estimate of the diffusion of fission products from UO_2 (App. A) indicate that the release of the various nuclides of interest is dependent upon two major factors, the temperature of the UO_2 and the half life of the nuclide. As expected, increasing the temperature increases the diffusion coefficient and thus increases fission-product release. There is a sharp increase in the diffusion rate at a temperature of 1000°C, with the amount of diffusion being about constant at temperatures of 1000°C or less. Therefore, it is important to minimize the amount of fuel that will be at temperatures in excess of 1000°C. There is, however, a lower limit on the amount of activity released from the UO_2, since, even at the lowest temperatures, significant amounts of activity will be released from the UO_2 by the recoil mechanism, as indicated by Fig. C.1 of App. C. The effect of half life on the amount of activity release from UO_2 is also indicated in Fig. C.1 of App. C. For a given temperature, the fraction of a nuclide that escapes from the UO_2 increases quite rapidly with increasing half life. This means, in effect, that the material through which the nuclide diffuses acts as a holdup medium. If the half life of a nuclide is less than the time required to diffuse out of the medium, the fraction of the nuclides escaping will be small. An increase in temperature would reduce the time required to diffuse out of the medium, and thus the fractional release of a nuclide increases with temperature.

Fission products are also released from the UO_2 by the recoil of the fission fragments. Since the range of the fission fragments is established by the energy of these fragments, the fractional release of the fission fragments will depend only on the size of the UO_2 particles. As Fig. C.1 of App. C indicates, there is an incentive to go to large particle sizes (greater than 100 μ).

Release of Fission Products from Graphite

The release of fission products from graphite was estimated by the same method as that used for estimating the diffusion of fission products from UO_2. The analysis of the diffusion of fission products from graphite is given in detail in App. B. It was assumed that the source of the fission products which diffused through the graphite

was the recoil of fission products from UO_2. Further, because of the structure of the UO_2-graphite fuel, it was assumed that the recoil particles from the UO_2 were embedded in the graphite and therefore had to diffuse out of the graphite in the same manner that the fission fragments diffused out of the UO_2. Fission products which were released from the UO_2 by diffusion were not considered to be held up in the graphite but were assumed to diffuse almost instantaneously to the gas stream.

As in the case of diffusion from UO_2, in order to investigate diffusion of fission products from graphite, the diffusion coefficients as a function of temperature are required. Experimental investigations have been carried out by North American Aviation[3-6] to determine the diffusion of the various fission products from impregnated graphite. Although the fuel material for this study was assumed to be a mixture of UO_2 and graphite, the disposition of the fission products in the graphite was the same as in an impregnated fuel. Therefore, using the values of fractional release of a given fission product as a function of both time and temperature, it is possible to calculate a diffusion coefficient by applying the NAA data to the expression that relates the fractional release of a nuclide to the temperature, time, and particulate material. Equation (1) was used for these calculations, since the experiments were performed on long-lived nuclides. The resulting values of the diffusion coefficients for various fission products as a function of temperature are tabulated in Table B.1 of App. B and are shown in Fig. B.2 of App. B. It may be seen from the figure that the various fission products diffuse at various rates from graphite. It is of interest to note that the diffusion of fission products in graphite is not limited to the low-melting-point nuclides or to the gaseous fission products. The diffusion of cesium, bromine, and strontium occurs at a more rapid rate than the diffusion of xenon. Since there were no experimental data for the diffusion rate of krypton in graphite, it was assumed that the diffusion coefficient for krypton was the same as for xenon. Table B.1 of App. B indicates that most of the experimental data were obtained at temperatures appreciably above those of interest for this study. The curves shown in Fig. B.2 of App. B were obtained by a straight-line extrapolation of the higher temperature data. A comparison of the diffusion coefficients for fission products in graphite (Fig. B.2, App. B) with the diffusion coefficient of xenon and krypton in UO_2 (Fig. A.1, App. A) indicates that, in general, the diffusion

---

[3]L. B. Doyle, *High-Temperature Diffusion of Individual Fission Elements from Uranium Carbide–Impregnated Graphite*, NAA-SR-255 (Sept. 11, 1953).

[4]C. A. Smith and C. T. Young, *Diffusion of Fission Fragments from Uranium-Impregnated Graphite*, NAA-SR-72 (May 4, 1951).

[5]D. Cubicciotti, *The Diffusion of Xenon from Uranium Carbide–Impregnated Graphite at High Temperatures*, NAA-SR-194 (Oct. 13, 1952).

[6]C. T. Young and C. A. Smith, *Preliminary Experiments on Fission Product Diffusion from Uranium-Impregnated Graphite in the Range 1800°–2200° C*, NAA-SR-232 (March 25, 1953).

rates of fission products from graphite are more rapid. If the mechanism for diffusion of graphite changed at lower temperatures as it appears to for UO_2 and if the transition temperature were appreciably above 800°C, the extrapolation of the curves would tend to underestimate the activity release from graphite.

The values of diffusion coefficients given by Fig. B.2 of App. B, and Eq. (2), which takes into account the half life of the diffusing nuclei, were used to calculate the release of fission products from graphite. The results are presented in App. B. The study indicated, as in the case of diffusion of fission products from UO_2, that the activity release is strongly dependent on temperature and half life. Since only the temperature of the graphite may be altered in a design, it would be advantageous to maintain a low graphite temperature. Since the reason for using ceramic materials is to attain high temperatures, the release of fission products by diffusion from the graphite may be reduced by increasing the UO_2 particle size and by decreasing the temperature drop in the fuel element. This suggests that flat plates or tubes would be preferable to solid rods.

Total Activity Release from UO_2-Graphite Fuel

The activity to be expected in the gas stream by diffusion from UO_2 of the various important gamma-emitting nuclides is given in Table A.5 of App. A for temperatures of 1000, 1200, and 1400°C. These activities are due to an assumed power density of 1000 w/cm^3. The activity to be expected in the gas stream by diffusion of the nuclides from graphite at temperatures in the range of 800 to 1400°C is given in Table C.1 of App. C. As may be seen, the activity release is greatly influenced by the fuel temperature. In order to estimate the activity in the HGCR-1, the volume of fuel as a function of temperature was calculated;[7] some of these results are presented in Table C.3 of App. C. Based on the temperature structure in the HGCR-1 and an assumed UO_2 particle size of 200 μ, the activity in the coolant would be about 10^7 curies. Since the helium volume of the system would be approximately 5×10^9 cm^3, the specific activity in the system, assuming no purification system and no deposition, would be about 2000 μc/cm^3. The relative importance of the two methods of releasing activity to the coolant and the important nuclides that contribute to the total system activity are shown in Table 5. As may be seen, the results are quite dependent upon the assumptions made for the diffusion coefficients for fission products in UO_2. Even assuming that iodine, xenon, krypton, rubidium, bromine, and cesium diffuse at the same rate from UO_2, the resulting isotopic activity in the gas from this process (case II) is less than that from recoil and diffusion through the graphite (case I) for all elements except

[7] M. H. Fontana, *Fuel Element Temperature Distribution in the HGCR-1*, ORNL CF-58-12-3 (Dec. 1958).

Table 5. Activity Release from UO_2-Graphite Fuel

Case I: Fission products recoil from UO_2 into the graphite and then diffuse out of the graphite.

Case II: Fission products diffuse out of the UO_2 directly into the gas stream. The graphite does not act as a barrier to release.

Nuclide	Activity in Primary System (curies)		Dose Rate with 3.5 ft of Concrete (mr/hr)	
	Case I	Case II	Case I	Case II
Xe^{135}	3.86×10^5	2.78×10^5	1.15×10^{-6}	8.29×10^{-7}
Br^{84}	1.21×10^4	8.91×10^3	2.7×10^{-1}	1.99×10^{-1}
Br^{87}	2.20×10^3	3.07×10^2	3.83×10^{-1}	5.35×10^{-2}
Kr^{87}	9.15×10^4	3.66×10^4	3.69×10^{-1}	1.48×10^{-1}
Kr^{88}	1.82×10^5	5.76×10^4	1.05×10^0	3.33×10^{-1}
Rb^{88}	2.09×10^5	7.56×10^4	8.03×10^{-1}	2.91×10^{-1}
Rb^{89}	8.45×10^4	2.95×10^4	5.38×10^{-1}	1.87×10^{-1}
Y^{90}	6.57×10^5	1.73×10^4	2.76×10^{-4}	7.27×10^{-6}
Y^{91m}	2.08×10^5	9.68×10^3	9.36×10^{-6}	4.35×10^{-7}
Y^{91}	7.73×10^5	2.43×10^4	3.48×10^{-4}	1.09×10^{-5}
Y^{92}	2.82×10^5	8.83×10^4	1.73×10^{-1}	5.41×10^{-2}
Y^{93}	6.87×10^4	1.07×10^3	1.02×10^{-2}	1.59×10^{-4}
Y^{94}	3.11×10^4	5.76×10^2	1.31×10^{-2}	2.43×10^{-4}
Zr^{95}	2.43×10^3	2.96×10^4	1.39×10^{-6}	1.70×10^{-5}
Nb^{95}	2.43×10^3	2.96×10^4	1.97×10^{-6}	2.36×10^{-5}
I^{131}	5.11×10^3	3.75×10^5	8.57×10^{-8}	6.28×10^{-6}
I^{132}	1.04×10^4	5.95×10^4	4.27×10^{-3}	2.44×10^{-2}
Te^{133}	1.17×10^3	0	2.33×10^{-5}	0
I^{133}	4.88×10^3	2.91×10^5	2.04×10^{-5}	1.22×10^{-3}
I^{134}	2.51×10^3	5.84×10^5	2.11×10^{-3}	4.90×10^{-1}
I^{135}	6.28×10^2	1.33×10^5	5.40×10^{-4}	1.15×10^{-1}
Xe^{135m}	2.3×10^4	4.61×10^4	4.74×10^{-7}	9.51×10^{-7}
I^{136}	5.0×10^1	4.22×10^4	2.09×10^{-4}	1.77×10^{-1}
Ba^{137m}	5.14×10^5	1.07×10^6	9.24×10^{-5}	1.92×10^{-4}
Cs^{138}	2.16×10^5	5.72×10^4	9.01×10^{-1}	2.39×10^{-1}
Ba^{139}	1.28×10^5	2.58×10^4	1.24×10^{-2}	2.50×10^{-1}
La^{140}	6.47×10^5	9.18×10^3	1.12×10^0	1.59×10^{-2}
La^{141}	2.67×10^5	1.39×10^4	1.06×10^{-2}	5.51×10^{-4}
La^{142}	2.66×10^4	1.74×10^4	1.09×10^{-5}	7.14×10^{-6}
Ce^{143}	2.23×10^3	4.26×10^3	6.82×10^{-6}	1.31×10^{-5}

Table 5 (continued)

Nuclide	Activity in Primary System (curies)		Dose Rate with 3.5 ft of Concrete (mr/hr)	
	Case I	Case II	Case I	Case II
Ba^{140}	6.47×10^5	9.18×10^3	4.0×10^{-6}	5.68×10^{-8}
Sr^{91}	6.1×10^5	2.42×10^4	2.21×10^{-2}	8.77×10^{-4}
Te^{129}	1.63×10^3	0	7.34×10^{-6}	0
Te^{131}	3.41×10^2	0	2.45×10^{-6}	0
Total	6.1×10^6	3.45×10^6	5.68	2.58
Total case I and case II	9.55×10^6		8.26	

iodine. However, even on that basis, Table 5 indicates that the total activity released to the gas stream is not increased greatly by the contribution of the activity that diffuses from UO_2.

It should be pointed out that the relative importance of the release of activity by diffusion from UO_2 and by diffusion from the graphite depends upon the temperature in the fuel and the fuel element configuration, both of which are dependent upon the material and design proposed for various unclad-fuel reactors. Table 6 indicates the effect of varying the makeup of the fuel. For a gas-cooled reactor with a fuel matrix (fuel B in Table 6) such as that proposed for the HGCR-1, the activity in the coolant would be that shown in Table 5. Since the calculations for the 200-μ UO_2 particles resulted in a recoil release to the graphite of 3.5% for heavy nuclei and 4.5% for light nuclei, it would be expected that impregnated fuel (fuel A, Table 6) would release approximately 16 times as much activity (assuming that 65% of the fission products recoil into the graphite).[6] Since diffusion from the graphite would be the same as for the case of the matrix of UO_2 and graphite, the activity release from the graphite would be 16 times greater. On the other hand, the release from UO_2 by diffusion would be less, since there would be only about one-third of the fission products remaining to diffuse out.

The lumped fuel would release relatively little recoil activity, and therefore the activity would result principally from UO_2 diffusion. However, the use of large lumps of UO_2 would tend to increase the temperature in the UO_2 and would result in significantly higher activity release than indicated in Table 6 for fuel C.

Increasing the temperature of the three types of fuel would increase the activity release from each of the fuels. Since fission products tend to diffuse from graphite more readily than from UO_2, it would be expected that fuel A would be most sensitive to increased temperature and that fuel C would be least sensitive. For a given fuel

Table 6. Comparison of Activity Released from Various Types of Fuels for Same Temperature Structure

Fuel Type	Method of Fabrication	Diffusion of Activity from UO_2 (curies)	Diffusion of Recoil Activity from Graphite (curies)	Total Activity Released (curies)
A	Impregnation	1.2×10^6	97.6×10^6	98.8×10^6
B	HGCR-1 matrix and UO_2 and graphite (200-μ UO_2)	3.45×10^6	6.1×10^6	9.55×10^6
C	UO_2 clad with graphite	3.45×10^6	~ 0	3.45×10^6

surface temperature the relative release of activity from fuel B or C would depend upon the particle size of fuel B and upon the dimensions of the UO_2 in fuel C. An increase in the particle size from 200 to 2000 μ would essentially result in activity releases similar to those of fuel C without imposing the penalty of the increased temperature difference associated with fuel C.

DISPOSITION OF ACTIVITY IN PRIMARY SYSTEM

In addition to decay, the other possible processes for removing nuclides from the circulating gas are (1) deposition on primary surfaces, (2) leakage from the primary system, and (3) removal to a bypass purification system. There is insufficient experimental information available to predict deposition rates for removing the fission products. Since the leakage from the system must be minimized, this process for removal will not be significant. Most of the nuclides listed in Table 5 have sufficiently short half lives for a purification rate of the order of $\gg 1\%$ bypass to give significant reductions in activity during operation (see Fig. C.5, App. C). Since the problems and cost associated with handling such a large volume of gas would be excessive, the reduction of important gamma-emitting activity during operation by this process is impractical. The operation of the purification system would be important for reducing the activity of the long-lived nuclides. Although this would not significantly decrease the gross activity during operation, it might bring about large decreases in after-shutdown activity.

The purification system proposed for the HGCR-1 is similar to the system described for the GCR-2 (see Chap. 5). With a flow rate of 1% per hour, the reduction in the operating activity in the system would be only about 15% (see Fig. C.5, App. C), if the effect of deposition were neglected. However, with this flow rate and with the long-lived nuclides neglected, the La^{140} activity would be reduced by a factor of 5, and the Ba^{137} and Y^{90} activities would be essentially eliminated. The reduction or elimination of these long-lived activities would, of course, reduce the dose rate after shutdown quite significantly and would simplify the problems associated with maintenance.

The importance of the removal of activity by deposition would depend upon the rate and position at which deposition took place. Significant deposition would decrease the contamination leaking from the system and eventually released from the stack. Deposition would also decrease the problem of shielding if it occurred primarily in the core. However, preferential deposition in equipment could complicate maintenance and increase shielding requirements.

SHIELDING REQUIREMENTS FOR THE HGCR-1

An investigation of the amount of shielding of the HGCR-1 that would be required during reactor operation indicated that with 3.5 ft of concrete the dose rate would be 2.5 mr/hr. The important nuclides that contribute to the total dose rate are shown in Table 5. For the shielding calculations it was assumed that (1) no activity had been removed by the purification system, (2) all the activity in the primary system was concentrated in the heat exchanger, and (3) the system leakage was negligible. The plant layout and shielding costs, given in App. D, were based on the use of 3.5 ft of concrete and were for the case of diffusion of fission products from the graphite.

SHUTDOWN DOSE CALCULATIONS

In order to establish maintenance procedures for the major pieces of equipment in the HGCR-1 plant, it was necessary to estimate the dose rates that would prevail at the equipment after shutdown. Dose rate calculations (App. D) for the case of diffusion from the graphite indicated that the dose rate one day after shutdown would be primarily due to La^{140}. After about three months the dose rate would be due to Y^{90} and Ba^{137m}. Since the dose rate from La^{140} and Y^{90} due to direct diffusion from the UO_2 is negligible (see Table 5), the results shown in App. D (which are based upon case I) indicate the dose rates that could be expected for various times after shutdown. Figure D.5 of App. D indicates that it would be possible to do direct maintenance on the steam generators 100 days after reactor shutdown and that the dose rate would be about 200 mr/hr. As pointed out previously, the use of a bypass purification system could be quite effective for removing long-lived activity if it were competitive with the deposition rate. Since deposition rates are unknown it is impossible to predict what reduction in long-lived activity could be possible or what methods would be most promising. The possibility of decontaminating equipment prior to maintenance work also offers a means of reducing the time required to attain a reasonable dose rate.

CONTAINMENT REQUIREMENTS

The necessity of making special provisions for containing radioactivity depends to a large extent upon the hazards associated with a particular type of reactor. In order to prevent the escape of radioactivity from the reactor area it is necessary to have two independent barriers. The GCR-2 reactor satisfied the containment requirements, since

the stainless-steel-clad material on the fuel elements was in effect the first barrier, and the primary system was the second barrier. Preliminary studies had indicated that these two barriers were sufficiently independent, so the conditions for penetrating both barriers and releasing large amounts of radioactivity as a consequence of a single failure were improbable. Therefore, no containment vessel was provided for the GCR-2.

The elimination of the fuel element cladding material, as in the HGCR-1 design, places the reactor in the category of contaminated coolant systems, since the release of fission products to the primary system would be about 10^7 curies. The hazards associated with releasing this amount of activity to the atmosphere in the event of a failure of the primary system would make it necessary to provide a containment vessel around the primary system. Since the possibility of penetrating both the primary system and the containment vessel simultaneously seems unlikely, the HGCR-1 system with a containment vessel should be at least as safe as the GCR-2.

Activity due to minor leakage from the primary system would be controlled inside the containment vessel by directing air through the cells containing the equipment in the primary system. This air would be monitored and sent to a cleanup system before being recycled within the containment vessel.

The diameter of the sphere containing the primary system was established as 220 ft. Such a vessel would be more than large enough to accommodate the release of fluid from the primary system and one loop of the steam system in the event of a rupture in the gas system. The pressure buildup in the sphere following such an incident would be only a few pounds per square inch. The diameter of the sphere was determined by the plant layout. Since maintenance on contaminated systems must be done remotely or semiremotely, the location of equipment was determined by maintenance procedures, not by attempting to obtain the most compact reactor complex. The thickness of the containment sphere would be determined by the thickness required to carry its normal structural dead and live loads. The pressure rise would not add an appreciable stress to the sphere.

8. INSTRUMENTATION, CONTROLS, AND OPERATION

No new work was done in connection with instrumentation and controls, and, with but few significant exceptions, the instrumentation and controls, as well as the operating procedures for the contaminated gas-cooled reactor systems, would be similar to those for the GCR-2.[1] Operations that would involve maintenance, which would be considerably more difficult with the contaminated system, are discussed in Chap. 9.

The instrumentation would be similar to that of the GCR-2, except for the omission of the fuel element leak-detection system and the more extensive nuclear instrumentation, temperature measuring devices, and radiation monitors throughout the plant. Instrumentation costs would be higher than for the GCR-2 because of the additional cost of penetration through the containment vessel, as well as the cost of running the instrumentation leads through a coaxial duct. It is anticipated that the additional nuclear instrumentation would be required to minimize the problems associated with xenon tilt in a large graphite reactor.

The stainless-steel-clad silver control rods employed in the GCR-2 might have to be modified to a cruciform shape in order to provide adequate control, but they would be compatible with the higher operating temperature. The canned control rod drive units would, of course, be even more essential with a contaminated system. Sufficient control rods would have to be provided so that failure of the drive mechanism in one or more rods would not require a shutdown. The repair work could thus be accomplished during a scheduled shutdown.

The operational criteria for this reactor would be the same as for the GCR-2, with added incentive for not subjecting the reactor to temperature transients which might be expected to have an important bearing on fission-product release. The steam generators would be the once-through type in which the boiler-feedwater flow would be controlled by the steam pressure which would be regulated by the turbogenerator speed, that is, the load.

The reactor is designed for operation with a fixed temperature gradient, and the power output would be controlled by bypassing a portion of the gas flow around the reactor. The fraction of the flow bypassed would be determined by the reactor inlet temperature; a control rod operating on a servo mechanism would maintain the reactor outlet temperature at the design value.

All continuously manned stations associated with the plant, that is, control rooms, shops, etc., would be located outside the containment vessel. However, to prohibit all access to the containment vessel during operation would be unrealistic, since it is quite conceivable that it would be advantageous to enter the vessel through appropriate locks for inspection and maintenance.

---

[1] *The ORNL Gas-Cooled Reactor*, ORNL-2500, pt 3 (April 1, 1958).

9. MAINTENANCE

In dealing with the problems of servicing contaminated systems, such as reactors, fuel reprocessing plants, or radiation laboratories, five basic schemes for such work may be considered. The five schemes are listed below in the order of cost in terms of capital investment in maintenance facilities, with the lower numbered techniques being the least expensive:

1. servicing by contact without decontamination,
2. servicing by contact after decontamination,
3. servicing in place with remotely controlled devices,
4. replacing with remotely controlled devices, rather than servicing,
5. using built-in spares, rather than servicing.

Of course, combinations of these methods could also be used. Each of the five basic methods was considered in order to arrive at a servicing scheme for the HGCR-1.

The activity level throughout the HGCR-1 was assumed to be sufficiently high during operation and immediately after shutdown (see Chap. 7) to preclude the use of contact servicing without decontamination, except in a few isolated instances. On the other hand, the techniques 2 through 5 are each theoretically capable of providing the means of effecting the desired maintenance. The ultimate selection of a specific technique for a particular failure must be made on the basis of an economic study which takes into account the cost of maintenance equipment and facilities, the cost of down time, and the probable number of failures. In lieu of adequate data upon which to base such an analysis, an intuitive criterion of selecting a maintenance scheme was employed, that is, minimum shutdown time. While this might seem to be somewhat arbitrary, the cost of shutdown time (~$7500 per hour) provides such a big incentive that this seems reasonable as a first approach.

In any of the maintenance work involving the primary system, the containment of gaseous and particulate activity and the provision for shielding from radiation are important problems. It is intended that air flow within the containment vessel be controlled so that all flow will be from areas of low contamination to areas of higher contamination. In this way the spread of contaminated gases, dusts, etc., would be controlled.

The cubicles surrounding each of the blowers and motors, the fuel charge–discharge area above the reactor, the helium purification system, and the spent fuel discharge chute are areas where contamination could exist. The whole containment vessel would have to be treated as a "hot" area, and a change room would be required at the entrance portal, since, if the system were opened, contamination could be spread by parts being handled. Air-conditioning equipment to cool the air within the containment cell and to accommodate heat loss from the reactor would be needed, as well as a cleanup system to remove airborne contaminants.

The suitability of one of the above maintenance schemes for a particular maintenance function on contaminated equipment is a function of the state of the several arts and techniques suitable for a particular servicing method. Accordingly, before discussing in more detail the proposed technique for performing maintenance on the various components, it is appropriate to review the status of the techniques.

MAINTENANCE TECHNIQUES AND PROBLEMS

Contact Servicing Without Decontamination

Where radiation levels are sufficiently low (that is, <200 mr/hr) and the operation will be of such a short duration that installation of elaborate equipment is not justified, contact maintenance work can be done without decontamination of the equipment. With respect to HGCR-1, it was felt that the activity levels, the massiveness of the equipment, and the economics of maintaining on-stream efficiency precluded contact servicing in most instances. The most notable exception in the HGCR-1 would be the work required to plug a steam generator tube at the header. The headers would be external to the secondary system shielding, and could be approached for servicing after the reactor had been shut down.

Contact Servicing After Decontamination

Decontamination is usually carried out by spraying or rinsing with suitable liquids which wash away most of the contamination. In liquid systems it may involve replacing the process fluid with a decontaminant, which is then circulated. This technique results in better decontamination than the spraying, but it is not practical for the large equipment used in gas-cooled reactors.

Decontamination factors of the order of 2 to several thousand have been obtained under carefully controlled laboratory conditions in which contaminated stainless steel was suspended in several different decontaminating solutions for periods up to several weeks.[1] However, in the decontamination of an actual system, such as the HRT, the attainable decontamination factors were only 22 to 25 (including decay) after treatment with a number of solutions but without descaling the system.[2] It was reported, however, that removal of the corrosion film would have given an additional decontamination factor of about 100. While it may be suspected that the activity in a gas-cooled system would not be as tightly bound to the metal surface, this potential advantage may be offset by the difficulty in flushing the contaminated surfaces in a large gas system.

The decontamination factors cited above apply to stainless steel systems. The factors allowable with other metal surfaces, such as the low-alloy steels, are less than

[1] D. O. Campbell, *Decontamination of Stainless Steel*, ORNL-1826 (March 2, 1955).

[2] D. O. Campbell, *Decontamination of the Homogeneous Reactor Experiment*, ORNL-1839 (June 12, 1956).

for stainless steels, which not only have a low affinity for activity but also a low corrosion rate.[3]

The activity level of long-lived contaminants in the HGCR-1 (assuming the purification system is unable to reduce this activity) means that decontamination must be employed if direct maintenance is to be used. Considerations of the problems associated with achieving the desired decontamination factors and with ensuring removal of the fluid used for decontaminating the system, as well as the involved and expensive procedures associated with even a minor repair, lead to the conclusion that decontamination will not be economical with equipment as large and complicated as the steam generator and helium blower units.

Remote Servicing in Place

In order to make repairs on contaminated equipment in place, remotely controlled servicing and viewing equipment would be required. In the HGCR-1, the equipment would be so large and cleanliness requirements so rigid that in-place maintenance would not only require an expensive array of servicing equipment, but it would also involve shutdowns of longer duration than could be justified.

A special technique for effecting in-place maintenance was adopted for the Homogeneous Reactor Test in which the cell containing the equipment to be serviced is flooded with water and the required maintenance is performed from above the water using long-handled tools.[4] While this technique may have merit for liquid systems (even though it was considered and rejected for use in the PAR),[5] it is apparent that it would be unsuitable for large gas systems, particularly in systems such as the HGCR-1 in which it would be important not to expose the graphite to moisture.

If the repair work or equipment replacement required welding, there would be the further problem of inspecting the weld in the radiation field. Section UW2 of the ASME Unfired Pressure Vessel Code, 1956 edition, requires that "all longitudinal and circumferential joints of vessels that are to contain lethal substances, either liquid or gaseous, shall be of the double-welded, butt-type or its equivalent, and shall be fully radiographed"; furthermore, "when fabricated of carbon or low-alloy steel, such vessels shall be stress relieved." The problems associated with full radiography of the reactor system are many. Section UW12 of the Code permits a weld joint efficiency of 95% for radiographed and thermally stress-relieved vessels, and 85% for vessels which are only

---

[3] F. N. Browder, *Summary of Surface Decontamination Experience at ORNL*, ORNL-158 (Aug. 20, 1948).

[4] S. E. Beall and R. W. Jurgensen, *Direct Maintenance Practices for the Homogeneous Reactor Test*, ORNL CF-58-4-101 (April 18, 1958).

[5] W. E. Johnson *et al.*, *Design Considerations for the Pennsylvania Advanced Reactor Slurry Homogeneous Plant*, 1958 Geneva Conference Paper No. 2356.

thermally stress-relieved. If a pipeline were to require repair due to the loss of an expansion joint, it is conceivable that the activity level at the surface of the pipe to be welded might be high enough to interfere with the radiography of the repaired joint. If such were the case, according to the present code the allowable pressure for the system would have to be decreased. This would, of course, affect plant efficiency and capacity. To accommodate this situation in a highly contaminated plant such as the HGCR-1, it might be necessary to design all pressure-containing equipment with the reduced weld joint efficiency of 85%. This would, of course, increase plant costs considerably. It would seem desirable that the Code Committee be requested to study this situation and provide clarification. It may be that alternate testing methods such as ultrasonics or proof-testing could be substituted for radiography.

Remote Replacement

Remote servicing and viewing equipment would be required to remove a unit from the operating system and replace it with a spare unit. The damaged equipment could then be repaired in a separate hot cell after the plant was back in operation. The virtue of this technique is that operation could be resumed without waiting for repair of the failed item. The failed unit could be discarded or repaired. This technique is recommended for the HGCR-1 for maintenance of blowers, motors, and valves.

A significant modification of this technique would be to decontaminate the component after having removed it to the special hot cell for repair. In this manner the component could possibly be cleaned up sufficiently to permit direct-contact servicing; but even if the activity level were not reduced to this extent, the subsequent servicing, reinstallation, and contamination control would have improved by the extent to which the activity level had been reduced. A disadvantage of decontamination is the problem of assuring that all decontaminating material is removed from the equipment.

Built-In Spare Equipment

A system in which the cost of individual components is low and value of on-stream time is high could be economically equipped with built-in spares. Valves would be required that would be actuated by failure of a piece of equipment and would rapidly place a new unit on stream. Because of the high cost of the major HGCR-1 components and the lack of reliable valves to isolate spare units, it is intended that this scheme be used only for the purification system. However, even in this instance, it would be expected that the failed item would eventually be removed, repaired, and replaced by remote control.

MAINTENANCE OF SPECIFIC COMPONENTS

Maintenance Philosophy

From the above considerations it may be seen that no single servicing scheme would suffice for the HGCR-1 and that the servicing of each component in which trouble might be expected would have to be accomplished in the most appropriate manner. In order to evaluate the maintenance problems associated with the reactor, it would first be necessary to evaluate the types of failures expected and then to decide what equipment and/or techniques may be advantageously provided to effect the anticipated maintenance. Any failure in the reactor core (which could not be repaired through the charge nozzles), reactor vessel, main coolant piping (within the reactor shield), or steam generator shell is so improbable that to provide in advance a means of coping with the different possible failures of these components would not be justified. This means that, should failure occur in one of these items, it would be handled by methods improvised at the time. The failure of all other components was considered as being sufficiently probable that advance provisions should be made for maintenance.

In all instances in which the maintenance was to be performed by remote replacement of the failed component, the equipment would be positioned so that it could be conveniently removed from above by remotely operated equipment. The failed component would be removed and replaced by a spare unit. The failed component would then be removed to the "hot" shop outside the containment vessel where it could be repaired, if practicable.

In all maintenance operations involving cutting into the main system piping, such as replacing an expansion joint, the reactor would not only have to be shut down and cooled, but after adequate cooling the fuel elements would have to be removed from the core. The contaminated helium would then be evacuated to the contaminated helium storage tanks and the system pressure raised to slightly below atmospheric pressure with clean helium. The necessary cuts could then be made using remote maintenance equipment and the defective unit could be replaced.

The required equipment for these remote operations does not exist, although equipment is being developed at several installations.[5,6] In view of the current state of the development, it is not possible to assign accurate cost figures to this equipment, but liberal sums have been allocated in both HGCR-1 capital and operating costs for maintenance and maintenance tools.

Fuel Element Failure

The fuel element in this reactor system would be particularly insensitive to the type of failure normally associated with reactor fuel elements, that is, cladding defects

[6] *Molten Salt Reactor Program Quarterly Progress Report for Period Ending June 30, 1958*, ORNL-2551 (Sept. 24, 1958).

that result in the loss of fission products. The fuel would have no cladding to become defective, and the UO_2-graphite matrix would be insensitive to the possible hot spots which could exist in the reactor core. Failures of the fuel element would, in general, be mechanical failures that would cause elements to become jammed or otherwise unremovable from a fuel channel. In view of the large size of the reactor, a fuel element could become stuck without seriously impairing the reactivity, although it would be desirable to be able to remove the element. If an element could not be extracted by the fuel-handling machine, that channel would be "abandoned" until a major shutdown occurred. The element could then be drilled out of the channel. The chips and particulate matter which would result from the drilling would be removed from the core through a vacuum-cleaning system.

Although the fuel-handling machine has not been designed, it is felt that it should not differ markedly from other on-stream fuel-handling machines. It would probably be desirable to incorporate the service functions described above in connection with drilling jammed fuel elements into a separate machine that would have sufficient flexibility to perform other in-pile functions of probable interest, that is, handling, control rods, television equipment, instrumentation, etc.

Steam Generator

The only failure postulated for a steam generator component for which repairs would be attempted is the locating and plugging of a leaking tube. A tube failure is considered to be the most probable failure, and therefore equipment and techniques for tube plugging would have to be developed. As shown in Fig. 1, the steam generator tubes are brought through the concrete shielding. In this position the direct radiation dose from the nearby contaminated equipment does not preclude the use of direct-maintenance techniques in locating and plugging off the defective tube. However, the leak connects the contaminated primary system to the steam system so that once the steam header flange is removed, the surrounding environment is "open" to the primary system. Accordingly, the primary system pressure would be reduced to slightly below atmospheric (and the steam system drained) before the steam system would be opened. The system pressure would also be a few pounds per square inch below the steam pressure at all times during pressure letdown.

The seal welds on the header flanges would be manually ground off and the flanges on both steam and water headers removed. Each tube would then be plugged at both ends and tested for leaks. This could be done either manually (by personnel with adequate protective clothing) or remotely (using machines especially developed for this purpose).

The leak would be located by plugging the tube and noting the pressure drop. With the leaking tube located, it would be isolated rather than repaired. The defective tube

could be plugged within the header or cut and capped external to the header. At present the latter technique appears to be the more expeditious. The water and steam header flanges could then be reinstalled and seal-welded. The air which would leak into the gas system during maintenance would be removed; the helium pressure would be raised to normal; the steam system would be filled; and plant operation would be resumed.

Blower and Blower Motor

Two methods of installing the blower-motor combination are possible. In one the equipment would be enclosed within a welded pressure vessel, while in the other the blower would have a shaft seal and the motor would be mounted conventionally. With the former scheme, the entire pressure vessel containing the blower and motor would be changed if a repair were to be made. The latter technique would permit servicing of the motor without "cutting" into the contaminated primary system. Much of the information required to choose intelligently between these two techniques is not available; for example, the required seals have not been developed; the contamination level is not known; and remote welding techniques are in a rudimentary stage. Accordingly, in the HGCR-1 design the blower and motor are enclosed in a pressure vessel in the belief that this represents the more conservative approach.

Any failure would require that this unit be replaced. Roof plugs have been provided over the blower-motor cubicle and a viewing window located in the wall for this operation. The unit would first be cut out of the system remotely, and a new unit would be placed in its stead. The piping joint would then be remotely prepared, welded, and inspected.

Were the motor to be externally mounted and a shaft seal employed, a labyrinth type of seal with a planned leakage would be preferred. The leakage would enter a plenum chamber from which it would pass to the helium purification system. After purification and decontamination, the helium would be pumped back to the main stream. A bleed flow of clean helium would be used to seal the outboard seal of the plenum chamber. The outflow to atmosphere from this seal would be vented to the stack and the small helium losses would be made up through the seal in the blower of the helium purification system.

Valves

The butterfly valves which control the helium flow and provide the blower bypass control are also located within the blower-motor cubicle. The actuators for these valves would be in a welded tank and mounted on the valve with a seal-welded flange.

The manipulator within the cubicle would be used to remove the actuator should trouble develop. The valves would not be expected to give trouble, since they would

not be required to shut tight. They could be cut out of the line, however, and replaced if trouble should occur. The device for doing this would be the same as that which would perform the similar function for the blower-motor units.

Piping System

The high activity level (2000 $\mu c/cm^3$) in the circulating gas would preclude direct maintenance work on the ducting after the plant had operated for a few weeks. However, it is not expected that any maintenance or repair of the main coolant piping would be required. The only items which would be likely to fail would be the system expansion bellows. Adequate space would be provided around these units to permit their repair by removing the section of pipe containing them and replacing it with a spare section. A failure of any of this equipment would be a major one, and considerable time would be required in which to accomplish repairs. Viewing and remotely operated equipment would be brought in to accomplish this operation.

Helium Purification System

Spare helium purification equipment would be provided so that in the event a unit failed it could be valved off and the spare unit employed. If there were a multiplicity of failures, the purification system would be shut down and repairs accomplished. Because small lines and low temperatures would be involved, it is felt that tight valves could be obtained which would permit repair of this system without shutting the plant down. Such repairs would have to be completed with remotely operated equipment. The system would be designed to permit access from above to planned cutoff points. Because this system is designed, in part, to contain liquids and heavy concentrations of water vapor, decontamination might prove advantageous. However, since the purification system has the function of removing activity (mostly long-lived activity), the amount of contamination in this system would probably exceed that associated with other equipment. In any event, repairs to this system are expected to be such that normally they could be handled during a scheduled plant shutdown.

Helium Storage and Vent System

The clean helium storage system would be maintained directly since it would not be contaminated. The amount of contamination in the contaminated helium storage system has not been thoroughly investigated, but it is expected that the activity level would not be as high as that associated with the other equipment. However, some remote or semiremote maintenance expense has been included. Valving should permit necessary maintenance to be accomplished with the reactor plant operating. It is expected that valve replacement would be the most frequent problem in this system. System layout will facilitate access to valves and other equipment from above. Any air that got into

the storage system or the purification system during repair work would be removed by the evacuation equipment before reconnection of the system to the main coolant stream.

Fuel Storage Heat Removal Equipment

Before fuel was transferred to the fuel storage area it would be cooled in the reactor charge machine. The activity released at the lower temperature, as discussed in Chap. 7, would be considerably less than during operation in the reactor. The cooled element would be placed in a container and transferred to the storage area. The container actually would be part of the storage equipment, and air flow would be relied upon to keep the element cool during transit and in storage. In the storage area, air would be blown over the spent elements to keep them cool. The air would then pass to a cleanup system and a water-cooled coil before it returned to the circulator. All equipment would be shielded, and remote manipulators and viewing equipment would be provided. A small stream of air would be introduced into this room from the cell ambient through the transfer tunnel and vented to the stack to dilute the room air and reduce any tendency for gaseous activity to build up. The discharge to the stack would have to be equipped with valves which would close and seal in the event of a rupture of the primary system.

10. COST ANALYSIS

CAPITAL COSTS

The cost estimates for the GCR-2 were used as the basis for estimating the HGCR-1 costs, since the cost basis for the GCR-2 was evolved after considerable detailed design and extensive contacts with equipment vendors. The costs of HGCR-1 components, when only preliminary designs were available, were assumed to be the same as for similar GCR-2 components, but they were supplemented by greater contingency factors. Vendors were not contacted for most items, since it was felt that neither time nor the preliminary nature of the design would permit the vendors to provide meaningful numbers. This rather preliminary study was intended to evaluate the potential worth of a system of this type and to obtain some idea of the economic feasibility of the system when the rather serious operating and maintenance problems were considered. It was felt that if this cursory look indicated that an unclad fuel element system of large power output would be as economical as, or more economical than, a clad-element system, then a more detailed study would be justified.

Steam Generator

The steam generator shells of the HGCR-1 would be 6 ft shorter and 1 ft larger in diameter than those of the GCR-2. The same material of construction would be used as for the GCR-2 generators. The larger diameter would cause an increase in the HGCR-1 shell cost over that for the GCR-2 of a factor[1] of 7300/6300 = 1.16 per foot of length, which would be partially offset by a factor of 54/60 = 0.9 to take into account the decrease in length from 60 to 54 ft. The tube headers on the GCR-2 design were inside the shell, while on the HGCR-1 they would be external, but recent information indicates that there should be no significant difference in cost between the two arrangements. Changes in length of tubing used result in the following factors:[2]

Economizer $\frac{26,820}{25,100} = 1.07$

Boiler $\frac{22,830}{28,400} = 0.803$

Superheater $\frac{16,100}{25,300} = 0.637$

The change from T-12 chromium-molybdenum tubing to T-11 chromium-molybdenum would modify the cost of the superheater tubing by a factor of 4.3. The final factor on the

[1] *The ORNL Gas-Cooled Reactor*, ORNL-2500, pt 3, Fig. 9.10 (April 1, 1958).

[2] *The ORNL Gas-Cooled Reactor*, ORNL-2500, sec 6.4, Table 6.2 (April 1, 1958).

superheater tubing would then be:

$$4.3 \times 0.637 = 2.74 \ .$$

These factors would then be applied to the GCR-2 cost estimates[3] as follows:

Component	GCR-2 Costs	Factor Increase	HGCR-1 Costs
Shells and heads	$ 532,800	1.16 × 0.9	$ 550,000
Superheater tubing	150,400	2.74	412,000
Boiler tubing	235,100	0.803	189,000
Economizer tubing	211,200	1.07	226,000
Total	$1,369,400		$1,621,900

This indicates a factor of 1.185 (1,621,900/1,369,400) increase in cost for a single steam generator. Recent information from boiler vendors indicates that the GCR-2 steam generator estimate was low by a factor of 1.33 (ref 4). It follows then that the cost of the eight HGCR-1 steam generators would be 1.185 × 1.33 × 8 × 1,369,400 = $17,250,000.

Valves

Valving for the HGCR-1 is the same as for the GCR-2, with the same line sizes and approximate temperatures. Since it has been assumed that the unit valve costs would be the same and there are twice the number of systems in the HGCR-1, the valve costs would be 86 000 × 2 = $172,000 (ref 5). To this, $21,500 was added to provide for one set of spares. The total valve cost would therefore be $193,500. No credit was taken for a probable decrease in unit costs with an increase in the number of units.

Expansion Joints

The expansion joints for the cold lines would be similar to those for GCR-2. Some of the cold lines would be concentric about hot lines, however, and the joints would be larger than those used for GCR-2. The effective cross section of the larger diameter pipe would require extremely heavy reinforcing of the wall to transmit the end thrust across pinned joints. The assumption was made that the cost of these joints would vary as the square of the diameter,[5] and therefore

$$\text{cost} = \frac{(84)^2}{(60)^2} 100{,}000 = \$196{,}000 \ .$$

---

[3] *The ORNL Gas-Cooled Reactor*, ORNL-2500, pt 4 (April 1, 1958).

[4] TVA Staff, *Gas-Cooled Nuclear Power Reactor Review* (unpublished).

[5] *The ORNL Gas-Cooled Reactor*, ORNL-2500, pt 4, p 11.7 (April 1, 1958).

The hot joints are a major unknown. It was assumed that because of the higher temperature these costs would be the same as for the GCR-2 hot joints, even though they would be smaller and would operate at much lower pressure differentials. Since there would be twice as many joints in the HGCR-1, the total cost for joints would be:

$$(132{,}000 \times 2) + (196{,}000 \times 2) = \$656{,}000 \quad .$$

An allowance of 12.5% for spares to permit expansion joint replacement would bring the total cost to $738,000.

Piping

Piping systems of this type with doubly insulated, concentric pipes are quite sensitive to fabrication and installation costs. Installation costs are considered to include all labor and materials for the installation and any hangers or supports required for the piping. One fabricator has estimated that for carbon steel piping 24 in. and below, field erection costs would be approximately 95% of fabricated pipe cost. The same fabricator indicates that for stainless steel piping the field erection cost would be lower, being closer to 65%, because of the high material cost for the stainless steel. Even if stainless steel piping were employed for the inner hot pipe, it would require external insulation to minimize the heat loss to the cooler annulus gas. Since the insulation problem cannot be avoided and techniques for the installation of contained insulation in cylindrical ducts are well developed, insulated chromium-molybdenum steel was used for estimating the cost of the hot inner pipe.[6] For the cold lines, carbon steel costs were used. A fabricated piping cost of

$$68 \times 8 \times 580 = \$315{,}000 \text{ for 60-in. cold pipe,}$$
$$48 \times 8 \times 180 = \$69{,}000 \text{ for 30-in. cold pipe,}$$
$$64 \times 8 \times 1000 = \$512{,}000 \text{ for 60-in. hot pipe,}$$
$$64 \times 8 \times 1080 = \$552{,}000 \text{ for 84-in. cold pipe,}$$

or a total of $1,448,000, was thus obtained. It was assumed that for these larger pipes, the installation cost would be 75% of the pipe fabrication cost, or $1,078,600, for a total installed cost of $2,526,600. To this would be added 20% of the installed cost for the 60-in. hot line to allow for the internal insulation, or $102,400. The final piping cost would be $2,629,000.

Neutron Curtain and Shield Cooling

No calculations were made to check the required thickness of the neutron shield, but it was felt that because of the higher power level the thickness and weight would increase. A factor of approximately 2 was chosen to give a cost of $75,000.

---

[6] *Ibid.*, Fig. 11.2.

Since the shield cooling required is related to the number of shielded enclosures, which would be doubled, the shield cooling cost was increased to $100,000.

Reactor Pressure Vessel, Including Supports

The HGCR-1 reactor pressure vessel would be the same size as the pressure vessel for the GCR-2. However, the outlet gas temperature would be higher, more gas nozzles would be required, and the vessel would have to be erected within the containment cell; therefore the cost estimate was increased by 50% to $3,500,000.

Fuel-Handling Costs

No detailed study was made of the fuel-handling equipment. It was felt that dry fuel storage could be accomplished at the same cost as wet storage. The fuel element charge machine and associated auxiliaries would be essentially the same as for the GCR-2, except for modifications to permit remote operation and on-stream loading. An allowance of 10% has been added to cover such changes. The cost allowed for the charge machine was then doubled to provide for a service machine to perform maintenance functions. The cost breakdown is shown in Table 7, which may be compared with data in Table 11.7, p 11.13, of the GCR-2 study.[6]

Helium Gas System

Two sets of helium storage and pumping equipment would be required for HGCR-1. One set would handle only clean helium which had not been through the reactor, and the other set would be used when contaminated helium had to be handled. Provision would be made to permit venting of either system to the stack. To provide for this dual system, the GCR-2 gas storage system costs were doubled.

Although the helium inventory in the HGCR-1 would be only 1.78 times that of the GCR-2, the capacity of the helium purification equipment was doubled for cost estimating. This was done to provide for equipment to ensure continuous operation. It is also felt that increased flow through this system would be desirable in the removal of activity which diffused from elements.

Helium Blowers and Motors

The blowers for the HGCR-1 would be the same size as those for the GCR-2, with changes as necessary in the blower blades to allow for the increased flow. Since twice as many blowers and motors would be used, the cost was doubled. A correction factor[7] of 1.5 was then added to account for the horsepower increasing from 6000 to 9000. The blower-motor cost would then be 3 times the GCR-2 blower-motor cost. In addition, one spare blower-motor set was provided to permit replacement of a failed unit.

---

[7] *Westinghouse Catalog Price List No. 3125*, p 5, April 2, 1958.

Instruments and Controls

In general, instrumentation costs were doubled. This was done because the number of units to be controlled in the HGCR-1 would be about twice that in GCR-2. Where units would not be added, as in the case of the reactor, it was felt that the additional complications resulting from the contaminated coolant would double the cost of instrumentation for these units. Since no fuel cladding would be used, the leak detection system of GCR-2 was eliminated from the costs, but, in its place, $150,000 was included for detecting leaks in the piping system or vessels. This would consist of equipment to locate leaks detected by sampling the air between the piping and the concrete. Because the containment cell separates the reactor system from the control room, an allowance of $1,000,000 is arbitrarily added to instrument costs to cover telemonitoring of instrument information and television signals.

Miscellaneous Laboratory Equipment

Because of the contaminated coolant it is felt that additional laboratory equipment and space would be required in conjunction with plant operation. For this reason the GCR-2 estimate was doubled.

Remote Maintenance Equipment

In addition to the standard items of maintenance equipment required by a plant of this size, various items would be required to permit remote maintenance work on the components. A General Mills type of manipulator would cost from $50,000 to $75,000, depending upon the trolley and telescoping scheme used for moving it to the point of operation.[8] Television equipment for viewing what the manipulator was doing could cost another $15,000. If television were not used, viewing windows which would restrict the work location would be required, and therefore television for use in HGCR-1 maintenance was included in the costs.

If defective equipment is to be removed from the operating system and sent to a hot cell for repair, the cost of the hot cell must be included. The cost, $175,000, of a hot cell constructed for the Oak Ridge Research Reactor (ORR),[9] approximately 10 ft square and 12 ft high, was used as a basis for estimating the cost of necessary remote maintenance equipment for the HGCR-1. It was assumed that a motor-blower set would be the largest item of equipment which might have to be disassembled or repaired in the hot cell. This unit would be approximately 12 ft in diameter and 24 ft long. To be able to work on such a unit with remotely controlled manipulators in a hot cell would require a cell at

---

[8] Personal communication from C. A. Mills to V. J. Kelleghan, Nov. 1958.

[9] T. E. Cole and J. A. Cox, *Design and Operation of the ORR*, 1958 Geneva Conference Paper No. 420.

least 40 ft × 32 ft × 20 ft high. Based on the ORR cell cost of $155 per cubic foot, the large cell would cost approximately $4,000,000 if the cost per unit volume were the same. Equipment for this cell, which would include a manipulator and other tools, was estimated to cost $400,000.

The removal of a motor-blower set would require a remote manipulator within the motor-blower cell or a remotely placeable and operable pipe-cutting and welding mechanism. Present work at ORNL on welding with remote manipulators indicates that such cutting and welding may be possible. In order to estimate a dollar value for this operation it was assumed that one manipulator and television system would be available for each motor-blower cubicle, along with one portable manipulator that could be placed as needed in any cell. This would be equivalent to a two-armed man able to work in the radiation field. It was also presumed that welding with remote manipulators would be feasible by the time required, so the cost of a remote welding machine was not included. This would mean a cost of

$$9 \times 75{,}000 = \$675{,}000 \text{ for manipulators,}$$
$$8 \times 15{,}000 = \$120{,}000 \text{ for television equipment .}$$

Additional tools and fixtures to be used by the manipulators were assumed to cost $200,000 to give a total cost of all this equipment of $1,000,000. In order to provide some margin in the event special tools were required, the estimate was then doubled.

Remote manipulators would be required for operation of the pumping equipment for handling the contaminated helium and for the helium purification systems. For estimating purposes it was assumed that one manipulator would be used in the contaminated helium storage area and one in each of the two helium purification systems. This amounts to an allowance of $500,000.

Thus the total capital charge to remote maintenance equipment is as follows:

Hot cell	$4,000,000
Hot cell tools	400,000
Remote tools and viewing equipment (in primary system cells)	2,000,000
Remote tools and viewing equipment (in auxiliary equipment cells)	500,000
Total	$6,900,000

Containment Vessel

The cost of the containment vessel is comprised of the cost of the foundation for the sphere and the spherical shell itself. It is estimated that the foundation would require about 16,200 yd^3 at $60 per cubic yard, or $972,000. The vessel cost was obtained by

extrapolating a Chicago Bridge and Iron Company estimate for two spheres, 200 ft and 210 ft in diameter, to obtain an estimate for the 220-ft-dia containment vessel for the HGCR-1. This gave a cost of $2,900,000 for the vessel. Costs for cooling and filtering the cell ambient air were then added, as well as the costs of providing access and venting. It was assumed that these added costs would be $250,000, and thus the total cell cost would be $4,122,000.

Steam Plant Equipment

The steam plant equipment for the HGCR-1 has not been studied. Without a design, it was felt that the capacity ratio to the 0.6 power times the GCR-2 cost[10] might give a reasonable estimate. For the HGCR-1, this factor is

$$\left(\frac{1130}{225}\right)^{0.6} = 2.64 \ .$$

Accordingly, the GCR-2 steam plant costs were multiplied by this factor to arrive at the steam plant costs for the HGCR-1.

Turbine and Electrical Equipment

It was assumed that the cost of the turbines and other electrical auxiliary equipment would vary directly with the power level.[11]

Moderator and Reflector

The estimate of the cost of fabrication of the graphite moderator and reflector was evaluated in the following manner. The material cost was based on the use of National Carbon Company TSF-grade graphite at 62¢ per pound, with the raw blocks having 1-in. oversize dimensions for machining. Since special extrusions were not recommended by the National Carbon Company to reduce costs, the cross-shaped moderator blocks were assumed to be machined from solid, square, graphite blocks. Machining estimates were obtained from the Y-12 graphite machine shop. A contingency of 30% was added to allow for design refinements. The cost of installation of the blocks was assumed to be 20¢ per pound of finish-machined graphite, with a contingency of 33% added to allow for design uncertainties.

The installed cost of the graphite moderator and reflector prism 35 ft in diameter and 25 ft high containing 2,136,000 lb of graphite (net weight) is summarized below:

---

[10] W. L. Nelson, *Cost-imating*, p 57, pamphlet compiled from Oil and Gas Journal.

[11] M. Bender and R. D. Stulting, *Cost Comparisons of Capital Investment in Various Nuclear Power Plants for Central Station Application*, ORNL CF-58-10-49 (Oct. 14, 1958).

Raw material, 3,992,000 lb	$2,475,000
Machining	154,000
Machining contingency	46,000
Packaging	19,000
Fabrication subtotal	$2,694,000
Shipping	67,000
Installation	567,000
Installation contingency	170,000
Installation subtotal	$ 804,000
Total installed cost	$3,498,000

Summary of Capital Costs

The capital costs discussed above are compiled and tabulated in Tables 7 and 8.

Table 7. Capital Costs

Listed by FPC account numbers

10.	Land and land rights (double GCR-2)		$ 900,000
11.	Structures and improvements		
	111.	Preparation of site (double GCR-2)	1,400,000
	113.	Powerhouse	
		A. Substructure	5,600,000
		B. Superstructure $(115 \times 420 \times 60 + 50 \times 70 \times 60)$ ft^3 at $2 per ft^3	6,216,000
	118.	Shoreline improvements	
		Intake and discharge canals, including weir $(5.02)^{0.6}$ (410,000)	1,080,000
	Total structures and improvements		$14,296,000
13A.	Reactor plant facilities		
	13A1.	Reactor shielding	
		Neutron curtain	75,000
		Biological shield walls, 25,800 yd^3 at $150 per yd^3	3,870,000
		Shield cooling	100,000
		Total shielding	$ 4,045,000
	13A2.	Reactor pressure vessel, including supports and insulation	3,500,000
	13A3.	Graphite	3,498,000
	13A4.	Fuel-handling equipment	
		Loading machinery	550,000
		Service machinery (including tools)	550,000
		Indexing chutes	250,000
		Loading racks	60,000
		Television inspection cameras	50,000
		Dry storage room and element-handling equipment	175,000
		Fuel transfer dolly	100,000
		Total fuel-handling equipment	$ 1,735,000

Table 7 (continued)

13A6.	Helium system	
	Helium storage and evacuation system	882,000
	Helium cleanup system	128,000
	Helium piping, including valves, expansion joints, and insulation	3,560,500
	Blowers and motors, including containers	7,104,500
	Total helium system	$11,675,000
13A7.	Instruments and controls	
	Instrument boards	566,000
	Local instruments	180,000
	Health physics monitors	200,000
	Control rods and drives	463,500
	Leak-detection system	150,000
	Telemetering to outside of containment cell	1,000,000
	Communications and miscellaneous	124,000
	Total instruments and controls	$ 2,683,500
13A8.	Steam generators, including insulation	17,250,000
13A9.	Miscellaneous laboratory equipment	100,000
13A10.	Containment cell	4,122,000
13A11.	Hot cell and remote-maintenance equipment	6,900,000
	Total reactor plant facilities (13A)	$55,508,500
13B.	Steam plant equipment	
	Feedwater equipment	1,700,000
	Water supply and treatment system	2,440,000
	Steam plant boards, instruments, and controls	1,115,000
	Steam plant piping	3,580,000
	Total steam plant equipment	$ 8,835,000
14.	Turbine-generator units, total	60,400,000
15.	Total accessory electrical equipment	20,500,000
16.	Miscellaneous power plant equipment, total (double GCR-2)	1,750,000

Table 8. Summary of Capital Costs

Listed by FPC account numbers

10.	Land and land rights	$ 900,000
11.	Structures and improvements	14,296,000
13A.	Reactor system	55,508,500
B.	Steam system	8,835,000
14.	Turbine-generator plant	60,400,000
15.	Accessory electrical equipment	20,500,000
16.	Miscellaneous power plant equipment	1,750,000
	Direct costs subtotal	$162,189,500
	Indirect costs (15% of direct costs)	24,328,500
	Subtotal	$186,518,000
	Escalation at 5% per year for half of construction period (2 years)	22,382,000
	Subtotal	$208,900,000
	Contingency (20% of direct costs, indirect costs, and escalation)	41,780,000
	Design, including contingency (12% of direct costs, indirect costs, and escalation)	25,068,000
	Total	$275,748,000

OPERATING COSTS

General

The operating costs fall into two categories: (1) those associated with the fuel and (2) the operating costs exclusive of the fuel. The latter include wages, supplies, and maintenance, and the former include fuel replacement fabrication, reprocessing, and burnup. All these costs are summarized in Table 9, and each item is described separately below. For most charges the costs indicated for the HGCR-1 were modified from corresponding costs for the GCR-2. In a few instances the GCR-2 costs are known to be in error, as by the omission of such charges as the recovery process, the conversion of $UO_2(NO_3)_2$ to UF_6, transportation costs, and conversion of plutonium nitrate to the metal. However, these errors are small and would be applicable to both the GCR-2 and HGCR-1 costs, and were therefore also omitted in this study so that these results would be more directly comparable to the published GCR-2 costs.

Wages

A staff of 100 was specified for the operation of the GCR-2. However, the HGCR-1 has twice as many turbogenerators (that is, eight 157-kw units), and, accordingly, the operating staff of the HGCR-1 was estimated to be 200, including supervision but not

Table 9. Summary of Operating Costs

	Annual Cost	Mills per Kilowatt-Hour
Wages (200 men at $6000 per year)	$1,200,000	0.16
Supplies (H_2O, He, lubrication, etc.)	1,000,000	0.13
Maintenance	3,100,000	0.42
Fuel fabrication (for replacement at $32.38 per kg of U)	2,740,000	0.37
Fuel reprocessing (multipurpose plant)	1,440,000	0.20
Fuel burnup (less Pu credit at $12 per g)	6,180,000	0.83
Fuel in process (for 66% of inventory at 4% per year)	495,000	0.07
		2.18

maintenance labor, as discussed below. At an average cost of $6000 per man per year, the annual cost for wages would be $1,200,000.

Supplies

The cost of water, lubrication, helium, and sundry supplies for the operation and maintenance of the plant, exclusive of the replacement items which were included in the capital costs and the contaminated components discussed below, was estimated to be $1,000,000, that is, approximately 2½ times the comparable GCR-2 cost.

Maintenance

The portion of the maintenance costs that would be chargeable to operating costs was estimated at $2,600,000 per year. Of this amount, $600,000 was for maintenance labor at the plant, $1,500,000 for consumed spare parts and tools, and $1,000,000 for the disposal of contaminated used parts and tools. In view of the uncertainties associated with the maintenance of a large contaminated system (see Chap. 9), each of these three items was intentionally estimated high. The maintenance labor allowance provides for 100 men at $6000 per year. The $1,500,000 allowance for spare parts is sufficient to cover the cost of one of each of the replaceable system components, as well as service tools.

In addition to the charge listed here as an operating expense under maintenance, there are at least two other significant cost items "hidden" elsewhere in the power costs which are directly attributable to maintenance in this plant – the plant factor and spare components.

In view of the difficulty of effecting hot maintenance, the plant factor was decreased from 0.80, as in the GCR-2, to 0.75. At the same time it must be appreciated that the HGCR-1 has on-stream fuel loading and a lower expected fuel element failure rate, both of which should help improve the relative HGCR-1 down time.

The maintenance philosophy of the HGCR-1 would be to remove a defective component from the system, replace it with a spare unit, and either dispose of or service the defective unit in a special hot cell. Accordingly, there are other charges included under capital costs for the initial purchase of spare components, remote tools, and handling equipment, as well as the hot shops.

Fuel Element Fabrication

The cost estimate for the fabrication of the initial graphite fuel element loading was based on the items described below and summarized in Table 10.

Table 10. Fuel Element Fabrication Costs for HGCR-1

	Total Cost	Cost per Kilogram of U*
Graphite stock	$ 525,000	$ 6.15
Processing UF_6 to UO_2	1,158,000	13.56**
Graphite-UO_2 sintering	100,000	1.17
Machining	506,000	5.93
Machining contingency	152,000	1.78
Cementing	54,000	0.63
Packaging	19,000	0.22
Miscellaneous	251,000	2.94
Total	$2,765,000	$32.38
Annual charge at 14% per year	387,000	

*$13.56 per kilogram of U, $12.00 per kilogram of UO_2.
**Uranium content taken as 85,390 kg.

In an effort to reduce the material cost of graphite, the feasibility of extruding special shapes, such as angles, channels, and hollow squares, was discussed with the National Carbon Company.[12] These shapes could be extruded; however, it was the opinion of the National Carbon Company that the cheapest solution would be to machine solid square stock into two channel sections, insert the fuel element plates, and then dowel and cement the channel sections together. The cost estimate was based upon the latter method of fabrication and assembly of the fuel element.

The stock cost was based on the use of National Carbon Company TSF-grade graphite at 62¢ per pound, with raw blocks having 1-in. oversize dimensions for machining. Five per cent spoilage was assumed.

[12]Personal communication, S. W. Palmer, National Carbon Company, to G. C. Robinson, Oct. 20, 1958.

Uranium oxide processing costs, that is, chemical processing, firing, and grinding to the desired particle size and density, were obtained from the Y-12 Process Analysis Group.[13] The estimated cost was $12 per kilogram of UO_2. The cost of sintering the uranium oxide (25% by volume) and graphite (75% by volume) mixture to form the fuel plates was taken to be 62¢ per pound of graphite. Although the sintering cost is uncertain, several possible errors would cause an error of only about 10% in the total estimate.

Machining estimates were obtained from the Y-12 graphite machine shop. A contingency of 30% was added to allow for design refinements such as dowels, keys, and bolts, which could possibly be required in the fabrication of the fuel element.

Cementing of the channel pieces was assumed to take place in a slightly reducing atmosphere at −60°F dew point at 1200°C temperature in a continuous belt-driven furnace.[14] Costs were based upon an approximate current rental fee charged by outside shops, $35 per hour, with belt speeds of approximately 15 to 30 fph.[15]

Miscellaneous costs were taken to be 10% of the subtotal of all previous costs. This cost was arbitrarily taken in order to provide a contingency to cover the uncertainties in the other fuel fabrication costs, such as the graphite coating discussed in Chap. 4.

For the HGCR-1, the UO_2 was considered to have a density of 10.4 g/cm^3 and to be 25% by volume of a fuel element plate having a cross section of 4.5 by 0.372 in. These figures result in a uranium inventory of 85.39 tonnes (96.88 tonnes of UO_2). (Note that the specific power for the HGCR-1 system is 36.2 w/g as compared with 4.95 w/g for GCR-2.) The fuel element fabrication cost contributes to the power cost in two ways: (1) fabrication of the first core, which is discussed below under "Total Power Cost," and (2) fabrication of replacement fuel elements, which is regarded as an operating expense.

Although no lifetime studies were performed, the fuel exposure of 10,000 Mwd/tonne of uranium used is conservative on the basis of GCR-2 data. However, lifetime studies should be undertaken to obtain reliable values for fuel costs. Both the HGCR-1 conversion ratio and k_{eff} are higher than the corresponding value for the GCR-2, for which a fuel exposure of 7400 Mwd/tonne was used that was based on a metallurgical limitation. With an average fuel exposure of 10,000 Mwd/tonne and a load factor of 0.75, the fueling

---

[13]Personal communication, A. C. Ayers, Y-12, to G. C. Robinson, Oct. 20, 1958.

[14]Personal communication, A. J. Toylor, ORNL, to G. C. Robinson, Oct. 2, 1958.

[15]Personal communication, W. T. Carey, Y-12, to G. C. Robinson, Oct. 2, 1958.

rate for the HGCR-1 would average 84.7 tonnes of uranium per year. The annual charge would be 84.7 × 32,380 = $2,740,000. Therefore, the contribution to the power cost is

$$\frac{32{,}380 \text{ dollars/tonne}}{24 \times 0.365 \times 10{,}000 \text{ Mwd/tonne}} = 0.37 \text{ mill/kwhr} \ .$$

Fuel Reprocessing

Fuel reprocessing costs were based on an assumed multipurpose plant with a 1-tonne daily uranium capacity, which would require an eight-day cleanup operation after fuel reprocessing. Although no detailed study has been made of the reprocessing costs of a graphite-UO_2 fuel element, several processes are available for the recovery of the spent uranium from the fuel elements.[16] However, it is suspected that the cost of reprocessing the graphite-UO_2 fuel elements would be somewhat higher than that for the stainless-steel-clad UO_2 fuel elements used in the GCR-2.[17] In lieu of experimental data, a 25% increase was assumed in the fuel reprocessing charge per unit mass. A charge of $15,500 per tonne of uranium was used in this study. With an average fuel exposure of 10,000 Mwd/tonne and a load factor of 0.75, the fueling rate for the HGCR-1 would average 84.7 tonnes per year. This amount of fuel would be processed in a single batch at a cost of

$$(15{,}500 \text{ dollars/day} \times 1 \text{ tonne/day} \times 84.7 \text{ tonnes}) + \\ + (8 \text{ days} \times 15{,}500 \text{ dollars/day}) = \$1{,}440{,}000 \text{ per year} \ .$$

The cost per kilowatt-hour is

$$\frac{1{,}440{,}000 \text{ dollars/year}}{1130 \text{ Mw} \times 8760 \text{ hr/year} \times 0.75} = 0.20 \text{ mill/kwhr} \ .$$

Fuel Burnup

The fuel burnup cost, based on a $12 per gram of plutonium credit, is shown in Table 11. It was found that the burnup cost for a given initial enrichment of the fuel was not strongly dependent upon the fuel exposure if the plutonium were valued at $12 per gram. Since the initial enrichment and the plutonium credit were the same as for the GCR-2 and the isotopic compositions at 10,000 Mwd/tonne fuel exposure were taken from the GCR-2 results,[18] the resulting burnup costs for the two systems are similar. HGCR-1 lifetime studies are expected to result in a reduction in the burnup cost.

---

[16] F. E. Faris, *Reactor Sci. Technol.*, vol 2, No. 4, TID-2004 (Dec. 1952).

[17] Personal communication, H. E. Goeller, ORNL, to W. B. Cottrell, ORNL, Dec. 1, 1958.

[18] *The ORNL Gas-Cooled Reactor*, ORNL-2500, Fig. 2.35 (April 1, 1958).

Table 11. Fuel Burnup Cost

Annual replacement rate of 84.7 tonnes of U per year, exposure of 10,000 Mwd/tonne, $12 per gram of Pu credit

	Annual Cost
Initial value of fuel 2% enriched in U^{235} at $220 per kg	$18,600,000
Value of spent fuel containing 1.0% U^{235} at $77 per kg	6,520,000
Net U^{235} burnup	$12,080,000
Plutonium credit (5.8 g of Pu per kg of U)	5,900,000
Net fuel burnup cost	$ 6,180,000
Net cost, mills/kwhr	0.83

Fuel in Process

The out-of-pile fuel holdup times were assumed to be the same as those used for the GCR-2, that is, eight months. Since the average fuel replacement rate is 99% per year, that is, 84.7 tonnes/year divided by the 85.39-tonne inventory, the out-of-pile inventory is $(8/12) \times 99 = 66\%$ of the in-pile inventory. The rental charge for the out-of-pile inventory will be 66% of the in-pile inventory, and thus, as mentioned below, the annual and power costs are $495,000 per year and 0.07 mill/kwhr, respectively.

TOTAL POWER COST

Fuel Inventory Costs

Included in the fixed costs is a rental charge for the uranium (which is owned by the AEC) based upon the initial value of the fuel. The rate currently established by the AEC is 4% per year. For the HGCR-1 the uranium inventory would be 85.39 tonnes. At a value of $220,000 per tonne for uranium enriched to 2% U^{235}, the uranium inventory would be valued at $18,800,000. For a load factor of 0.75, therefore, the contribution to the power cost is

$$\frac{\$18.8 \times 10^6 \times 0.04 \text{ per year}}{1130 \text{ Mw(e)} \times 8760 \times 0.75 \text{ hr/year}} = 0.10 \text{ mill/kwhr} \ .$$

An annual capital charge must also be applied to the cost of fabrication of the first set of fuel elements. An annual rate of 14% has been applied in this case as for the other investment items. For the HGCR-1 with a fuel fabrication cost of $32.38 per kilogram of uranium, this charge amounts to

$$\frac{32{,}380 \text{ dollars/tonne} \times 85.39 \text{ tonnes} \times 0.14 \text{ per year}}{1130 \text{ Mw(e)} \times 8760 \times 0.75 \text{ hr/year}} = 0.05 \text{ mill/kwhr} \ .$$

The two fixed fuel charges add 0.15 mill/kwhr to the power cost, as shown in Table 12.

Table 12. Comparison of Cost and Performance Data for HGCR-1 and GCR-2

	GCR-2*	HGCR-1
General data		
Net electrical rating, Mw	225	1130
Total generator rating, Mw	252	1256
Thermal efficiency, over-all, %	32.8	36.5
Steam pressure, psia	950	1450
Steam temperature, initial superheater, °F	950	1050
Plant factor	0.80	0.75
Investment data (dollars per kilowatt, base)		
(310) Land	3.12	1.22
(311) Structures and improvements	53.33	19.35
(312) Reactor plant	157.60	87.10
(314) Turbine-generator plant	83.25	81.75
(315) Accessory electrical system	28.32	27.75
(316) Miscellaneous plant equipment	6.06	2.37
Total	331.68	219.54
Total, less reactor	174.08	137.11
Cost of energy (mills/net kwhr), fixed charges		
A. Plant costs at 14%	7.42	5.20
B. Fuel inventory at 4%	0.76	0.10
C. Fuel element fabrication at 14%	0.38	0.05
Total fixed	8.56	5.35
Operating costs (mills/net kwhr)		
A. Wages (including supervision)	0.38	0.16
B. Supplies, water, lubrication, etc.	0.25	0.13
C. Maintenance (equipment and wages)	0.26	0.42
D. Fuel	1.73	1.47
Total operating	2.62	2.18
Total power	11.18	7.53

**The Gas-Cooled Reactor*, ORNL-2500, pt 1, p 15 (April 1, 1958).

Power Cost

The total cost of power from the HGCR-1 is given in Table 12. The table combines the capital costs (with contingency and escalation as shown in Table 8) and fuel inventory charges with the operating cost (Table 9). Also shown in Table 12 are the comparable figures for the GCR-2.

COMPARISON OF HGCR-1 AND GCR-2 POWER COSTS

Direct comparison of the cost of power from the two reactors, as summarized in Table 12, can be misleading because of the disparity in size between the two plants. Furthermore, there is no good means of obtaining comparable cost figures short of optimizing both reactor designs for the same size plant. An attempt was made, however, to estimate the cost of power from an 1130-Mw(e) GCR-2 type of power plant in which heat would be generated in four 282-Mw(e) GCR-2 type reactors. A total of four rather than five reactors was chosen for this comparison in order to allow for some modifications in the GCR-2 design. In the capital cost summary given in Table 13 for the scaled-up GCR-2 type of plant, the following assumptions are implicit, although the actual scale factor in most instances is admittedly only a best guess:

1. Since power plant sites always require the bulk of the area for auxiliary facilities and construction, land costs would not exceed twice those for GCR-2, although site preparation costs would be treble because of the additional buildings required.

2. Careful arrangement of the reactors and consolidation of the turbine installation would reduce the cost of structural improvements per unit of capacity.

3. The reactor vessel and core would realize some unit cost savings by increased quantities and broader distribution of tooling costs, even though the individual pressure vessels would be somewhat larger.

4. Graphite unit costs would remain the same, but the amount required might not vary directly with power.

5. Fuel service equipment could be managed in a way which would give a higher utilization factor by programing reactor refueling cycles so that fueling machinery could be used for more than one reactor.

6. Blower, steam generator, and instrument costs would benefit from quantity purchase, and some saving over an increase proportional to power was assumed.

7. Steam plant equipment and shoreline improvement costs could be scaled on the basis of the capacity ratio to the 0.6 power.

8. Turbine and electrical equipment would vary directly with the power level, although a small saving for quantity purchase was allowed.

9. Miscellaneous power plant equipment and laboratories costs would be increased but to not more than twice the GCR-2 cost.

10. All top charges were taken to be the same as in the HGCR-1 estimate.

Table 13. Capital Cost Estimate for 1130-Mw GCR-2 Type of Reactor Based on Scaling GCR-2 Costs

		Scale Factor	Cost Estimate
10.	Land	2	$ 900,000
11.	Site preparation	3	2,100,000
	Power house	3.5	23,000,000
	Shoreline improvements	$(5.02)^{(0.6)}$	1,080,000
13a.	Reactor shielding	4.5	6,900,000
	Pressure vessel	4	9,300,000
	Graphite	4.9	14,700,000
	Fuel handling	3	3,700,000
	Gas system	4	15,400,000
	Instruments and controls	4	7,800,000
	Steam generators	4	21,800,000
	Miscellaneous laboratory equipment	2	100,000
13b.	Steam plant equipment	$(5.02)^{(0.6)}$	8,800,000
14.	Turbine equipment	4.9	59,000,000
15.	Accessory electrical	4.9	20,000,000
16.	Miscellaneous equipment	2	1,750,000
	Direct costs subtotal		$196,330,000
	Indirect costs at 15%		30,450,000
	Subtotal		$226,780,000
	Escalation at 12% (6% for 2 years)		27,213,000
	Subtotal		$253,993,000
	Contingency (20% of direct costs, indirect costs, and escalation)		50,799,000
	Design (12% of direct costs, indirect costs, and escalation)		30,479,000
	Grand total		$335,271,000

The resulting costs of power from a 225-Mw(e) GCR-2 and from an 1130-Mw(e) GCR-2 type of plant are shown in Table 14. The capital cost charge for the 1130-Mw(e) GCR-2 plant was obtained from Table 13 by assuming an annual interest charge of 14% and an 0.80 load factor. The fuel inventory fabrication and cycle costs were held constant. The charge for wages was reduced because of some savings in administration and maintenance despite the multiplicity of units, but supplies and maintenance costs were not affected.

Table 14. Estimated Power Costs from 225-Mw(e) GCR-2 Plant and 1130-Mw(e) GCR-2 Type of Plant

	Estimated Power Costs (mills/kwhr)	
	225-Mw(e) GCR-2	1130-Mw(e) GCR-2
Plant costs at 14%	7.42	5.92
Fuel inventory at 4%	0.76	0.76
Fuel element fabrication at 14%	0.38	0.38
Wages	0.38	0.27
Supplies	0.25	0.25
Maintenance	0.26	0.26
Fuel	1.73	1.73
Total	11.18	9.57

Some additional improvements in the GCR-2 design were postulated in the original design study,[19] but in view of subsequent work it would be premature to take credit for this uncertain potential. It may be shown, however, that a modification to double the specific power of the GCR-2 by increasing the allowable fuel element surface temperature 100°F might effect a reduction of more than 0.5 mill/kwhr in the power cost. Such extrapolations as these are extremely tenuous and assume the feasibility and practicability of a modification that only a detailed design study could substantiate.

There are at least two considerations which have not been mentioned in comparing HGCR-1 and GCR-2 costs, both of which argue the disadvantage of the HGCR-1:

1. Contingency factors for the HGCR-1 may need to be higher in relation to the GCR-2 because of the greater extension of technology.

2. Design costs for the GCR-2 design are likely to represent a smaller percentage of the capital investment than for the HGCR-1, but both are probably too high.

It is significant, however, that for reactor plants of this capacity an error of $4,000,000 in the charges to capital costs represents a differential of only 0.1 mill/kwhr in the power cost. Thus the saving that might accrue from the construction of a large GCR-2 type of plant in which the design and contingency costs were half those allowed in Table 13 would be equivalent to about 1 mill/kwhr.

In view of the many uncertainties inherent in the costs and the extrapolations which have been presented in this report, undue merit should not be given to the absolute value of the cost figures herein. The relative costs of components and power of two systems analyzed on a comparable basis are of much greater significance. The estimated cost of

[19] *The ORNL Gas-Cooled Reactor*, ORNL-2500, pt 1, p 16 (April 1, 1958).

power for the 1130-Mw(e) GCR-2 type of system is of interest not only because it is appreciably less than that for the GCR-2, but also because it is still significantly higher than that for the HGCR-1. This cost analysis does not include development costs, and no attempt was made in this analysis to provide a refined correction of escalation. As the numbers stand, all components of both plants were assumed to be developed, both plants were to be completed in four years, and the costs were escalated accordingly.

It cannot be claimed that the spread in the cost of power between these two systems is absolutely irretrievable, although an underestimate of the HGCR-1 by about 20%, or an overestimate of the 1130-Mw(e) GCR-2 by a comparable amount, would be required to change the competitive cost position of these two plants. Not only would these errors in costing have to be applicable to only one of the two plants (otherwise the equalizing effect would be nullified), but they would represent a sum of approximately $80,000,000 in capital charges, or $15,000,000 in annual operating expenses. While it is conceivable that large sums of money may be required for the development work on contaminated systems, it does not seem likely – granting the feasibility of the equipment and fuel elements assumed herein – that as large a unilateral error in costs as indicated above exists in the *n*th generation of either of the two plants.

11. DISCUSSION AND RECOMMENDATIONS

All the advantages generally associated with high-temperature operation may be claimed for the contaminated gas-cooled reactor. A low-temperature system could also be contaminated, but in this instance contamination results from the desire for high temperatures and the inability of existing materials to contain fission products within the fuel elements at temperatures of approximately 2000°F and above.

With the high-temperature fuel element, a large temperature difference exists between the fuel element and the coolant, which results in high heat fluxes and high power densities in the reactor. These, in turn, tend to reduce both reactor capital costs and fuel charges. By increasing the outlet gas temperature (1500°F was the design condition for these studies), lower steam generator costs result because of the high heat transfer efficiencies on the controlling gas side.

Although it is necessary because of the desired temperature (>2000°F for the fuel element) to employ refractory fuel elements, it would be quite surprising if the fuel element selected for this study were to prove to be the optimum combination of materials and configuration. Physics and heat transfer studies should be performed on a number of other promising fuel element configurations. A UO_2-graphite fuel element of the type proposed does appear to be very attractive, but many of the particular features remain to be proved. The inclusion of the 200-μ UO_2 particles with 75 vol % graphite to form plates of the required structural and irradiation integrity should be demonstrated, as well as the manufacture of the box-type fuel element assembly. Not only are other fuel element configurations possible, but it might be expected that studies on the densification of graphite and on surface coatings would have significant implications for the release of fission products from these fuels. While not specifically mentioned, it is intended that future studies should include ceramic fuel elements, as well as graphite-coated and ceramic-coated graphite fuel elements.

The physics calculations were performed as a function of a number of parameters with values in the vicinity of those of the final design. Although this limited approach indicated that the design was not far from optimum, these and other parameters should be further examined. Enrichments less than 2% may be advantageous in this system in which the parasitic absorptions are so low that the higher conversion ratios associated with lower enrichment might compensate for the lower U^{235} concentration. Detailed lifetime studies were not performed, and it is probable that lifetimes greater than 10,000 Mwd/tonne could be attained. Other fuel element configurations may have nuclear, as well as thermal, advantages, particularly with regard to the resonance escape probability, which is a function of the fraction of moderator mixed with the fuel, fuel element temperature, etc.

The control problems associated with this reactor were examined only cursorily, but a number of interesting questions has evolved. The probable change in the fuel temperature coefficient with exposure, the xenon poisoning, and the effect of control rods on the power distribution must be examined analytically, as well as the effect of the "xenon tilt."

An area of particular concern in this study has been the calculations on the release of activity from the fuel. The data for the release of fission products from UO_2 were based on diffusion of krypton from UO_2. The diffusion of other fission products from UO_2 is still unknown. The calculations of diffusion of fission products from graphite were based on limited data for smaller specimens which were tested at higher temperatures than of interest to the HGCR-1. The applicability of the analytical model which permitted the calculation of activity released with the fuel element and temperature in question should be verified experimentally. These studies should then be extended to an investigation of techniques which would reduce the fission-product release.

Intimately associated with the problem of the release of activity is the ultimate disposition of the activity in the primary system. Activity may be removed from a circulating fluid by deposition on the walls of the system, holdup in a purification system, leakage from the primary system, and decay. Since there is no control over the process, and leakage from a contaminated system must be minimized, deposition and purification are the important parameters to be manipulated. Unfortunately, suitable techniques have not been developed to filter the main gas stream economically (assuming that this would be desirable). At the same time, activity deposition rates from a contaminated gas stream are virtually unknown. Experimental work would have to be performed in order to establish deposition rates for the important activities. These results would have significant implications for both the purification technique and maintenance requirements, since, if the deposition rates are high, the activity could plate out on the walls of the primary system before it had a chance to be removed by the purification system unless the latter were to consist of a total stream filter rather than a bypass cleanup system.

The maintenance cost of a contaminated system is difficult to estimate even after deciding on a particular maintenance philosophy. Inasmuch as the maintenance philosophy is dependent on the calculated activity releases, the locale and rates of deposition, and the effectiveness of the cleanup system, maintenance may actually be somewhat simpler than proposed herein. Nevertheless, it is difficult to conceive of a system in which remote cutting, grinding, welding, and inspection will not be required. These techniques should be developed for pipe sections of a fraction of a foot in diameter up to the 6- and 7-ft-dia ducts used in large gas systems.

The suitability of decontamination techniques and their ability to attain the desired decontamination factors should be considered further. If decontamination permitted direct maintenance of components in the gas loop external to the primary shielding, it would result in a considerable saving. In any event, decontamination of equipment removed from the system would expedite maintenance, even if it were not practical to decontaminate in place.

Closely associated with the maintenance problem is the plant layout. To simplify the work, the basic layout of the GCR-2 formed the basis for this study, but other layouts might prove substantially better and should be studied. Here a compromise must be made between the desire to spread the system out to expedite remote maintenance and the cost of larger cells, building, and containment vessel. While the entire system could have been enclosed in a containment vessel some 50 ft in diameter less than that shown in the final design, the additional space was provided for remote access to the equipment. In this connection the feasibility of containment provisions other than that provided by the containment sphere should be investigated.

Although further analytical studies are needed, particularly in areas such as physics and heat transfer, much pertinent basic information does exist that can be developed into design data only through an experimental program. At the present time it would appear that the greatest returns could be realized from an in-pile loop in which full-scale unclad fuel elements could be tested at design temperature. The phenomena of activity release, deposition, and purification could be studied in the same loop, in addition to determining the effects of radiation on various fuel elements. A substantial effort would also be required for the development of the fuel elements, decontamination techniques, and remote maintenance methods, as well as for analytical studies and for the analytical evaluation of the material and loop test programs.

The results of this design study indicate that the HGCR-1 could be expected to produce power at a cost significantly less than that for a GCR-2 type of power plant. Since the GCR-2 plant showed promise of attaining a lower power cost than that from any existing nuclear plant, it would appear that an extensive development program of the problems associated with the HGCR-1 system is warranted. Much of the work would be applicable to any reactor system designs employing unclad fuel elements. These and other promising designs, such as a package unit in which the reactor and heat exchanger are enclosed within the same cylindrical pressure vessel, should be examined.

APPENDIX A. RELEASE OF FISSION PRODUCTS FROM UO_2

The fuel element designed for the HGCR-1 is composed of 200-μ-dia particles of UO_2 mixed with graphite. The release of fission products from UO_2 is brought about by two processes: (1) the diffusion of fission products from the UO_2 and (2) the recoil of fission-product fragments out of the UO_2.

DIFFUSION OF FISSION PRODUCTS OUT OF UO_2

The diffusion of fission products from the UO_2 may be estimated by the following expression:[1]

$$N_i = 4\pi a^3 f\gamma R \quad , \tag{1}$$

where

N_i = total number of active atoms external to the equivalent sphere at any time, t,

a = radius of equivalent sphere, cm,

f = fissioning rate per unit volume, fissions/sec·cm^3,

γ = fission yield, atoms/fission,

and R is defined by

$$R = \left\{ \left[\sqrt{\frac{d}{\lambda}} \frac{\cosh\sqrt{\lambda/d}}{\sinh\sqrt{\lambda/d}} - \frac{d}{\lambda} \right] \frac{(1 - e^{-\lambda t})}{\lambda} - \left[\frac{2}{\pi^2} e^{-\lambda t} \sum_{n=1}^{\infty} \frac{1 - e^{-n^2\pi^2 dt}}{n^2(n^2\pi^2 d + \lambda)} \right] \right\} , \tag{2}$$

and

$d = D/a^2$, sec^{-1},

D = diffusion coefficient, cm^2/sec,

λ = radioactive decay constant, sec^{-1},

t = time of operation, sec.

If the total number of equivalent spheres in a cubic centimeter of fuel is expressed as

$$n = \frac{1}{\frac{4}{3}\pi a^3} ,$$

then the total number of atoms released from 1 cm^3 of fuel is

$$N = N_i n = 3f\gamma R \quad . \tag{3}$$

For this study a power density of 1000 w/cm^3 was chosen and was converted to the actual power density for the final results. Therefore, Eq. (3) may be rewritten as

$$\begin{aligned} N &= 3 \times (3 \times 10^{10}) \times 10^3 \gamma R \\ &= 9 \times 10^{13} \gamma R \quad . \end{aligned} \tag{3a}$$

[1] J. D. Eichenberg *et al.*, *Effects of Irradiation on Bulk UO_2*, WAPD-183 (Oct. 1957).

In order to evaluate Eq. (3*a*) it is necessary to have adequate information about the diffusion of fission products in UO_2 at various temperatures.

Since the information on the diffusion of fission products in UO_2 is limited to that for krypton and xenon, it was assumed for this study that bromine, iodine, and cesium would diffuse at the rate given for krypton in Fig. A.1. The diffusion curves given in a Geneva paper[2] include additional data, but they were not used because they were not available at the time this study was begun. Although the Geneva paper data are more recent, a comparison of the curves indicates that the values used tend to give a conservative result.

The solution to Eq. (2) involves many parameters with values that range over many orders of magnitude, and therefore a machine calculation was made on the IBM 704 to evaluate Eq. (2) for the following range of parameters:[3]

$$10^9 \geqq t \geqq 10^5 \ ,$$

$$10^0 \geqq \lambda \geqq 10^{-9} \ ,$$

$$10^4 \geqq d \geqq 10^{-15} \ .$$

The solution to Eq. (2) is plotted in Fig. A.2 for $t = 10^8$ and 10^9 sec. Subsequent calculations were based on a fuel lifetime of $\sim 3 \times 10^8$ sec. Since the actual fuel lifetime would be nearer to 3×10^7 sec, the results overestimated the escape of the longer lived nuclides and therefore overestimated any daughters of these nuclides.

The radius of the equivalent sphere, a, may be found from the following expression:[1]

$$a = \frac{3\rho}{S} \ , \tag{4}$$

where

ρ = fraction of theoretical density,

S = surface area, cm^2/cm^3.

A value of S is given in ref 1 for a theoretical density of 0.91 as $S = 2.5 \times 10^3$. Therefore

$$a = \frac{(3)(0.91)}{2.5 \times 10^3} = 1.09 \times 10^{-3} \ .$$

Values of d for various temperatures were calculated by using the values of D obtained from Fig. A.1. Then, from the data of Fig. A.2, the value of R for the given nuclide could be found by using its half life and the value of d associated with the isotope at a given temperature. Values of R for the various nuclides which can diffuse out of UO_2 are given in Table A.1. Although many of these nuclides are not important

---

[2] J. Belle, *Properties of Uranium Dioxide*, 1958 Geneva Conference Paper No. 2404.

[3] W. B. Cottrell and H. N. Culver, *Machine Calculation for the Diffusion of Fission Products*, ORNL CF-59-1-1 (Jan. 1959).

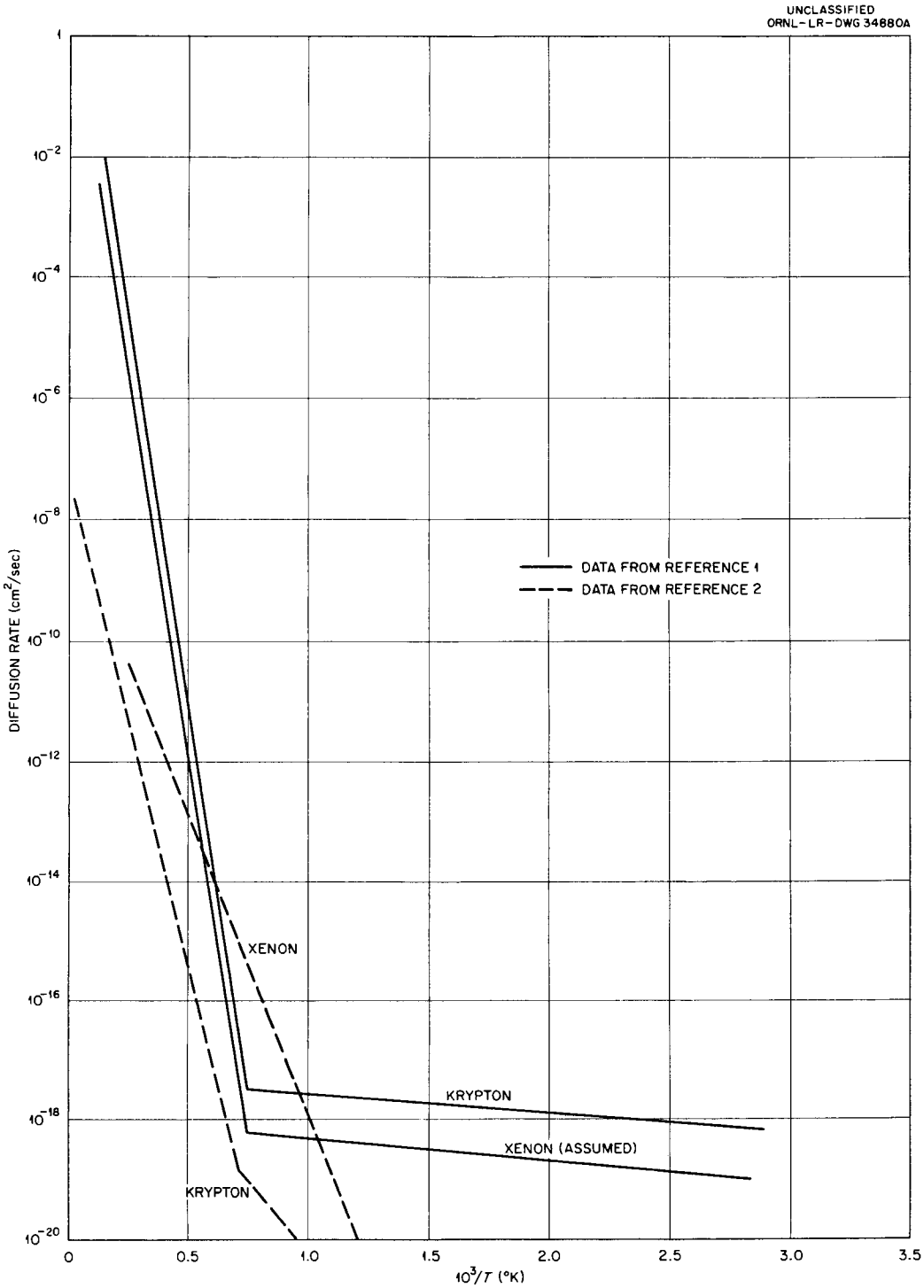

Fig. A.1. Diffusion Rates for Xenon and Krypton in UO_2.

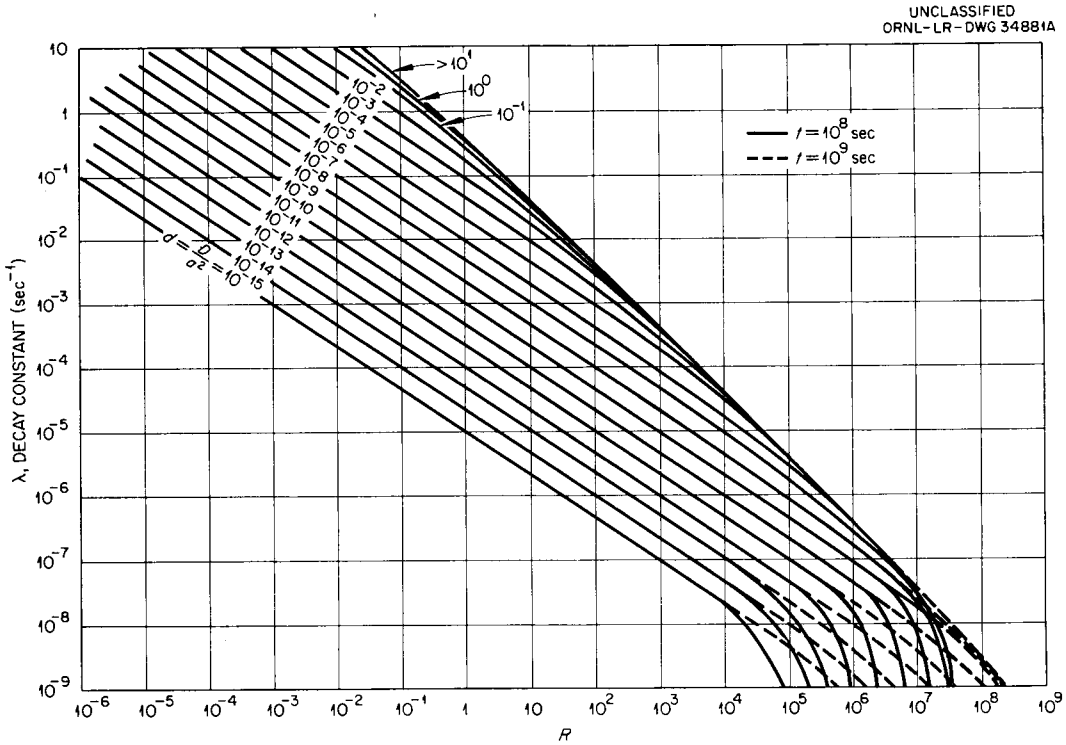

Fig. A.2. Graphical Solution to Diffusion Equation (2).

gamma-ray emitters, they decay into gamma-ray emitters and are therefore important sources of activity for dose-rate calculations.

The important nuclides of interest in this study are underlined in Table A.2. Since many of these nuclides do not diffuse out of UO_2, the only method of obtaining these nuclides in the coolant is by decay of precursor nuclides. Table A.3 indicates the method used to predict the number of atoms of a given nuclide in the gas stream. Included in this table are the equations used and definitions of the symbols used. Table A.4 gives detailed results for diffusion at 1400°C, and Table A.5 lists the number of atoms and the activity of the important gamma-ray-emitting nuclides.

An analysis of the results for the 1400°C case indicates that the activity in the gas may be approximated for the 1000 and 1200°C cases by comparing the R values at 1400, 1200, and 1000°C.

Since the R values for 1000, 1200, and 1400°C are in the following ratios:

$$R_{1200}/R_{1000} \approx 12.5 \ ,$$

$$R_{1400}/R_{1200} \cong 10.5 \ ,$$

the activity for the 1200 and 1000°C cases may be expressed as

$$A_{1200} = A_{1400}/10.5 \ ,$$

$$A_{1000} = A_{1400}/131 \ .$$

The values of D were all based on the value for krypton, and therefore the R values for a given value of λ will be proportional. This will not be the case for diffusion in graphite since the various elements will have different diffusion coefficients. The activities for the 1200 and 1000°C cases are given in Table A.5.

RECOIL OF FISSION PRODUCTS FROM UO_2

The range of fission fragments in air is[4] 2.3 cm for light nuclei and 1.8 cm for heavy nuclei. The range in a material other than air may be expressed as

$$\bar{R}(E) = 0.56\ A^{1/3}\ R(E)_{air},\ \text{cm};$$

$$\bar{R} = 0.56\ A^{1/3}\ (2.3),\ \text{for light nuclei},$$

$$\bar{R} = 0.56\ A^{1/3}\ (1.8),\ \text{for heavy nuclei};$$

$$A_{UO_2} = A\ (U^{238})\ \frac{\rho_{UO_2}}{\rho_{U^{238}}}$$

$$= 238\ \frac{10.5}{18} = 139,$$

$$\bar{R} = 5.18 \times 0.56 \times 2.3 = 6.67\ \text{mg/cm}^2,\ \text{for light nuclei},$$

$$\bar{R} = 5.18 \times 0.56 \times 1.8 = 5.22\ \text{mg/cm}^2,\ \text{for heavy nuclei}.$$

The density of UO_2 is 10.5 g/cm^3; therefore, the range of the fission fragments in UO_2 is

$$\bar{R} = \frac{6.67 \times 10^{-3}}{10.5} = 6.35 \times 10^{-4}\ \text{cm, for light nuclei},$$

$$\bar{R} = \frac{5.22 \times 10^{-3}}{10.5} = 4.98 \times 10^{-4}\ \text{cm, for heavy nuclei}.$$

With a 200-μ particle size (0.02 cm),

$$\text{volume of particle} = \frac{4}{3}\pi r^3 = \frac{4}{3}\pi(1 \times 10^{-2})^3$$

$$= \frac{4\pi \times 10^{-6}}{3}\ \text{cm}^3\ ,$$

$$\text{volume of outer shell} = \frac{4}{3}\pi[r^3 - (r - R)^3]\ .$$

---

[4] J. F. Hogerton and R. C. Grass (eds.), *The Reactor Handbook*, vol I, AECD-3645 (March 1955).

Therefore, for the light nuclei,

$$V = \frac{4}{3}\pi[10^{-6} - (9.365 \times 10^{-3})^3]$$

$$= \frac{4}{3}\pi[10^{-6} - (8.213 \times 10^{-7})]$$

$$= \frac{4}{3}\pi[1.787 \times 10^{-7}] \ ;$$

$$\text{fraction of fragments out} = \frac{(0.25)\ 1.787 \times 10^{-7}}{10^{-6}}$$

$$= 4.47 \times 10^{-2} \ .$$

For heavy nuclei,

$$\text{fraction of fragments out} = \frac{(0.25)\ 1.421 \times 10^{-7}}{10^{-6}}$$

$$= 3.55 \times 10^{-2} \ .$$

Table A.1. Values* of R for Radionuclides Diffusing from UO_2

Nuclide	λ (sec^{-1})	Values of R		
		For UO_2 at 1000°C and $d = 1.92 \times 10^{-12}$ sec^{-1}	For UO_2 at 1200°C and $d = 3.94 \times 10^{-10}$ sec^{-1}	For UO_2 at 1400°C and $d = 4.54 \times 10^{-8}$ sec^{-1}
Br^{84}	3.85×10^{-4}	2.4×10^{-1}	3.0×10^{0}	3.2×10^{1}
Br^{87}	1.25×10^{-2}	1×10^{-3}	1.3×10^{-2}	1.4×10^{-1}
Kr^{87}	1.48×10^{-4}	1×10^{0}	1.3×10^{1}	1.4×10^{2}
Br^{88}	4.47×10^{-2}	1.7×10^{-4}	2.2×10^{-3}	2.3×10^{-2}
Kr^{88}	6.95×10^{-5}	2.4×10^{0}	3.0×10^{1}	3.2×10^{2}
Rb^{88}	6.49×10^{-4}	9.0×10^{-2}	1.14×10^{0}	1.2×10^{1}
Kr^{89}	3.63×10^{-3}	6.3×10^{-3}	8.0×10^{-2}	8.4×10^{-1}
Rb^{89}	7.50×10^{-4}	7.0×10^{-2}	8.9×10^{-1}	9.3×10^{0}
Kr^{90}	2.10×10^{-2}	5.6×10^{-4}	7.1×10^{-3}	7.5×10^{-2}
Rb^{90}	4.22×10^{-3}	5.6×10^{-3}	7.1×10^{-2}	7.5×10^{-1}
Kr^{91}	7.08×10^{-2}	6.5×10^{-5}	8.3×10^{-4}	8.7×10^{-3}
Rb^{91}	8.25×10^{-4}	5.6×10^{-2}	7.1×10^{-1}	7.5×10^{0}
Kr^{92}	2.31×10^{-1}	1.5×10^{-5}	1.9×10^{-4}	2.0×10^{-3}
Rb^{92}	8.66×10^{-3}	2.0×10^{-3}	2.5×10^{-2}	2.6×10^{-1}
Kr^{93}	3.47×10^{-1}	9.0×10^{-6}	1.14×10^{-4}	1.2×10^{-3}
Rb^{93}	$\sim 6.94 \times 10^{-1}$	2.7×10^{-6}	3.4×10^{-5}	3.6×10^{-4}
Kr^{94}	4.95×10^{-1}	4.0×10^{-6}	5.1×10^{-5}	5.4×10^{-4}
Rb^{94}	$\sim 6.94 \times 10^{-1}$	2.7×10^{-6}	3.4×10^{-5}	3.6×10^{-4}
I^{131}	9.96×10^{-7}	1.5×10^{3}	1.9×10^{4}	2.0×10^{5}
I^{132}	8.02×10^{-5}	2.0×10^{0}	2.5×10^{1}	2.6×10^{2}
I^{133}	9.25×10^{-6}	5.6×10^{1}	7.1×10^{2}	7.5×10^{3}
I^{134}	2.20×10^{-4}	4.0×10^{-1}	5.1×10^{0}	5.4×10^{1}
I^{135}	2.89×10^{-5}	9.0×10^{0}	1.14×10^{2}	1.2×10^{3}
Xe^{135m}	7.40×10^{-4}	6.3×10^{-2}	8.0×10^{-1}	8.4×10^{0}
I^{136}	8.06×10^{-3}	2.0×10^{-3}	2.5×10^{-2}	2.6×10^{-1}
I^{137}	3.15×10^{-2}	2.4×10^{-4}	3.0×10^{-3}	3.2×10^{-2}
Xe^{137}	2.96×10^{-3}	8.0×10^{-3}	1.0×10^{-1}	1.1×10^{0}
Cs^{137}	8.27×10^{-10}	2.9×10^{6}	4.6×10^{7}	9×10^{7}
I^{138}	1.17×10^{-1}	3.3×10^{-5}	4.2×10^{-4}	4.4×10^{-3}
Xe^{138}	6.79×10^{-4}	7.0×10^{-2}	8.9×10^{-1}	9.3×10^{0}
Cs^{138}	3.62×10^{-4}	1.9×10^{-1}	2.4×10^{0}	2.5×10^{1}
I^{139}	2.57×10^{-1}	1.1×10^{-5}	1.4×10^{-4}	1.5×10^{-3}

Table A.1 (continued)

Nuclide	λ (sec^{-1})	Values of R		
		For UO_2 at 1000°C and $d = 1.92 \times 10^{-12}$ sec^{-1}	For UO_2 at 1200°C and $d = 3.94 \times 10^{-10}$ sec^{-1}	For UO_2 at 1400°C and $d = 4.54 \times 10^{-8}$ sec^{-1}
Xe^{139}	1.69×10^{-2}	7.0×10^{-4}	8.9×10^{-3}	9.3×10^{-2}
Cs^{139}	1.22×10^{-3}	3.3×10^{-2}	4.2×10^{-1}	4.4×10^{0}
Xe^{140}	4.33×10^{-2}	1.3×10^{-4}	1.7×10^{-3}	1.8×10^{-2}
Cs^{140}	1.05×10^{-2}	1.3×10^{-3}	1.7×10^{-2}	1.8×10^{-1}
Xe^{141}	4.08×10^{-1}	5.6×10^{-6}	7.1×10^{-5}	7.5×10^{-4}
Cs^{141}	$\sim 6.94 \times 10^{-1}$	2.7×10^{-6}	3.4×10^{-5}	3.6×10^{-4}

*Parameter values assumed in calculations:

$\rho_{UO_2} = 0.91$,

$a = 1.09 \times 10^{-3}$,

$d = \frac{D}{a^2} = 8.4 \times 10^5\ D\ (\text{sec}^{-1})$,

time = 3×10^8 sec (~ 10 years),

power density = 1000 w/cm^3.

Table A.2. Radionuclides Contributing to Primary System Contamination

Chain	Decay Scheme*			
	A	*B*	*C*	*D*
84	30m Br 1.1			
87	55.6s Br —98%→ 2.7	78m Kr 2.7	→ Rb	
88	15.5s Br → (2.9)	2.77h Kr 3.7 (0.8)	→ 17.8m Rb 3.7	
89	3.18m Kr → (4.6)	15.4m Rb 4.8 (0.2)		
90	33s Kr → (5.2)	2.74m Rb → 4.9 (0.7)	28y Sr → 5.9	64.5h Y 5.9
91	9.8s Kr → (3.7)	1.67m Rb → 14m Rb 5.7 (2.0)	9.7h Sr (0.2) 5.9	—40%→ 51m Y 2.4 —60%→ 58d Y 5.9
92	3.0s Kr → (2.7)	8s Rb → 5.5 (2.8)	2.7h Sr → (0.6) 6.1	3.6h Y 6.1

Table A.2 (continued)

Chain	Decay Scheme*				
	A	*B*	*C*	*D*	
93	2s Kr (1.3)	Short Rb 4.4 (3.1)	7m Sr 6.4 (2.0)	10.0h Y 6.5 (0.1)	
94	1.4s Kr (0.6)	Short Rb 2.9 (2.3)	2m Sr 5.8 (2.9)	16.5m Y 6.5 (0.7)	
95	10.5m Y 6.4	63d Zr 6.4	35d Nb 6.4		
129	33d Te 0.24	72m Te 1.0			
131	30h Te 0.44	24.8m Te 2.9	8.05d I 2.9		
132	77h Te 4.4 (1.0)	2.4h I 4.4	Xe		
133	63m Te 4.6	2m Te 6.0	20.8h I 6.5 (0.5)		
134	44m Te 6.7 (3.7)	52.5m I 7.6 (0.9)	Xe		
135	2m Te (4.2)	6.68h I (1.7) 5.9	30% → 15.6m Xe 1.8 70% → 9.13h Xe 6.2 (0.3)	Cs	
136	86s I (3.1)	Xe			
137	22s I (4.9)	~6% → ; ~94% → 3.9m Xe (1.3) 5.9	26.6y Cs 5.9	92% → 2.6m Ba 5.4 8% → Stable Ba	
138	5.9s I (3.4)	17m Xe 5.5 (2.1)	32m Cs 5.8 (0.3)	Ba	
139	2.7s I (1.8)	41s Xe 4.7 (2.9)	9.5m Cs 5.9 (1.2)	85m Ba (0.1) 6.0	La
140	16s Xe (3.7)	66s Cs 6.0 (2.3)	12.8d Ba (0.3) 6.3	40.2h La 6.3	Ce
141	1.7s Xe (1.8)	Short Cs 4.7 (2.9)	18m Ba 5.9 (1.2)	3.7h La (0.1) 6.0	32d Ce
142	1m Cs (3.4)	6m Ba (2.2) 5.6	74m La (0.3) 5.9		
143	0.5m Ba (4.9)	19m La (1.3) 6.2	32h Ce 6.2		

*A, B, C, and D indicate the members of a chain. The nuclides which are underlined are the gamma-ray-emitting nuclides of interest for shielding calculations. Some of the chains are simplified for cases where initial members of a chain do not affect the calculations. Direct yields (in per cent) are given beneath the nuclides in parentheses; cumulative yields are not enclosed in parentheses.

Table A.3. Schematic Distribution of Radioactive Nuclides for Unclad Fuel Elements*

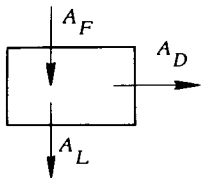	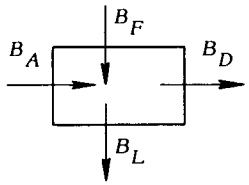	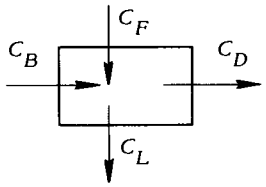	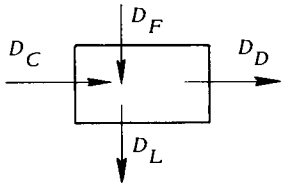
$A_G = A_L$	$B_G = B_L + \frac{A_L \lambda_A}{\lambda_B}$	$C_G = C_L + \frac{B_G \lambda_B}{\lambda_C}$	$D_G = D_L + \frac{C_G \lambda_C}{\lambda_D}$
$A_F = \frac{3 \times 10^{13}\, \gamma_A}{\lambda_A}$	$B_F = \frac{3 \times 10^{13}\, \gamma_B}{\lambda_B}$	$C_F = \frac{3 \times 10^{13}\, \gamma_C}{\lambda_C}$	$D_F = \frac{3 \times 10^{13}\, \gamma_D}{\lambda_D}$
	$B_A = A_D \frac{\lambda_A}{\lambda_B}$	$C_B = B_D \frac{\lambda_B}{\lambda_C}$	$D_C = C_D \frac{\lambda_C}{\lambda_D}$
$A_L = 3/\gamma_A R_A$	$B_L = 3/R_B \gamma_B'$	$C_L = 3/R_C \gamma_C'$	$D_L = 3/R_D \gamma_D'$
$\gamma_A = \gamma_A$	$\gamma_B' = \gamma_B + \frac{A_D}{A_D + A_L} \gamma_A$	$\gamma_C' = \gamma_C + \frac{B_D}{B_D + B_L} \gamma_B'$	$\gamma_D' = \gamma_D + \frac{C_D}{C_D + C_L} \gamma_C'$
$A_D = A_F - A_L$	$B_D = B_F + B_A - B_L$	$C_D = C_F + C_B - C_L$	$D_D = D_F + D_C - D_L$

*Definition of symbols:

A, B, C, D indicate the members of a chain.

Subscripts denote:

F = generation term,
L = leakage by diffusion,
D = decay to daughter,
A, B, C = gain of nuclide by decay process,
G = nuclides in gas stream.

Table A.4. Results Obtained in Calculation of Diffusion of Fission Products from UO_2 at 1400°C

Decay Scheme $A \rightarrow B \rightarrow C \rightarrow D$				Chain	γ_A	R_A	$A_L = A_G$	R_B	γ'_B	B_L	B_G	R_C	γ'_C	C_L	C_G	D_G
Br				84	1.1×10^{-2}	3.2×10^{1}	2.88×10^{13}									
Br	Kr			87	2.7×10^{-2}	1.4×10^{-1}	3.1×10^{10}	1.4×10^{2}	2.7×10^{-2}	3.09×10^{14}	3.11×10^{14}					
Br	Kr	Rb		88	2.9×10^{-2}	2.3×10^{-2}	5.45×10^{10}	3.2×10^{2}	3.7×10^{-2}	9.7×10^{14}	1.05×10^{15}	1.2×10^{1}	3.48×10^{-2}	3.42×10^{13}	1.47×10^{14}	
Kr	Rb			89	4.6×10^{-2}	8.4×10^{-1}	3.16×10^{12}	9.3×10^{0}	4.76×10^{-2}	3.62×10^{13}	4.96×10^{13}					
Kr	Rb	Sr	Y^m	90	5.2×10^{-2}	7.5×10^{-2}	3.19×10^{11}	7.5×10^{-1}	5.88×10^{-2}	3.61×10^{12}	5.19×10^{12}				2.78×10^{19}	7.34×10^{15}
			Y													5.41×10^{13}
Kr	Rb	Sr	Y	91	3.7×10^{-2}	8.7×10^{-3}	2.64×10^{10}	7.5×10^{0}	5.7×10^{-2}	3.5×10^{13}	3.7×10^{13}		5.81×10^{-2}		1.54×10^{15}	2.22×10^{17}
Kr	Rb	Sr	Y	92	2.7×10^{-2}	2.0×10^{-3}	4.42×10^{9}	2.6×10^{-1}	5.5×10^{-2}	1.17×10^{12}	1.29×10^{12}				1.57×10^{14}	2.09×10^{14}
Kr	Rb	Sr	Y	93	1.3×10^{-2}	1.2×10^{-3}	1.28×10^{9}	3.6×10^{-4}	4.4×10^{-2}	1.3×10^{9}	1.94×10^{9}				8.15×10^{11}	6.96×10^{13}
Kr	Rb	Sr	Y	94	6×10^{-3}	5.4×10^{-4}	2.66×10^{8}	3.6×10^{-4}	2.9×10^{-2}	8.56×10^{8}	1.05×10^{9}				1.26×10^{11}	1.04×10^{12}
Te^m	Te	I		131	4×10^{-3}				2.9×10^{-2}			2.0×10^{5}	2.9×10^{-2}	4.75×10^{17}	4.75×10^{17}	
Te	I			132	4.6×10^{-2}			2.6×10^{2}	4.6×10^{-2}	9.37×10^{14}	9.37×10^{14}					
Te^m	Te	I		133	4.6×10^{-2}				6.0×10^{-2}			7.5×10^{3}	6.5×10^{-2}	3.98×10^{16}	3.98×10^{16}	
Te	I			134	6.7×10^{-2}			5.4×10^{1}	7.6×10^{-2}	3.36×10^{14}	3.36×10^{14}					
Te	I	Xe^m		135	4.2×10^{-2}			1.2×10^{3}	5.9×10^{-2}	5.8×10^{15}	5.8×10^{15}	8.4×10^{0}	1.6×10^{-2}	1.1×10^{13}	7.88×10^{13}	
I				136	3.1×10^{-2}	2.6×10^{-1}	6.6×10^{11}									
I	Xe	Cs	Ba^m	137	4.9×10^{-2}	3.2×10^{-2}	1.28×10^{11}	1.1×10^{0}	5.88×10^{-2}	5.3×10^{12}	6.66×10^{12}	9×10^{7}	5.87×10^{-2}	4.32×10^{20}	1.65×10^{21}	3.08×10^{14}
I	Xe	Cs		138	3.4×10^{-2}	4.4×10^{-3}	1.22×10^{10}	9.3×10^{0}	5.5×10^{-2}	4.19×10^{13}	4.4×10^{13}	2.5×10^{1}	5.7×10^{-2}	1.17×10^{14}	1.99×10^{14}	
I	Xe	Cs	Ba	139	1.8×10^{-2}	1.5×10^{-3}	2.21×10^{9}	9.3×10^{-2}	4.7×10^{-2}	3.58×10^{11}	3.91×10^{11}	4.4×10^{0}	5.9×10^{-2}	2.13×10^{13}	2.67×10^{13}	2.4×10^{14}
Xe	Cs	Ba	La	140	3.7×10^{-2}	1.8×10^{-2}	5.45×10^{10}	1.8×10^{-1}	6.0×10^{-2}	8.84×10^{11}	1.11×10^{12}				1.85×10^{16}	2.42×10^{15}
Xe	Cs	Ba	La	141	1.8×10^{-2}	7.5×10^{-4}	1.11×10^{9}	3.6×10^{-4}	4.7×10^{-2}	1.385×10^{9}	2.04×10^{9}				2.2×10^{12}	2.73×10^{13}
Y	Zr	Nb		95	6.4×10^{-2}	6.5×10^{0}	3.4×10^{13}				2.95×10^{17}				1.64×10^{17}	
Cs	Ba	La		142	3.4×10^{-2}	1.3×10^{-1}	3.62×10^{11}	2×10^{0}		9.18×10^{12}	1.14×10^{13}				1.41×10^{14}	
Ba	La	Ce		143	4.9×10^{-2}	6×10^{-2}	2.4×10^{11}								8.83×10^{14}	

Table A.5. Activity of Fission Products Diffusing from UO_2 at 1000, 1200, and 1400°C*

Nuclide	λ (sec^{-1})	N at 1400°C	A at 1400°C (curies/cm^3)	A at 1200°C (curies/cm^3)	A at 1000°C (curies/cm^3)
Br^{84}	3.85×10^{-4}	2.88×10^{13}	3.0×10^{-1}	2.9×10^{-2}	2.32×10^{-3}
Br^{87}	1.25×10^{-2}	3.1×10^{10}	1.05×10^{-2}	1.0×10^{-3}	8.0×10^{-5}
Kr^{87}	1.48×10^{-4}	3.11×10^{14}	1.25×10^{0}	1.19×10^{-1}	9.52×10^{-3}
Kr^{88}	6.95×10^{-5}	1.05×10^{15}	1.97×10^{0}	1.88×10^{-1}	1.50×10^{-2}
Rb^{88}	6.49×10^{-4}	1.47×10^{14}	2.58×10^{0}	2.46×10^{-1}	1.97×10^{-2}
Rb^{89}	7.5×10^{-4}	4.96×10^{13}	1.01×10^{0}	9.6×10^{-2}	7.68×10^{-3}
Y^{90}	2.98×10^{-6}	7.34×10^{15}	5.9×10^{-1}	5.62×10^{-2}	4.50×10^{-3}
Y^{91m}	2.26×10^{-4}	5.41×10^{13}	3.31×10^{-1}	3.15×10^{-2}	2.52×10^{-3}
Y^{91}	1.38×10^{-7}	2.22×10^{17}	8.29×10^{-1}	7.9×10^{-2}	6.32×10^{-3}
Y^{92}	5.35×10^{-5}	2.09×10^{14}	3.02×10^{-1}	2.88×10^{-2}	2.30×10^{-3}
Y^{93}	1.93×10^{-5}	6.96×10^{13}	3.64×10^{-2}	3.47×10^{-3}	2.78×10^{-4}
Y^{94}	7.0×10^{-4}	1.04×10^{12}	1.97×10^{-2}	1.88×10^{-3}	1.50×10^{-4}
Zr^{95}	1.27×10^{-7}	2.95×10^{17}	1.01×10^{0}	9.63×10^{-2}	7.7×10^{-3}
Nb^{95}	2.29×10^{-7}	1.64×10^{17}	1.01×10^{0}	9.63×10^{-2}	7.7×10^{-3}
I^{131}	9.96×10^{-7}	4.75×10^{17}	1.28×10^{1}	1.22×10^{0}	9.76×10^{-2}
I^{132}	8.02×10^{-5}	9.37×10^{14}	2.04×10^{0}	1.94×10^{-1}	1.55×10^{-2}
Te^{133}	5.78×10^{-3}	0	0	0	0
I^{133}	9.25×10^{-6}	3.98×10^{16}	9.95×10^{0}	9.48×10^{-1}	7.58×10^{-2}
I^{134}	2.2×10^{-4}	3.36×10^{14}	2.0×10^{0}	1.9×10^{-1}	1.52×10^{-1}
I^{135}	2.89×10^{-5}	5.8×10^{15}	4.54×10^{0}	4.32×10^{-1}	3.46×10^{-2}
Xe^{135m}	7.4×10^{-4}	7.88×10^{13}	1.57×10^{0}	1.5×10^{-1}	1.2×10^{-2}
I^{136}	8.06×10^{-3}	6.6×10^{11}	1.44×10^{-1}	1.37×10^{-1}	1.10×10^{-2}
Ba^{137m}	4.4×10^{-3}	3.08×10^{14}	3.66×10^{1}	3.49×10^{0}	2.79×10^{-1}
Cs^{138}	3.62×10^{-4}	1.99×10^{14}	1.95×10^{0}	1.86×10^{-1}	1.49×10^{-2}
Ba^{139}	1.36×10^{-4}	2.4×10^{14}	8.82×10^{-1}	8.4×10^{-2}	6.72×10^{-3}
Ba^{140}	6.27×10^{-7}	1.85×10^{16}	3.14×10^{-1}	2.99×10^{-2}	2.39×10^{-3}
La^{140}	4.79×10^{-6}	2.42×10^{15}	3.12×10^{-1}	2.97×10^{-2}	2.38×10^{-3}
La^{141}	6.42×10^{-4}	2.73×10^{13}	4.74×10^{-1}	4.51×10^{-2}	3.61×10^{-3}
La^{142}	1.56×10^{-4}	1.41×10^{14}	5.94×10^{-1}	5.65×10^{-2}	4.52×10^{-3}
Ce^{143}	6.01×10^{-6}	8.83×10^{14}	1.44×10^{-1}	1.37×10^{-2}	1.11×10^{-3}
Xe^{135}	2.11×10^{-5}	1.67×10^{16}	9.52×10^{0}	9.06×10^{-1}	7.25×10^{-2}
Sr^{91}	1.99×10^{-5}	1.54×10^{15}	8.28×10^{-1}	7.89×10^{-2}	6.3×10^{-3}
$Te^{129-131}$		0	0	0	0
Total			95.9	9.26	1.02

*Assumptions: $\rho_{UO_2} = 0.91$, $t = 3 \times 10^8$ sec, power density = 1000 w/cm^3.

APPENDIX B. RELEASE OF FISSION PRODUCTS FROM THE GRAPHITE

The release of fission products from the graphite will be by diffusion of the fission products in the graphite. The source of the fission products in the graphite depends upon the UO_2 particle size. The half life of the nuclides is of greatest importance, since both the UO_2 and the graphite serve as excellent materials for retaining fission products for long enough times to allow short-lived nuclides to decay. For this study, with a UO_2 particle size of 200 μ, the source of fission products in the graphite due to recoil is assumed to be 3.5% for the heavy nuclides and 4.5% for the light nuclides. Calculations were based on 100% of the generated fission products being in the graphite, and then a correction was made to reflect the results for the 200-μ UO_2 particles.

The method used for the calculation of the release of activity was the same as that used for calculating the diffusion of fission products from UO_2. However, in this case the values of the diffusion coefficients used were for the diffusion of the various nuclides in graphite.

Since there was no information available which gave values of the diffusion coefficients of various fission-product elements in graphite as a function of temperature, the data for the release of various fission products as a function of time and temperature given in refs 1–5 were used to calculate a diffusion coefficient from the following expression, given in ref 1:

$$F = 1 + \frac{6}{\pi^4 \gamma^2} \sum_{n=1}^{\infty} \frac{1}{n^4} (e^{-n^2 \pi^2 \gamma^2} - 1) \ , \tag{5}$$

where

F = fractional release,

$\gamma = (Dt/a^2)^{1/2}$,

t = time, sec,

D = diffusion coefficient, cm^2/sec,

a = radius of sphere, cm.

---

[1] L. B. Doyle, *High-Temperature Diffusion of Individual Fission Elements from Uranium Carbide–Impregnated Graphite*, NAA-SR-255 (Sept. 11, 1953).

[2] C. A. Smith and C. T. Young, *Diffusion of Fission Fragments from Uranium-Impregnated Graphite*, NAA-SR-72 (May 4, 1951).

[3] C. T. Young and C. A. Smith, *Preliminary Experiments on Fission Product Diffusion from Uranium-Impregnated Graphite in the Range 1800°–2200° C*, NAA-SR-232 (March 25, 1953).

[4] D. Cubicciotti, *The Diffusion of Xenon from Uranium Carbide–Impregnated Graphite at High Temperatures*, NAA-SR-194 (Oct. 13, 1952).

[5] G. A. Cowan and C. J. Orth, *Diffusion of Fission Products at High Temperatures from Refractory Matrices*, 1958 Geneva Conference Paper No. 613.

Since the data in refs 1–5 gave values of F, t, and temperature, it was possible to obtain a value of D for a given temperature. To simplify the procedure, a curve of F vs γ was plotted based on Eq. (5). This is shown in Fig. B.1. A value of a was

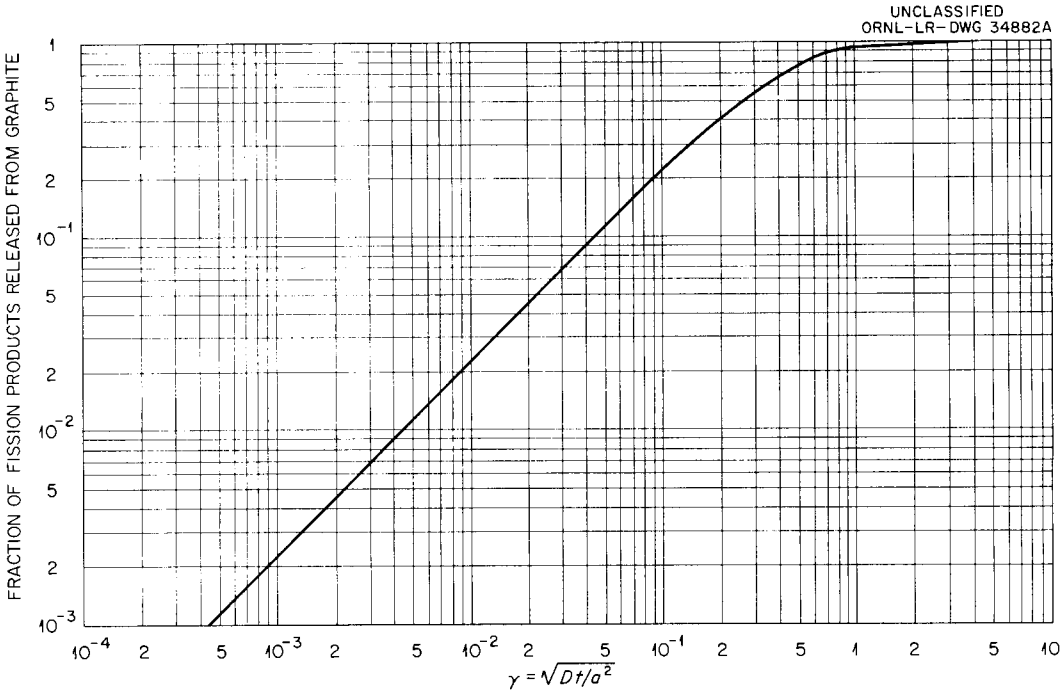

Fig. B.1. Fractional Release of Fission Products from Graphite.

calculated, using Eq. (4), based on the properties of graphite (ρ = 1.7 g/cm^3, S = 0.5 m^2/g),[6] and thus the value for the diffusion coefficient was

$$D = \frac{5.78 \times 10^{-8} \gamma^2}{t} .$$

Values of D are given in Table B.1 for the fission-product elements and are plotted in Fig. B.2.

With the values of D from Fig. B.2 it is possible to calculate d and obtain values of R from Fig. A.2, App. A. The method used is the same as outlined in App. A. Values of D and D/a^2 are given in Table B.2, values of R are given in Tables B.3 and B.4, and the results of the calculations of diffusion in the graphite are presented in Tables B.5–B.8.

---

[6] L. M. Currie, V. C. Hamister, and H. G. MacPherson, "The Production and Properties of Graphite for Reactors," *Proc. Intern. Conf. Peaceful Uses Atomic Energy, Geneva, 1955* 8, 451 (1955).

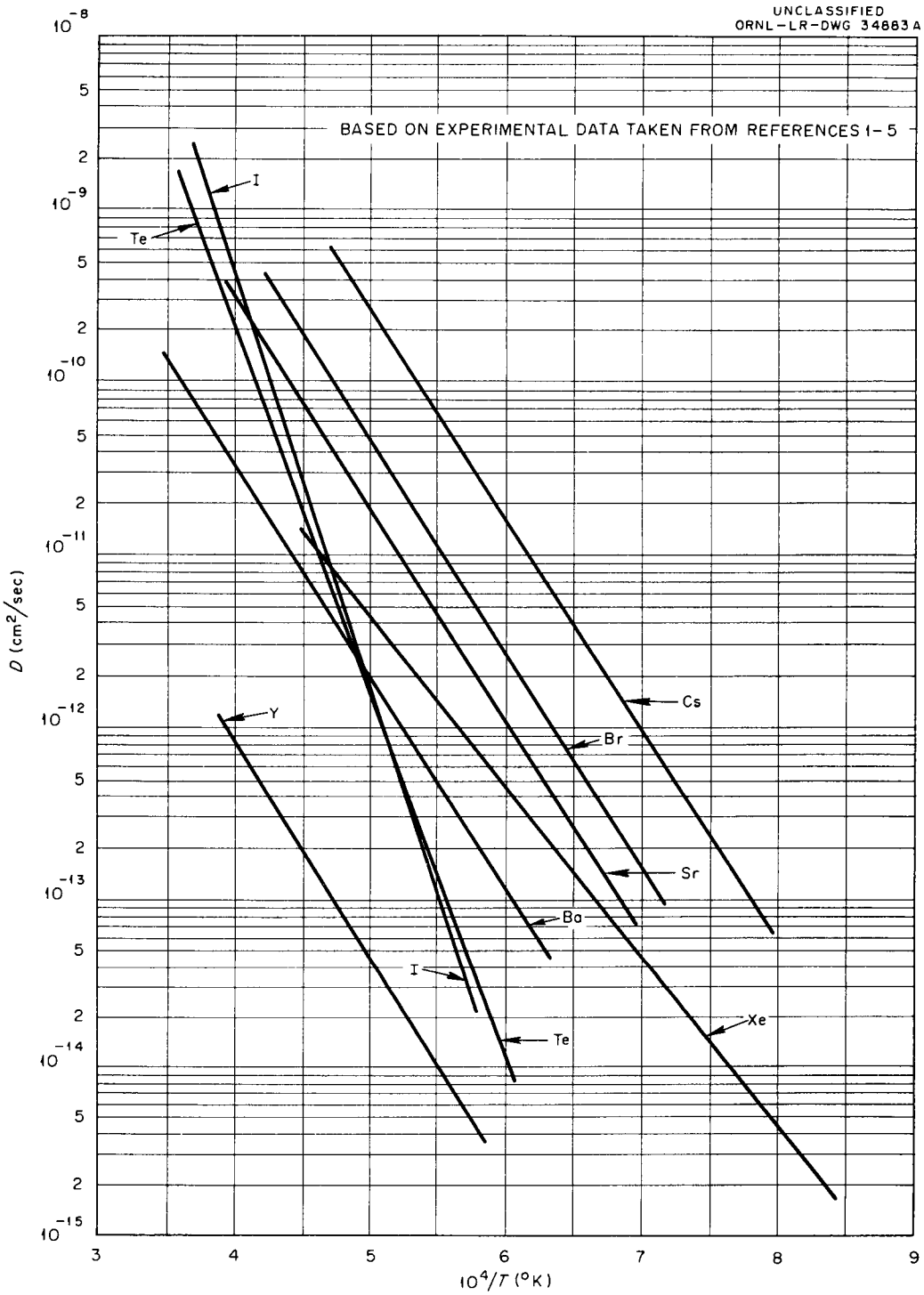

Fig. B.2. Diffusion Coefficients for Fission Products in Graphite.

Table B.1. Determination of Diffusion Coefficients for Fission Products in Graphite Based on Experimental Results in References 1 Through 5

Reference	Nuclide	Temperature (°C)	Time (sec)	Fraction Released	γ	γ^2	$D = \frac{5.78 \times 10^{-8} \gamma^2}{t}$	$10^4/T$ (°K^{-1})
1	Ba	1900	4800	0.90	8×10^{-1}	6.4×10^{-1}	7.71×10^{-12}	
		1700	7.2×10^{3}	0.53	2.9×10^{-1}	8.4×10^{-2}	6.75×10^{-13}	
		1500	5.4×10^{3}	0.15	6.7×10^{-2}	4.49×10^{-3}	4.8×10^{-14}	
		1700	4.32×10^{4}	0.947	1.3×10^{0}	1.69×10^{0}	2.26×10^{-12}	
		1700	2.16×10^{4}	0.80	5.4×10^{-1}	2.92×10^{-1}	7.81×10^{-13}	
		1700	1200	0.30	1.45×10^{-1}	2.1×10^{-2}	1.01×10^{-12}	
2	Ba	1560	1.8×10^{4}	0.81	5.6×10^{-1}	3.14×10^{-1}	1.01×10^{-12}	
1	Ba	1500	4.32×10^{4}	0.75	4.85×10^{-1}	2.35×10^{-1}	3.14×10^{-13}	
		1500	2.16×10^{4}	0.50	2.7×10^{-1}	7.3×10^{-2}	1.945×10^{-13}	
		1400	2700	0.80	5.4×10^{-1}	2.92×10^{-1}	6.25×10^{-12}	
		1400	1350	0.70	4.3×10^{-1}	1.85×10^{-1}	7.91×10^{-12}	
5	Ba	2600	30	0.50	2.7×10^{-1}	7.3×10^{-2}	1.4×10^{-10}	
		2200	30	0.09	3.9×10^{-2}	1.52×10^{-3}	2.93×10^{-12}	
3	Ba	1560	1.662×10^{4}	0.80	5.4×10^{-1}	2.92×10^{-1}	1.01×10^{-12}	
		1760	2.34×10^{3}	0.60	3.5×10^{-1}	1.23×10^{-1}	3.04×10^{-12}	
2	Sr	1200	9×10^{3}	0.40	2×10^{-1}	4×10^{-2}	2.56×10^{-13}	6.78
		1200	4320	0.20	9×10^{-2}	8.1×10^{-3}	1.08×10^{-13}	6.78
		1200	1.44×10^{4}	0.60	3.5×10^{-1}	1.23×10^{-1}	4.94×10^{-13}	6.78
3	Sr	1560	900	0.20	9×10^{-2}	8.1×10^{-3}	5.2×10^{-13}	5.45
		1560	1620	0.40	2×10^{-1}	4×10^{-2}	1.44×10^{-12}	5.45
		1560	2520	0.60	3.5×10^{-1}	1.23×10^{-1}	2.82×10^{-12}	5.45
		1760	840	0.40	2×10^{-1}	4×10^{-2}	2.75×10^{-12}	4.93
		1760	1200	0.60	3.5×10^{-1}	1.23×10^{-1}	5.92×10^{-12}	4.93
		1760	1800	0.89	7.3×10^{-1}	5.34×10^{-1}	1.71×10^{-11}	4.93
		1880	240	0.80	5.4×10^{-1}	2.92×10^{-1}	7.03×10^{-11}	4.65
		2100	90	0.80	5.4×10^{-1}	2.92×10^{-1}	1.87×10^{-10}	4.22
		2400	30	0.972	1.8×10^{0}	3.24×10^{0}	6.24×10^{-9}	3.74
		2400	40	0.99	3.0×10^{0}	9×10^{0}	1.3×10^{-8}	3.74
1	Cs	1500	1350	0.925	1×10^{0}	1×10^{0}	4.3×10^{-11}	5.63
		1500	600	0.7	3.5×10^{-1}	1.22×10^{-1}	1.2×10^{-11}	5.63
		1700	600	0.97	2×10^{0}	4×10^{0}	3.85×10^{-10}	5.06
		1700	300	0.83	6×10^{-1}	3.6×10^{-1}	7.0×10^{-11}	5.06
5	Br	1800	30	0.337	1.65×10^{-1}	2.72×10^{-2}	5.24×10^{-11}	4.83
		2000	30	0.434	2.25×10^{-1}	5.06×10^{-2}	9.75×10^{-11}	4.40
		2200	30	0.861	6.5×10^{-1}	4.225×10^{-1}	8.14×10^{-10}	4.05
		2400	30	0.915	8.3×10^{-1}	6.89×10^{-1}	1.33×10^{-9}	3.74
		2600	30	0.946	1.25×10^{0}	1.56×10^{0}	3.0×10^{-9}	3.48
5	I	1600	30	0.07	3×10^{-2}	9×10^{-4}	1.73×10^{-12}	5.33
		1800	30	0.09	4×10^{-2}	1.6×10^{-3}	3.08×10^{-12}	4.83
		2000	30	0.22	1×10^{-1}	1×10^{-2}	1.93×10^{-11}	4.40
		2200	30	0.45	2.35×10^{-1}	5.52×10^{-2}	1.06×10^{-10}	4.05
		2400	30	0.94	1.2×10^{0}	1.44×10^{0}	2.78×10^{-9}	3.74
1	I	1500	1350	0.13	5.8×10^{-2}	3.36×10^{-3}	1.44×10^{-13}	5.63
		1500	5400	0.27	1.3×10^{-1}	1.69×10^{-2}	1.81×10^{-13}	5.63

Table B.1 (continued)

Reference	Nuclide	Temperature (°C)	Time (sec)	Fraction Released	γ	γ^2	$D = \frac{5.78 \times 10^{-8} \gamma^2}{t}$	$10^4/T$ (°K^{-1})
1	I	1500	1.08×10^4	0.25	1.2×10^{-1}	1.44×10^{-2}	7.7×10^{-14}	5.63
		1500	2.16×10^4	0.33	1.6×10^{-1}	2.56×10^{-2}	6.85×10^{-14}	5.63
		1500	8.64×10^4	0.40	2×10^{-1}	4.0×10^{-2}	2.68×10^{-14}	5.63
		1700	1350	0.35	1.7×10^{-1}	2.89×10^{-2}	1.24×10^{-12}	5.06
		1700	2700	0.43	2.3×10^{-1}	5.29×10^{-2}	1.13×10^{-12}	5.06
		1700	5400	0.43	2.3×10^{-1}	5.29×10^{-2}	5.65×10^{-13}	5.06
		1700	1.08×10^4	0.58	3.3×10^{-1}	1.09×10^{-1}	5.84×10^{-13}	5.06
		1700	2.16×10^4	0.67	4.1×10^{-1}	1.68×10^{-1}	4.5×10^{-13}	5.06
		1700	8.64×10^4	0.85	6.15×10^{-1}	3.78×10^{-1}	2.53×10^{-13}	5.06
		1900	1350	0.858	6.5×10^{-1}	4.22×10^{-1}	1.81×10^{-11}	4.61
		1900	2700	0.929	1.05×10^0	1.1×10^0	2.35×10^{-11}	4.61
		1900	5400	0.958	1.4×10^0	1.96×10^0	2.1×10^{-11}	4.61
		1900	1.08×10^4	0.978	2×10^0	4×10^0	2.14×10^{-11}	4.61
		1900	2.16×10^4	0.9854	2.9×10^0	8.4×10^0	2.25×10^{-11}	4.61
		1900	4.32×10^4	0.993	3.4×10^0	1.15×10^1	1.54×10^{-11}	4.61
4	Xe	900	3600	0.0682	3×10^{-2}	9×10^{-4}	1.44×10^{-14}	8.51
		900	7200	0.072	3.1×10^{-2}	9.6×10^{-4}	7.7×10^{-15}	8.51
		1060	3600	0.0447	1.95×10^{-2}	3.8×10^{-4}	6.1×10^{-15}	7.5
		1060	7200	0.053	2.3×10^{-2}	5.3×10^{-4}	4.25×10^{-15}	7.5
		1020	3600	0.0682	3×10^{-2}	9×10^{-4}	1.44×10^{-14}	7.73
		1020	7200	0.072	3.1×10^{-2}	9.6×10^{-4}	7.7×10^{-15}	7.73
		1050	3600	0.0836	3.65×10^{-2}	1.33×10^{-3}	2.13×10^{-14}	7.55
		1050	7200	0.0894	3.9×10^{-2}	1.52×10^{-3}	1.22×10^{-14}	7.55
		1205	3600	0.167	7.5×10^{-2}	5.62×10^{-3}	9.0×10^{-14}	6.78
		1205	7200	0.179	8.2×10^{-2}	6.72×10^{-3}	5.4×10^{-14}	6.78
		1250	3600	0.1265	5.6×10^{-2}	3.14×10^{-3}	5.04×10^{-14}	6.56
		1250	7200	0.143	6.4×10^{-2}	4.1×10^{-3}	3.29×10^{-14}	6.56
		1200	3600	0.118	5.2×10^{-2}	2.7×10^{-3}	4.33×10^{-14}	6.78
		1200	7200	0.128	5.6×10^{-2}	3.14×10^{-3}	2.52×10^{-14}	6.78
		1225	3600	0.218	1.0×10^{-1}	1.0×10^{-2}	1.6×10^{-13}	6.68
		1225	7200	0.234	1.1×10^{-1}	1.21×10^{-2}	9.71×10^{-14}	6.68
		1500	3600	0.49	2.6×10^{-1}	6.75×10^{-2}	1.08×10^{-12}	5.63
		1500	7200	0.528	2.9×10^{-1}	8.4×10^{-2}	6.74×10^{-13}	5.63
		1500	3600	0.381	1.9×10^{-1}	3.61×10^{-2}	5.79×10^{-13}	5.63
		1500	7200	0.425	2.2×10^{-1}	4.84×10^{-2}	3.88×10^{-13}	5.63
		1490	3600	0.458	2.4×10^{-1}	5.76×10^{-2}	9.25×10^{-13}	5.97
		1490	7200	0.485	2.6×10^{-1}	6.76×10^{-2}	5.43×10^{-13}	5.97
		1490	3600	0.354	1.75×10^{-1}	3.06×10^{-2}	4.91×10^{-13}	5.97
		1490	7200	0.385	1.95×10^{-1}	3.8×10^{-2}	3.05×10^{-13}	5.97
5	Te	1800	30	0.02	8.7×10^{-3}	7.56×10^{-5}	1.46×10^{-13}	4.83
		2000	30	0.27	1.3×10^{-1}	1.69×10^{-2}	3.26×10^{-11}	4.40
		2200	30	0.35	1.7×10^{-1}	2.89×10^{-2}	5.36×10^{-11}	4.05
		2600	30	0.65	4.0×10^{-1}	1.6×10^{-1}	3.08×10^{-10}	3.48
		2400	30	0.84	6.0×10^{-1}	3.6×10^{-1}	6.92×10^{-10}	3.74
		2400	60	0.948	1.4×10^0	1.96×10^0	1.88×10^{-9}	3.74

Table B.1 (continued)

Reference	Nuclide	Temperature (°C)	Time (sec)	Fraction Released	γ	γ^2	$D = \frac{5.78 \times 10^{-8} \gamma^2}{t}$	$10^4/T$ (°K^{-1})
5	Te	2400	120	0.952	1.5×10^0	2.25×10^0	1.08×10^{-9}	3.74
		2400	240	0.966	1.7×10^0	2.9×10^0	6.98×10^{-10}	3.74
1	Te	1500	1350	0.20	9.1×10^{-2}	8.29×10^{-3}	3.55×10^{-13}	5.63
		1500	5400	0.24	1.15×10^{-1}	1.32×10^{-2}	1.41×10^{-13}	5.63
		1500	1.08×10^4	0.23	1.1×10^{-1}	1.21×10^{-2}	6.48×10^{-14}	5.63
		1500	2.16×10^4	0.30	1.45×10^{-1}	2.1×10^{-2}	5.61×10^{-14}	5.63
		1500	8.64×10^4	0.43	2.25×10^{-1}	5.06×10^{-2}	3.4×10^{-14}	5.63
		1700	1350	0.42	2.15×10^{-1}	4.63×10^{-2}	1.98×10^{-12}	5.06
		1700	2700	0.51	2.8×10^{-1}	7.85×10^{-2}	1.68×10^{-12}	5.06
		1700	5400	0.55	3.1×10^{-1}	9.6×10^{-2}	1.03×10^{-12}	5.06
		1700	1.08×10^4	0.65	3.9×10^{-1}	1.52×10^{-1}	8.14×10^{-13}	5.06
		1700	2.16×10^4	0.67	4.1×10^{-1}	1.68×10^{-1}	4.5×10^{-13}	5.06
		1700	8.64×10^4	0.92	9×10^{-1}	8.1×10^{-1}	5.43×10^{-13}	5.06
		1900	1350	0.83	5.9×10^{-1}	3.48×10^{-1}	1.49×10^{-11}	4.61
		1900	2700	0.905	8×10^{-1}	6.4×10^{-1}	1.37×10^{-11}	4.61
		1900	5400	0.94	1.2×10^0	1.44×10^0	1.54×10^{-11}	4.61
		1900	1.08×10^4	0.968	1.7×10^0	2.89×10^0	1.55×10^{-11}	4.61
		1900	4.32×10^4	0.987	2.8×10^0	7.85×10^0	1.05×10^{-11}	4.61
1	Y	1700	2.16×10^4	~0.15	6.7×10^{-2}	4.49×10^{-3}	1.2×10^{-14}	5.06
		1700	8.64×10^4	0.45	2.35×10^{-1}	5.52×10^{-2}	3.7×10^{-14}	5.06
		1900	1.08×10^4	~0.15	6.7×10^{-2}	4.49×10^{-3}	2.4×10^{-14}	4.61
		1900	4.32×10^4	0.56	3.15×10^{-1}	9.9×10^{-2}	1.33×10^{-13}	4.61

Table B.2. Diffusion Coefficients, D, and the Values of d for Fission Products in Graphite at Various Temperatures

Element	Values of D				$d = D/a^2$			
	At 1000°C	At 1200°C	At 1400°C	At 800°C	At 1200°C	At 1400°C	At 700°C	At 1000°C
Br	1.2×10^{-15}	2.6×10^{-13}	2.3×10^{-12}	1.8×10^{-16}	4.5×10^{-6}	3.4×10^{-5}	3.1×10^{-9}	2.08×10^{-8}
Kr	5.7×10^{-15}	6.7×10^{-14}	4.0×10^{-13}	2×10^{-16}	1.16×10^{-6}	6.92×10^{-6}	3.46×10^{-9}	9.86×10^{-8}
Rb	8×10^{-14}	1.7×10^{-12}	1.6×10^{-11}	1.4×10^{-15}	2.94×10^{-5}	2.77×10^{-4}	2.42×10^{-8}	1.38×10^{-7}
Sr	5×10^{-15}	1.2×10^{-13}	1.0×10^{-12}	7×10^{-17}	2.08×10^{-6}	1.73×10^{-5}	1.21×10^{-9}	8.65×10^{-8}
Y	5.3×10^{-18}	2.6×10^{-16}	2.0×10^{-15}	1.2×10^{-19}	4.5×10^{-9}	3.46×10^{-8}	2.08×10^{-12}	9.17×10^{-11}
Te	1×10^{-18}	2.6×10^{-16}	1.0×10^{-14}		4.5×10^{-9}	1.73×10^{-7}		1.73×10^{-11}
I	2.4×10^{-19}	1.0×10^{-16}	6.0×10^{-15}		1.73×10^{-9}	1.04×10^{-7}		4.15×10^{-12}
Xe	5.7×10^{-15}	6.7×10^{-14}	4.0×10^{-13}	2×10^{-16}	1.16×10^{-6}	6.92×10^{-6}	3.46×10^{-9}	9.86×10^{-8}
Cs	8×10^{-14}	1.7×10^{-12}	1.6×10^{-11}	1.4×10^{-15}	2.94×10^{-5}	2.77×10^{-4}	2.42×10^{-8}	1.38×10^{-7}
Bo	4.2×10^{-16}	1.0×10^{-14}	1.0×10^{-13}	5.6×10^{-18}	1.73×10^{-7}	1.73×10^{-6}	9.68×10^{-11}	7.27×10^{-9}

Table B.3. R Values for Various Fission Products at Fuel Temperatures of 800 and 1000°C

Nuclide	Decay Constant, λ (sec^{-1})	UO_2 at 800°C		UO_2 at 1000°C	
		$d = D/a^2$ (sec^{-1})	R	$d = D/a^2$ (sec^{-1})	R
Br^{84}	3.85×10^{-4}	3.1×10^{-9}	7.23×10^{0}	2.08×10^{-8}	1.87×10^{1}
Br^{87}	1.25×10^{-2}	3.1×10^{-9}	1.67×10^{-2}	2.08×10^{-8}	4.32×10^{-2}
Kr^{87}	1.48×10^{-4}	3.46×10^{-9}	3.23×10^{1}	9.86×10^{-8}	1.73×10^{2}
Br^{88}	4.47×10^{-2}	3.1×10^{-9}	6.12×10^{-3}	2.08×10^{-8}	1.56×10^{-2}
Kr^{88}	6.95×10^{-5}	3.46×10^{-9}	1.0×10^{2}	9.86×10^{-8}	5.34×10^{2}
Rb^{88}	6.49×10^{-4}	2.42×10^{-8}	9.95×10^{0}	1.38×10^{-7}	2.38×10^{1}
Kr^{89}	3.63×10^{-3}	3.46×10^{-9}	2.82×10^{-1}	9.86×10^{-8}	1.51×10^{0}
Rb^{89}	7.50×10^{-4}	2.42×10^{-8}	7.78×10^{0}	1.38×10^{-7}	1.86×10^{1}
Kr^{90}	2.10×10^{-2}	3.46×10^{-9}	2.0×10^{-2}	9.86×10^{-8}	1.07×10^{-1}
Rb^{90}	4.22×10^{-3}	2.42×10^{-8}	5.91×10^{-1}	1.38×10^{-7}	1.41×10^{0}
Sr^{90}	7.85×10^{-10}	1.21×10^{-9}	4.5×10^{7}	8.65×10^{-8}	6.5×10^{7}
Y^{90}	2.98×10^{-6}	2.08×10^{-12}	2.74×10^{2}	9.17×10^{-11}	1.82×10^{3}
Kr^{91}	7.08×10^{-2}	3.46×10^{-9}	3.18×10^{-3}	9.86×10^{-8}	1.70×10^{-2}
Rb^{91}	8.25×10^{-4}	2.42×10^{-8}	6.84×10^{0}	1.38×10^{-7}	1.63×10^{1}
Sr^{91}	1.99×10^{-5}	1.21×10^{-9}	4.0×10^{2}	8.65×10^{-8}	3.38×10^{3}
Y^{91m}	2.26×10^{-4}	2.08×10^{-12}	4.03×10^{-1}	9.17×10^{-11}	2.68×10^{0}
Y^{91}	1.38×10^{-7}	2.08×10^{-12}	2.74×10^{4}	9.17×10^{-11}	1.82×10^{5}
Kr^{92}	2.31×10^{-1}	3.46×10^{-9}	5.29×10^{-4}	9.86×10^{-8}	2.83×10^{-3}
Rb^{92}	8.66×10^{-3}	2.42×10^{-8}	2.02×10^{-1}	1.38×10^{-7}	4.83×10^{-1}
Sr^{92}	7.13×10^{-5}	1.21×10^{-9}	5.57×10^{1}	8.65×10^{-8}	4.70×10^{2}
Y^{92}	5.35×10^{-5}	2.08×10^{-12}	3.60×10^{0}	9.17×10^{-11}	2.40×10^{1}
Kr^{93}	3.47×10^{-1}	3.46×10^{-9}	2.94×10^{-4}	9.86×10^{-8}	1.57×10^{-3}
Rb^{93}	$\sim 6.94 \times 10^{-1}$	2.42×10^{-8}	2.72×10^{-4}	1.38×10^{-7}	6.5×10^{-4}
Sr^{93}	1.65×10^{-3}	1.21×10^{-9}	5.22×10^{-1}	8.65×10^{-8}	4.41×10^{0}
Y^{93}	1.93×10^{-5}	2.08×10^{-12}	1.73×10^{1}	9.17×10^{-11}	1.15×10^{2}
Kr^{94}	4.95×10^{-1}	3.46×10^{-9}	1.71×10^{-4}	9.86×10^{-8}	9.11×10^{-4}
Rb^{94}	$\sim 6.94 \times 10^{-1}$	2.42×10^{-8}	2.72×10^{-4}	1.38×10^{-7}	6.5×10^{-4}
Sr^{94}	5.78×10^{-3}	1.21×10^{-9}	8.0×10^{-2}	8.65×10^{-8}	6.76×10^{-1}
Y^{94}	7.0×10^{-4}	2.08×10^{-12}	7.93×10^{-2}	9.17×10^{-11}	5.27×10^{-1}
Te^{129m}	2.43×10^{-7}			1.73×10^{-11}	3.33×10^{4}
Te^{129}	1.6×10^{-4}			1.73×10^{-11}	1.58×10^{0}
Te^{131m}	6.42×10^{-5}			1.73×10^{-11}	7.90×10^{0}
Te^{131}	4.66×10^{-4}			1.73×10^{-11}	2.91×10^{-1}
I^{131}	9.96×10^{-7}			4.15×10^{-12}	2.04×10^{3}

Table B.3 (continued)

Nuclide	Decay Constant, λ (sec^{-1})	UO_2 at 800°C		UO_2 at 1000°C	
		$d = D/a^2$ (sec^{-1})	R	$d = D/a^2$ (sec^{-1})	R
Te^{132}	2.5×10^{-6}			1.73×10^{-11}	1.04×10^{3}
I^{132}	8.02×10^{-5}			4.15×10^{-12}	2.85×10^{0}
Te^{133m}	1.83×10^{-4}			1.73×10^{-11}	1.25×10^{0}
Te^{133}	5.78×10^{-3}			1.73×10^{-11}	9.57×10^{-3}
I^{133}	9.25×10^{-6}			4.15×10^{-12}	7.34×10^{1}
Te^{134}	2.63×10^{-4}			1.73×10^{-11}	9.15×10^{-1}
I^{134}	2.2×10^{-4}			4.15×10^{-12}	8.97×10^{-1}
Te^{135}	5.78×10^{-3}			1.73×10^{-11}	9.57×10^{-3}
I^{135}	2.89×10^{-5}			4.15×10^{-12}	1.32×10^{0}
Xe^{135m}	7.4×10^{-4}	3.46×10^{-9}	2.94×10^{0}	9.86×10^{-8}	1.57×10^{1}
I^{136}	8.06×10^{-3}			4.15×10^{-12}	2.85×10^{-3}
I^{137}	3.15×10^{-2}			9.15×10^{-12}	3.67×10^{-4}
Xe^{137}	2.96×10^{-3}	3.46×10^{-9}	3.82×10^{-1}	9.86×10^{-8}	2.04×10^{0}
Cs^{137}	8.27×10^{-10}	2.42×10^{-8}	6×10^{7}	1.38×10^{-7}	6.5×10^{7}
Ba^{137m}	4.44×10^{-3}	9.68×10^{-11}	3.44×10^{-2}	7.27×10^{-9}	2.98×10^{-1}
I^{138}	1.17×10^{-1}			4.15×10^{-12}	5.10×10^{-5}
Xe^{138}	6.79×10^{-4}	3.46×10^{-9}	3.35×10^{0}	9.86×10^{-8}	1.79×10^{1}
Cs^{138}	3.62×10^{-4}	2.42×10^{-8}	2.18×10^{1}	1.38×10^{-7}	5.2×10^{1}
I^{139}	2.57×10^{-1}			4.15×10^{-12}	1.53×10^{-5}
Xe^{139}	1.69×10^{-2}	3.46×10^{-9}	2.65×10^{-2}	9.86×10^{-8}	1.41×10^{-1}
Cs^{139}	1.22×10^{-3}	2.42×10^{-8}	3.73×10^{0}	1.38×10^{-7}	8.92×10^{0}
Ba^{139}	1.36×10^{-4}	9.68×10^{-11}	5.9×10^{0}	7.27×10^{-9}	5.11×10^{1}
Xe^{140}	4.33×10^{-2}	3.46×10^{-9}	6.47×10^{-3}	9.86×10^{-8}	3.45×10^{-2}
Cs^{140}	1.05×10^{-2}	2.42×10^{-8}	1.56×10^{-1}	1.38×10^{-7}	3.72×10^{-1}
Ba^{140}	6.27×10^{-7}	9.68×10^{-11}	1.97×10^{4}	7.27×10^{-9}	1.7×10^{5}
Xe^{141}	4.08×10^{-1}	3.46×10^{-9}	2.23×10^{-4}	9.86×10^{-8}	1.19×10^{-3}
Cs^{141}	$\sim 6.94 \times 10^{-1}$	2.42×10^{-8}	2.72×10^{-4}	1.38×10^{-7}	6.50×10^{-4}
Ba^{141}	6.42×10^{-4}	9.68×10^{-11}	6.4×10^{-1}	7.27×10^{-9}	5.55×10^{0}

Table B.4. R Values for Various Fission Products at Fuel Temperatures of 1200 and 1400°C

Nuclide	Decay Constant, λ (sec^{-1})	UO_2 at 1400°C		UO_2 at 1200°C	
		$d = D/a^2$ (sec^{-1})	R	$d = D/a^2$ (sec^{-1})	R
Br^{84}	3.85×10^{-4}	3.4×10^{-5}	5×10^{2}	4.5×10^{-6}	2.3×10^{2}
Br^{87}	1.25×10^{-2}	3.4×10^{-5}	3×10^{0}	4.5×10^{-6}	1×10^{0}
Kr^{87}	1.48×10^{-4}	6.92×10^{-6}	9×10^{2}	1.16×10^{-6}	6×10^{2}
Br^{88}	4.47×10^{-2}	3.4×10^{-5}	4.5×10^{-1}	4.5×10^{-6}	1.8×10^{-1}
Kr^{88}	6.95×10^{-5}	6.92×10^{-6}	2.8×10^{3}	1.16×10^{-6}	1.6×10^{3}
Rb^{88}	6.49×10^{-4}	2.77×10^{-4}	7.0×10^{2}	2.94×10^{-5}	2×10^{2}
Kr^{89}	3.63×10^{-3}	6.92×10^{-6}	9×10^{0}	1.16×10^{-6}	6×10^{0}
Rb^{89}	7.50×10^{-4}	2.77×10^{-4}	7×10^{2}	2.94×10^{-5}	2×10^{2}
Kr^{90}	2.10×10^{-2}	6.92×10^{-6}	7×10^{-1}	1.16×10^{-6}	4.5×10^{-1}
Rb^{90}	4.22×10^{-3}	2.77×10^{-4}	4×10^{1}	2.94×10^{-5}	1.5×10^{1}
Sr^{90}	7.85×10^{-10}	1.73×10^{-5}	7×10^{7}	2.08×10^{-6}	7×10^{7}
Y^{90}	2.98×10^{-6}	3.46×10^{-8}	2.5×10^{4}	4.5×10^{-9}	1×10^{4}
Kr^{91}	7.08×10^{-2}	6.92×10^{-6}	1×10^{-1}	1.16×10^{-6}	6.5×10^{-2}
Rb^{91}	8.25×10^{-4}	2.77×10^{-4}	6.5×10^{2}	2.94×10^{-5}	1.6×10^{2}
Sr^{91}	1.99×10^{-5}	1.73×10^{-5}	1.8×10^{4}	2.08×10^{-6}	1.0×10^{4}
Y^{91m}	2.26×10^{-4}	3.46×10^{-8}	4×10^{1}	4.5×10^{-9}	1.8×10^{1}
Y^{91}	1.38×10^{-7}	3.46×10^{-8}	1.5×10^{6}	4.5×10^{-9}	9.0×10^{5}
Kr^{92}	2.31×10^{-1}	6.42×10^{-6}	2.0×10^{-2}	1.16×10^{-6}	1.2×10^{-2}
Rb^{92}	8.66×10^{-3}	2.77×10^{-4}	1.8×10^{1}	2.94×10^{-5}	6.0×10^{0}
Sr^{92}	7.13×10^{-5}	1.73×10^{-5}	3.5×10^{3}	2.08×10^{-6}	1.8×10^{3}
Y^{92}	5.35×10^{-5}	3.46×10^{-8}	3.5×10^{2}	4.5×10^{-9}	1.4×10^{2}
Kr^{93}	3.47×10^{-1}	6.92×10^{-6}	1.1×10^{-2}	1.16×10^{-6}	7.0×10^{-3}
Rb^{93}	$\sim 6.94 \times 10^{-1}$	2.77×10^{-4}	2.5×10^{-2}	2.94×10^{-5}	1.7×10^{-2}
Sr^{93}	1.65×10^{-3}	1.73×10^{-5}	6.5×10^{1}	2.08×10^{-6}	2.0×10^{1}
Y^{93}	1.93×10^{-5}	3.46×10^{-8}	1.6×10^{3}	4.5×10^{-9}	6.5×10^{2}
Kr^{94}	4.95×10^{-1}	6.92×10^{-6}	6.5×10^{-3}	1.16×10^{-6}	4.0×10^{-3}
Rb^{94}	$\sim 6.94 \times 10^{-1}$	2.77×10^{-4}	2.4×10^{-2}	2.94×10^{-5}	9.0×10^{-3}
Sr^{94}	5.78×10^{-3}	1.73×10^{-5}	1.0×10^{1}	2.08×10^{-6}	3.2×10^{0}
Y^{94}	7.0×10^{-4}	3.46×10^{-8}	8×10^{0}	4.5×10^{-9}	3.0×10^{0}
Te^{129m}	2.43×10^{-7}	1.73×10^{-7}	1.1×10^{6}	4.5×10^{-9}	4.0×10^{5}
Te^{129}	1.6×10^{-4}	1.73×10^{-7}	2.1×10^{2}	4.5×10^{-9}	3.2×10^{1}
Te^{131m}	6.42×10^{-5}	1.73×10^{-7}	8×10^{2}	4.5×10^{-9}	1.1×10^{2}
Te^{131}	4.66×10^{-4}	1.73×10^{-7}	4.5×10^{1}	4.5×10^{-9}	5.8×10^{0}
I^{131}	9.96×10^{-7}	1.04×10^{-7}	2.2×10^{5}	1.73×10^{-9}	4.0×10^{4}

Table B.4 (continued)

Nuclide	Decay Constant, λ (sec^{-1})	UO_2 at 1400°C		UO_2 at 1200°C	
		$d = D/a^2$ (sec^{-1})	R	$d = D/a^2$ (sec^{-1})	R
Te^{132}	2.5×10^{-6}	1.73×10^{-7}	7.0×10^{4}	4.5×10^{-9}	1.3×10^{4}
I^{132}	8.02×10^{-5}	1.04×10^{-7}	5×10^{2}	1.73×10^{-9}	7.0×10^{1}
Te^{133m}	1.83×10^{-4}	1.73×10^{-7}	2.0×10^{2}	4.5×10^{-9}	3.0×10^{1}
Te^{133}	5.78×10^{-3}	1.73×10^{-7}	1.0×10^{0}	4.5×10^{-9}	1.4×10^{-1}
I^{133}	9.25×10^{-6}	1.04×10^{-7}	1.1×10^{4}	1.73×10^{-9}	1.5×10^{3}
Te^{134}	2.63×10^{-4}	1.73×10^{-7}	1.1×10^{2}	4.5×10^{-9}	1.5×10^{1}
I^{134}	2.2×10^{-4}	1.04×10^{-7}	1.1×10^{2}	1.73×10^{-9}	1.2×10^{1}
Te^{135}	5.78×10^{-3}	1.73×10^{-7}	1.0×10^{0}	4.5×10^{-9}	1.4×10^{-1}
I^{135}	2.89×10^{-5}	1.04×10^{-7}	2.3×10^{3}	1.73×10^{-9}	3.0×10^{2}
Xe^{135m}	7.4×10^{-4}	6.92×10^{-6}	2.3×10^{2}	1.16×10^{-6}	1.2×10^{2}
I^{136}	8.06×10^{-3}	1.04×10^{-7}	5.0×10^{-1}	1.73×10^{-9}	6.5×10^{-2}
I^{137}	3.15×10^{-2}	1.04×10^{-7}	6.5×10^{-2}	1.73×10^{-9}	8.0×10^{-3}
Xe^{137}	2.96×10^{-3}	6.92×10^{-6}	1.2×10^{1}	1.16×10^{-6}	7.0×10^{0}
Cs^{137}	8.27×10^{-10}	2.77×10^{-4}	7.0×10^{7}	2.94×10^{-5}	7.0×10^{7}
Ba^{137m}	4.44×10^{-3}	1.73×10^{-6}	4.0×10^{0}	1.73×10^{-7}	1.3×10^{0}
I^{138}	1.17×10^{-1}	1.04×10^{-7}	8.0×10^{-3}	1.73×10^{-9}	1.0×10^{-3}
Xe^{138}	6.79×10^{-4}	6.92×10^{-6}	1.0×10^{2}	1.16×10^{-6}	6.0×10^{1}
Cs^{138}	3.62×10^{-4}	2.77×10^{-4}	9.0×10^{2}	2.94×10^{-5}	5.5×10^{2}
I^{139}	2.57×10^{-1}	1.04×10^{-7}	2.7×10^{-3}	1.73×10^{-9}	3.5×10^{-4}
Xe^{139}	1.69×10^{-2}	6.92×10^{-6}	8.0×10^{-1}	1.16×10^{-6}	4.0×10^{-1}
Cs^{139}	1.22×10^{-3}	2.77×10^{-4}	2.0×10^{2}	2.94×10^{-5}	9.0×10^{1}
Ba^{139}	1.36×10^{-4}	1.73×10^{-6}	7.0×10^{2}	1.73×10^{-7}	3.0×10^{2}
Xe^{140}	4.33×10^{-2}	6.92×10^{-6}	2.0×10^{-1}	1.16×10^{-6}	1.2×10^{-1}
Cs^{140}	1.05×10^{-2}	2.77×10^{-4}	1.1×10^{1}	2.94×10^{-5}	4.0×10^{0}
Ba^{140}	6.27×10^{-7}	1.73×10^{-6}	6.5×10^{5}	1.73×10^{-7}	4.0×10^{5}
Xe^{141}	4.08×10^{-1}	6.92×10^{-6}	8.0×10^{-3}	1.16×10^{-6}	4.5×10^{-3}
Cs^{141}	$\sim 6.94 \times 10^{-1}$	2.77×10^{-4}	2.5×10^{-2}	2.94×10^{-5}	1.7×10^{-2}
Ba^{141}	6.42×10^{-4}	1.73×10^{-6}	7.0×10^{1}	1.73×10^{-7}	2.6×10^{1}

Table B.5. Results of Calculations of Diffusion of Fission Products in Graphite at 800°C

Decay Scheme $A \rightarrow B \rightarrow C \rightarrow D$				Chain	R_A	γ_A	$A_L = A_G$	R_B	γ'_B	B_L	B_G	R_C	γ'_C	C_L	C_G	R_D	γ'_D	D_L	D_G
Br				84	7.23×10^{0}	1.1×10^{-2}	4.87×10^{12}												
Br	Kr			87	1.67×10^{-2}	2.7×10^{-2}	2.76×10^{10}	3.23×10^{1}	2.64×10^{-2}	5.22×10^{13}	5.45×10^{13}								
Br	Kr	Rb		88	6.12×10^{-3}	2.9×10^{-2}	1.09×10^{10}	1.0×10^{2}	3.7×10^{-2}	2.26×10^{14}	2.33×10^{14}	9.95×10^{0}	3.7×10^{-2}	2.25×10^{13}	4.54×10^{13}				
Kr	Rb			89	2.82×10^{-1}	4.6×10^{-2}	7.94×10^{11}	7.78×10^{0}	4.8×10^{-2}	2.29×10^{13}	2.63×10^{13}								
Kr	Rb	Sr	Y	90	2.0×10^{-2}	5.2×10^{-2}	6.36×10^{10}	5.91×10^{-1}	5.9×10^{-2}	2.13×10^{12}	2.44×10^{12}	4.5×10^{7}	5.9×10^{-2}	1.62×10^{20}	1.75×10^{20}	2.74×10^{2}	$\sim 4 \times 10^{-2}$	6.7×10^{14}	4.69×10^{16}
			Y^m													4.03×10^{-1}	2.4×10^{-2}	5.92×10^{11}	3.4×10^{13}
Kr	Rb	Sr	Y	91	3.18×10^{-3}	3.7×10^{-2}	7.2×10^{9}	6.84×10^{0}	5.7×10^{-2}	2.34×10^{13}	2.40×10^{13}	4.0×10^{2}	5.9×10^{-2}	1.44×10^{15}	2.44×10^{15}	2.74×10^{4}	5.9×10^{-2}	9.89×10^{16}	4.5×10^{17}
Kr	Rb	Sr	Y	92	5.29×10^{-4}	2.7×10^{-2}	8.74×10^{8}	2.02×10^{-1}	5.5×10^{-2}	6.80×10^{11}	7.03×10^{11}	5.57×10^{1}	6.1×10^{-2}	2.08×10^{14}	2.93×10^{14}	3.6×10^{0}	6.1×10^{-2}	1.34×10^{13}	4.03×10^{14}
Kr	Rb	Sr	Y	93	2.94×10^{-4}	1.3×10^{-2}	2.34×10^{8}	2.72×10^{-4}	4.4×10^{-2}	7.32×10^{8}	8.49×10^{8}	5.22×10^{-1}	6.4×10^{-2}	2.04×10^{12}	2.4×10^{12}	1.73×10^{1}	6.5×10^{-2}	6.88×10^{13}	2.74×10^{14}
Kr	Rb	Sr	Y	94	1.71×10^{-4}	6×10^{-3}	6.28×10^{7}	2.72×10^{-4}	2.9×10^{-2}	4.83×10^{8}	5.28×10^{8}	8.0×10^{-2}	5.8×10^{-2}	2.84×10^{11}	3.47×10^{11}	7.93×10^{-2}	6.5×10^{-2}	3.15×10^{11}	3.18×10^{12}
Te^m	Te			129		2.4×10^{-3}			1.0×10^{-2}										
Te^m	Te	I		131		4×10^{-3}			2.9×10^{-2}				2.9×10^{-2}						
Te	I			132		4.4×10^{-2}			4.4×10^{-2}										
Te^m	Te	I		133		4.6×10^{-2}			6.0×10^{-2}				6.5×10^{-2}						
Te	I			134		6.7×10^{-2}			7.6×10^{-2}										
Te	I	Xe^m		135		4.2×10^{-2}			5.9×10^{-2}			2.94×10^{0}	1.8×10^{-2}	3.24×10^{12}	3.24×10^{12}				
I				136		3.1×10^{-2}													
I	Xe	Cs	Ba^m	137		4.9×10^{-2}		3.82×10^{-1}	5.9×10^{-2}	1.38×10^{12}	1.38×10^{12}	6×10^{7}	5.9×10^{-2}	2.17×10^{20}	2.22×10^{20}	3.44×10^{-2}	$\sim 3.5 \times 10^{-2}$	7.37×10^{10}	3.82×10^{13}
I	Xe	Cs		138		3.4×10^{-2}		3.35×10^{0}	5.5×10^{-2}	1.13×10^{13}	1.13×10^{13}	2.18×10^{1}	5.8×10^{-2}	7.74×10^{13}	9.85×10^{13}				
I	Xe	Cs	Ba	139		1.8×10^{-2}		2.65×10^{-2}	4.7×10^{-2}	7.62×10^{10}	7.62×10^{10}	3.73×10^{0}	5.9×10^{-2}	1.35×10^{13}	1.46×10^{13}	5.9×10^{0}	6.0×10^{-2}	2.17×10^{13}	1.53×10^{14}
Xe	Cs	Ba	La	140	6.47×10^{-3}	3.7×10^{-2}	1.47×10^{10}	1.56×10^{-1}	6.0×10^{-2}	5.73×10^{11}	6.34×10^{11}	1.97×10^{4}	6.3×10^{-2}	7.60×10^{16}	8.66×10^{16}				1.13×10^{16}
Xe	Cs	Ba	La	141	2.23×10^{-4}	1.8×10^{-2}	2.46×10^{8}	2.72×10^{-4}	4.7×10^{-2}	7.82×10^{8}	9.27×10^{8}	6.4×10^{-1}	5.9×10^{-2}	2.31×10^{12}	3.31×10^{12}				4.1×10^{13}
Y	Zr	Nb		95	4×10^{-2}	6.4×10^{-2}	1.54×10^{11}				1.335×10^{15}				7.41×10^{14}				
Cs	Ba	La		142	1.2×10^{-1}	3.4×10^{-2}	2.5×10^{11}	1×10^{-1}	5.6×10^{-2}	3.42×10^{11}	1.84×10^{12}				2.28×10^{13}				
Ba	La	Ce		143	2×10^{-3}	4.9×10^{-2}	6×10^{9}								2.3×10^{13}				

Table B.6. Results of Calculations of Diffusion of Fission Products in Graphite at 1000°C

Decay Scheme $A \rightarrow B \rightarrow C \rightarrow D$				Chain	R_A	γ_A	$A_L = A_G$	R_B	γ'_B	B_L	B_G	R_C	γ'_C	C_L	C_G	R_D	γ'_D	D_L	D_G
Br				84	1.87×10^{1}	1.1×10^{-2}	1.26×10^{13}												
Br	Kr			87	4.32×10^{-2}	2.7×10^{-2}	7.14×10^{10}	1.73×10^{2}	2.64×10^{-2}	2.80×10^{14}	2.86×10^{14}								
Br	Kr	Rb		88	1.56×10^{-2}	2.9×10^{-2}	2.77×10^{10}	5.34×10^{2}	3.7×10^{-2}	1.21×10^{15}	1.23×10^{15}	2.38×10^{1}	3.7×10^{-2}	5.39×10^{13}	1.86×10^{14}				
Kr	Rb			89	1.51×10^{0}	4.6×10^{-2}	4.25×10^{12}	1.86×10^{1}	4.8×10^{-2}	5.46×10^{13}	7.26×10^{13}								
Kr	Rb	Sr	Y	90	1.07×10^{-1}	5.2×10^{-2}	3.41×10^{11}	1.41×10^{0}	5.9×10^{-2}	5.09×10^{12}	6.78×10^{12}	6.5×10^{7}	5.9×10^{-2}	2.35×10^{20}	2.72×10^{20}	1.82×10^{3}	4.5×10^{-2}	5.02×10^{15}	7.68×10^{16}
Kr	Rb	Sr	Y^m	91												2.68×10^{0}	2.4×10^{-2}	3.94×10^{12}	5.21×10^{14}
			Y	91	1.70×10^{-2}	3.7×10^{-2}	3.85×10^{10}	1.63×10^{1}	5.7×10^{-2}	5.69×10^{13}	6.02×10^{13}	3.38×10^{3}	5.9×10^{-2}	1.22×10^{16}	1.47×10^{16}	1.82×10^{5}	5.9×10^{-2}	6.57×10^{17}	2.78×10^{18}
Kr	Rb	Sr	Y	92	2.83×10^{-3}	2.7×10^{-2}	4.68×10^{9}	4.83×10^{-1}	5.5×10^{-2}	1.63×10^{12}	1.75×10^{12}	4.70×10^{2}	6.1×10^{-2}	1.75×10^{15}	1.96×10^{15}	2.40×10^{1}	6.1×10^{-2}	8.96×10^{13}	2.70×10^{15}
Kr	Rb	Sr	Y	93	1.57×10^{-3}	1.3×10^{-2}	1.25×10^{9}	6.5×10^{-4}	4.4×10^{-2}	1.75×10^{9}	2.38×10^{9}	4.41×10^{0}	6.4×10^{-2}	1.73×10^{13}	1.83×10^{13}	1.15×10^{2}	6.5×10^{-2}	4.57×10^{14}	2.02×10^{15}
Kr	Rb	Sr	Y	94	9.11×10^{-4}	6.0×10^{-3}	3.35×10^{8}	6.5×10^{-4}	2.9×10^{-2}	1.15×10^{9}	1.39×10^{9}	6.76×10^{-1}	5.8×10^{-2}	2.40×10^{12}	2.57×10^{12}	5.27×10^{-1}	6.5×10^{-2}	2.10×10^{12}	2.33×10^{13}
Te^m	Te			129	3.33×10^{4}	2.4×10^{-3}	4.89×10^{15}	1.58×10^{0}	1.0×10^{-2}	9.67×10^{11}	8.40×10^{12}								
Te^m	Te	I		131	7.9×10^{0}	4.0×10^{-3}	1.93×10^{12}	2.91×10^{-1}	2.9×10^{-2}	5.16×10^{11}	5.43×10^{11}	2.04×10^{3}	2.9×10^{-2}	3.62×10^{15}	4.15×10^{15}				
Te	I			132	1.04×10^{3}	4.4×10^{-2}	2.80×10^{15}	2.85×10^{0}	4.4×10^{-2}	7.67×10^{12}	9.51×10^{13}								
Te^m	Te	I		133	1.25×10^{0}	4.6×10^{-2}	3.52×10^{12}	9.57×10^{-3}	6.0×10^{-2}	3.51×10^{10}	1.47×10^{11}	7.34×10^{1}	6.5×10^{-2}	2.92×10^{14}	3.84×10^{14}				
Te	I			134	9.15×10^{-1}	6.7×10^{-2}	3.75×10^{12}	8.97×10^{-1}	7.6×10^{-2}	4.17×10^{12}	8.63×10^{12}								
Te	I	Xe^m		135	9.57×10^{-3}	4.2×10^{-2}	2.46×10^{10}	1.32×10^{0}	5.9×10^{-2}	4.04×10^{12}	8.96×10^{12}	1.57×10^{1}	1.8×10^{-2}	1.73×10^{13}	1.74×10^{13}				
I				136	2.85×10^{-3}	3.1×10^{-2}	5.41×10^{9}												
I	Xe	Cs	Ba^m	137	3.67×10^{-4}	4.9×10^{-2}	1.10×10^{9}	2.04×10^{0}	5.9×10^{-2}	7.37×10^{12}	7.38×10^{12}	6.5×10^{7}	5.9×10^{-2}	2.35×10^{20}	2.61×10^{20}	2.98×10^{-1}	4×10^{-2}	7.3×10^{11}	4.56×10^{13}
I	Xe	Cs		138	5.1×10^{-5}	3.4×10^{-2}	1.06×10^{8}	1.79×10^{1}	5.5×10^{-2}	6.03×10^{13}	6.03×10^{13}	5.2×10^{1}	5.8×10^{-2}	1.85×10^{14}	2.95×10^{14}				
I	Xe	Cs	Ba	139	1.53×10^{-5}	1.8×10^{-2}	1.69×10^{7}	1.41×10^{-1}	4.7×10^{-2}	4.06×10^{11}	4.06×10^{11}	8.92×10^{0}	5.9×10^{-2}	3.22×10^{13}	3.78×10^{13}	5.11×10^{1}	6.0×10^{-2}	1.87×10^{14}	5.26×10^{14}
Xe	Cs	Ba	La	140	3.45×10^{-2}	3.7×10^{-2}	7.81×10^{10}	3.72×10^{-1}	6.0×10^{-2}	1.37×10^{12}	1.69×10^{12}	1.7×10^{5}	6.3×10^{-2}	6.55×10^{17}	6.38×10^{17}				8.95×10^{16}
Xe	Cs	Ba	La	141	1.19×10^{-3}	1.8×10^{-2}	1.31×10^{9}	6.5×10^{-4}	4.7×10^{-2}	1.87×10^{9}	2.64×10^{9}	5.55×10^{0}	5.9×10^{-2}	2.0×10^{13}	2.29×10^{13}				2.84×10^{14}
Y	Zr	Nb		95	3×10^{-1}	6.4×10^{-2}	1.175×10^{12}				1.02×10^{16}				5.66×10^{15}				
Cs	Ba	La		142	3.7×10^{-1}	3.4×10^{-2}	7.7×10^{11}	9×10^{-1}	5.6×10^{-2}	3.08×10^{12}	7.72×10^{12}				9.56×10^{13}				
Ba	La	Ce		143	2.2×10^{-2}	4.9×10^{-2}	6.6×10^{10}								2.54×10^{14}				

Table B.7. Results of Calculations of Diffusion of Fission Products in Graphite at 1200°C

Decay Scheme $A \rightarrow B \rightarrow C \rightarrow D$	Chain	R_A	γ_A	$A_L = A_G$	R_B	γ'_B	B_L	B_G	R_C	γ'_C	C_L	C_G	R_D	γ'_D	D_L	D_G
Br	84	2.3×10^{2}	1.1×10^{-2}	1.55×10^{14}												
Br Kr	87	1×10^{0}	2.7×10^{-2}	1.65×10^{12}	6×10^{2}	2.61×10^{-2}	9.6×10^{14}	1.18×10^{15}								
Br Kr Rb	88	1.8×10^{-1}	2.9×10^{-2}	3.2×10^{11}	1.6×10^{3}	3.66×10^{-2}	3.58×10^{15}	3.79×10^{15}	2×10^{2}	2.83×10^{-2}	3.46×10^{14}	7.51×10^{14}				
Kr Rb	89	6.0×10^{0}	4.6×10^{-2}	1.69×10^{13}	2×10^{2}	4.6×10^{-2}	5.64×10^{14}	6.36×10^{14}								
Kr Rb Sr Y	90	4.5×10^{-1}	5.2×10^{-2}	1.43×10^{12}	1.5×10^{1}	5.8×10^{-2}	5.33×10^{13}	6.04×10^{13}	7×10^{7}	5.05×10^{-2}	2.16×10^{20}	5.4×10^{20}	1×10^{4}	5×10^{-2}	3.06×10^{16}	1.73×10^{17}
Kr Rb Sr Y^m	91												1.8×10^{1}	1.03×10^{-2}	1.13×10^{13}	4.43×10^{15}
Y	91	6.5×10^{-2}	3.7×10^{-2}	1.47×10^{11}	1.6×10^{2}	5.68×10^{-2}	5.57×10^{14}	5.70×10^{14}	1×10^{4}	4.35×10^{-2}	2.66×10^{16}	5.02×10^{16}	9.0×10^{5}	2.58×10^{-2}	1.42×10^{18}	8.65×10^{18}
Kr Rb Sr Y	92	1.2×10^{-2}	2.7×10^{-2}	1.99×10^{10}	6.0×10^{0}	5.48×10^{-2}	2.01×10^{13}	2.06×10^{13}	1.8×10^{3}	5.5×10^{-2}	6.06×10^{15}	8.57×10^{15}	1.4×10^{2}	4.05×10^{-2}	3.47×10^{14}	1.17×10^{16}
Kr Rb Sr Y	93	7.0×10^{-3}	1.3×10^{-2}	5.55×10^{9}	1.7×10^{-2}	4.4×10^{-2}	4.58×10^{10}	4.86×10^{10}	2.0×10^{1}	6.3×10^{-2}	7.71×10^{13}	9.75×10^{13}	6.5×10^{2}	3.46×10^{-2}	1.38×10^{15}	9.69×10^{15}
Kr Rb Sr Y	94	4.0×10^{-3}	6.0×10^{-3}	1.47×10^{9}	9.0×10^{-3}	2.9×10^{-2}	1.6×10^{10}	1.71×10^{10}	3.2×10^{0}	5.76×10^{-2}	1.13×10^{13}	1.33×10^{13}	3.0×10^{0}	6.25×10^{-2}	1.14×10^{13}	1.21×10^{14}
Te^m Te	129	4.0×10^{5}	2.4×10^{-3}	5.87×10^{16}	3.2×10^{1}	9.5×10^{-3}	1.86×10^{13}	1.078×10^{14}								
Te^m Te I	131	1.1×10^{2}	4.0×10^{-3}	2.69×10^{13}	5.8×10^{0}	2.89×10^{-2}	1.025×10^{13}	1.06×10^{13}	4×10^{4}	2.87×10^{-2}	7.03×10^{16}	8.09×10^{16}				
Te I	132	1.3×10^{4}	4.4×10^{-2}	3.50×10^{16}	7.0×10^{1}	4.11×10^{-2}	1.76×10^{14}	1.27×10^{15}								
Te^m Te I	133	3.0×10^{1}	4.6×10^{-2}	8.45×10^{13}	1.4×10^{-1}	5.95×10^{-2}	5.1×10^{11}	3.19×10^{12}	1.5×10^{3}	6.45×10^{-2}	5.94×10^{15}	7.93×10^{15}				
Te I	134	1.5×10^{1}	6.7×10^{-2}	6.15×10^{13}	1.2×10^{1}	7.55×10^{-2}	5.55×10^{13}	1.286×10^{14}								
Te I Xe^m	135	1.4×10^{-1}	4.2×10^{-2}	3.6×10^{11}	3.0×10^{2}	5.9×10^{-2}	1.08×10^{15}	1.15×10^{15}	1.2×10^{2}	1.74×10^{-2}	1.28×10^{14}	1.42×10^{14}				
I	136	6.5×10^{-2}	3.1×10^{-2}	1.24×10^{11}												
I Xe Cs Ba^m	137	8.0×10^{-3}	4.9×10^{-2}	2.4×10^{10}	7.0×10^{0}	5.9×10^{-2}	2.52×10^{13}	2.54×10^{13}	7.0×10^{7}	5.65×10^{-2}	2.42×10^{20}	3.33×10^{20}	1.3×10^{0}	4.6×10^{-2}	3.66×10^{12}	6.03×10^{13}
I Xe Cs	138	1.0×10^{-3}	3.4×10^{-2}	2.08×10^{9}	6.0×10^{1}	5.5×10^{-2}	2.02×10^{14}	2.02×10^{14}	5.5×10^{2}	5.35×10^{-2}	1.81×10^{15}	2.19×10^{15}				
I Xe Cs Ba	139	3.5×10^{-4}	1.8×10^{-2}	3.86×10^{8}	4.0×10^{-1}	4.7×10^{-2}	1.15×10^{12}	1.15×10^{12}	9.0×10^{1}	5.83×10^{-2}	3.21×10^{14}	3.37×10^{14}	3.0×10^{2}	4.62×10^{-2}	8.48×10^{14}	3.87×10^{15}
Xe Cs Ba La	140	1.2×10^{-1}	3.7×10^{-2}	2.72×10^{11}	4.0×10^{0}	5.97×10^{-2}	1.46×10^{13}	1.57×10^{13}	4.0×10^{5}	5.76×10^{-2}	1.41×10^{18}	1.67×10^{18}				2.19×10^{17}
Xe Cs Ba La	141	4.5×10^{-3}	1.8×10^{-2}	4.96×10^{9}	1.7×10^{-2}	4.7×10^{-2}	4.89×10^{10}	5.18×10^{10}	2.6×10^{1}	5.8×10^{-2}	9.22×10^{13}	1.48×10^{14}				1.84×10^{15}
Y Zr Nb	95	1.8×10^{0}	6.4×10^{-2}	7.05×10^{12}				6.12×10^{16}				3.4×10^{16}				
Cs Ba La	142	3.7×10^{0}	3.4×10^{-2}	7.7×10^{12}	4.5×10^{0}		1.54×10^{13}	6.17×10^{13}				7.65×10^{14}				
Ba La Ce	143	1.2×10^{-1}	4.9×10^{-2}									1.38×10^{15}				

Table B.8. Results of Calculations of Diffusion of Fission Products in Graphite at 1400°C

Decay Scheme $A \rightarrow B \rightarrow C \rightarrow D$				Chain	γ_A	R_A	$A_L = A_G$	R_B	γ'_B	B_L	B_G	R_C	γ'_C	C_L	C_G	R_D	γ'_D	D_L	D_G
Br				84	1.1×10^{-2}	5×10^{2}	3.37×10^{14}												
Br	Kr			87	2.7×10^{-2}	3×10^{0}	4.95×10^{12}	9×10^{2}	2.44×10^{-2}	1.34×10^{15}	1.75×10^{15}								
Br	Kr	Rb		88	2.9×10^{-2}	4.5×10^{-1}	8.0×10^{11}	2.8×10^{3}	3.58×10^{-2}	6.15×10^{15}	6.67×10^{15}	7×10^{2}	2.15×10^{-2}	9.3×10^{14}	1.64×10^{15}				
Kr	Rb			89	4.6×10^{-2}	9×10^{0}	2.54×10^{13}	7×10^{2}	4.5×10^{-2}	1.93×10^{15}	2.04×10^{15}								
Kr	Rb	Sr	Y	90	5.2×10^{-2}	7×10^{-1}	2.22×10^{12}	4×10^{1}	5.75×10^{-2}	1.41×10^{14}	1.52×10^{14}	7×10^{7}	3.68×10^{-2}	1.59×10^{-2}	9.77×10^{20}	2.5×10^{4}	3.26×10^{-2}	5.0×10^{16}	3.08×10^{17}
Kr	Rb	Sr	Y^m	91												4×10^{1}	2.16×10^{-4}	5.3×10^{11}	8.5×10^{15}
			Y	91	3.7×10^{-2}	1×10^{-1}	2.26×10^{11}	6.5×10^{2}	5.65×10^{-2}	2.25×10^{15}	2.27×10^{15}	1.8×10^{4}	2×10^{-3}	2.2×10^{15}	9.65×10^{16}	1.5×10^{6}	5.4×10^{-4}	4.96×10^{16}	1.39×10^{19}
Kr	Rb	Sr	Y	92	2.7×10^{-2}	2×10^{-2}	3.32×10^{10}	1.8×10^{1}	5.48×10^{-2}	6.06×10^{13}	6.15×10^{13}	3.5×10^{3}	4.32×10^{-2}	9.27×10^{15}	1.68×10^{16}	3.5×10^{2}	2.1×10^{-2}	4.52×10^{14}	2.26×10^{16}
Kr	Rb	Sr	Y	93	1.3×10^{-2}	1.1×10^{-2}	8.72×10^{9}	2.5×10^{-2}	4.39×10^{-2}	6.71×10^{10}	7.15×10^{10}	6.5×10^{1}	6.22×10^{-2}	2.48×10^{14}	2.78×10^{14}	1.6×10^{3}	4.96×10^{-2}	4.86×10^{15}	2.87×10^{16}
Kr	Rb	Sr	Y	94	6.0×10^{-3}	6.5×10^{-3}	2.38×10^{9}	2.5×10^{-2}	2.895×10^{-2}	4.42×10^{10}	4.59×10^{10}	1.0×10^{1}	5.7×10^{-2}	3.49×10^{13}	4.04×10^{13}	8×10^{0}	5.73×10^{-2}	2.8×10^{13}	3.61×10^{14}
Te^m	Te			129	2.4×10^{-3}	1.1×10^{6}	1.62×10^{17}	2.1×10^{2}	8.9×10^{-3}	1.14×10^{14}	3.6×10^{14}								
Te^m	Te	I		131	4.0×10^{-3}	8.0×10^{2}	1.96×10^{14}	4.5×10^{1}	2.86×10^{-2}	7.88×10^{13}	8.15×10^{13}	2.2×10^{5}	2.72×10^{-2}	3.66×10^{17}	4.45×10^{17}				
Te	I			132	4.4×10^{-2}	7.0×10^{4}	1.88×10^{17}	5.0×10^{2}	2.84×10^{-2}	8.71×10^{14}	6.40×10^{15}								
Te^m	Te	I		133	4.6×10^{-2}	2.0×10^{2}	5.65×10^{14}	1.0×10^{0}	5.85×10^{-2}	3.58×10^{12}	2.15×10^{13}	1.1×10^{4}	6.28×10^{-2}	4.23×10^{16}	5.57×10^{16}				
Te	I			134	6.7×10^{-2}	1.1×10^{2}	4.51×10^{14}	1.1×10^{2}	7.2×10^{-2}	4.85×10^{14}	1.02×10^{15}								
Te	I	Xe^m		135	4.2×10^{-2}	1.0×10^{0}	2.57×10^{12}	2.3×10^{3}	5.85×10^{-2}	8.25×10^{15}	8.76×10^{15}	2.3×10^{2}	1.51×10^{-2}	2.13×10^{14}	3.16×10^{14}				
I				136	3.1×10^{-2}	5×10^{-1}	9.53×10^{11}												
I	Xe	Cs	Ba^m	137	4.9×10^{-2}	6.5×10^{-2}	1.95×10^{11}	1.2×10^{1}	5.88×10^{-2}	4.32×10^{13}	4.53×10^{13}	7×10^{7}	5.46×10^{-2}	2.34×10^{20}	3.96×10^{20}	4.0×10^{0}	4.44×10^{-2}	1.08×10^{13}	7.88×10^{13}
I	Xe	Cs		138	3.4×10^{-2}	8×10^{-3}	1.66×10^{10}	1.0×10^{2}	5.49×10^{-2}	3.36×10^{14}	3.39×10^{14}	9×10^{2}	5.02×10^{-2}	2.76×10^{15}	3.39×10^{15}				
I	Xe	Cs	Ba	139	1.8×10^{-2}	2.7×10^{-3}	2.98×10^{9}	8×10^{-1}	4.7×10^{-2}	2.3×10^{12}	2.35×10^{12}	2×10^{2}	5.79×10^{-2}	7.08×10^{14}	7.40×10^{14}	7×10^{2}	3.01×10^{-2}	1.29×10^{15}	7.94×10^{15}
Xe	Cs	Ba	La	140	3.7×10^{-2}	2×10^{-1}	4.54×10^{11}	1.1×10^{1}	5.94×10^{-2}	4.0×10^{13}	4.19×10^{13}	6.5×10^{5}	4.83×10^{-2}	1.92×10^{18}	2.62×10^{18}				3.43×10^{17}
Xe	Cs	Ba	La	141	1.8×10^{-2}	8×10^{-3}	8.83×10^{9}	2.5×10^{-2}	4.7×10^{-2}	7.19×10^{10}	7.71×10^{10}	7.0×10^{1}	5.74×10^{-2}	2.45×10^{14}	3.28×10^{14}				4.07×10^{15}
Y	Zr	Nb		95	6.4×10^{-2}	4.5×10^{0}					1.53×10^{17}				8.5×10^{16}				
Cs	Ba	La		142	3.4×10^{-2}	1.1×10^{1}	2.29×10^{13}	1.2×10^{1}		4.11×10^{13}	1.79×10^{14}				2.22×10^{15}				
Ba	La	Ce		143	4.9×10^{-2}	3.8×10^{-1}									4.37×10^{15}				

APPENDIX C. ACTIVITY IN THE PRIMARY GAS SYSTEM

The activity of the various nuclides in the primary system at temperatures of 800, 1000, 1200, and 1400°C is given in Table C.1 for the assumed power density of 1000 w/cm^3 and for an assumed volume of fuel of 1 cm^3. Case I gives the various activities if all the fission products recoil into the graphite. Case II gives the activity in the gas stream if the fission products in the graphite are from the recoil of fission fragments from a 200-μ UO_2 particle.

In order to establish the relative importance of diffusion and recoil from UO_2 in the HGCR-1, and to see how modifications to the system would affect the activity release, a comparison of the activity release from UO_2 by the processes of recoil and diffusion was made. From Table A.3 in App. A, it may be shown that the fractional release of activity from the UO_2 by diffusion may be expressed as:

$$F_{UO_2} = \frac{3 \times (3 \times 10^{10})\, R\gamma}{\dfrac{3 \times 10^{13}\, \gamma\, (1 - e^{-\lambda t})}{\lambda}} = \frac{3R\lambda}{1 - e^{-\lambda t}} \; .$$

The values of R were obtained for a time of 3×10^8 sec so that for all the cases, except Cs^{137}, the fractional release of nuclides depended only on the factor $R\lambda$. The values of R were taken from Table A.1 of App. A, and the results of the calculations of the release of the various nuclides as a function of temperature are given in Table C.2. The values for the release of the nuclides as a function of particle size are compared in Fig. C.1 with the release by the diffusion mechanism.

For the 200-μ UO_2 particles, it may be seen that only when the decay constant is less than 10^{-8} sec^{-1} does the diffusion from UO_2 become as significant as the recoil from UO_2. Therefore, only Cs^{137} is released from UO_2 more by diffusion than by the recoil process. Figure C.1 shows that for a higher temperature in the fuel element, diffusion becomes more significant. It also indicates that for the HGCR-1 temperatures, the activity may be reduced by increasing the particle size.

Figure C.1 also presents a comparison of the release of activity from the UO_2 by the processes of diffusion and recoil. The activity which has recoiled from the UO_2 must diffuse out of the graphite in order to get into the gas stream. However, it is assumed that the activity which has been released from the UO_2 by diffusion is not retained by the graphite, but is immediately released to the gas stream. Therefore, when comparing the relative importance of diffusion and recoil from UO_2, it is necessary to take into account the fraction of the fission products which diffuse out of the graphite.

The fractional release of activity from the UO_2 is given by

$$F_{UO_2} = \frac{3R\lambda}{(1 - e^{-\lambda t})} \; .$$

UNCLASSIFIED
ORNL-LR-DWG 34884A

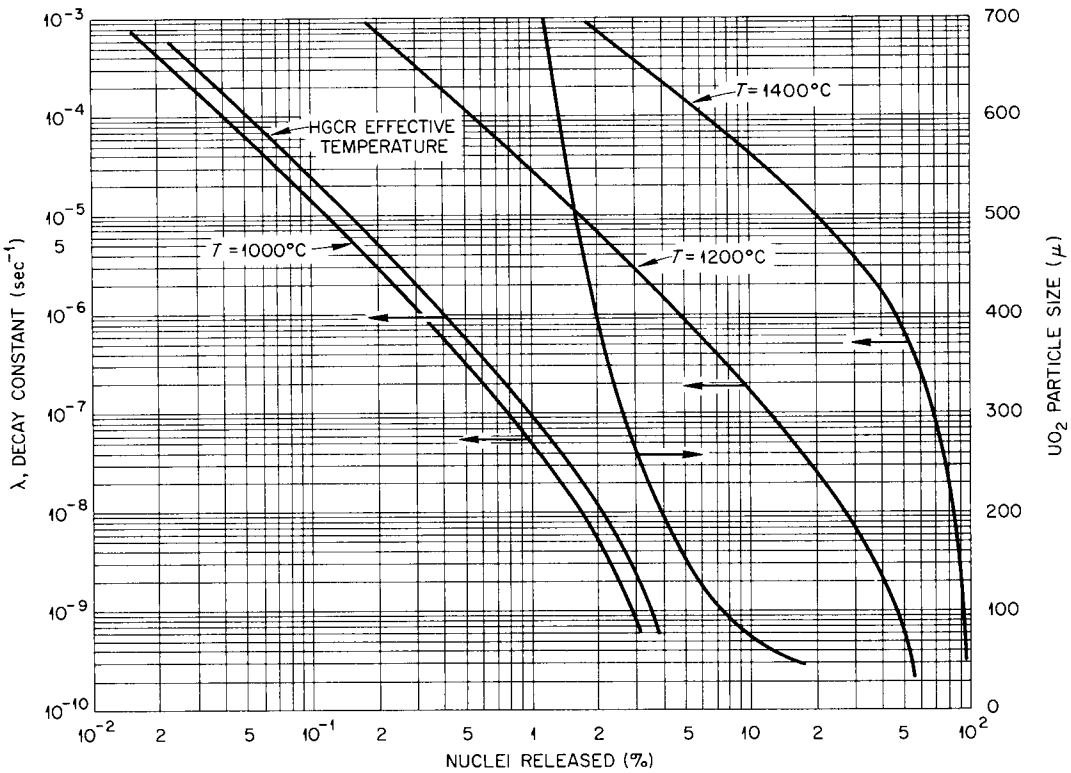

Fig. C.1. Nuclides Released from UO_2 by Diffusion and by Recoil.

The fractional release of activity from the graphite is given by

$$F_G = \frac{3R\lambda}{(1 - e^{-\lambda t})} f ,$$

where f is the fractional release of activity from UO_2 by recoil. Therefore the ratio of the release of activity by diffusion from the graphite to that diffusing directly from the UO_2 is given by

$$\frac{F_G}{F_{UO_2}} = \frac{3R_G f}{3R_{UO_2}} = f \frac{R_G}{R_{UO_2}} .$$

By comparing the R values for UO_2 diffusion with those for graphite diffusion, the relative importance of diffusion and recoil processes may be determined. For the temperature distribution in the HGCR-1, the contribution of total activity due to diffusion from the UO_2 is significantly less, and therefore the values given in Table C.1, case II, are used in the following calculations.

Since the thermal power output from the reactor is $\sim 3 \times 10^9$ w, the activity in the system may be approximated by multiplying the values in Table C.1, case II, by 3×10^6.

The activities of the various nuclides in the system as a function of fuel element temperature are given in Figs. C.2, C.3, and C.4. Since the amount of a given nuclide in the gas stream is strongly dependent upon temperature, it is necessary to estimate the fraction of the fuel at various temperatures. The temperatures in the HGCR-1 fuel

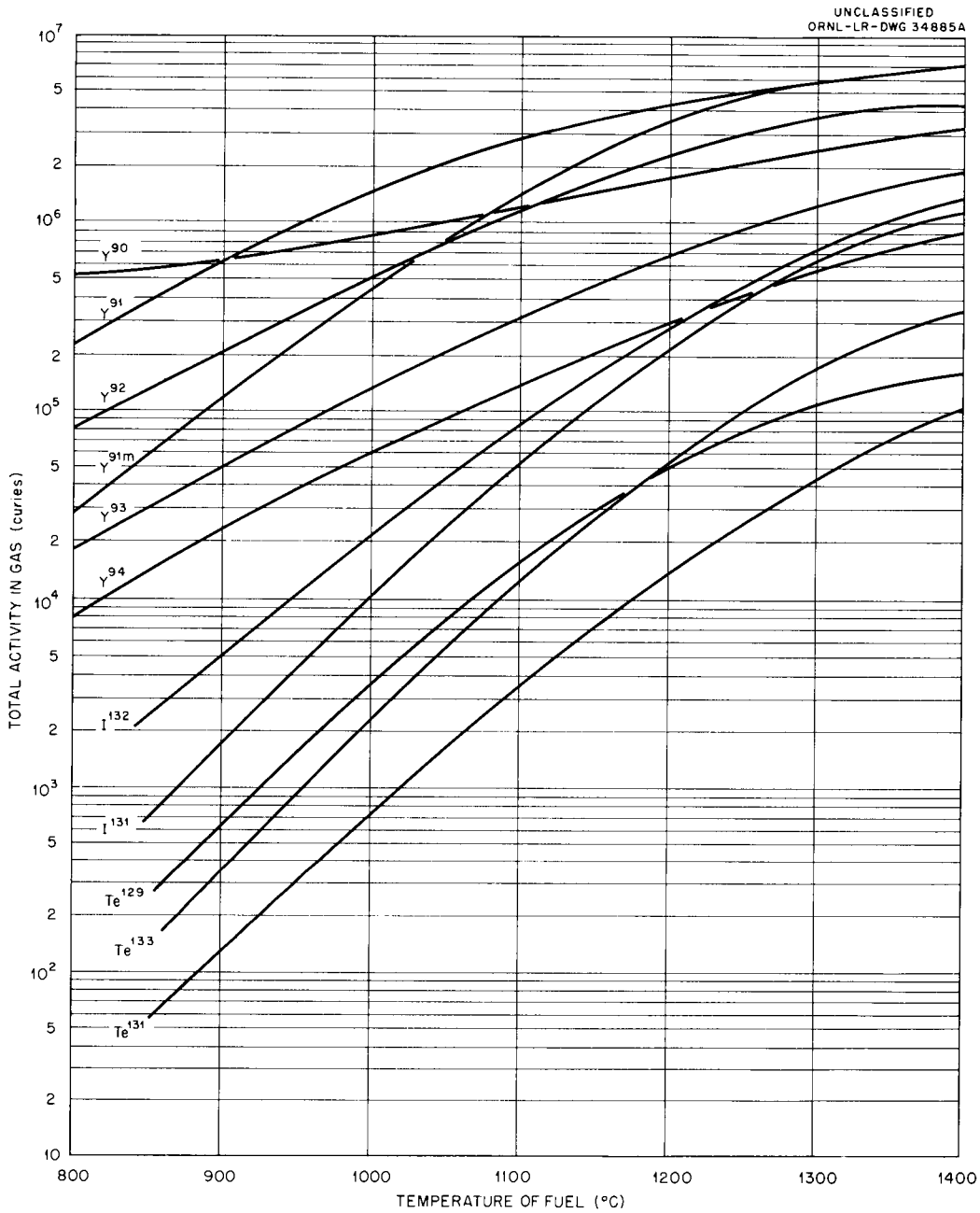

Fig. C.2. Effect of Fuel Element Temperature on Fission-Product Activity in the Primary Gas System.

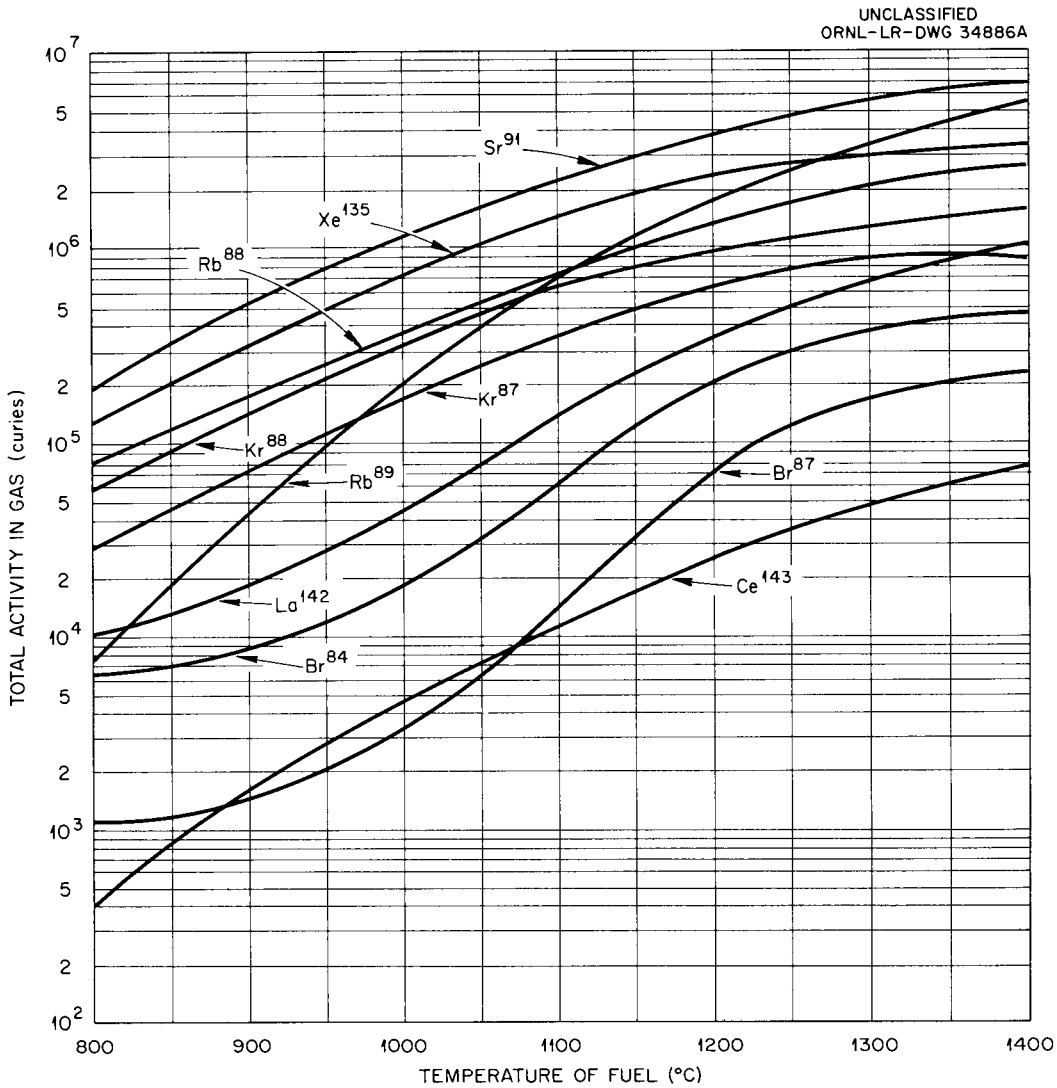

Fig. C.3. Effect of Fuel Element Temperature on Fission-Product Activity in the Primary Gas System.

elements were calculated,[1] and the fractions for various temperature ranges are shown in Table C.3. The activity which would be present in the gas stream if all the fuel were at the highest temperature in the temperature increment is also shown in Table C.3. By taking these activities and multiplying by the fraction of fuel at the temperatures in the temperature increment, the activity in the system is obtained, as shown in Table C.4.

The activities given in Table C.4 represent the maximum amount that would be circulating around the primary system (for the assumptions made for this system). There

[1] M. H. Fontana, *Fuel Element Temperature Distribution in the HGCR-1*, ORNL CF-58-12-3 (Dec. 1958).

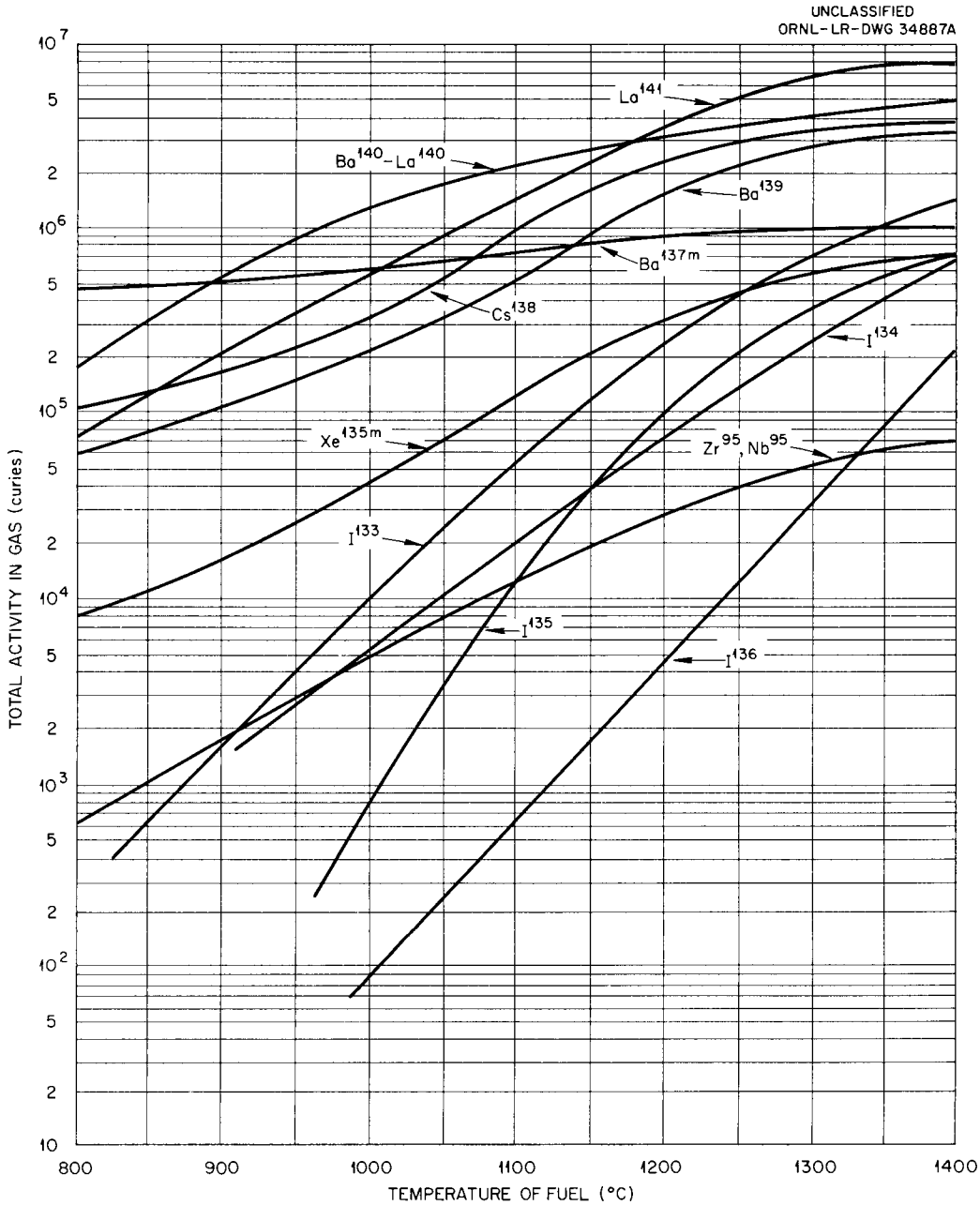

Fig. C.4. Effect of Fuel Element Temperature on Fission-Product Activity in the Primary Gas System.

would be three processes, however, for decreasing activity in the loop during normal operation: (1) system leakage, (2) deposition, and (3) purification of the gas.

Since the system leakage would have to be minimized in order to have an operational system, the reduction of activity by this method would not be significant.

Deposition would decrease the activity being circulated, but it is difficult to predict how important such a process would be, since its importance would depend upon the rate of deposition and the place of deposition. Deposition in the core or pressure vessel would reduce maintenance problems, whereas deposition in the blowers or heat exchangers would make maintenance more difficult. In any event, there are no data upon which to base a calculation of activity deposition in a gas system.

With a purification system, the only removal processes (neglecting deposition) are decay and the purification. The calculated activity in the system as a function of the purification rate is given in Table C.5. As may be seen in Table C.5 and Fig. C.5, the effectiveness of the purification system during operation is not very great, since most of the nuclides are short-lived and therefore the reduction $\lambda[\lambda + (\alpha/T)]$ is not significant. In order to get an activity reduction of a factor of about 8, it is necessary to bypass 1% of the gas stream. Since the problems and costs associated with doing this are very great, the use of the purification system for reducing activity during operation would be quite limited.

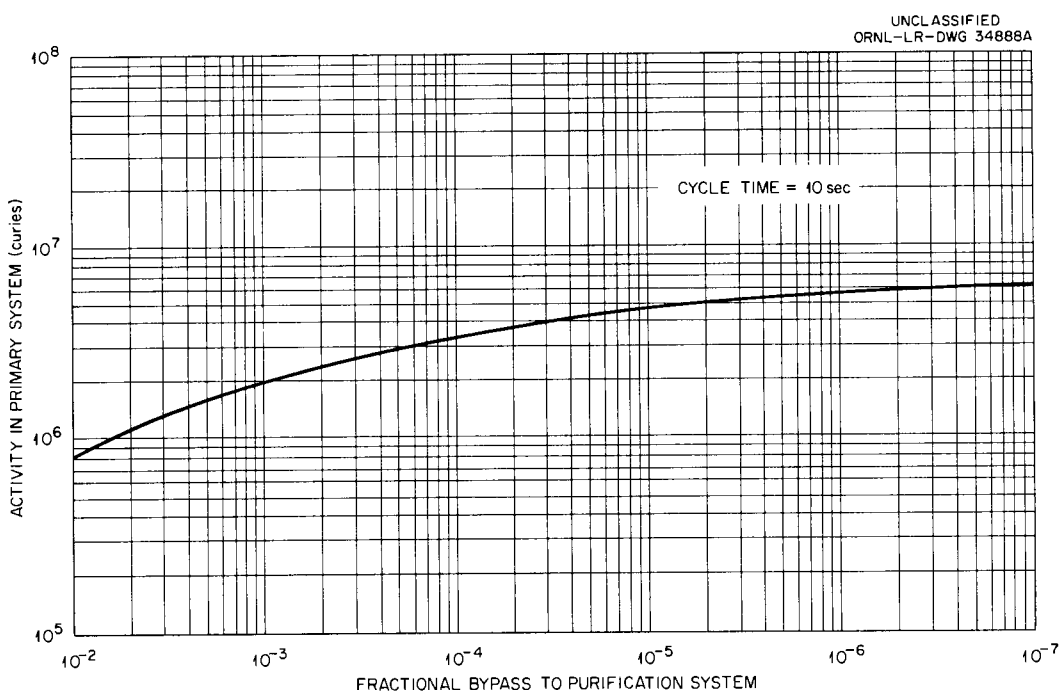

Fig. C.5. Effect of the Purification System on Primary System Activity (Assuming No Deposition).

Table C.1. Activity in the Primary System for Fuel Temperatures of 800, 1000, 1200, and 1400°C and a Power Density of 1000 w/cm^3

Case I: All fission products born in UO_2 released to graphite

Case II: Only fission products in graphite are recoil fragments from UO_2

Nuclide	λ (sec^{-1})	N at 1200°C	A at 1200°C (curies/cm^3)	N at 1400°C	A at 1400°C (curies/cm^3)	N at 1000°C	A at 1000°C (curies/cm^3)	N at 800°C	A at 800°C (curies/cm^3)
					Case I				
Xe^{135}	2.11×10^{-5}	3.54×10^{16}	2.02×10^{1}	5.63×10^{16}	3.21×10^{1}	1.16×10^{16}	6.61×10^{0}	1.95×10^{15}	1.11×10^{0}
Br^{84}	3.85×10^{-4}	1.55×10^{14}	1.61×10^{0}	3.37×10^{14}	3.5×10^{0}	1.26×10^{13}	1.31×10^{-1}	4.87×10^{12}	5.05×10^{-2}
Br^{87}	1.25×10^{-2}	1.65×10^{12}	5.57×10^{-1}	4.95×10^{12}	1.67×10^{0}	7.14×10^{10}	2.41×10^{-2}	2.76×10^{10}	9.33×10^{-3}
Kr^{87}	1.48×10^{-4}	1.18×10^{15}	4.73×10^{0}	1.75×10^{15}	7.01×10^{0}	2.86×10^{14}	1.14×10^{0}	5.45×10^{13}	2.18×10^{-1}
Kr^{88}	6.95×10^{-5}	3.79×10^{15}	7.11×10^{0}	6.67×10^{15}	1.25×10^{1}	1.23×10^{15}	2.31×10^{0}	2.33×10^{14}	4.38×10^{-1}
Rb^{88}	6.49×10^{-4}	7.51×10^{14}	9.9×10^{0}	1.64×10^{15}	1.97×10^{1}	1.86×10^{14}	2.45×10^{0}	4.54×10^{13}	5.97×10^{-1}
Rb^{89}	7.5×10^{-4}	6.36×10^{14}	1.29×10^{1}	2.04×10^{15}	4.13×10^{1}	7.26×10^{13}	1.47×10^{0}	2.63×10^{13}	5.33×10^{-1}
Y^{90}	2.98×10^{-6}	1.73×10^{17}	1.39×10^{1}	3.08×10^{17}	2.48×10^{1}	7.68×10^{16}	6.16×10^{0}	4.69×10^{16}	3.76×10^{0}
Y^{91m}	2.26×10^{-4}	4.43×10^{15}	2.76×10^{1}	8.5×10^{15}	5.17×10^{1}	5.21×10^{14}	3.25×10^{0}	3.4×10^{13}	2.12×10^{-1}
Y^{91}	1.38×10^{-7}	8.65×10^{18}	3.23×10^{1}	1.39×10^{19}	5.19×10^{1}	2.78×10^{18}	1.04×10^{1}	4.5×10^{17}	1.68×10^{0}
Y^{92}	5.35×10^{-5}	1.17×10^{16}	1.69×10^{1}	2.26×10^{16}	3.26×10^{1}	2.7×10^{15}	3.9×10^{0}	4.03×10^{14}	5.81×10^{-1}
Y^{93}	1.93×10^{-5}	9.69×10^{15}	5.04×10^{0}	2.87×10^{16}	1.49×10^{1}	2.02×10^{15}	1.05×10^{0}	2.74×10^{14}	1.42×10^{-1}
Y^{94}	7.0×10^{-4}	1.21×10^{14}	2.29×10^{0}	3.61×10^{14}	6.83×10^{0}	2.33×10^{13}	4.4×10^{-1}	3.18×10^{12}	6.01×10^{-2}
Te^{129}	1.6×10^{-4}	1.08×10^{14}	4.68×10^{-1}	3.6×10^{14}	1.56×10^{0}	8.4×10^{12}	3.64×10^{-2}		
Te^{131}	4.66×10^{-4}	1.06×10^{13}	1.34×10^{-1}	8.15×10^{13}	1.03×10^{0}	5.43×10^{11}	6.85×10^{-3}		
I^{131}	9.96×10^{-7}	8.09×10^{16}	2.17×10^{0}	4.45×10^{17}	1.18×10^{1}	4.15×10^{15}	1.11×10^{-1}		
I^{132}	8.02×10^{-5}	1.27×10^{15}	2.76×10^{0}	6.4×10^{15}	1.39×10^{1}	9.51×10^{13}	2.07×10^{-1}		
Te^{133}	5.78×10^{-3}	3.19×10^{12}	4.99×10^{-1}	2.15×10^{13}	3.36×10^{0}	1.47×10^{11}	2.3×10^{-2}		

Table C.1 (continued)

Nuclide	λ (sec^{-1})	N at 1200°C	A at 1200°C (curies/cm^3)	N at 1400°C	A at 1400°C (curies/cm^3)	N at 1000°C	A at 1000°C (curies/cm^3)	N at 800°C	A at 800°C (curies/cm^3)
I^{133}	9.25×10^{-6}	7.93×10^{15}	1.98×10^{0}	5.57×10^{16}	1.39×10^{1}	3.84×10^{14}	9.6×10^{-2}		
I^{134}	2.2×10^{-4}	1.29×10^{14}	7.66×10^{-1}	1.02×10^{15}	6.06×10^{0}	8.63×10^{12}	5.14×10^{-2}		
I^{135}	2.89×10^{-5}	1.15×10^{15}	8.98×10^{-1}	8.76×10^{15}	6.85×10^{0}	8.96×10^{12}	6.99×10^{-3}		
Xe^{135m}	7.4×10^{-4}	1.42×10^{14}	2.84×10^{0}	3.16×10^{14}	6.31×10^{0}	1.70×10^{13}	3.98×10^{-1}	3.24×10^{12}	7.41×10^{-2}
I^{136}	8.06×10^{-3}	1.24×10^{11}	2.7×10^{-2}	9.53×10^{11}	2.08×10^{-1}	5.41×10^{9}	1.18×10^{-3}		
Ba^{137m}	4.4×10^{-3}	6.6×10^{13}	7.85×10^{0}	7.88×10^{13}	9.37×10^{0}	4.56×10^{13}	5.43×10^{0}	3.82×10^{13}	4.55×10^{0}
Cs^{138}	3.62×10^{-4}	2.19×10^{15}	2.14×10^{1}	3.39×10^{15}	3.31×10^{1}	2.98×10^{14}	2.91×10^{0}	9.85×10^{13}	9.6×10^{-1}
Ba^{139}	1.36×10^{-4}	3.87×10^{15}	1.42×10^{1}	7.94×10^{15}	2.91×10^{1}	5.26×10^{14}	1.93×10^{0}	1.53×10^{14}	5.61×10^{-1}
Ba^{140}	6.27×10^{-7}	1.67×10^{18}	2.83×10^{1}	2.62×10^{18}	4.45×10^{1}	6.83×10^{17}	1.16×10^{1}	8.66×10^{16}	1.47×10^{0}
La^{140}	4.79×10^{-6}	2.19×10^{17}	2.83×10^{1}	3.43×10^{17}	4.43×10^{1}	8.95×10^{16}	1.16×10^{1}	1.13×10^{16}	1.46×10^{0}
La^{141}	6.42×10^{-4}	1.84×10^{15}	3.2×10^{1}	4.07×10^{15}	7.07×10^{1}	2.84×10^{14}	4.95×10^{0}	4.1×10^{13}	7.13×10^{-1}
Zr^{95}	1.27×10^{-7}	6.12×10^{16}	2.1×10^{-1}	1.53×10^{17}	5.25×10^{-1}	1.02×10^{16}	3.5×10^{-2}	1.34×10^{15}	4.6×10^{-3}
Nb^{95}	2.29×10^{-7}	3.4×10^{16}	2.1×10^{-1}	8.5×10^{16}	5.25×10^{-1}	5.66×10^{15}	3.5×10^{-2}	7.41×10^{14}	4.6×10^{-3}
Sr^{91}	1.99×10^{-5}	5.02×10^{16}	2.7×10^{1}	9.65×10^{16}	5.2×10^{1}	1.47×10^{16}	7.92×10^{0}	2.44×10^{15}	1.31×10^{0}
La^{142}	1.56×10^{-4}	7.65×10^{14}	3.22×10^{0}	2.22×10^{15}	9.37×10^{0}	9.56×10^{13}	4.04×10^{-1}	2.28×10^{13}	9.61×10^{-2}
Ce^{143}	6.01×10^{-6}	1.38×10^{15}	2.24×10^{-1}	4.37×10^{15}	7.11×10^{-1}	2.54×10^{14}	4.14×10^{-2}	2.3×10^{13}	3.74×10^{-3}
					Case II				
Xe^{135}			7.17×10^{-1}		1.14×10^{0}		2.35×10^{-1}		3.94×10^{-2}
Br^{84}			7.20×10^{-2}		1.56×10^{-1}		5.86×10^{-3}		2.26×10^{-3}
Br^{87}			2.49×10^{-2}		7.46×10^{-2}		1.08×10^{-3}		4.17×10^{-4}
Kr^{87}			2.11×10^{-1}		3.13×10^{-1}		5.10×10^{-2}		9.74×10^{-3}

Table C.1 (continued)

Nuclide	λ (sec^{-1})	N at 1200°C	A at 1200°C (curies/cm^3)	N at 1400°C	A at 1400°C (curies/cm^3)	N at 1000°C	A at 1000°C (curies/cm^3)	N at 800°C	A at 800°C (curies/cm^3)
Kr^{88}			3.18×10^{-1}		5.59×10^{-1}		1.03×10^{-1}		1.96×10^{-2}
Rb^{88}			4.43×10^{-1}		8.81×10^{-1}		1.10×10^{-1}		2.67×10^{-2}
Rb^{89}			5.77×10^{-1}		1.85×10^{0}		6.57×10^{-2}		2.38×10^{-2}
Y^{90}			6.21×10^{-1}		1.11×10^{0}		2.75×10^{-1}		1.68×10^{-1}
Y^{91m}			1.23×10^{0}		2.13×10^{0}		1.45×10^{-1}		9.48×10^{-3}
Y^{91}			1.44×10^{0}		2.32×10^{0}		4.65×10^{-1}		7.51×10^{-2}
Y^{92}			7.55×10^{-1}		1.46×10^{0}		1.74×10^{-1}		2.60×10^{-2}
Y^{93}			2.25×10^{-1}		6.66×10^{-1}		4.69×10^{-2}		6.35×10^{-3}
Y^{94}			1.02×10^{-1}		3.05×10^{-1}		1.97×10^{-2}		2.69×10^{-3}
Te^{129}			1.66×10^{-2}		5.54×10^{-2}		1.29×10^{-3}		
Te^{131}			4.76×10^{-3}		3.66×10^{-2}		2.43×10^{-4}		
I^{131}			7.70×10^{-2}		4.19×10^{-1}		3.94×10^{-3}		
I^{132}			9.80×10^{-2}		4.93×10^{-1}		7.35×10^{-3}		
Te^{133}			1.77×10^{-2}		1.19×10^{-1}		8.17×10^{-4}		
I^{133}			7.03×10^{-2}		4.93×10^{-1}		3.41×10^{-3}		
I^{134}			2.72×10^{-2}		2.15×10^{-1}		1.82×10^{-3}		
I^{135}			3.19×10^{-2}		2.43×10^{-1}		2.48×10^{-4}		
Xe^{135m}			1.01×10^{-1}		2.24×10^{-1}		1.41×10^{-2}		2.63×10^{-3}
I^{136}			9.59×10^{-4}		7.38×10^{-2}		4.19×10^{-5}		
Ba^{137m}			2.79×10^{-1}		3.33×10^{-1}		1.93×10^{-1}		1.62×10^{-1}
Cs^{138}			7.60×10^{-1}		1.18×10^{0}		1.03×10^{-1}		3.41×10^{-2}

Table C.1 (continued)

Nuclide	λ (sec^{-1})	N at 1200°C	A at 1200°C (curies/cm^3)	N at 1400°C	A at 1400°C (curies/cm^3)	N at 1000°C	A at 1000°C (curies/cm^3)	N at 800°C	A at 800°C (curies/cm^3)
Ba^{139}			5.04×10^{-1}		1.03×10^{0}		6.85×10^{-2}		1.99×10^{-2}
Ba^{140}			1.00×10^{0}		1.58×10^{0}		4.12×10^{-1}		5.22×10^{-2}
La^{140}			1.00×10^{0}		1.57×10^{0}		4.12×10^{-1}		5.18×10^{-2}
La^{141}			1.14×10^{0}		2.51×10^{0}		1.76×10^{-1}		2.53×10^{-2}
Zr^{95}			9.39×10^{-3}		2.35×10^{-2}		1.56×10^{-3}		2.06×10^{-4}
Nb^{95}			9.39×10^{-3}		2.35×10^{-2}		1.56×10^{-3}		2.06×10^{-4}
Sr^{91}			1.21×10^{0}		2.32×10^{0}		3.54×10^{-1}		5.86×10^{-2}
La^{142}			1.14×10^{-1}		3.33×10^{-1}		1.43×10^{-2}		3.41×10^{-3}
Ce^{143}			7.95×10^{-3}		2.52×10^{-2}		1.47×10^{-3}		1.33×10^{-4}
Total for Case II			13.22		26.44		3.47		0.82

Table C.2. Release of Nuclides by Diffusion from UO_2

Nuclide	Light Nuclei Released (%)			Nuclide	Heavy Nuclei Released (%)		
	At 1000°C	At 1200°C	At 1400°C		At 1000°C	At 1200°C	At 1400°C
Br^{84}	2.52×10^{-2}	3.17×10^{-1}	3.36×10^{0}	I^{131}	4.07×10^{-1}	5.16×10^{0}	5.43×10^{1}
Br^{87}	3.41×10^{-3}	4.45×10^{-2}	4.78×10^{-1}	I^{132}	4.37×10^{-2}	5.46×10^{-1}	5.71×10^{0}
Kr^{87}	4.04×10^{-2}	5.24×10^{-1}	5.65×10^{0}	I^{133}	1.41×10^{-1}	1.79×10^{0}	1.89×10^{1}
Br^{88}	2.07×10^{-3}	2.68×10^{-2}	2.81×10^{-1}	I^{134}	2.40×10^{-2}	3.06×10^{-1}	3.25×10^{0}
Kr^{88}	4.56×10^{-2}	5.71×10^{-1}	6.06×10^{0}	I^{135}	7.10×10^{-2}	8.98×10^{-1}	9.47×10^{0}
Rb^{88}	1.59×10^{-2}	2.02×10^{-1}	2.13×10^{0}	Xe^{135m}	1.27×10^{-2}	1.62×10^{-1}	1.70×10^{0}
Kr^{89}	6.25×10^{-3}	7.92×10^{-2}	8.33×10^{-1}	I^{136}	4.40×10^{-3}	5.51×10^{-2}	5.73×10^{-1}
Rb^{89}	1.43×10^{-2}	1.82×10^{-1}	1.91×10^{0}	I^{137}	2.06×10^{-3}	2.58×10^{-2}	2.76×10^{-1}
Kr^{90}	3.22×10^{-3}	4.07×10^{-2}	4.31×10^{-1}	Xe^{137}	6.47×10^{-3}	8.08×10^{-2}	8.90×10^{-1}
Rb^{90}	6.44×10^{-3}	8.19×10^{-2}	8.65×10^{-1}	Cs^{137}	2.98×10^{0}	4.72×10^{1}	9.22×10^{1}
Kr^{91}	1.26×10^{-3}	1.61×10^{-2}	1.68×10^{-1}	I^{138}	1.05×10^{-3}	1.34×10^{-2}	1.41×10^{-1}
Rb^{91}	1.26×10^{-2}	1.60×10^{-1}	1.69×10^{0}	Xe^{138}	1.30×10^{-2}	1.65×10^{-1}	1.72×10^{0}
Kr^{92}	9.47×10^{-4}	1.20×10^{-2}	1.26×10^{-1}	Cs^{138}	1.88×10^{-2}	2.37×10^{-1}	2.47×10^{0}
Rb^{92}	4.72×10^{-3}	5.92×10^{-2}	6.14×10^{-1}	I^{139}	7.73×10^{-4}	9.83×10^{-3}	1.05×10^{-1}
Kr^{93}	8.52×10^{-4}	1.08×10^{-2}	1.14×10^{-1}	Xe^{139}	3.22×10^{-3}	4.10×10^{-2}	4.29×10^{-1}
Rb^{93}	5.11×10^{-4}	6.44×10^{-3}	6.83×10^{-2}	Cs^{139}	1.10×10^{-2}	1.40×10^{-1}	1.47×10^{0}
Kr^{94}	5.41×10^{-4}	6.88×10^{-3}	7.29×10^{-2}	Xe^{140}	1.54×10^{-3}	2.10×10^{-2}	2.13×10^{-1}
Rb^{94}	5.11×10^{-4}	6.44×10^{-3}	6.83×10^{-2}	Cs^{140}	3.74×10^{-3}	4.89×10^{-2}	5.16×10^{-1}
				Xe^{141}	6.22×10^{-4}	7.92×10^{-3}	8.35×10^{-2}
				Cs^{141}	5.11×10^{-4}	6.44×10^{-3}	6.83×10^{-2}

Table C.3. Activity of the Fission Products in the Gas Stream If All the Fuel Is at the Highest Temperature in the Temperature Increment

Temperature Increment	Temperature Range (°C)	Fuel at Temperatures in Temperature Increment (%)	Activity (curies)			
			Sr^{91}	Rb^{89}	Xe^{135}	Rb^{88}
1	<871	66.21	3.9×10^5	2.6×10^4	2.4×10^5	1.4×10^5
2	871–899	5.70	5.0×10^5	4.0×10^4	3.0×10^5	1.7×10^5
3	899–927	6.05	6.3×10^5	6.6×10^4	3.9×10^5	2.1×10^5
4	927–954	4.94	8.0×10^5	1.0×10^5	4.9×10^5	2.7×10^5
5	954–982	4.83	9.9×10^5	1.5×10^5	6.0×10^5	3.2×10^5
6	982–1010	3.98	1.3×10^6	2.3×10^5	7.8×10^5	4.0×10^5
7	1010–1038	3.26	1.5×10^6	3.2×10^5	9.9×10^5	4.8×10^5
8	1038–1066	2.38	1.7×10^6	4.6×10^5	1.2×10^6	5.9×10^5
9	1066–1093	1.81	2.0×10^6	6.2×10^5	1.5×10^6	7.0×10^5
10	1093–1121	0.79	2.4×10^6	8.3×10^5	1.7×10^6	8.3×10^5
11	1121–1149	0.05	2.8×10^6	1.2×10^6	1.9×10^6	9.9×10^5

Temperature Increment*	Activity (curies)					
	Kr^{88}	La^{142}	Kr^{87}	Br^{84}	Br^{87}	Ce^{143}
1	1.2×10^5	1.6×10^4	5.5×10^4	8.0×10^3	1.3×10^3	1.2×10^3
2	1.5×10^5	1.8×10^4	7.0×10^4	9.0×10^3	1.4×10^3	1.6×10^3
3	1.8×10^5	2.3×10^4	9.0×10^4	1.1×10^4	1.7×10^3	2.2×10^3
4	2.4×10^5	3.0×10^3	1.3×10^5	1.3×10^4	2.1×10^3	2.9×10^3
5	2.9×10^5	3.9×10^4	1.6×10^5	1.6×10^4	2.8×10^3	3.8×10^3
6	3.6×10^5	5.0×10^4	1.9×10^5	1.9×10^4	3.7×10^3	4.9×10^3
7	4.2×10^5	6.9×10^4	2.3×10^5	2.6×10^4	5.2×10^3	6.2×10^3
8	5.1×10^5	9.2×10^4	2.9×10^5	3.7×10^4	8.0×10^3	8.0×10^3
9	6.0×10^5	1.3×10^5	3.4×10^5	5.8×10^4	1.3×10^4	1.0×10^4
10	7.0×10^5	1.7×10^5	4.0×10^5	8.8×10^4	2.0×10^4	1.4×10^4
11	8.0×10^5	2.2×10^5	4.8×10^5	1.3×10^5	3.2×10^4	1.7×10^4

Table 3 (continued)

Temperature Increment*	Activity (curies)					
	La^{141}	Ba^{140}	La^{140}	Cs^{138}	Ba^{139}	I^{133}
1	1.5×10^5	4.0×10^5	4.0×10^5	1.5×10^5	8.5×10^4	1.0×10^3
2	1.9×10^5	5.5×10^5	5.5×10^5	1.7×10^5	1.0×10^5	1.7×10^3
3	2.5×10^5	7.0×10^5	7.0×10^5	1.9×10^5	1.3×10^5	2.7×10^3
4	3.2×10^5	8.8×10^5	8.8×10^5	2.3×10^5	1.5×10^5	4.6×10^3
5	4.2×10^5	1.2×10^6	1.2×10^6	2.9×10^5	1.8×10^5	7.5×10^3
6	5.6×10^5	1.4×10^6	1.4×10^6	3.6×10^5	2.3×10^5	1.3×10^4
7	7.1×10^5	1.6×10^6	1.6×10^6	4.6×10^5	2.8×10^5	1.9×10^4
8	9.5×10^5	1.8×10^6	1.8×10^6	6.1×10^5	3.8×10^5	3.0×10^4
9	1.3×10^6	2.0×10^6	2.0×10^6	8.5×10^5	4.9×10^5	4.8×10^4
10	1.7×10^6	2.3×10^6	2.3×10^6	1.3×10^6	6.8×10^5	7.5×10^4
11	2.2×10^6	2.6×10^6	2.6×10^6	1.6×10^6	9.0×10^5	1.1×10^5

Temperature Increment*	Activity (curies)					
	Te^{131}	Te^{129}	Ba^{137m}	I^{135}	Xe^{135m}	I^{134}
1	8×10^1	3.8×10^2	4.9×10^5	8.0×10^0	1.3×10^4	8.0×10^2
2	1.3×10^2	6.0×10^2	5.0×10^5	2.0×10^1	1.7×10^4	1.3×10^3
3	2.0×10^2	1.1×10^3	5.1×10^5	7.0×10^1	2.0×10^4	1.9×10^3
4	3.3×10^2	1.7×10^3	5.2×10^5	1.5×10^2	2.7×10^4	2.8×10^3
5	5.4×10^2	2.8×10^3	5.6×10^5	4.2×10^2	3.5×10^4	4.2×10^3
6	8.4×10^2	4.2×10^3	5.9×10^5	1.0×10^3	4.5×10^4	6.0×10^3
7	1.4×10^3	6.8×10^3	6.1×10^5	2.3×10^3	6.0×10^4	9.0×10^3
8	2.0×10^3	1.0×10^4	6.6×10^5	5.0×10^3	8.1×10^4	1.4×10^4
9	3.1×10^3	1.4×10^4	7.0×10^5	1.0×10^4	1.2×10^5	1.9×10^4
10	5.0×10^3	2.1×10^4	7.3×10^5	2.0×10^4	1.6×10^5	2.8×10^4
11	7.0×10^3	2.9×10^4	7.6×10^5	3.4×10^4	1.9×10^5	3.9×10^4

Table C.3 (continued)

Temperature Increment*	Activity (curies)					
	I^{136}	Zr^{95}	Nb^{95}	Y^{91}	Y^{91m}	Y^{92}
1	8.0×10^0	1.3×10^3	1.3×10^3	4.8×10^5	8.0×10^4	1.7×10^5
2	1.4×10^1	1.8×10^3	1.8×10^3	6.0×10^5	1.3×10^5	2.1×10^5
3	2.3×10^1	2.3×10^3	2.3×10^3	8.0×10^5	1.7×10^5	2.7×10^5
4	3.8×10^1	3.0×10^3	3.0×10^3	1.0×10^6	2.5×10^5	3.5×10^5
5	6.8×10^1	4.0×10^3	4.0×10^3	1.4×10^6	3.7×10^5	4.6×10^5
6	1.2×10^2	5.1×10^3	5.1×10^3	1.6×10^6	5.0×10^5	5.7×10^5
7	1.8×10^2	6.9×10^3	6.9×10^3	1.9×10^6	7.0×10^5	7.1×10^5
8	3.2×10^2	8.9×10^3	8.9×10^3	2.3×10^6	1.0×10^6	9.0×10^5
9	5.9×10^2	1.2×10^4	1.2×10^4	2.7×10^6	1.4×10^6	1.2×10^6
10	1.0×10^3	1.5×10^4	1.5×10^4	3.1×10^6	1.8×10^6	1.5×10^6
11	1.7×10^3	1.8×10^4	1.8×10^4	3.5×10^6	2.4×10^6	1.7×10^6

Temperature Increment*	Activity (curies)					
	Y^{90}	Y^{93}	I^{132}	I^{131}	Y^{94}	Te^{133}
1	5.8×10^5	3.8×10^4	3.1×10^3	1.0×10^3	1.8×10^4	2×10^2
2	6.0×10^5	5.0×10^4	5.0×10^3	1.8×10^3	2.3×10^4	3.7×10^2
3	6.5×10^5	6.6×10^4	7.8×10^3	3.0×10^3	3.0×10^4	6.0×10^2
4	7.0×10^5	8.5×10^4	1.3×10^4	4.8×10^3	4.0×10^4	1.0×10^3
5	7.9×10^5	1.3×10^5	1.7×10^4	8.0×10^3	5.1×10^4	1.8×10^3
6	8.5×10^5	1.5×10^5	2.6×10^4	1.3×10^4	6.4×10^4	2.9×10^3
7	9.5×10^5	1.8×10^5	3.7×10^4	2.0×10^4	8.1×10^4	4.7×10^3
8	1.1×10^6	2.4×10^5	5.5×10^4	3.3×10^4	1.1×10^5	7.5×10^3
9	1.3×10^6	3.0×10^5	8.0×10^4	5.0×10^4	1.3×10^5	1.3×10^4
10	1.4×10^6	3.8×10^5	1.3×10^5	7.8×10^4	1.7×10^5	1.9×10^4
11	1.5×10^6	4.7×10^5	1.6×10^5	1.2×10^5	2.0×10^5	2.6×10^4

*The temperature range and percentage of fuel at temperatures in the temperature range are the same as given initially.

Table C.4. Activity of the Fission Products in the Gas Stream for the HGCR-1 Temperature Distribution

Temperature Increment*	Activity (curies)					
	Sr^{91}	Rb^{89}	Xe^{135}	Rb^{88}	Kr^{88}	La^{142}
1	2.58×10^5	1.72×10^4	1.59×10^5	9.27×10^4	7.95×10^4	1.06×10^4
2	2.85×10^4	2.28×10^3	1.71×10^4	9.69×10^3	8.55×10^3	1.03×10^3
3	3.81×10^4	3.99×10^3	2.36×10^4	1.27×10^4	1.09×10^4	1.39×10^3
4	3.95×10^4	4.94×10^3	2.42×10^4	1.33×10^4	1.19×10^4	1.48×10^3
5	4.78×10^4	7.25×10^3	2.90×10^4	1.55×10^4	1.40×10^4	1.88×10^3
6	5.17×10^4	9.15×10^3	3.10×10^4	1.59×10^4	1.43×10^4	1.99×10^3
7	4.89×10^4	1.04×10^4	3.23×10^4	1.56×10^4	1.37×10^4	2.25×10^3
8	4.05×10^4	1.09×10^4	2.86×10^4	1.40×10^4	1.21×10^4	2.19×10^3
9	3.62×10^4	1.12×10^4	2.72×10^4	1.27×10^4	1.09×10^4	2.35×10^3
10	1.90×10^4	6.56×10^3	1.34×10^4	6.56×10^3	5.53×10^3	1.34×10^3
11	1.40×10^3	6.00×10^2	9.50×10^2	4.95×10^2	4.00×10^2	1.10×10^2
Total	6.10×10^5	8.45×10^4	3.86×10^5	2.09×10^5	1.82×10^5	2.66×10^4

Temperature Increment*	Activity (curies)					
	Kr^{87}	Br^{84}	Br^{87}	Ce^{143}	La^{141}	Ba^{140}
1	3.64×10^4	5.30×10^3	8.61×10^2	7.95×10^2	9.93×10^4	2.65×10^5
2	3.49×10^3	5.13×10^2	7.98×10^1	9.12×10^1	1.08×10^4	3.14×10^4
3	5.45×10^3	6.66×10^2	1.03×10^2	1.33×10^2	1.51×10^4	4.24×10^4
4	6.42×10^3	6.42×10^2	1.04×10^2	1.43×10^2	1.58×10^4	4.35×10^4
5	7.73×10^3	7.73×10^2	1.35×10^2	1.84×10^2	2.03×10^4	5.80×10^4
6	7.56×10^3	7.56×10^2	1.47×10^2	1.95×10^2	2.23×10^4	5.57×10^4
7	7.50×10^3	8.48×10^2	1.70×10^2	2.02×10^2	2.31×10^4	5.22×10^4
8	6.90×10^3	8.81×10^2	1.90×10^2	1.90×10^2	2.26×10^4	4.28×10^4
9	6.15×10^3	1.05×10^3	2.35×10^2	1.81×10^2	2.35×10^4	3.62×10^4
10	3.16×10^3	6.95×10^2	1.58×10^2	1.11×10^2	1.34×10^4	1.82×10^4
11	2.40×10^2	6.50×10^1	1.60×10^1	8.50×10^0	1.10×10^3	1.30×10^3
Total	9.15×10^4	1.21×10^4	2.20×10^3	2.23×10^3	2.67×10^5	6.47×10^5

Table C.4 (continued)

Temperature Increment*	Activity (curies)					
	La^{140}	Cs^{138}	Ba^{139}	I^{133}	Te^{131}	Te^{129}
1	2.65×10^5	9.93×10^4	5.63×10^4	6.62×10^2	5.30×10^1	2.52×10^2
2	3.14×10^4	9.69×10^3	5.70×10^3	9.69×10^1	7.41×10^0	3.42×10^1
3	4.24×10^4	1.15×10^4	7.87×10^3	1.63×10^2	1.21×10^1	6.66×10^1
4	4.35×10^4	1.14×10^4	7.41×10^3	2.27×10^2	1.63×10^1	8.40×10^1
5	5.80×10^4	1.40×10^4	8.69×10^3	3.62×10^2	2.61×10^1	1.35×10^2
6	5.57×10^4	1.43×10^4	9.15×10^3	5.17×10^2	3.34×10^1	1.67×10^2
7	5.22×10^4	1.50×10^4	9.13×10^3	6.19×10^2	4.56×10^1	2.22×10^2
8	4.28×10^4	1.45×10^4	9.04×10^3	7.14×10^2	4.76×10^1	2.38×10^2
9	3.62×10^4	1.54×10^4	8.87×10^3	8.69×10^2	5.61×10^1	2.53×10^2
10	1.82×10^4	1.03×10^4	5.37×10^3	5.93×10^2	3.95×10^1	1.66×10^2
11	1.30×10^3	8.00×10^2	4.50×10^2	5.50×10^1	3.50×10^0	1.45×10^1
Total	6.47×10^5	2.16×10^5	1.28×10^5	4.88×10^3	3.41×10^2	1.63×10^3

Temperature Increment*	Activity (curies)					
	Ba^{137m}	I^{135}	Xe^{135m}	I^{134}	I^{136}	Zr^{95}
1	3.24×10^5	5.30×10^0	8.61×10^3	5.30×10^2	5.30×10^0	8.61×10^2
2	2.85×10^4	1.14×10^0	9.69×10^2	7.41×10^1	7.98×10^{-1}	1.03×10^2
3	3.09×10^4	4.24×10^0	1.21×10^3	1.15×10^2	1.39×10^0	1.39×10^2
4	2.57×10^4	7.41×10^0	1.33×10^3	1.38×10^2	1.88×10^0	1.48×10^2
5	2.70×10^4	2.03×10^1	1.69×10^3	2.03×10^2	3.28×10^0	1.93×10^2
6	2.35×10^4	3.98×10^1	1.79×10^3	2.39×10^2	4.78×10^0	2.03×10^2
7	1.99×10^4	7.50×10^1	1.96×10^3	2.93×10^2	5.87×10^0	2.25×10^2
8	1.57×10^4	1.19×10^2	1.93×10^3	3.33×10^2	7.62×10^0	2.12×10^2
9	1.27×10^4	1.81×10^2	2.17×10^3	3.44×10^2	1.03×10^1	2.17×10^2
10	5.77×10^3	1.58×10^2	1.26×10^3	2.21×10^2	7.90×10^0	1.19×10^2
11	3.80×10^2	1.70×10^1	9.50×10^1	1.95×10^1	8.50×10^{-1}	9.00×10^0
Total	5.14×10^5	6.28×10^2	2.30×10^4	2.51×10^3	5.00×10^1	2.43×10^3

Table C.4 (continued)

Temperature Increment*	Activity (curies)					
	Nb^{95}	Y^{91}	Y^{91m}	Y^{92}	Y^{90}	Y^{93}
1	8.61×10^2	3.18×10^5	5.30×10^4	1.13×10^5	3.84×10^5	2.52×10^4
2	1.03×10^2	3.42×10^4	7.41×10^3	1.20×10^4	3.42×10^4	2.85×10^3
3	1.39×10^2	4.84×10^4	1.03×10^4	1.63×10^4	3.93×10^4	3.99×10^3
4	1.48×10^2	4.94×10^4	1.24×10^4	1.73×10^4	3.46×10^4	4.20×10^3
5	1.93×10^2	6.76×10^4	1.79×10^4	2.22×10^4	3.82×10^4	6.28×10^3
6	2.03×10^2	6.37×10^4	1.99×10^4	2.27×10^4	3.38×10^4	5.97×10^3
7	2.25×10^2	6.19×10^4	2.28×10^4	2.31×10^4	3.10×10^4	5.87×10^3
8	2.12×10^2	5.47×10^4	2.38×10^4	2.14×10^4	2.62×10^4	5.71×10^3
9	2.07×10^2	4.89×10^4	2.53×10^4	2.17×10^4	2.35×10^4	5.43×10^4
10	1.19×10^2	2.45×10^4	1.42×10^4	1.19×10^4	1.11×10^4	3.00×10^4
11	9.00×10^0	1.75×10^3	1.20×10^3	8.50×10^2	7.50×10^2	2.35×10^2
Total	2.43×10^3	7.73×10^5	2.08×10^5	2.82×10^5	6.57×10^5	6.87×10^4

Temperature Increment*	Activity (curies)			
	I^{132}	I^{131}	Y^{94}	Te^{133}
1	2.06×10^3	6.62×10^2	1.19×10^4	1.32×10^2
2	2.85×10^2	1.03×10^2	1.31×10^3	2.11×10^1
3	4.72×10^2	1.82×10^2	1.82×10^3	3.63×10^1
4	6.42×10^2	2.37×10^2	1.98×10^3	4.94×10^1
5	8.21×10^2	3.86×10^2	2.46×10^3	8.69×10^1
6	1.03×10^3	5.17×10^2	2.55×10^3	1.15×10^2
7	1.21×10^3	6.52×10^2	2.64×10^3	1.53×10^2
8	1.31×10^3	7.85×10^2	2.62×10^3	1.79×10^2
9	1.45×10^3	9.05×10^2	2.35×10^3	2.35×10^2
10	1.03×10^3	6.16×10^2	1.34×10^4	1.50×10^2
11	8.00×10^1	6.00×10^1	1.00×10^2	1.30×10^1
Total	1.04×10^4	5.11×10^3	3.11×10^4	1.17×10^3

*The temperature range of the temperature increment and the amount of fuel at temperatures in the temperature increment are the same as given in Table C.3.

Table C.5. Effect of the Purification System on Fission-Product Activity in the Primary Gas System

Nuclide	λ (sec^{-1})	Activity, with $\alpha/T = 0$ (curies)	Activity, with $\alpha/T = 10^{-3}$ (curies)	Activity, with $\alpha/T = 10^{-4}$ (curies)	Activity, with $\alpha/T = 10^{-5}$ (curies)	Activity, with $\alpha/T = 10^{-6}$ (curies)
Br^{84}	3.85×10^{2}	1.21×10^{4}	3.36×10^{3}	9.61×10^{3}	1.18×10^{4}	1.21×10^{4}
Br^{87}	1.25×10^{4}	2.20×10^{3}	2.04×10^{3}	2.18×10^{3}	2.20×10^{3}	2.20×10^{3}
Kr^{87}	1.48×10^{2}	9.15×10^{4}	1.18×10^{4}	5.46×10^{4}	8.57×10^{4}	9.10×10^{4}
Kr^{88}	6.95×10^{1}	1.82×10^{5}	1.18×10^{4}	7.46×10^{4}	1.59×10^{5}	1.79×10^{5}
Rb^{88}	6.49×10^{2}	2.09×10^{5}	8.23×10^{4}	1.81×10^{5}	2.06×10^{5}	2.09×10^{5}
Rb^{89}	7.5×10^{2}	8.45×10^{4}	3.63×10^{4}	7.45×10^{4}	8.34×10^{4}	8.45×10^{4}
Y^{90}	2.98×10^{0}	6.57×10^{5}	1.96×10^{3}	1.91×10^{4}	1.51×10^{5}	4.92×10^{5}
Sr^{91}	1.99×10^{1}	6.10×10^{5}	1.19×10^{4}	1.01×10^{5}	4.06×10^{5}	5.81×10^{5}
Y^{91m}	2.26×10^{2}	2.08×10^{5}	3.83×10^{4}	1.44×10^{5}	1.99×10^{5}	2.07×10^{5}
Y^{91}	1.38×10^{-1}	7.73×10^{5}	1.07×10^{2}	1.07×10^{3}	1.05×10^{4}	9.43×10^{4}
Y^{92}	5.35×10^{1}	2.82×10^{5}	1.44×10^{4}	9.84×10^{4}	2.38×10^{5}	2.77×10^{5}
Y^{93}	1.93×10^{1}	6.87×10^{4}	1.31×10^{3}	1.11×10^{4}	4.53×10^{4}	6.53×10^{4}
Y^{94}	7.0×10^{2}	3.11×10^{4}	1.28×10^{4}	2.72×10^{4}	3.06×10^{4}	3.11×10^{4}
Zr^{95}	1.27×10^{-1}	2.43×10^{3}	3.09×10^{-1}	3.09×10^{0}	3.04×10^{1}	2.75×10^{2}
Nb^{95}	2.29×10^{-1}	2.43×10^{3}	5.56×10^{-1}	5.56×10^{0}	5.44×10^{1}	4.54×10^{2}
Te^{129}	1.6×10^{2}	1.63×10^{3}	2.25×10^{2}	1.00×10^{3}	1.53×10^{3}	1.62×10^{3}
Te^{131}	4.66×10^{2}	3.41×10^{2}	1.08×10^{2}	2.81×10^{2}	3.34×10^{2}	3.41×10^{2}
I^{131}	9.96×10^{-1}	5.11×10^{3}	5.09×10^{0}	5.05×10^{1}	4.65×10^{2}	2.56×10^{3}
I^{132}	8.05×10^{1}	1.04×10^{4}	7.73×10^{2}	4.64×10^{3}	9.26×10^{3}	1.03×10^{4}
Te^{133}	5.78×10^{3}	1.17×10^{3}	9.98×10^{2}	1.15×10^{3}	1.17×10^{3}	1.17×10^{3}
I^{133}	9.25×10^{0}	4.88×10^{3}	4.48×10^{1}	4.12×10^{2}	2.35×10^{3}	4.41×10^{3}
I^{134}	2.20×10^{2}	2.51×10^{3}	4.52×10^{2}	1.72×10^{3}	2.40×10^{3}	2.50×10^{3}
I^{135}	2.89×10^{1}	6.28×10^{2}	1.77×10^{1}	1.41×10^{2}	4.67×10^{2}	6.07×10^{2}
Xe^{135m}	7.4×10^{2}	2.30×10^{4}	9.78×10^{3}	2.02×10^{4}	2.27×10^{4}	2.30×10^{4}
Xe^{135}	2.11×10^{1}	3.86×10^{5}	7.95×10^{3}	6.72×10^{4}	2.62×10^{5}	3.69×10^{5}
I^{136}	8.06×10^{3}	5.00×10^{1}	4.45×10^{1}	4.94×10^{1}	5.0×10^{1}	5.0×10^{1}
Ba^{137m}	4.4×10^{3}	5.14×10^{5}	4.19×10^{5}	5.01×10^{5}	5.13×10^{5}	5.14×10^{5}
Cs^{138}	3.62×10^{2}	2.16×10^{5}	5.72×10^{4}	1.69×10^{5}	2.10×10^{5}	2.15×10^{5}
Ba^{139}	1.36×10^{2}	1.28×10^{5}	1.54×10^{4}	7.37×10^{4}	1.19×10^{5}	1.27×10^{5}
Ba^{140}	6.27×10^{-1}	6.47×10^{5}	4.06×10^{2}	4.06×10^{3}	3.82×10^{4}	2.50×10^{5}
La^{140}	4.79×10^{0}	6.47×10^{5}	3.10×10^{3}	2.96×10^{4}	2.10×10^{5}	5.36×10^{5}
La^{141}	6.42×10^{2}	2.67×10^{5}	1.04×10^{5}	2.31×10^{5}	2.63×10^{5}	2.67×10^{5}
La^{142}	1.56×10^{2}	2.66×10^{4}	3.59×10^{3}	1.62×10^{4}	2.50×10^{4}	2.64×10^{4}
Ce^{143}	6.01×10^{0}	2.23×10^{3}	1.34×10^{1}	1.27×10^{2}	8.38×10^{2}	1.91×10^{3}
Total		6.10×10^{6}	8.51×10^{5}	1.92×10^{6}	3.31×10^{6}	4.68×10^{6}

APPENDIX D. DOSE RATE AT STEAM GENERATORS

The calculation of the dose rate at the steam generator was based on the assumptions that (1) no credit would be taken for the reduction in activity due to a purification system (since, if the deposition rate were high, the purification system would be ineffective), (2) the total system activity would be divided equally between the eight steam generators, and (3) the steam generators would be similar in geometry to the GCR-2 steam generators.

The source in the steam generator was assumed to be of various energies and to have a strength of 1 curie/cm^3. The geometry used for calculating the steam generator shielding is shown in Fig. D.1. The expressions and symbols used are from ref 1. Table D.1 gives the doses for 3, 4, and 5 ft of concrete for 1-curie/cm^3 sources of various energies. Figure D.2 shows the relationship of shield thickness, dose rate, and energy of the assumed source. For the calculation of the data of Table D.1, t_c, the thickness of the concrete, was given the values of 3, 4, and 5 ft, and the following expressions were evaluated:

UNCLASSIFIED
ORNL-LR-DWG 38864

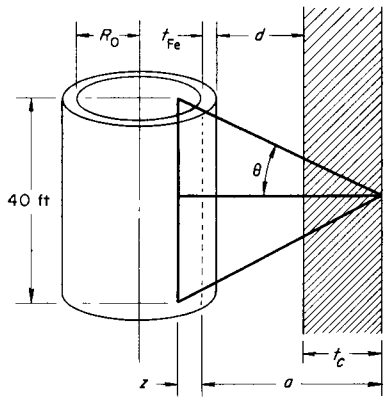

R_0 = 305 cm
t_{Fe} = 7.62 cm
d = 91.4 cm

Fig. D.1. Geometry Used in Shielding Calculation.

$$\phi = \frac{BpR_0^2}{2\,(a+z)}\,F\,(\theta, b_2)\ ,$$

$$b_2 = \mu_{Fe}t_{Fe} + \mu_c t_c + \mu_s z\ ,$$

$$a = 91.4 + 7.62 + t_c = 99.02 + t_c\ ,$$

$$b_1 = \mu_{Fe}t_{Fe} + \mu_c t_c\ ,$$

$$\phi = \frac{(3.7 \times 10^{10})(305)^2}{2\,(a+z)}\,F\,(\theta, b_2)\,B\ .$$

Dose buildup factors for concrete, based on a point isotropic source, were obtained from the expression

$$B\,(E, b_2) = A_1 e^{-a_1 b_2} + A_2 e^{-a_2 b_2}\ ,$$

[1] T. Rockwell III (ed.), *Reactor Shielding Design Manual*, TID-7004 (March 1956).

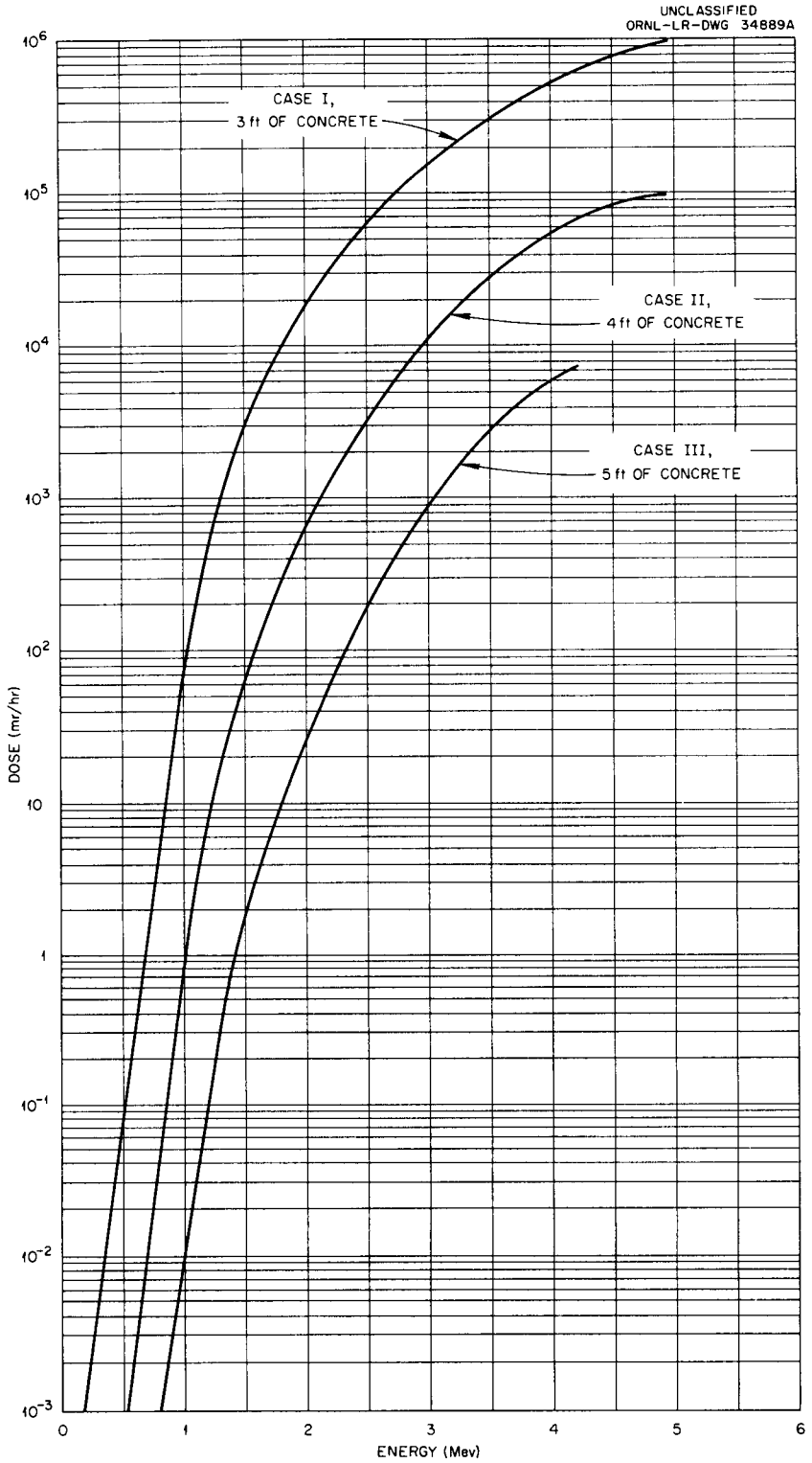

Fig. D.2. Dose from Sources of Various Energies with a Strength of 1 Curie/cm^3.

which was evaluated from the following data:

Energy (Mev)	$-a_1$	$-a_2$	A_1	A_2
0.5	0.11	−0.01	12.5	−11.5
1	0.088	−0.03	10	−9
1.5	0.079	−0.045	8	−7
2	0.063	−0.058	6.3	−5.3
2.5	0.054	−0.067	5.4	−4.4
3	0.062	−0.073	4.7	−3.7
3.5	0.061	−0.077	4.25	−3.25
4	0.059	−0.079	3.9	−2.9

For $E = 0.5$,

$$B = 12.5e^{0.11\,b_2} - 11.5e^{-0.01\,b_2} \;;$$

$E = 1.0$,

$$B = 10.0e^{0.088\,b_2} - 9.0e^{-0.03\,b_2} \;;$$

$E = 1.5$,

$$B = 8.0e^{0.079\,b_2} - 7.0e^{-0.045\,b_2} \;;$$

$E = 2.0$,

$$B = 6.3e^{0.063\,b_2} - 5.3e^{-0.058\,b_2} \;;$$

$E = 2.5$,

$$B = 5.4e^{0.054\,b_2} - 4.4e^{-0.067\,b_2} \;;$$

$E = 3.0$,

$$B = 4.7e^{0.062\,b_2} - 3.7e^{-0.073\,b_2} \;;$$

$E = 3.5$,

$$B = 4.25e^{0.061\,b_2} - 3.25e^{-0.077\,b_2} \;;$$

$E = 4.0$,

$$B = 3.9e^{0.059\,b_2} - 2.9e^{-0.079\,b_2} \;.$$

The gamma energy and the number of photons per disintegration for the nuclides of interest are given in Table D.2. The dose rate from a 1-curie/cm^3 source of the nuclides

is also shown. The values were obtained by using the number of photons per disintegration of a given energy and the data of Fig. D.2. The values of dose rate from a 1-curie/cm^3 source (Table D.2) and from the actual source in the steam generator (Table D.3) were used to obtain the dose rate for various assumed purification rates; the results are presented in Table D.3 and plotted in Fig. D.3. Figure D.3 indicates that about 3 ft of concrete would be required to reduce the dose rate to approximately 7.5 mr/hr during operation. The use of a purification system would only decrease the shield thickness by about 6 in. if it were competitive with deposition in reducing activity.

The amount of activity concentrated in a steam generator was estimated from the following relationship, based on the assumption that all the activity would be uniformly distributed in each of the eight steam generators:

$$S_i = \frac{A_i}{nV} ,$$

where S_i is the activity due to nuclide i in the steam generator (in curies/cm^3), A_i is the total system activity from nuclide i if no purification is assumed (values given in Table C.5), V is the volume of a steam generator, and n is the number of steam generators. Since each steam generator has a volume of about 4×10^8 cm^3,

$$S_i \approx \frac{A_i}{3.2 \times 10^9} \approx 3 \times 10^{-10} A_i .$$

A comparison of the dose rate and shield thickness required for the case of no retention of fission products is presented in Fig. D.4. The effectiveness of graphite in retaining and in holding up fission products results in a decrease in shield thickness for a given dose rate by a factor of 2.

The activity and dose rates during normal operation decay rapidly after shutdown. The shutdown doses from the various nuclides for concrete shield thicknesses of 3 and 4 ft, and for times from shutdown to 10^7 sec, are tabulated in Table D.4. The values of Table D.4 are plotted in Fig. D.5 as functions of shield thickness. From the curves of Fig. D.5, it is possible to determine what thickness of concrete would be necessary to maintain a dose rate of 7.5 mr/hr. This is shown in Fig. D.6, as well as the shielding necessary to maintain a dose rate at 200 mr/hr. From Table D.4 it may be seen that soon after shutdown the main contributor to the dose rate is La^{140} and that this activity predominates until about 10^7 sec (three months), when Y^{90} and Ba^{137m} become the most important activities. Figure D.5 indicates that the problem of doing maintenance on major pieces of equipment may not be too great. The replacement of major pieces of equipment, such as a heat exchanger or a blower, could be done in about 100 days with no shielding; the dose rate would be <200 mr/hr. However, the most significant factor

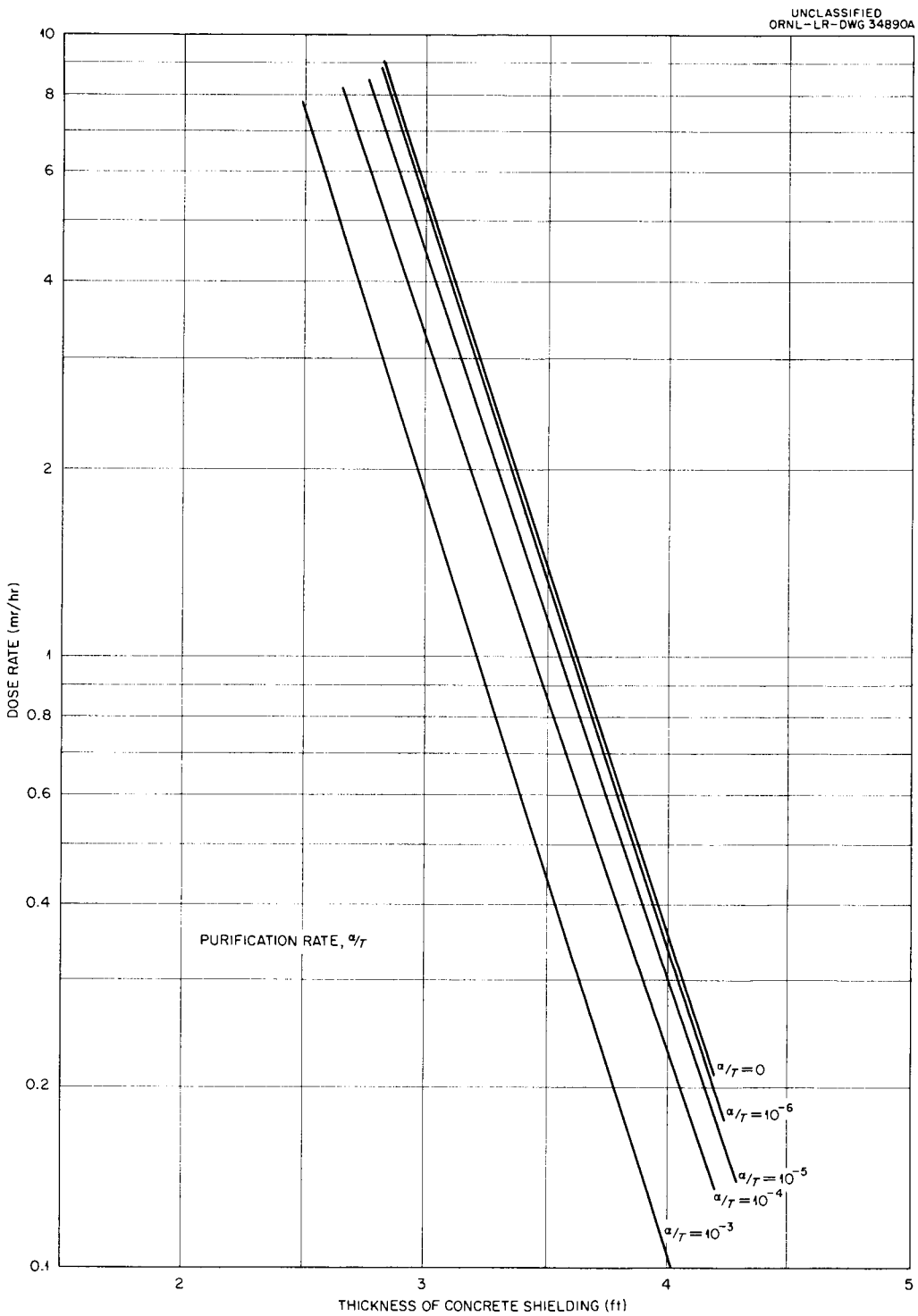

Fig. D.3. Effect of Purification Rate on Dose Rate External to Shielding at the Steam Generators During Normal Operation.

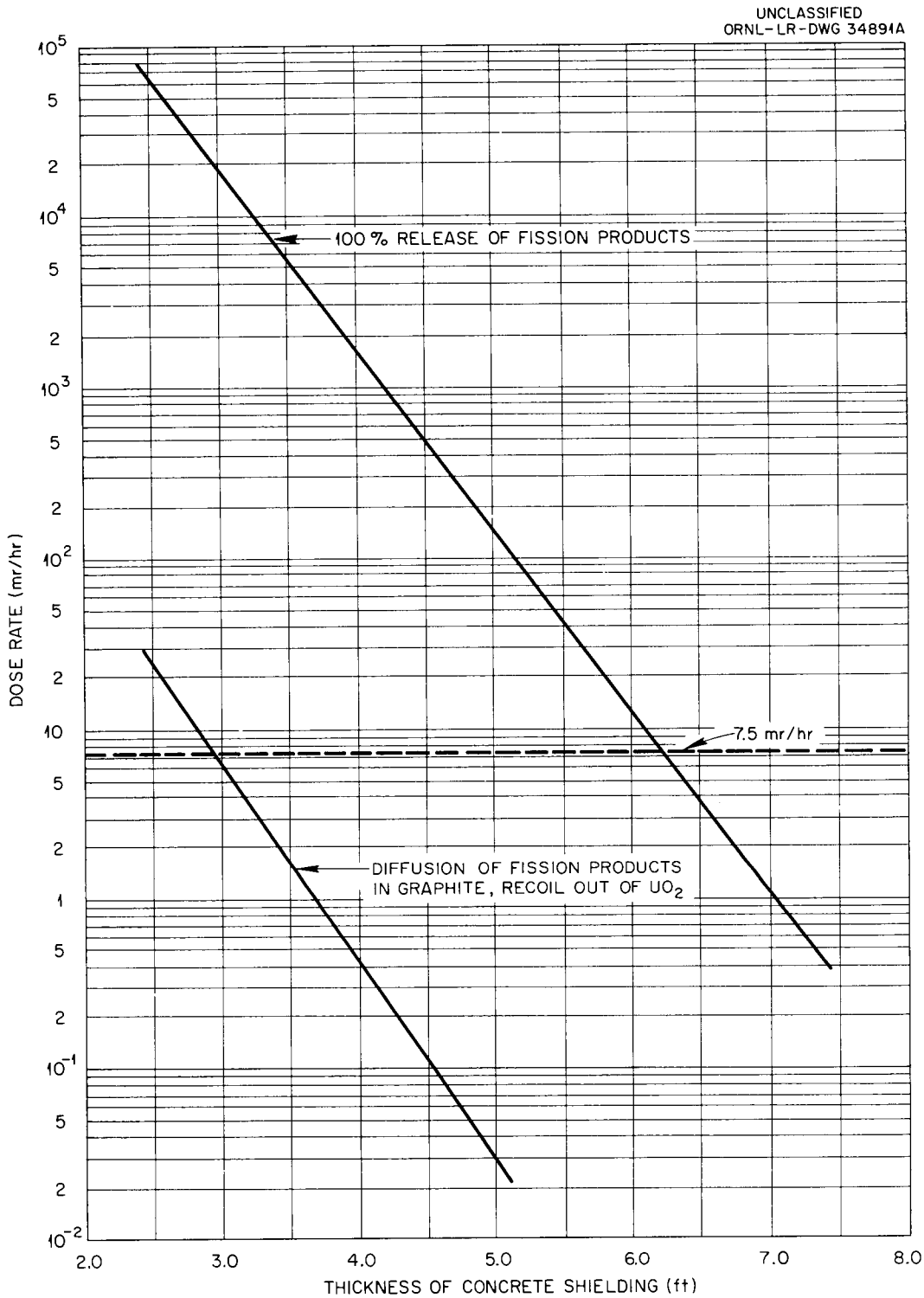

Fig. D.4. Dose Rate External to Shielding at Steam Generators.

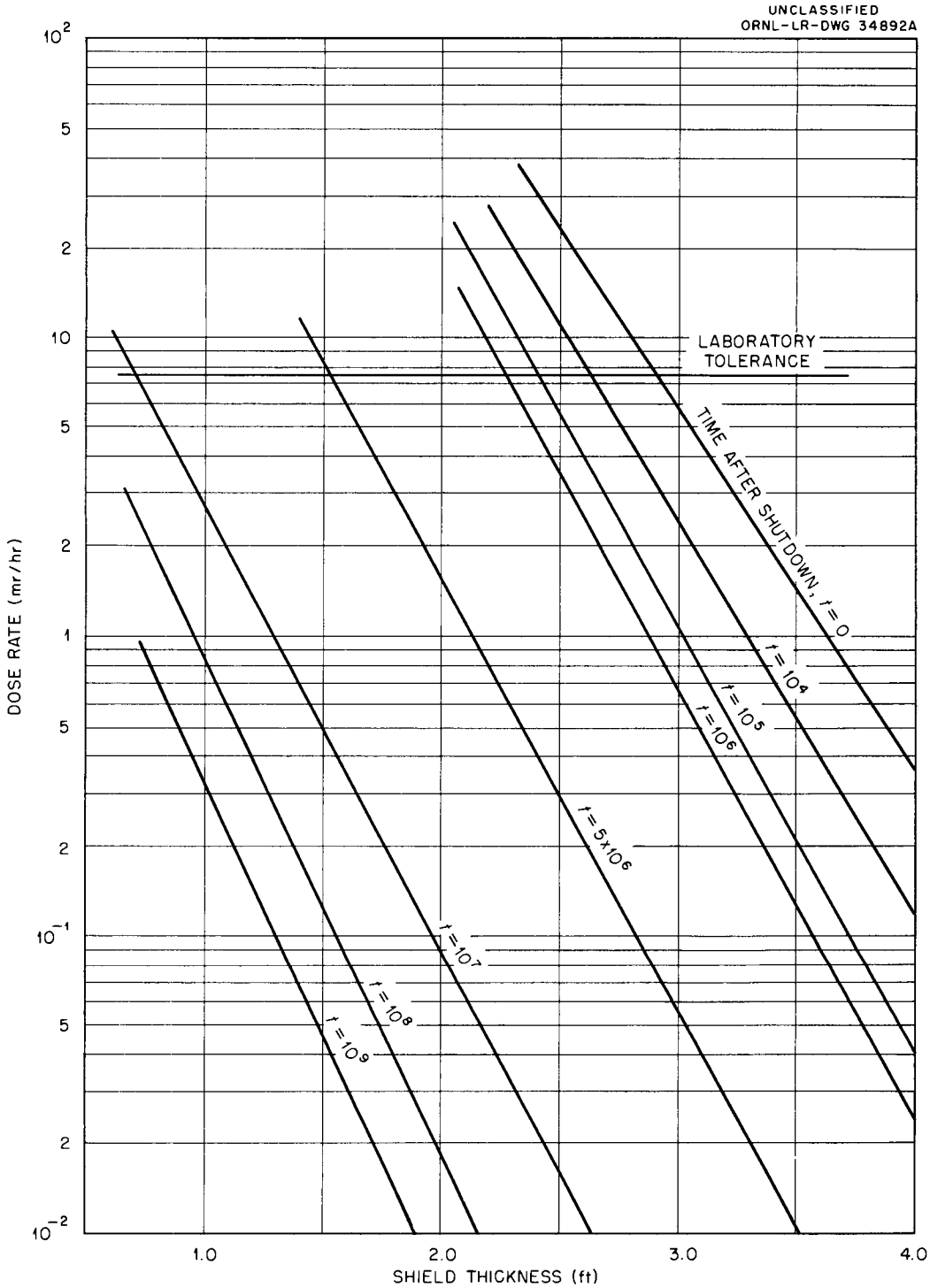

Fig. D.5. Dose Rates at Steam Generators for Various Shield Thicknesses and for Various Times After Shutdown.

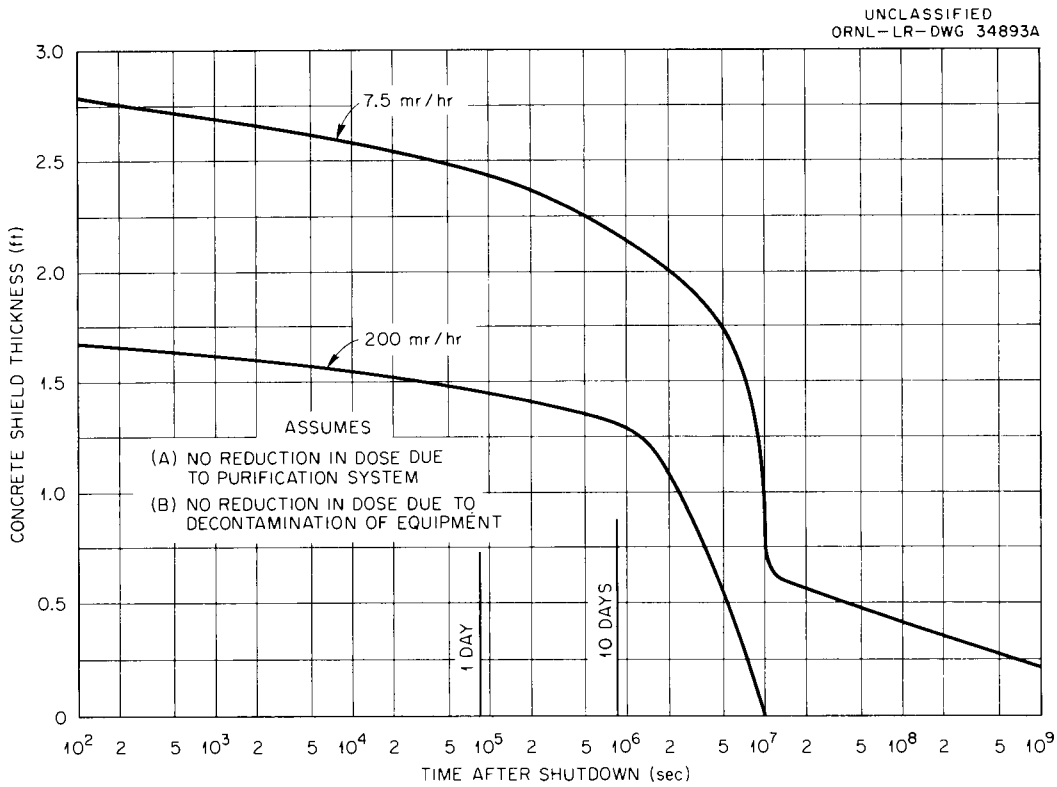

Fig. D.6. Shield Thickness Required To Reduce Dose Rate to 7.5 mr/hr and 200 mr/hr at Steam Generators.

to consider in evaluating the maintenance problem is that the doses shown in Fig. D.5 are upper-limit values. As mentioned earlier, the activity in the system may be reduced by the addition of a purification system. If the deposition rate for long-lived nuclides were not greater than the removal rate by a purification system, it would be possible to reduce the longer-lived nuclides by several orders of magnitude. Maintenance could then await decay of the short-lived activity. The additional possibility of decontamination of equipment could reduce the problem of maintenance. However, it will be necessary to study deposition in these systems before it will be possible to evaluate the usefulness of decontamination techniques.

Table D.1. Calculation of Dose Rate at Steam Generator Pits

Energy (Mev)	μ_s	μ_{Fe}	μ_c	$\mu_{Fe}t_{Fe}$	$\mu_c t_c$	b_1	m	$\frac{1}{m}\mu_s Z$	$\mu_s Z$	Z	b_2	F	B	ϕ	Dose Rate (mr/hr)
Case I: t_c = 3 ft = 91.4 cm (ordinary concrete); a/R_0 = 190.42/305 = 0.624															
0.5	0.0461	0.653	0.206	4.98	18.83	23.81	1.75	3.15	5.51	120	29.32	4×10^{-14}	310	6.87×10^{1}	6.87×10^{-2}
1.0	0.0328	0.465	0.150	3.54	13.71	17.25	1.57	2.7	4.24	129	21.49	1.1×10^{-10}	61.8	3.66×10^{4}	6.65×10^{1}
1.5	0.0266	0.376	0.122	2.86	11.15	14.01	1.45	2.45	3.55	133.5	17.56	6.7×10^{-9}	28.8	1.025×10^{6}	2.63×10^{3}
2.0	0.0232	0.329	0.105	2.51	9.60	12.11	1.38	2.33	3.22	139	15.33	6.7×10^{-8}	14.4	5.04×10^{6}	1.57×10^{4}
2.5	0.0214	0.299	0.094	2.28	8.59	10.87	1.35	2.28	3.08	144	13.95	2.75×10^{-7}	9.8	1.385×10^{7}	5.05×10^{4}
3.0	0.0197	0.279	0.086	2.13	7.86	9.99	1.30	2.28	2.96	150	12.95	7.8×10^{-7}	9.2	3.62×10^{7}	1.51×10^{5}
3.5	0.0189	0.265	0.080	2.02	7.31	9.33	1.28	2.28	2.92	154	12.25	1.6×10^{-6}	7.7	6.14×10^{7}	2.85×10^{5}
4.0	0.0181	0.257	0.075	1.96	6.86	8.82	1.25	2.26	2.82	156	11.64	3×10^{-6}	6.6	9.83×10^{7}	5.04×10^{5}
Case II: t_c = 4 ft = 122 cm (ordinary concrete); a/R_0 = 221.02/305 = 0.724															
0.5	0.0461	0.653	0.206	4.98	25.13	30.11	1.82	3.2	5.81	126	35.92	$\sim 10^{-16}$	642	3.18×10^{-1}	3.18×10^{-4}
1.0	0.0328	0.465	0.150	3.54	18.30	21.84	1.61	2.8	4.51	138	26.35	8×10^{-13}	98	3.76×10^{2}	6.84×10^{-1}
1.5	0.0266	0.376	0.122	2.86	14.88	17.74	1.49	2.53	3.77	142.5	21.51	1.1×10^{-10}	41	2.13×10^{4}	5.45×10^{1}
2.0	0.0232	0.329	0.105	2.51	12.81	15.32	1.43	2.40	3.43	148	18.75	2×10^{-9}	18.8	1.75×10^{5}	5.46×10^{2}
2.5	0.0214	0.299	0.094	2.28	11.47	13.75	1.38	2.32	3.20	150	16.95	1.25×10^{-8}	12	6.95×10^{5}	2.53×10^{3}
3.0	0.0197	0.279	0.086	2.13	10.49	12.62	1.35	2.26	3.06	155	15.68	4.75×10^{-8}	11.2	2.43×10^{6}	1.01×10^{4}
3.5	0.0189	0.265	0.080	2.02	9.76	11.78	1.32	2.23	2.94	155.5	14.72	1.2×10^{-7}	9.4	5.15×10^{6}	2.4×10^{4}
4.0	0.0181	0.251	0.075	1.96	9.15	11.11	1.29	2.20	2.84	157	13.95	2.75×10^{-7}	7.9	9.88×10^{6}	5.06×10^{4}
Case III: t_c = 5 ft = 152 cm (ordinary concrete); a/R_0 = 251.02/305 = 0.824															
0.5	0.0461	0.653	0.206	4.98	31.31	36.29	1.87	3.4	6.36	138	42.65	$\sim 10^{-19}$	1368	6.04×10^{-4}	6.04×10^{-7}
1.0	0.0328	0.465	0.150	3.54	22.80	26.34	1.67	2.75	4.60	140.5	30.94	7.5×10^{-15}	148.4	4.89×10^{0}	8.89×10^{-3}
1.5	0.0266	0.376	0.122	2.86	18.54	21.40	1.52	2.50	3.80	144.0	25.20	2.7×10^{-12}	56.1	6.6×10^{2}	1.7×10^{0}
2.0	0.0232	0.329	0.105	2.51	15.96	18.47	1.46	2.38	3.48	150	21.95	7×10^{-11}	23.6	7.08×10^{3}	2.21×10^{1}
2.5	0.0214	0.299	0.094	2.28	14.29	16.57	1.41	2.29	3.23	151	19.80	6.7×10^{-10}	14.5	4.15×10^{4}	1.51×10^{2}
3.0	0.0197	0.279	0.086	2.13	13.07	15.20	1.37	2.23	3.06	155	18.26	3.3×10^{-9}	13.6	1.9×10^{5}	7.83×10^{2}
3.5	0.0189	0.265	0.080	2.02	12.16	14.18	1.35	2.19	2.96	156.5	17.14	1×10^{-8}	11.2	4.73×10^{5}	2.2×10^{3}
4.0	0.0181	0.257	0.075	1.96	11.40	13.36	1.33	2.15	2.86	158	16.22	2.6×10^{-8}	9.4	1.03×10^{6}	5.28×10^{3}

Table D.2. Dose Rates from a 1-Curie/cm^3 Source

Nuclide	Gamma Emission		Dose Rate for Photons of Energy E (mr/hr)		
	Energy, E (Mev)	Disintegrations of Energy E (%)	Case I, 3 ft of Concrete	Case II, 4 ft of Concrete	Case III, 5 ft of Concrete
Br^{84}	3.93	10	4.8×10^4	4.7×10^3	4.9×10^2
	3.28	4.0	8.8×10^3	6.8×10^2	5.6×10^1
	3.03	3.3	4.95×10^3	3.3×10^2	2.48×10^1
	2.82	2.7	2.97×10^3	1.78×10^2	1.16×10^1
	2.47	12	6.0×10^3	3.0×10^2	1.68×10^1
	2.17	2.7	6.75×10^2	2.56×10^1	1.08×10^0
	2.05	1.6	2.88×10^2	1.04×10^1	4.0×10^{-1}
	1.90	20	2.6×10^3	7.6×10^1	3.0×10^0
	1.74	1.6	Neg.	Neg.	Neg.
	1.57	1.3	Neg.	Neg.	Neg.
	1.47	1.6	Neg.	Neg.	Neg.
	1.21	3.3	Neg.	Neg.	Neg.
	1.01	15	Neg.	Neg.	Neg.
	0.88	50	Neg.	Neg.	Neg.
	0.81	5	Neg.	Neg.	Neg.
		Total	7.428×10^4	6.3×10^3	6.343×10^2
Br^{87}	5.4	56	5.6×10^5	5.6×10^4	5.6×10^3
	3.0	14	1.96×10^4	1.4×10^3	1.06×10^2
		Total	5.796×10^5	5.74×10^4	5.706×10^3
Kr^{87}	2.55	21	1.26×10^4	6.7×10^2	3.56×10^1
	2.10	4	8.0×10^2	3.2×10^1	1.2×10^0
	0.85	9	Neg.	Neg.	Neg.
	0.405	91	Neg.	Neg.	Neg.
		Total	1.34×10^4	7.02×10^2	3.68×10^1
Kr^{88}	2.4	35	1.47×10^4	7×10^2	3.5×10^1
	2.19	18	4.5×10^3	1.8×10^2	8.17×10^0
	1.55	14	Neg.	Neg.	Neg.
	0.85	23	Neg.	Neg.	Neg.
		Total	1.92×10^4	8.8×10^2	4.32×10^1
Rb^{88}	4.87	0.46	4.14×10^3	4.14×10^2	4.14×10^1
	3.68	0.13	4.55×10^2	4.17×10^1	4.04×10^0
	3.52	0.37	1.11×10^3	9.62×10^1	9.25×10^0

Table D.2 (continued)

Nuclide	Gamma Emission		Dose Rate for Photons of Energy E (mr/hr)		
	Energy, E (Mev)	Disintegrations of Energy E (%)	Case I, 3 ft of Concrete	Case II, 4 ft of Concrete	Case III, 5 ft of Concrete
Rb^{88}	3.24	0.46	9.65×10^{2}	6.9×10^{1}	6.44×10^{0}
	3.01	0.46	6.9×10^{2}	4.6×10^{1}	3.45×10^{0}
	2.68	2.5	1.93×10^{3}	1.1×10^{2}	6.75×10^{0}
	2.11	1.2	2.52×10^{2}	9.6×10^{0}	4.2×10^{-1}
	1.85	32.6	3.26×10^{3}	6.52×10^{1}	3.26×10^{0}
	1.39	2.0	Neg.	Neg.	Neg.
	0.908	18	Neg.	Neg.	Neg.
		Total	1.28×10^{4}	8.52×10^{2}	7.5×10^{1}
Rb^{89}	3.52	2.16	6.48×10^{3}	5.84×10^{2}	5.4×10^{1}
	2.75	2.74	2.48×10^{3}	1.49×10^{2}	9.35×10^{0}
	2.59	12.5	8.11×10^{3}	4.25×10^{2}	2.5×10^{1}
	2.20	14.1	3.67×10^{3}	1.41×10^{2}	7.05×10^{0}
	1.55	3.5	1.05×10^{2}	2.45×10^{0}	7×10^{-2}
	1.26	53.2	3.19×10^{2}	5.32×10^{0}	1.06×10^{-1}
	1.05	70.8	Neg.	Neg.	Neg.
	0.663	16.0	Neg.	Neg.	Neg.
		Total	2.12×10^{4}	1.38×10^{3}	9.56×10^{1}
Sr^{91}	1.413	7	9.8×10^{1}	2.1×10^{0}	4.9×10^{-1}
	1.025	33	2.31×10^{1}	2.31×10^{-1}	Neg.
	0.747	29	Neg.	Neg.	Neg.
	0.65	44	Neg.	Neg.	Neg.
		Total	1.21×10^{2}	2.3×10^{0}	4.9×10^{-1}
Y^{90}	1.734	0.02	1.4×10^{0}	3.6×10^{-2}	1.2×10^{-3}
		Total	1.4×10^{0}	3.6×10^{-2}	1.2×10^{-3}
Y^{91m}	0.551	100	1.5×10^{-1}	$\sim 1.5 \times 10^{-2}$	$\sim 1.5 \times 10^{-3}$
		Total	1.5×10^{-1}	$\sim 1.5 \times 10^{-2}$	$\sim 1.5 \times 10^{-3}$
Y^{91}	1.22	0.3	1.5×10^{0}	2.4×10^{-2}	3.9×10^{-4}
		Total	1.5×10^{0}	2.4×10^{-2}	3.9×10^{-4}
Y^{92}	2.4	1	4.4×10^{2}	2.0×10^{1}	1×10^{0}
	1.9	5	6.0×10^{2}	1.9×10^{1}	6.5×10^{-1}

Table D.2 (continued)

Nuclide	Gamma Emission		Dose Rate for Photons of Energy E (mr/hr)		
	Energy, E (Mev)	Disintegrations of Energy E (%)	Case I, 3 ft of Concrete	Case II, 4 ft of Concrete	Case III, 5 ft of Concrete
Y^{92}	1.45	50	1.0×10^{3}	2.0×10^{1}	5×10^{-1}
	0.94	150	Neg.	Neg.	Neg.
		Total	2.04×10^{3}	5.9×10^{1}	2.15×10^{0}
Y^{93}	2.14	0.9	2.16×10^{2}	8.1×10^{0}	3.51×10^{-1}
	1.88	2.2	2.64×10^{2}	7.05×10^{0}	2.64×10^{-1}
	1.40	1.0	1.4×10^{1}	3×10^{-1}	7×10^{-3}
	1.15	0.5	Neg.	Neg.	Neg.
	0.94	3.56	Neg.	Neg.	Neg.
	0.68	1.44	Neg.	Neg.	Neg.
		Total	4.94×10^{2}	1.545×10^{1}	6.22×10^{-1}
Y^{94}	1.4	100	1.4×10^{3}	3×10^{1}	7×10^{-1}
		Total	1.4×10^{3}	3×10^{1}	7×10^{-1}
Te^{129}	1.1	10	1.5×10^{1}	2.6×10^{-1}	7×10^{-3}
	0.74	4	Neg.	Neg.	Neg.
	0.47	15	Neg.	Neg.	Neg.
		Total	1.5×10^{1}	2.6×10^{-1}	7×10^{-3}
Te^{131}	1.14	10	2.4×10^{1}	4.0×10^{-1}	9×10^{-3}
	0.95	5	Neg.	Neg.	Neg.
	0.60	5	Neg.	Neg.	Neg.
	0.45	20	Neg.	Neg.	Neg.
		Total	2.4×10^{1}	4.0×10^{-1}	9.0×10^{-3}
Te^{133}	1.0	100	6.6×10^{1}	6.84×10^{-1}	8.9×10^{-3}
	0.6	100	3×10^{-1}	Neg.	Neg.
		Total	6.63×10^{1}	6.84×10^{-1}	8.9×10^{-3}
I^{131}	0.722	2.8	5.6×10^{-2}	$\sim 1.4 \times 10^{-3}$	$\sim 2.04 \times 10^{-6}$
	0.637	9.3	Neg.	Neg.	Neg.
		Total	5.6×10^{-2}	$\sim 1.4 \times 10^{-3}$	$\sim 2.0 \times 10^{-6}$
I^{132}	2.2	2	5.2×10^{2}	2×10^{1}	1×10^{0}
	1.96	5	7.0×10^{2}	2.2×10^{1}	8.5×10^{-1}
	1.4	11	1.54×10^{2}	3.3×10^{0}	7.7×10^{-2}
	1.16	8	Neg.	Neg.	Neg.

Table D.2 (continued)

Nuclide	Gamma Emission		Dose Rate for Photons of Energy E (mr/hr)		
	Energy, E (Mev)	Disintegrations of Energy E (%)	Case I, 3 ft of Concrete	Case II, 4 ft of Concrete	Case III, 5 ft of Concrete
I^{132}	0.96	20	Neg.	Neg.	Neg.
	0.777	75	Neg.	Neg.	Neg.
	0.673	100	Neg.	Neg.	Neg.
	0.624	6	Neg.	Neg.	Neg.
	0.528	25	Neg.	Neg.	Neg.
		Total	1.374×10^3	4.5×10^1	1.92×10^0
I^{133}	1.4	1	1.4×10^1	3×10^{-1}	7×10^{-3}
	0.85	5	Neg.	Neg.	Neg.
	0.53	94	Neg.	Neg.	Neg.
		Total	1.4×10^1	3×10^{-1}	7×10^{-3}
I^{134}	1.78	35	2.8×10^3	7.0×10^1	2.45×10^0
	1.1	35	Neg.	Neg.	Neg.
	0.86	30	Neg.	Neg.	Neg.
		Total	2.8×10^3	7.0×10^1	2.45×10^0
I^{135}	1.8	11	9.9×10^2	2.53×10^1	8.8×10^{-1}
	1.72	19	1.33×10^3	3.04×10^1	1.14×10^0
	1.46	12	2.4×10^2	4.8×10^0	1.2×10^{-1}
	1.28	34	2.2×10^2	3.4×10^0	6.8×10^{-2}
	1.14	37	8.5×10^1	1.4×10^0	2.2×10^{-2}
	1.04	9	Neg.	Neg.	Neg.
	0.86	11	Neg.	Neg.	Neg.
	0.53	27	Neg.	Neg.	Neg.
	0.42	6.9	Neg.	Neg.	Neg.
		Total	2.87×10^3	6.53×10^1	2.23×10^0
I^{136*}	2.6	20	1.34×10^4	7.2×10^2	4×10^1
	1.3	60	4.8×10^2	8.4×10^0	1.8×10^{-1}
		Total	1.39×10^4	7.28×10^2	4.02×10^1
Xe^{135m}	0.5	100	6.87×10^{-2}	3.18×10^{-4}	6.04×10^{-7}
		Total	6.87×10^{-2}	3.18×10^{-4}	6.04×10^{-7}

*Estimated.

Table D.2 (continued)

Nuclide	Gamma Emission		Dose Rate for Photons of Energy E (mr/hr)		
	Energy, E (Mev)	Disintegrations of Energy E (%)	Case I, 3 ft of Concrete	Case II, 4 ft of Concrete	Case III, 5 ft of Concrete
Cs^{138}	3.34	0.5	1.2×10^3	9.0×10^1	8.0×10^0
	2.63	9	6.39×10^3	3.6×10^2	2.16×10^1
	2.21	18	5.05×10^3	2.16×10^2	9.36×10^0
	1.43	73	1.24×10^3	2.55×10^1	6.56×10^{-1}
	1.01	25	1.66×10^1	1.71×10^{-1}	2.22×10^{-3}
	0.87	4	Neg.	Neg.	Neg.
	0.55	8	Neg.	Neg.	Neg.
	0.463	23	Neg.	Neg.	Neg.
		Total	1.39×10^4	9.21×10^2	3.96×10^1
Ba^{137m}	0.661	100	6×10^{-1}	$\sim 10^{-3}$	$\sim 10^{-6}$
		Total	6×10^{-1}	$\sim 10^{-3}$	$\sim 10^{-6}$
Ba^{139}	1.43	19	3.23×10^2	6.65×10^0	1.71×10^{-1}
		Total	3.23×10^2	6.65×10^0	1.71×10^{-1}
Ba^{140}	0.54	30	2.06×10^{-2}	9.5×10^{-5}	1.8×10^{-7}
		Total	2.06×10^{-2}	9.5×10^{-5}	1.8×10^{-7}
La^{140}	3.0	1	1.51×10^3	1.01×10^2	7.83×10^0
	2.5	5.4	5.05×10^2	2.53×10^1	1.51×10^0
	1.6	94	3.76×10^3	8.46×10^1	2.72×10^0
	0.81	29	Neg.	Neg.	Neg.
	5	3.9	Neg.	Neg.	Neg.
		Total	5.77×10^3	2.11×10^2	1.21×10^1
La^{141}	1.5	5	1.32×10^2	2.73×10^0	8.5×10^{-2}
		Total	1.32×10^2	2.73×10^0	8.5×10^{-2}
Zr^{95}	0.757	49	1.13×10^0	6.85×10^{-3}	1.96×10^{-5}
	0.724	49	7.83×10^{-1}	4.4×10^{-3}	1.08×10^{-5}
		Total	1.91×10^0	1.12×10^{-2}	3.04×10^{-5}
Nb^{95}	0.768	100	2.7×10^0	1.7×10^{-2}	5.4×10^{-5}
		Total	2.7×10^0	1.7×10^{-2}	5.4×10^{-5}
La^{142}	0.87	10	1×10^0	8×10^{-3}	5×10^{-5}
	0.63	90	3.6×10^{-1}	1.98×10^{-3}	4.5×10^{-6}
		Total	1.36×10^0	1×10^{-2}	5.5×10^{-5}

Table D.2 (continued)

Nuclide	Gamma Emission		Dose Rate for Photons of Energy E (mr/hr)		
	Energy, E (Mev)	Disintegrations of Energy E (%)	Case I, 3 ft of Concrete	Case II, 4 ft of Concrete	Case III, 5 ft of Concrete
Xe^{135}	0.6	4	1×10^{-2}	5.6×10^{-5}	2.0×10^{-7}
		Total	1×10^{-2}	5.6×10^{-5}	2.0×10^{-7}
Ce^{143}	1.1	6	9.6×10^{0}	1.56×10^{-1}	4.2×10^{-3}
	0.86	6	6×10^{-1}	4.8×10^{-3}	3.0×10^{-5}
	0.57	6	Neg.	Neg.	Neg.
	0.72	1	Neg.	Neg.	Neg.
	0.67	4	Neg.	Neg.	Neg.
		Total	1.02×10^{1}	1.61×10^{-1}	4.23×10^{-3}

Table D.3. Dose Rate at Steam Generators for Various Purification Rates*

S_i = source strength of indicated nuclide in curies/cm^3
D_i = dose rate from indicated nuclide in mr/hr

Nuclide, N_i	S_i for $\alpha/T = 0$	D_i with 3 ft of Concrete	D_i with 4 ft of Concrete	S_i for $\alpha/T = 10^{-3}$	D_i with 3 ft of Concrete	D_i with 4 ft of Concrete	S_i for $\alpha/T = 10^{-4}$	D_i with 3 ft of Concrete	D_i with 4 ft of Concrete	S_i for $\alpha/T = 10^{-5}$	D_i with 3 ft of Concrete	D_i with 4 ft of Concrete	S_i for $\alpha/T = 10^{-6}$	D_i with 3 ft of Concrete	D_i with 4 ft of Concrete
Br^{84}	3.63×10^{-6}	2.70×10^{-1}	2.29×10^{-2}	1.01×10^{-6}	7.50×10^{-2}	6.36×10^{-3}	2.88×10^{-6}	2.14×10^{-1}	1.81×10^{-2}	3.54×10^{-6}	2.63×10^{-1}	2.23×10^{-2}	3.63×10^{-6}	2.70×10^{-1}	2.29×10^{-2}
Br^{87}	6.6×10^{-7}	3.83×10^{-1}	3.79×10^{-2}	6.12×10^{-7}	3.55×10^{-1}	3.51×10^{-2}	6.54×10^{-7}	3.79×10^{-1}	3.75×10^{-2}	6.60×10^{-7}	3.83×10^{-1}	3.79×10^{-2}	6.60×10^{-7}	3.83×10^{-1}	3.79×10^{-2}
Kr^{87}	2.75×10^{-5}	3.69×10^{-1}	1.93×10^{-2}	3.54×10^{-6}	4.74×10^{-2}	2.49×10^{-3}	1.63×10^{-5}	2.18×10^{-1}	1.14×10^{-2}	2.57×10^{-5}	3.44×10^{-1}	1.80×10^{-2}	2.73×10^{-5}	3.66×10^{-1}	1.92×10^{-2}
Kr^{88}	5.46×10^{-5}	1.05×10^{0}	4.80×10^{-2}	3.54×10^{-6}	6.80×10^{-2}	3.12×10^{-3}	2.23×10^{-5}	4.28×10^{-1}	1.96×10^{-2}	4.77×10^{-5}	9.16×10^{-1}	4.20×10^{-2}	5.37×10^{-5}	1.03×10^{0}	4.73×10^{-2}
Rb^{88}	6.27×10^{-5}	8.03×10^{-1}	6.84×10^{-2}	2.47×10^{-5}	3.16×10^{-1}	2.10×10^{-2}	5.43×10^{-5}	6.95×10^{-1}	4.63×10^{-2}	6.18×10^{-5}	7.91×10^{-1}	5.27×10^{-2}	6.27×10^{-5}	8.03×10^{-1}	6.84×10^{-2}
Rb^{89}	2.54×10^{-5}	5.38×10^{-1}	4.65×10^{-2}	1.09×10^{-5}	2.31×10^{-1}	1.99×10^{-2}	2.23×10^{-5}	4.73×10^{-1}	4.08×10^{-2}	2.51×10^{-5}	5.32×10^{-1}	4.59×10^{-2}	2.54×10^{-5}	5.38×10^{-1}	4.65×10^{-2}
Y^{90}	1.97×10^{-4}	2.76×10^{-4}	7.09×10^{-6}	5.88×10^{-7}	8.23×10^{-7}	2.12×10^{-8}	5.73×10^{-6}	8.02×10^{-6}	2.06×10^{-7}	4.53×10^{-5}	6.34×10^{-5}	1.63×10^{-6}	1.48×10^{-4}	2.07×10^{-4}	5.33×10^{-6}
Sr^{91}	1.83×10^{-4}	2.21×10^{-2}	4.21×10^{-4}	3.57×10^{-6}	4.32×10^{-4}	8.21×10^{-6}	3.03×10^{-5}	3.67×10^{-3}	6.97×10^{-5}	1.22×10^{-4}	1.48×10^{-2}	2.81×10^{-4}	1.74×10^{-4}	2.11×10^{-2}	4.00×10^{-4}
Y^{91m}	6.24×10^{-5}	9.36×10^{-6}	9.36×10^{-7}	1.15×10^{-5}	1.73×10^{-6}	1.73×10^{-7}	4.32×10^{-5}	6.48×10^{-6}	6.48×10^{-7}	5.97×10^{-5}	8.93×10^{-6}	8.96×10^{-7}	6.21×10^{-5}	9.32×10^{-6}	9.32×10^{-7}
Y^{91}	2.32×10^{-4}	3.48×10^{-4}	5.57×10^{-6}	3.21×10^{-8}	4.82×10^{-8}	7.70×10^{-10}	3.21×10^{-7}	4.82×10^{-7}	7.70×10^{-4}	3.15×10^{-6}	4.73×10^{-6}	7.56×10^{-8}	2.83×10^{-5}	4.25×10^{-5}	6.79×10^{-7}
Y^{92}	8.46×10^{-5}	1.73×10^{-1}	4.99×10^{-3}	4.32×10^{-6}	8.81×10^{-3}	2.55×10^{-4}	2.95×10^{-5}	6.02×10^{-2}	1.74×10^{-3}	7.14×10^{-5}	1.46×10^{-1}	4.21×10^{-3}	8.31×10^{-5}	1.70×10^{-1}	4.90×10^{-3}
Y^{93}	2.06×10^{-5}	1.02×10^{-2}	3.19×10^{-4}	3.93×10^{-7}	1.94×10^{-4}	6.09×10^{-6}	3.33×10^{-6}	1.65×10^{-3}	5.16×10^{-5}	1.36×10^{-5}	6.72×10^{-3}	2.11×10^{-4}	1.96×10^{-5}	9.68×10^{-3}	3.04×10^{-4}
Y^{94}	9.33×10^{-6}	1.31×10^{-2}	2.78×10^{-4}	3.84×10^{-6}	5.38×10^{-3}	1.15×10^{-4}	8.16×10^{-6}	1.14×10^{-2}	2.45×10^{-4}	9.18×10^{-6}	1.29×10^{-2}	2.75×10^{-4}	9.33×10^{-6}	1.31×10^{-2}	2.78×10^{-4}
Zr^{95}	7.29×10^{-7}	1.39×10^{-6}	8.16×10^{-9}	9.27×10^{-11}	1.77×10^{-10}	1.04×10^{-12}	9.27×10^{-10}	1.77×10^{-9}	1.04×10^{-11}	9.12×10^{-9}	1.74×10^{-8}	1.02×10^{-10}	8.25×10^{-8}	1.58×10^{-7}	1.95×10^{-9}
Nb^{95}	7.29×10^{-7}	1.97×10^{-6}	1.24×10^{-8}	1.66×10^{-10}	4.48×10^{-10}		1.66×10^{-9}	4.48×10^{-9}		1.63×10^{-8}	4.40×10^{-8}		1.36×10^{-7}	3.67×10^{-7}	
Te^{129}	4.89×10^{-7}	7.34×10^{-6}	1.27×10^{-7}	6.75×10^{-8}	1.01×10^{-6}		3.00×10^{-7}	4.5×10^{-6}		4.59×10^{-7}	6.89×10^{-6}		4.86×10^{-7}	7.29×10^{-6}	
Te^{131}	1.02×10^{-7}	2.45×10^{-6}	4.08×10^{-8}	3.24×10^{-8}	7.78×10^{-7}		8.43×10^{-8}	2.02×10^{-6}		1.00×10^{-7}	2.4×10^{-6}		1.02×10^{-7}	2.45×10^{-6}	
I^{131}	1.53×10^{-6}	8.57×10^{-8}	2.14×10^{-9}	1.53×10^{-9}	8.57×10^{-11}		1.52×10^{-8}	8.51×10^{-10}		1.39×10^{-7}	7.78×10^{-9}		7.68×10^{-6}	4.30×10^{-7}	
I^{132}	3.12×10^{-6}	4.27×10^{-3}	1.40×10^{-4}	2.32×10^{-7}	3.18×10^{-4}	1.04×10^{-5}	1.39×10^{-6}	1.90×10^{-3}	6.26×10^{-5}	2.78×10^{-6}	3.81×10^{-3}	1.25×10^{-4}	3.09×10^{-6}	4.23×10^{-3}	1.39×10^{-4}
Te^{133}	3.51×10^{-7}	2.33×10^{-5}	2.40×10^{-7}	2.99×10^{-7}	1.98×10^{-5}		3.45×10^{-7}	2.29×10^{-5}		3.51×10^{-7}	2.33×10^{-5}		3.51×10^{-7}	2.33×10^{-5}	
I^{133}	1.46×10^{-6}	2.04×10^{-5}	4.38×10^{-7}	1.34×10^{-8}	1.88×10^{-7}		1.24×10^{-7}	1.74×10^{-6}		7.05×10^{-7}	4.87×10^{-6}		1.32×10^{-6}	1.85×10^{-5}	
I^{134}	7.53×10^{-7}	2.11×10^{-3}	5.27×10^{-5}	1.36×10^{-7}	3.81×10^{-4}	9.52×10^{-6}	5.16×10^{-7}	1.44×10^{-3}	3.61×10^{-5}	7.20×10^{-7}	2.20×10^{-3}	5.04×10^{-5}	7.50×10^{-7}	2.1×10^{-3}	5.25×10^{-5}
I^{135}	1.88×10^{-7}	5.40×10^{-4}	1.23×10^{-5}	5.31×10^{-9}	1.52×10^{-5}	3.47×10^{-7}	4.23×10^{-8}	1.21×10^{-4}	2.76×10^{-6}	1.40×10^{-7}	4.02×10^{-4}	9.14×10^{-6}	1.82×10^{-7}	5.22×10^{-4}	1.19×10^{-5}
Xe^{135m}	6.90×10^{-6}	4.74×10^{-7}	2.19×10^{-9}	2.93×10^{-6}	2.01×10^{-7}		6.06×10^{-6}	4.16×10^{-7}		6.81×10^{-6}	4.68×10^{-7}		6.90×10^{-6}	4.74×10^{-7}	
Xe^{135}	1.15×10^{-4}	1.15×10^{-6}	6.44×10^{-9}	2.38×10^{-6}	2.38×10^{-8}		2.20×10^{-5}	2.02×10^{-7}		7.86×10^{-5}	7.86×10^{-7}		1.11×10^{-4}	1.11×10^{-6}	
I^{136}	1.5×10^{-8}	2.09×10^{-4}	1.09×10^{-5}	1.33×10^{-8}	1.85×10^{-4}	9.68×10^{-6}	1.48×10^{-8}	2.06×10^{-4}	1.08×10^{-5}	1.50×10^{-8}	2.09×10^{-4}	1.09×10^{-5}	1.50×10^{-8}	2.09×10^{-4}	1.09×10^{-5}
Ba^{137m}	1.54×10^{-4}	9.24×10^{-5}	1.54×10^{-7}	1.24×10^{-4}	7.44×10^{-5}		1.5×10^{-4}	9.0×10^{-4}		1.54×10^{-4}	9.24×10^{-2}		1.54×10^{-4}	9.24×10^{-4}	
Cs^{138}	6.48×10^{-5}	9.01×10^{-1}	5.97×10^{-2}	1.72×10^{-5}	2.39×10^{-1}	1.58×10^{-2}	5.07×10^{-5}	7.05×10^{-1}	4.67×10^{-2}	6.30×10^{-5}	8.76×10^{-1}	5.80×10^{-2}	6.45×10^{-5}	8.97×10^{-1}	5.94×10^{-2}
Ba^{139}	3.84×10^{-5}	1.24×10^{-2}	2.55×10^{-4}	4.62×10^{-6}	1.49×10^{-3}	3.07×10^{-5}	2.21×10^{-5}	7.14×10^{-3}	1.47×10^{-4}	3.57×10^{-5}	1.15×10^{-2}	2.37×10^{-4}	3.81×10^{-5}	1.23×10^{-2}	2.53×10^{-4}
Ba^{140}	1.94×10^{-4}	4.00×10^{-6}	1.84×10^{-8}	1.22×10^{-7}	2.51×10^{-9}		1.22×10^{-6}	2.51×10^{-8}		1.15×10^{-5}	2.37×10^{-7}		7.5×10^{-5}	1.55×10^{-6}	
La^{140}	1.94×10^{-4}	1.12×10^{0}	4.09×10^{-2}	9.3×10^{-7}	5.37×10^{-3}	1.96×10^{-4}	8.88×10^{-6}	5.12×10^{-2}	1.87×10^{-3}	6.30×10^{-5}	3.64×10^{-1}	1.33×10^{-2}	1.61×10^{-4}	9.29×10^{-1}	3.40×10^{-2}
La^{141}	8.00×10^{-5}	1.06×10^{-2}	2.19×10^{-4}	3.12×10^{-5}	4.12×10^{-3}	8.52×10^{-5}	6.93×10^{-5}	9.15×10^{-3}	1.89×10^{-4}	7.89×10^{-5}	1.04×10^{-2}	2.15×10^{-4}	8.01×10^{-5}	1.06×10^{-2}	2.19×10^{-4}
La^{142}	7.98×10^{-6}	1.09×10^{-5}	7.98×10^{-8}	1.07×10^{-6}	1.46×10^{-6}		4.86×10^{-6}	6.61×10^{-6}		7.50×10^{-6}	1.02×10^{-5}		7.92×10^{-6}	1.08×10^{-5}	
Ce^{143}	6.69×10^{-7}	6.82×10^{-6}	1.08×10^{-7}	4.02×10^{-9}	4.10×10^{-8}		3.81×10^{-8}	3.89×10^{-7}		2.51×10^{-7}	2.56×10^{-6}		5.73×10^{-7}	5.84×10^{-6}	
Totals		5.68	0.350		1.85	0.104		3.26	0.224		4.68	0.298		5.46	0.342

*Dose rates for a 1-curie/cm^3 source are given in Table D.2.

Table D.4. Dose Rates at Steam Generator and Outside Shields of 3 and 4 ft of Concrete for Various Times After Shutdown*

Nuclide	Dose Rate (mr/hr)													
	At $t = 0$		At $t = 10^4$ sec			At $t = 10^5$ sec			At $t = 10^6$ sec			At $t = 10^7$ sec		
	3 ft of Concrete	4 ft of Concrete	Fraction of Dose at $t = 0$	3 ft of Concrete	4 ft of Concrete	Fraction of Dose at $t = 0$	3 ft of Concrete	4 ft of Concrete	Fraction of Dose at $t = 0$	3 ft of Concrete	4 ft of Concrete	Fraction of Dose at $t = 0$	3 ft of Concrete	4 ft of Concrete
Br^{84}	2.7×10^{-1}	2.29×10^{-2}	2.2×10^{-2}	5.94×10^{-3}	5.04×10^{-4}									
Br^{87}	3.83×10^{-1}	3.79×10^{-2}												
Kr^{87}	3.69×10^{-1}	1.93×10^{-2}	2.3×10^{-1}	8.49×10^{-2}	4.44×10^{-3}	10^{-6}	3.69×10^{-7}	1.93×10^{-8}						
Kr^{88}	1.05×10^{0}	4.80×10^{-2}	5.0×10^{-1}	5.25×10^{-1}	2.40×10^{-2}	9.0×10^{-4}	9.45×10^{-4}	4.22×10^{-5}						
Rb^{88}	8.03×10^{-1}	6.84×10^{-2}	5.5×10^{-1}	4.42×10^{-1}	3.76×10^{-2}	1.1×10^{-3}	8.83×10^{-4}	7.52×10^{-5}						
Rb^{89}	5.38×10^{-1}	4.65×10^{-2}	7×10^{-4}	3.77×10^{-4}	3.26×10^{-5}									
Y^{90}	2.76×10^{-4}	7.09×10^{-6}	1.0	2.76×10^{-4}	7.09×10^{-6}	1.0	2.76×10^{-4}	7.09×10^{-6}	1.0	2.76×10^{-4}	7.09×10^{-6}	1.0	2.76×10^{-4}	7.09×10^{-6}
Sr^{91}	2.21×10^{-2}	4.21×10^{-4}	8.5×10^{-1}	1.88×10^{-2}	3.58×10^{-4}	1.4×10^{-1}	3.09×10^{-3}	5.89×10^{-5}						
Y^{91m}	9.36×10^{-6}	9.36×10^{-7}	9.0×10^{-1}	8.42×10^{-6}	8.42×10^{-7}	1.5×10^{-1}	1.40×10^{-6}	1.40×10^{-7}						
Y^{91}	3.48×10^{-4}	5.57×10^{-6}	1.0	3.48×10^{-4}	5.57×10^{-6}	1.0	3.48×10^{-4}	5.57×10^{-6}	9.0×10^{-1}	3.13×10^{-4}	5.01×10^{-6}	2.6×10^{-1}	9.05×10^{-5}	1.45×10^{-6}
Y^{92}	1.73×10^{-1}	4.99×10^{-3}	8.4×10^{-1}	1.45×10^{-1}	4.19×10^{-3}	1.6×10^{-2}	2.77×10^{-3}	7.98×10^{-5}						
Y^{93}	1.02×10^{-2}	3.19×10^{-4}	8.5×10^{-1}	8.67×10^{-3}	2.71×10^{-4}	1.4×10^{-1}	1.43×10^{-3}	4.47×10^{-5}						
Y^{94}	1.31×10^{-2}	2.78×10^{-4}	1×10^{-3}	1.31×10^{-5}	2.78×10^{-7}									
Zr^{95}	1.39×10^{-6}	8.16×10^{-9}	1.0	1.39×10^{-6}	8.16×10^{-9}	1.0	1.39×10^{-6}	8.16×10^{-9}	1.0	1.39×10^{-6}	8.16×10^{-9}	3×10^{-1}	4.17×10^{-7}	2.45×10^{-9}
Nb^{95}	1.97×10^{-6}	1.24×10^{-8}	1.0	1.97×10^{-6}	1.24×10^{-8}	1.0	1.97×10^{-6}	1.24×10^{-8}	1.0	1.97×10^{-6}	1.24×10^{-8}	5×10^{-1}	9.35×10^{-7}	6.20×10^{-9}
Te^{129}	7.34×10^{-6}	1.27×10^{-7}	9.5×10^{-1}	6.97×10^{-6}	1.21×10^{-7}	3.5×10^{-1}	2.57×10^{-6}	4.45×10^{-8}	2.7×10^{-1}	1.98×10^{-6}	3.43×10^{-8}	3×10^{-2}	2.20×10^{-7}	3.81×10^{-9}
Te^{131}	2.45×10^{-6}	4.08×10^{-8}	1.4×10^{-1}	3.43×10^{-7}	5.71×10^{-9}	3.3×10^{-4}	8.09×10^{-10}	1.35×10^{-11}						
I^{131}	8.57×10^{-8}	2.14×10^{-9}	1.0	8.57×10^{-8}	2.14×10^{-9}	8.5×10^{-1}	7.28×10^{-8}	1.82×10^{-9}	3.7×10^{-1}	3.17×10^{-8}	7.92×10^{-10}	5×10^{-5}	4.29×10^{-12}	1.07×10^{-13}
I^{132}	4.27×10^{-3}	1.40×10^{-4}	1.0	4.27×10^{-3}	1.40×10^{-4}	8.0×10^{-1}	3.42×10^{-3}	1.12×10^{-4}	9.0×10^{-2}	3.84×10^{-4}	1.26×10^{-5}			
Te^{133}	2.33×10^{-5}	2.40×10^{-7}	1.8×10^{-1}	4.19×10^{-6}	4.32×10^{-8}									
I^{133}	2.04×10^{-5}	4.38×10^{-7}	1.0	2.04×10^{-5}	4.38×10^{-7}	4.3×10^{-1}	8.77×10^{-6}	1.88×10^{-7}	1.05×10^{-4}	2.14×10^{-9}	4.60×10^{-11}			
I^{134}	2.11×10^{-3}	5.27×10^{-5}	2.8×10^{-1}	5.91×10^{-4}	1.48×10^{-5}									
I^{135}	5.40×10^{-4}	1.23×10^{-5}	7.5×10^{-1}	4.05×10^{-4}	9.23×10^{-6}	5.5×10^{-2}	2.97×10^{-5}	6.77×10^{-7}						
Xe^{135m}	4.74×10^{-7}	2.19×10^{-9}	7.0×10^{-1}	3.32×10^{-7}	1.53×10^{-9}	5.8×10^{-2}	2.75×10^{-8}	1.27×10^{-10}						
Xe^{135}	1.15×10^{-6}	6.44×10^{-9}	1.1×10^{0}	1.27×10^{-6}	7.08×10^{-9}	5.0×10^{-1}	5.75×10^{-7}	3.22×10^{-9}						
I^{136}	2.09×10^{-4}	1.09×10^{-5}												
Ba^{137m}	9.24×10^{-5}	1.54×10^{-7}	1.0	9.24×10^{-5}	1.54×10^{-7}	1.0	9.24×10^{-5}	1.54×10^{-7}	1.0	9.24×10^{-5}	1.54×10^{-7}	1.0	9.24×10^{-5}	1.54×10^{-7}
Cs^{138}	9.01×10^{-1}	5.97×10^{-2}	5.3×10^{-2}	4.78×10^{-2}	3.16×10^{-3}									
Ba^{139}	1.24×10^{-2}	2.55×10^{-4}	3×10^{-1}	3.72×10^{-3}	7.65×10^{-5}	3×10^{-6}	3.72×10^{-8}	7.65×10^{-10}						
Ba^{140}	4.00×10^{-6}	1.84×10^{-8}	1.0	4.00×10^{-6}	1.84×10^{-8}	9.5×10^{-1}	3.8×10^{-6}	1.75×10^{-8}	5.4×10^{-1}	2.16×10^{-6}	9.94×10^{-9}	2.0×10^{-3}	8.00×10^{-9}	3.68×10^{-11}
La^{140}	1.12×10^{0}	4.09×10^{-2}	1.0	1.12×10^{0}	4.09×10^{-2}	9.5×10^{-1}	1.06×10^{0}	3.89×10^{-2}	5.8×10^{-1}	6.50×10^{-1}	2.37×10^{-2}	2.2×10^{-3}	2.46×10^{-3}	9.00×10^{-5}
La^{141}	1.06×10^{-2}	2.19×10^{-4}	6.4×10^{-1}	6.78×10^{-3}	1.40×10^{-4}	6×10^{-3}	6.36×10^{-5}	1.31×10^{-6}						
La^{142}	1.09×10^{-5}	7.98×10^{-8}	2.3×10^{-1}	2.51×10^{-6}	1.84×10^{-8}	$\sim 10^{-6}$	1.09×10^{-11}	7.98×10^{-14}						
Ce^{143}	6.82×10^{-6}	1.08×10^{-7}	1.0	6.82×10^{-6}	1.08×10^{-7}	6.0×10^{-1}	4.09×10^{-6}	6.48×10^{-8}	3×10^{-3}	2.05×10^{-8}	3.24×10^{-10}			
Total dose rate	5.68	0.350		2.41	0.115		1.07	3.93×10^{-2}		6.51×10^{-1}	2.37×10^{-2}		2.93×10^{-3}	9.87×10^{-5}

*The dose rates tabulated are for the case of a purification rate of $\alpha/T = 0$; the purification system was assumed to be ineffective for removing activity both during reactor operation and for periods after shutdown.

APPENDIX E. STEAM SYSTEM CALCULATIONS

NOMENCLATURE

A = area, ft^2

A_{lm} = log mean area, ft^2

A_f = fin area, ft^2

A_i = inside (water side) area, ft^2

A_o = tube outside area, ft^2

A_t = total gas side area, ft^2

C_p = specific heat, Btu/lb·ft

D_e = equivalent diameter, ft

D_i = inside diameter, ft

D_o = outside diameter, ft

f = friction factor, dimensionless

f_B = fraction of F_{B+S} that is transferred in the boiler

f_S = fraction of F_{B+S} that is transferred in the superheater

F_B = fraction of heat transferred in boiler

F_{B+S} = fraction of heat transferred in boiler and superheater

F_E = fraction of heat transferred in the economizer

F_S = fraction of heat transferred in superheater

F_{TPF} = two-phase flow factor

g_c = conversion factor, 4.18×10^8 $lb_m \cdot ft/lb_f \cdot hr$

G = mass flow rate, $lb/ft^2 \cdot °F$

h = enthalpy, Btu/lb

h = heat transfer coefficient, $Btu/hr \cdot ft^2 \cdot °F$

h_{FW} = feedwater enthalpy, Btu/lb

h_g = gas side heat transfer coefficient, $Btu/hr \cdot ft^2 \cdot °F$

h_i = inside heat transfer coefficient, $Btu/hr \cdot ft^2 \cdot °F$

h_w = water side heat transfer coefficient, $Btu/hr \cdot ft^2 \cdot °F$

H = matrix height, ft

ΔH = head loss, $ft \cdot lb_f/lb_m$

j = $(Nu)(Pr)^{2/3}$, dimensionless group

k = thermal conductivity, Btu/hr·ft^2·(°F/ft)

L = length, ft

N = number of tube banks normal to gas flow

Nu = Nusselt number, dimensionless

Δp = pressure drop, lb/ft^2

Δp_{lp} = pressure drop, liquid phase, lb/ft^2

P = wetted perimeter, ft

PP = pumping power

Pr = Prandtl number, dimensionless

q = rate of heat transfer, Btu/hr

r_h = hydraulic radius, ft

Re = Reynolds number, dimensionless

R_{foul} = fouling resistance to heat transfer, (Btu/hr·ft^2·°F)$^{-1}$

R_{wall} = wall resistance to heat transfer, (Btu/hr·ft^2·°F)$^{-1}$

t = temperature, °F

t_B = boiling temperature, °F

$t_{g_{B,S}}$ = gas temperature at the boiler-superheater interface, °F

t_{g_i} = gas inlet temperature to the superheater, °F

t_{g_o} = gas outlet temperature from the heat exchanger, °F

t_{S_o} = steam outlet temperature from superheater, °F

Δt = temperature difference, °F

Δt_{lm} = log mean temperature difference

Δt_{lm_B} = log mean temperature difference in the boiler

Δt_{lm_S} = log mean temperature difference in the superheater

Δt_p = "pinch" temperature difference, °F

T = absolute temperature, °F

U = over-all heat transfer coefficient, Btu/hr·ft^2·°F

w_g = gas flow rate, lb/hr

w_w = water flow rate, lb/hr

x = thickness of material through which heat flows, ft

η = efficiency

μ = viscosity, lb/hr·ft

ϕ = Gardner's fin efficiency

ρ = density, lb/ft^3

HEAT TRANSFER IN STEAM GENERATOR SECTIONS

The fraction of heat transferred in each section and the feedwater temperature as a function of the "pinch" temperature difference (Δt_p) were shown in Fig. 20, Chap. 6. The data were calculated in the manner described below.

Fraction of heat transferred in the boiler and superheater is

$$F_{B+S} = \frac{t_{\text{gas in superheater}} - t_{\text{gas out of boiler}}}{t_{\text{gas in superheater}} - t_{\text{gas out of economizer}}}$$

$$= \frac{1500 - (591.7 + \Delta t_p)}{1500 - 506} = \frac{908.3 - \Delta t_p}{994} .$$

The fraction of heat transferred in the boiler is

$$F_B = f_B F_{B+S} ,$$

where

f_B = the fraction of F_{B+S} that is transferred in the boiler

$$= \frac{h_{\text{boiler outlet}} - h_{\text{boiler inlet}}}{h_{\text{superheater outlet}} - h_{\text{boiler inlet}}} ,$$

h = steam and/or water enthalpy,

$$f_B = \frac{1170.7 - 605.2}{1521 - 605.2} = 0.617 ;$$

then

$$F_B = 0.617 F_{B+S} .$$

The fraction transferred in the superheater is

$$F_S = f_S F_{B+S} ,$$

where

$$f_S = 1 - f_B .$$

That is,

$$F_S = (1 - 0.617) F_{B+S} = 0.383 F_{B+S} .$$

The fraction of the heat transferred in the economizer is

$$F_E = 1 - F_{B+S} .$$

The required feedwater inlet enthalpy as a function of Δt_p is

$$\frac{h_{\text{boiler inlet}} - h_{\text{feedwater}}}{h_{\text{superheater outlet}} - h_{\text{feedwater}}} = F_E \ ,$$

$$\frac{605.2 - h_{FW}}{1521 - h_{FW}} = 1 - F_{B+S} \ ,$$

$$h_{FW} = \frac{605.2 - 1521\,(1 - F_{B+S})}{F_{B+S}} \ .$$

The corresponding temperature for the resultant h_{FW} was read from the steam tables[1] and plotted in Fig. 20, Chap. 6, along with F_B, F_S, and F_E.

LOG MEAN TEMPERATURE DIFFERENCES IN STEAM GENERATOR SECTIONS

The log mean temperature difference as a function of pinch temperature difference was given in Fig. 19, Chap. 6. These temperatures are calculated as follows:

$$\Delta t_{lm} = \frac{\Delta t_{\text{large}} - \Delta t_{\text{small}}}{\ln \dfrac{\Delta t_{\text{large}}}{\Delta t_{\text{small}}}} \ .$$

Superheater

$$\Delta t_{lm_S} = \frac{\left(t_{g_{B,S}} - t_B\right) - \left(t_{g_i} - t_{S_o}\right)}{\ln \dfrac{t_{g_{B,S}} - t_B}{t_{g_i} - t_{S_o}}} \ ,$$

where

$t_{g_{B,S}}$ = temperature of gas at boiler-superheater intersection,

t_B = boiling temperature of steam,

t_{g_i} = gas inlet temperature,

t_{S_o} = steam outlet temperature.

The term $t_{g_{B,S}}$ is related to the pinch temperature as follows:

$$t_{g_{B,S}} = t_{g_i} - \left(t_{g_i} - t_{g_o}\right) F_S \ ,$$

[1] J. H. Keenan and F. K. Keyes, *Thermodynamic Properties of Steam*, Wiley, New York, 1936.

where

$$F_S = (0.383)\frac{908.3 - \Delta t_p}{994} .$$

The quantity F_S can also be read from Fig. 20, Chap. 6. Substituting the relevant numbers in this case:

$$\Delta t_{lm_S} = \frac{[1500 - (1500 - 506)F_S - 591.7] - (1500 - 1050)}{\ln \dfrac{[1500 - (1500 - 506)F_S - 591.7]}{(1500 - 1050)}} .$$

Collecting terms:

$$\Delta t_{lm_S} = \frac{458.3 - 994F_S}{\ln \dfrac{908.3 - 994F_S}{450}} .$$

Boiler

$$\Delta t_{lm_B} = \frac{\left(t_{g_{B,S}} - t_B\right) - \left(t_{g_{B,E}} - t_B\right)}{\ln \dfrac{t_{g_{B,S}} - t_B}{t_{g_{B,E}} - t_B}} ,$$

where

$t_{g_{B,S}}$ = gas temperature at boiler-superheater interface,

$t_{g_{B,E}}$ = gas temperature at boiler-economizer interface

$= t_{g_{i\ \text{superheater}}} - \left(t_{g_{i\ \text{superheater}}} - t_{g_{o\ \text{economizer}}}\right)(F_{B+S})$.

Substituting the relevant numbers:

$$\Delta t_{lm_B} = \frac{[1500 - (1500 - 506)F_S - 591.7] - [1500 - (1500 - 506)F_{B+S} - 591.7]}{\ln \dfrac{[1500 - (1500 - 506)F_S - 591.7]}{[1500 - (1500 - 506)F_{B+S} - 591.7]}} .$$

Collecting terms:

$$\Delta t_{lm_B} = \frac{994F_{B+S} - 994F_S}{\ln \dfrac{908.3 - 994F_S}{908.3 - 994F_{B+S}}} ,$$

where

$F_{B+S} = F_B + F_S$,

and F_B and F_S are as shown in Fig. 20, Chap. 6.

Economizer

$$\Delta t_{lm_E} = \frac{\left(t_{g_{B,E}} - t_B\right) - \left(t_{g_o} - t_{FW}\right)}{\ln \dfrac{t_{g_{B,E}} - t_B}{t_{g_o} - t_{FW}}} ,$$

where t_{FW} is the feedwater temperature taken from Fig. 20, Chap. 6. Substituting numbers:

$$\Delta t_{lm_E} = \frac{[1500 - (1500 - 506)F_{B+S} - 591.7] - (506 - t_{FW})}{\ln \dfrac{[1500 - (1500 - 506)F_{B+S} - 591.7]}{(506 - t_{FW})}} .$$

Collecting terms:

$$\Delta t_{lm_E} = \frac{402.3 - 994F_{B+S} + t_{FW}}{\ln \dfrac{908.3 - 994F_{B+S}}{506 - t_{FW}}} .$$

PROCEDURE FOR SCALING GCR-2 STEAM GENERATORS

Power Output per Heat Exchanger

Power output of reactor = 3095 Mw.

Blower pumping power = 72,000 hp = 53.65 Mw.

Total power to be removed by heat exchanger = 3095 + 54 = 3149 Mw.

Power removed by GCR-2 steam generators = 700 Mw.

$$\frac{\text{Power removed HGCR-1}}{\text{Power removed GCR-2}} = \frac{3149}{700} = 4.5 .$$

The HGCR-1 has twice as many heat exchangers as the GCR-2.

Power removed per steam generator = 4.5/2 = 2.25 × GCR-2 power.

Temperature Rise Due to Pumping Power

The gas flow rate per heat exchanger is

$$w_g = \frac{q}{C_p\left(t_{g_i} - t_{g_o}\right)} \quad \frac{(3.095 \times 10^6)(3413)}{(1.248)(1500 - 525)(8)} = 1.085 \times 10^6 \text{ lb/hr} .$$

Power input per blower = (9000 hp) (0.7068) (3600) = 2.29×10^7 Btu/hr.

$$\text{Temperature rise through blower} = q/w_g C_p = \frac{2.29 \times 10^7}{(1.085 \times 10^6)(1.248)} = 16.9°\text{F}.$$

Feedwater Temperature

A temperature rise through the shell annulus of about 2°F was assumed. The temperature of the gas carried out of the economizer was 525 – 18.9 = 506.1°F, and a 50°F pinch temperature was assumed. Similar procedures would be followed for other pinch temperatures. From Fig. 20, Chap. 6, the feedwater inlet temperature was found to be 480°F.

Heat Removed by Each Section

The proportions of heat removed by each section (from Fig. 20, Chap. 6) are:

Heat removed by economizer = 13.5% .

Heat removed by boiler = 53.5% .

Heat removed by superheater = 33% .

The proportions of heat removed by each section of the GCR-2 exchangers are:[2]

Heat removed by economizer = 21.12% .

Heat removed by boiler = 54.8% .

Heat removed by superheater = 24.1% .

The ratio of heat removal by each section of the HGCR-1 to that removed by the corresponding GCR-2 section is:

1. Economizer

$$\left(\frac{q_{\text{HGCR-1}}}{q_{\text{GCR-2}}}\right)_{\text{economizer}} = \left(\frac{q_{\text{HGCR-1}}}{q_{\text{GCR-2}}}\right)_{\text{total per steam generator}} \left(\frac{F_{E_{\text{HGCR-1}}}}{F_{E_{\text{GCR-2}}}}\right)$$

$$= (2.25)\left(\frac{13.5}{21.12}\right) = 1.438 \ .$$

2. Boiler

$$\left(\frac{q_{\text{HGCR-1}}}{q_{\text{GCR-2}}}\right)_{\text{boiler}} = (2.25)\left(\frac{53.5}{54.8}\right) = 2.196 \ .$$

3. Superheater

$$\left(\frac{q_{\text{HGCR-1}}}{q_{\text{GCR-2}}}\right)_{\text{superheater}} = (2.25)\left(\frac{33.0}{24.1}\right) = 3.082 \ .$$

---

[2] *The ORNL Gas-Cooled Reactor*, ORNL-2500 (April 1, 1958).

The Over-All Heat Transfer Coefficient

The relationship for the gas-side heat transfer coefficient for cross flow outside a bank of finned tubes is

$$j = 1.38\ \mathrm{Re}^{-0.385}$$

(average of composite data of refs 3 and 4); that is,

$$\left(\frac{h}{C_p G}\right)\left(\frac{C_p \mu}{k}\right)^{2/3} = 1.38\left(\frac{\mu}{GD_e}\right)^{0.385} .$$

Solving for h:

$$h = 1.38\ \frac{C_p^{1/3} k^{2/3}}{\mu^{0.282}}\ \frac{G^{0.615}}{D^{0.385}} .$$

Since $k^{2/3}/\mu^{0.282}$ does not vary too greatly with temperature (about 6% in 300°F), for simplification let

$$h \sim G^{0.615} .$$

Since $G = w_g/A$, and for this compilation A, the free-flow area, is constant

$$\frac{h_{\mathrm{HGCR-1}}}{h_{\mathrm{GCR-2}}} = (1.224)^{0.615} = 1.1323 .$$

The ratio of water flow through the tubes is

$$\left(\frac{w_{\mathrm{HGCR-1}}}{w_{\mathrm{GCR-2}}}\right)_w = \frac{q_{\mathrm{HGCR-1}}}{q_{\mathrm{GCR-2}}}\ \frac{(h_S - h_{FW})_{\mathrm{GCR-2}}}{(h_S - h_{FW})_{\mathrm{HGCR-1}}}$$

$$= 2.25\ \frac{(1477.7 - 295.5)}{(1521 - 464)} = 2.25\ \frac{(1182.2)}{(1033.2)} = 2.52 .$$

The water-side heat transfer coefficient h_w is proportional to $G^{0.8}$ in the economizer and superheater, and because of lack of information is assumed to remain constant in the boiler. The ratios, then, are as follows:

$$\left(\frac{h_{\mathrm{HGCR-1}}}{h_{\mathrm{GCR-2}}}\right)_{w,\mathrm{economizer}} = (2.52)^{0.8} = 2.13 ,$$

---

[3] W. M. Kays and A. L. London, *Trans. ASME* 72, 1075 (1950).

[4] D. L. Katz *et al.*, *Correlation of Heat Transfer and Pressure Drop for Air Flowing Across Banks of Finned Tubes*, Engineering Research Institute Project 1592, Rep. 30, University of Michigan, Dec. 1954.

$$\left(\frac{h_{\text{HGCR-1}}}{h_{\text{GCR-2}}}\right)_{w,\text{boiler}} = 1 \ ,$$

$$\left(\frac{h_{\text{HGCR-1}}}{h_{\text{GCR-2}}}\right)_{w,\text{superheater}} = 2.13 \ .$$

The equation defining the over-all heat transfer coefficient U is

$$\frac{1}{UA_o} = \frac{1}{h_g(A_t + \phi A_f)} + \frac{1}{h_w A_i} + \frac{R_{\text{wall}}}{A_{lm}} + \frac{R_{\text{foul}}}{A_i} \ .$$

Since the fin efficiency ϕ is a function[5] of $\sqrt{h_g}$, and h_g varies only by about 13%, it is assumed that the same fin efficiency exists as in the GCR-2. The wall and fouling resistances were allowed to be constant since they are of a small order. Then

$$\frac{1}{(UA_o)_{\text{HGCR-1}}} = \frac{1}{h_{g\ \text{GCR-2}}\left(\frac{h_{\text{HGCR-1}}}{h_{\text{GCR-2}}}\right)_g (A_t + \phi A_f)} + \frac{1}{h_{w\ \text{GCR-2}}\left(\frac{h_{\text{HGCR-1}}}{h_{\text{GCR-2}}}\right)_w A_i} + \frac{R_{\text{wall}}}{A_{lm}} + \frac{R_{\text{foul}}}{A_i}$$

$$= \left(\frac{h_{\text{GCR-2}}}{h_{\text{HGCR-1}}}\right)_g \left[\frac{1}{h_{\text{GCR-2}}(A_t + \phi A_f)}\right] + \left(\frac{h_{\text{GCR-2}}}{h_{\text{HGCR-1}}}\right)_w \left(\frac{1}{h_{w\ \text{GCR-2}} A_i}\right) + \frac{R_{\text{wall}}}{A_{lm}} + \frac{R_{\text{foul}}}{A_i} \ .$$

For the economizer:

$$\frac{1}{(UA_o)_{\text{HGCR-1}}} = 0.00531\left(\frac{h_{\text{GCR-2}}}{h_{\text{HGCR-1}}}\right)_g + 0.00188\left(\frac{h_{\text{GCR-2}}}{h_{\text{HGCR-1}}}\right)_w + 0.00154 + 0.00151$$

$$= 0.00531\left(\frac{1}{1.323}\right) + 0.00188\left(\frac{1}{2.13}\right) + 0.00154 + 0.00151 \ .$$

$$(UA_o)_{\text{HGCR-1}} = 116.0 \ .$$

$$(UA_o)_{\text{GCR-2}} = 97.7 \ .$$

$$\left(\frac{U_{\text{HGCR-1}}}{U_{\text{GCR-2}}}\right)_{\text{economizer}} = \frac{116.0}{97.7} = 1.187 \ .$$

[5] K. A. Gardner, *Trans. ASME* **67**, 621 (1945).

For the boiler:

$$\frac{1}{(UA_o)_{HGCR-1}} = 0.0185\left(\frac{h_{GCR-2}}{h_{HGCR-1}}\right)_g + 0.00486\left(\frac{h_{GCR-2}}{h_{HGCR-1}}\right)_w + 0.005875 + 0.00486$$

$$= 0.185\left(\frac{1}{1.323}\right) + 0.00486\ (1) + 0.005875 + 0.00486$$

$$= 0.3190\ .$$

$$\frac{1}{(UA_o)_{GCR-2}} = 0.03409\ .$$

$$\left(\frac{U_{HGCR-1}}{U_{GCR-2}}\right)_{boiler} = \frac{0.03409}{0.03190} = 1.0667\ .$$

$$\frac{1}{U_{HGCR-1}} = 0.002158\left(\frac{h_{GCR-2}}{h_{HGCR-1}}\right)_w + 0.01048\left(\frac{h_{GCR-2}}{h_{HGCR-1}}\right)_g + 0.00125 + 0.000634$$

$$= 0.002158\left(\frac{1}{2.13}\right) + 0.01048\left(\frac{1}{1.323}\right) + 0.00125 + 0.000634$$

$$= 0.012157\ .$$

$$\left(\frac{U_{HGCR-1}}{U_{GCR-2}}\right)_{superheater} = \frac{0.01456}{0.012157} = 1.196\ .$$

Calculation of Tube Area, Length, and Matrix Height

The ratio of the areas for each section is

$$\frac{A_{HGCR-1}}{A_{GCR-2}} = \frac{q_{HGCR-1}}{q_{GCR-2}}\left(\frac{\Delta t_{GCR-2}}{\Delta t_{HGCR-1}}\right)_{lm}\frac{U_{GCR-2}}{U_{HGCR-1}} = \frac{L_{HGCR-1}}{L_{GCR-2}}\ .$$

The log mean temperature difference, Δt_{lm}, for the GCR-2 is

Economizer	54.1°F
Boiler	103.7°F
Superheater	139.8°F

These figures include an ignorance factor of 0.95 to account for the fact that the actual flow in the heat exchanger is not pure counterflow. The HGCR-1 Δt_{lm} is corrected in the same manner for consistency.

The HGCR-1 log mean temperature differences are shown as a function of pinch temperature difference in Fig. 19, Chap. 6. The results for the HGCR-1 at a 50°F pinch temperature difference corrected with the 0.95 factor are:

Economizer	39°F
Boiler	205.8°F
Superheater	488°F

The required surface area, tube length, and matrix height can now be found.

Economizer:

$$\frac{A_{HGCR-1}}{A_{GCR-2}} = 1.438\left(\frac{54.1}{38}\right)\left(\frac{1}{1.187}\right) = 1.726$$

Outside surface area

$$A_{HGCR-1} = 1.726\ (122{,}000) = 210{,}800\ \text{ft}^2$$

Tube length

$$L_{HGCR-1} = 1.726\ (25{,}100) = 43{,}350\ \text{ft}$$

Matrix height

$$H_{HGCR-1} = 1.726\ (8.9) = 15.35\ \text{ft}$$

Boiler:

$$\frac{A_{HGCR-1}}{A_{GCR-2}} = 2.196\left(\frac{103.7}{205.8}\right)\left(\frac{1}{1.0667}\right) = 1.037$$

Outside surface area

$$A_{HGCR-1} = 1.037\ (112{,}700) = 116{,}900\ \text{ft}^2$$

Tube length

$$L_{HGCR-1} = 1.037\ (28{,}400) = 29{,}450\ \text{ft}$$

Matrix height

$$H_{HGCR-1} = 1.037\ (11.7) = 12.14\ \text{ft}$$

Superheater:

$$\frac{A_{HGCR-1}}{A_{GCR-2}} = 3.082\left(\frac{139.8}{488}\right)\left(\frac{1}{1.196}\right) = 0.738$$

Outside surface area

$$A_{HGCR-1} = 0.738\ (15{,}750) = 11{,}620\ \text{ft}^2$$

Tube length

$$L = 0.738\ (25{,}300) = 18{,}670 \text{ ft}$$

Matrix height

$$H = 0.738\ (14.2) = 10.48 \text{ ft}$$

Total matrix height:

GCR-2 = 34.8 ft

HGCR-1 = 37.9 ft

The calculations were repeated for several pinch temperatures, and the required areas are shown in Fig. 19, Chap. 6. The fraction of heat transferred in each section is taken from Fig. 20, Chap. 6. Assigning an over-all cost of $7.8 per square foot of surface area, which was taken from GCR-2 costs and independent estimates by the ORNL staff, and a fixed capital charge of 14% per year, the calculated annual relative cost is as shown in Fig. 18, Chap. 6. Also, assigning a value of 10 mills/kwhr and assuming a 0.80 power factor gave the decrease in revenue as a result of the lower efficiency caused by the lower feedwater temperatures, which is also shown in Fig. 18, Chap. 6. The net saving in cost, using a 30°F pinch as a reference, is shown in Fig. 18, Chap. 6, to be greatest at a pinch temperature difference of about 80°F.

DETERMINATION OF ANNULUS SIZE

The equation for pressure drop, assuming incompressible flow, is[6]

$$\Delta p = \frac{fG^2L}{\rho^2 g_c r_h} ,$$

for

$$D_e = 4r_h = 4\ A/p$$

$$= \frac{D_o^2 - D_i^2}{D_o + D_i} ,$$

$$G = \frac{w_g}{A} = \frac{4w_g}{\pi(D_o^2 - D_i^2)} ,$$

$$\text{Re} = \frac{GD_e}{\mu} = \frac{4w_g}{\pi(D_o + D_i)\ \mu} ,$$

$f \sim 0.46\ (\text{Re})^{-0.2}$ in the turbulent range.

[6]Since the density of the gas leaving the annulus is about equal to thot of the gas entering, and the Mach number is very small, this is a valid assumption.

Substituting into the equation for Δp and canceling:

$$\Delta p = \frac{(0.046)(4^{1.8})(2)(L)(w_g^{1.8})(\mu^{0.2})}{(\pi)^{1.8}(g_c)(\rho)} \left[\frac{(D_o + D_i)^{1.2}}{(D_o^2 - D_i^2)^3}\right] .$$

Letting

$\mu = 0.072$ lb/hr·ft,

$\rho = 0.114$ lb/ft^3,

$D_i = 20$ ft,

$w_g = 302.6$ lb/sec = 1,088,000 lb/hr,

and substituting, the equation for Δp per foot of annulus length is

$$\Delta p = 129.5 \left[\frac{(D_o + 20)^{1.2}}{(D_o^2 - 400)^3}\right] ,$$

where D_o is expressed in feet. The pumping power expended per year at a 0.80 power factor is

$$PP = \left(\frac{\Delta p}{\rho} w_g\right) (7.356 \times 10^{-3})(365)(24)(0.8) \text{ kwhr} ,$$

where Δp is in lb/ft^2, ρ is in lb$_m$/ft^3, and w_g is in lb/sec.

The cost of the power is assumed to be 10 mills/kwhr and is plotted in Fig. 22, Chap. 6, for various shell outside diameters. The cost of the shell was taken from Fig. 9.10, ORNL-2500, Part 3, and is plotted in Fig. 22, Chap. 6. The point at which the sum of the two is a minimum is shown clearly on Fig. 22, Chap. 6, to be 21.5 ft.

TEMPERATURE RISE THROUGH ANNULUS

The previous assumption of an approximate temperature rise of 2°F will now be checked. Since about 5 in. of insulation exists between the hot and cold gas, it will be further assumed that the heat transferred from the hot gas to the annulus gas is negligible compared with that transferred to the steam. This allows the calculation of heat loss from the temperatures shown on Fig. 23, Chap. 6.

The heat transfer coefficient h on the inner wall of the annulus side was calculated from the following equation,[7] which is valid within the range of $1 < D_o/D_i < 10$:

$$j = \frac{h_i}{C_p G} \left(\frac{C_p \mu}{k}\right)^{2/3} = \frac{0.023\,\psi}{\frac{D_o G}{\mu}} ,$$

where $\psi = (D_o/D_i)^{0.45}$; $D_o/D_i = 1.075$ is within the range.

---

[7] W. H. McAdams, *Heat Transmission*, McGraw-Hill, New York, 1954.

The physical constants are evaluated at $t_{av} = 524°F$. The flow rate $w = 1.088 \times 10^6$ lb/hr. The cross-sectional area of the annulus is:

$$A = \pi(D_o^2 - D_i^2) = \pi[(21.5)^2 - (20)^2] = 195.5 \text{ ft}^2 ,$$

and

$$G = w/A = \frac{10.88 \times 10^6}{195.5} = 5570 \text{ lb/hr·ft}^2 ,$$

$$\left(\frac{C_p\mu}{k}\right)^{2/3} = (0.72)^{2/3} = 0.8032 ,$$

$$D_e = \frac{D_o^2 - D_i^2}{D_o + D_i} = \frac{(21.5)^2 - (20)^2}{21.5 + 20} = 1.5 \text{ ft} ,$$

$$\mu = 0.07 \text{ lb/hr·ft} ,$$

$$C_p = 1.248 \text{ lb/hr·ft} ,$$

and

$$\frac{h}{(1.248)(5570)}(0.8032) = \frac{(0.023)(1.075)^{0.45}}{\left[\frac{(1.5)(5570)}{0.0700}\right]^{0.2}} .$$

Solving for h in the annulus:

$$h = 17.7 \text{ Btu/hr·ft}^2\text{·°F} .$$

The thermal conductivity of the insulation, Thermobestos, will be the same as in GCR-2:

$$k = (0.705)(3) = 2.115 \text{ Btu/hr·ft·(°F/in.)} .$$

The over-all heat transfer coefficient U, based on the area of the outside of the insulation, A_o, is:

$$\frac{1}{UA_o} = \frac{1}{h_iA_i} + \frac{x}{kA_{lm}} + \frac{1}{h_oA_o} .$$

To assure a conservative solution, h_i is assumed to be infinite; that is, the inside surface of the insulation is at the same temperature as the gas. Then:

$$\frac{1}{UA_o} = \frac{x}{kA_{lm}} + \frac{1}{h_oA_o} ,$$

$$\frac{1}{U(62.8)} = \frac{5.0}{(2.155)(61.42)} + \frac{1}{(17.7)(62.8)} ,$$

$$\frac{1}{U} = 2.4725 ,$$

and

$$U = 0.4042 \text{ Btu/hr}\cdot\text{ft}^2\cdot{}^\circ\text{F} \quad .$$

The sections analyzed are:

1. hot length of annulus past superheater outlet,
2. length of annulus in same axial position as superheater,
3. length of annulus in same axial position as separation between superheater and boiler (1.5 ft),
4. length of annulus even with boiler,
5. length of annulus even with separation between boiler and economizer (3 ft),
6. length of annulus even with economizer.

The heat transferred in each section is found from the equations

$$q = \frac{UA_o}{L} \times L\ \Delta t$$

and

$$\Delta t_{lm} = \frac{\Delta t_{\text{large}} - \Delta t_{\text{small}}}{\ln \dfrac{\Delta t_{\text{large}}}{\Delta t_{\text{small}}}} \quad .$$

In the superheater section, the annulus gas temperature is assumed to be 525°F. This gives a Δt_{lm} of 793°F, and

$$t_o - t_i = \frac{q}{u_g C_p} = \frac{216{,}000}{(1.088 \times 10^6)(1.240)} = 0.1762^\circ\text{F} \quad .$$

Following the same procedure throughout the length of the shell annulus, the results are:

t_{rise} in region past superheater = 0.0302°F,
t_{rise} in superheater section = 0.1762°F,
t_{rise} in boiler superheater separator = 0.0201°F,
t_{rise} in boiler length = 0.0795°F,
t_{rise} in boiler economizer separator = 0.00725°F,
t_{rise} in economizer length = 0.01625°F.
Total temperature rise = 0.3295°F.

Thus it may be seen that the 2°F drop assumed is conservative. Such a small correction does not warrant recalculation.

GAS-SIDE PRESSURE DROP

The gas-side pressure drop along the matrix can be simply scaled up from the GCR-2 calculations as shown below for a 50°F pinch temperature difference. On the helium side,

$$G = 2.536 \times 1.224 = 3.103 \text{ lb/ft}^2\cdot\text{sec} \ .$$

The equation for pressure drop in the superheater (bare tube) sections is

$$\Delta p = \frac{4fNG^2}{2g_c\rho} \ .$$

The factor f scales as

$$\frac{f_{\text{HGCR-1}}}{f_{\text{GCR-2}}} = \left(\frac{GD_e}{\mu}\right)^{0.15}_{\text{GCR-2}} \left(\frac{\mu}{GD_e}\right)^{0.15}_{\text{HGCR-1}} \ .$$

Since the geometry is the same,

$$\frac{f_{\text{HGCR-1}}}{f_{\text{GCR-2}}} = \left(\frac{G_{\text{GCR-2}}}{G_{\text{HGCR-1}}} \frac{\mu_{\text{HGCR-1}}}{\mu_{\text{GCR-2}}}\right)^{0.15} ,$$

$$t_{\text{av GCR-2}} = \frac{1000 + 867.5}{2} = 933.7°\text{F} \ ,$$

$$\mu = 0.0840 \text{ lb/hr}\cdot\text{ft} \ ,$$

$$t_{\text{av HGCR-1}} = \frac{1500 + 1171.4}{2} = 1336°\text{F} \ ,$$

$$\mu = 0.107 \text{ lb/hr}\cdot\text{ft} \ ,$$

$$\rho_{\text{HGCR-1}} = 0.0625 \text{ lb/ft}^3 \ ,$$

$$f_{\text{HGCR-1}} = f_{\text{GCR-2}} \left(1.224 \times \frac{0.107}{0.084}\right)^{0.15}$$

$$= 0.085\ (1.585)^{0.15} = 0.0954 \ ,$$

$$\Delta p = \frac{4(0.0954)\,(27)\,(3.103)^2}{2(32.2)\,(0.0625)} = 24.71 \text{ lb/ft}^2 \ ,$$

$$\Delta p = \frac{24.71}{144} = 0.1717 \text{ psi} \ ,$$

$$\Delta H = \frac{24.71}{0.0675} = 398 \text{ ft} \ .$$

For the boiler section, with finned surface,

$$\Delta H = \frac{fAG^2}{2\rho_m^2 g_c A_c} \ ,$$

where

A = outside surface area,

A_c = free area,

and f varies as follows:

$$f = 0.060 \left(\frac{G_{GCR-2}}{G_{HGCR-1}}\right)^{0.253} \left(\frac{\mu_{HGCR-1}}{\mu_{GCR-2}}\right)^{0.253}$$

$$= 0.060 \left(\frac{1}{1.245}\right)^{0.253} \left(\frac{0.0825}{0.077}\right)^{0.253}$$

$$= 0.0573 \ .$$

The area A = 119,400 ft^2 for the HGCR-1, and A_c is the same as for the GCR-2. Substituting:

$$\Delta H = \frac{(0.0573)(119{,}400)(2.06 \times 1.224)^2}{2\,(0.092)^2\,(32.2)(118)} = 676 \text{ ft} \ ,$$

$$\Delta p = (676)(0.0818) = 55.25 \text{ lb/ft}^2 = 0.384 \text{ psi} \ .$$

For the economizer section:

$$\Delta H = \frac{fAG^2}{2\rho_m^2 g_c A_c} \ ,$$

where

$$A_{HGCR-1} = 184{,}000 \text{ ft}^2,$$

$$A_c = 126.7 \text{ ft}^2,$$

$$f = 0.051 \left(\frac{1}{1.245}\right)^{0.253} \left(\frac{0.74}{0.71}\right)^{0.253} = 0.0489,$$

$$\Delta H = \frac{(0.0489)(184{,}000)(2.35)^2}{(2)(0.1077)^2\,(32.2)(126.7)} = 525 \text{ ft},$$

$$\Delta p = \rho \Delta H = \frac{(0.1077)(525)}{144} = 0.3928 \text{ psi}.$$

Summarizing:

	ΔH (ft)		Δp (psi)	
	50°F Pinch	80°F Pinch	50°F Pinch	80°F Pinch
Pressure drop in				
Superheater	398	362	0.1717	0.1562
Boiler	676	520	0.384	0.2950
Economizer	525	325	0.3928	0.2432
Subtotal	1599	1207	0.9485	0.6942

WATER-SIDE PRESSURE DROP

The GCR-2 calculation was scaled up by the following equations.

Superheater:

$$\Delta p_{HGCR\text{-}1} = \Delta p_{GCR\text{-}2} \left(\frac{G_{HGCR\text{-}1}}{G_{GCR\text{-}2}}\right)^2 \frac{L_{HGCR\text{-}1}}{L_{GCR\text{-}2}} \frac{P_{GCR\text{-}2}}{P_{HGCR\text{-}1}} \left(\frac{T_{HGCR\text{-}1}}{T_{GCR\text{-}2}}\right)_{av}$$

$$= (27.2)(2.425)^2 \frac{10.48}{14.2} \frac{950}{1450} \frac{1610}{1410} = 88.2 \ .$$

Boiler:

$$\Delta p = \Delta p_{lp} \ F_{TPF} \ ,$$

where

$\Delta p_{lp} = \Delta p$ liquid phase,

F_{TPF} = two-phase flow factor = 8 (see ref 8).

Therefore,

$$\Delta p = (\Delta p_{GCR\text{-}2})_{lp} \left(\frac{G_{HGCR\text{-}1}}{G_{GCR\text{-}2}}\right)^2 \frac{L_{HGCR\text{-}1}}{L_{GCR\text{-}2}} (F_{TPF})$$

$$= (2.594)(2.425)^2 \frac{10.37}{11.7} (8) = 126.2 \text{ psia} \ .$$

Economizer:

$$\Delta p = (\Delta p_{GCR\text{-}2}) \left(\frac{G_{HGCR\text{-}1}}{G_{GCR\text{-}2}}\right)^2 \frac{L_{HGCR\text{-}1}}{L_{GCR\text{-}2}} = (4.18)(2.425)^2 \frac{9.5}{8.9} = 23.3 \ .$$

Total Δp = 88.2 + 126.2 + 23.3 = 237.7 psi .

Inlet pressure = 1450 + 237.7 = 1688 psia .

$$\text{Total water flow rate} = \frac{q}{h_S - h_{FW}} = \frac{(3{,}147{,}000)(3413)}{(1521 - 425)}$$

$$= 9{,}800{,}000 \text{ lb/hr} \ .$$

Water flow rate per exchanger = 9,800,000/8 = 1,225,000 lb/hr .

CALCULATION OF PUMPING POWER AND OVER-ALL EFFICIENCY

Pumping power = $(\Delta p/\rho)(w_w)$ (kwhr/ft·lb)

$$= \frac{(1688.5)(144)}{(60.15)} (9.8 \times 10^6) \frac{0.001356}{3600} = 14{,}900 \text{ kw.}$$

Water pumping power = 14.9 kw.

Gas pumping power = 54 Mw.

---

[8] R. C. Martinelli and D. B. Nelson, *Trans. ASME* 70, 695 (1948).

Gross electrical output = 1259 Mw.

Net electrical output[9] = 1259 − 68.9 = 1190.1 Mw.

Net efficiency[9] = 1190.1/3093 = 38.5%.

CALCULATION OF STEAM CYCLE EFFICIENCY

The efficiency of a regenerative feedwater heating, nonreheat cycle was calculated as outlined by Salisbury.[10] This shows improvements on a simple nonextraction cycle for various numbers of heaters with corrections for different condenser back pressures, inlet steam conditions, and expansion efficiency.

The basic, simple, cycle efficiency was calculated for the following conditions:

1. steam inlet pressure, 1450 psia,
2. steam outlet temperature, 1050°F,
3. over-all expansion efficiency, 85%,
4. condenser pressure, 2 in. Hg.

The efficiency is

$$\eta = \frac{h_{\text{steam inlet}} - h_{\text{steam at last stage}}}{h_{\text{steam inlet}} - h_{\text{feedwater}}} .$$

In the basic cycle, 1050°F, 1450-psi steam and 2-in. back pressure,

$$\eta = \frac{1521 - 1000}{1521 - 69.1} = \frac{521}{1451} = 35.9\% .$$

The quality of the steam at the state line end point is 10.2% moisture.

---

[9]Including auxiliary power requirements, the net electrical output is 1130 Mw, and the efficiency 36.5%.

[10]J. K. Salisbury, *Steam Turbines and Their Cycles*, Wiley, New York, 1950.

APPENDIX F. RELEASE OF RADIOACTIVITY

The use of an unclad fuel element which would release large amounts of activity would make it necessary to maintain control of the activity which could leak from the primary system. The consequences of releasing activity from the primary system were investigated in order to establish design features and conditions, such as the purification rate, stack height, allowable leakage rate, and maximum time of exposure.

The release of activity from the fuel and the resulting levels of activity are described in Chap. 7 and in Apps. A, B, and C. As was pointed out, the activity referred to was restricted to the important gamma-emitting nuclides, and therefore the low-energy gamma emitters, as well as the beta emitters, were not investigated. In determining the allowable leakage from the primary system, it was necessary to investigate all the fission products which would contribute to the activity concentration downstream from the plant stack exhaust.

Several processes would cause the activity to be reduced before it was discharged from the stack. The activity that had escaped from the fuel into the gas stream would reach an equilibrium activity that would depend on the four processes for removal of activity from the circulating gas in the primary system: (1) radioactive decay, (2) leakage, (3) purification, and (4) deposition. The activities listed in Table 5, Chap. 7, were obtained by assuming that the only method for removing a particular nuclide from the gas stream would be radioactive decay. This assumption was made in order to obtain a conservative result, since the uncertainty about the deposition rate did not allow a credit for the purification system. However, if the deposition rate exceeds the purification rate, then by assuming no reduction by deposition and assuming a particular purification rate, the equilibrium activity which exists in the circulating gas stream will be limited by either leakage, decay, or purification. The activity which exists in the circulating gas may be computed by using the values given in Table 5, Chap. 7, and the following expression:

$$A_i = A_{0_i} \frac{\lambda_i}{\lambda_i + \alpha_i + \beta_i + \gamma_i}, \tag{1}$$

where

A_i = activity of nuclide i in the gas stream, curies,

A_{0_i} = activity of nuclide i in primary system, assuming $\alpha = \beta = \gamma = 0$, curies,

λ_i = radioactive decay constant, sec^{-1},

α_i = purification rate, sec^{-1},

β_i = leakage rate, sec^{-1},

γ_i = deposition rate, sec^{-1}.

If it is assumed that the leakage rate for all the nuclides is the same as the system leakage rate, the activity released from the system by leakage is

$$A = \beta \sum_i A_{0_i} \frac{\lambda_i \delta_i}{\lambda_i + \alpha_i + \beta + \gamma_i} , \tag{2}$$

where

A = total activity leaking from the primary system, curies,

δ_i = decontamination factor associated with activity leaking through small passages.

The activity release (in curies/sec) from the stack due to nuclide i is given by

$$A_s = \frac{\beta A_{0_i} \lambda_i \delta_i \rho_i}{(\lambda_i + \alpha_i + \beta + \gamma_i)} , \tag{3}$$

where ρ_i is the fraction of activity passing through the filter in the stack. From Eq. (3) it may be seen that the activity previously calculated for shielding purposes may be reduced for the exposure calculations by several factors: the stack filter factor, a factor for the decontamination obtained during the process of leaking from the system, and a reduction factor due to the purification system, leakage from the primary system, or deposition on primary system surfaces.

As was indicated previously, if the deposition rate is assumed to be less than the purification rate, the results will be on the safe side. Since there is no way to evaluate the deposition rates, for this study it was assumed for all cases that $\gamma_i = 0$. Furthermore, since there are few data available for evaluating the decontamination factors associated with small leaks, values of δ_i were assumed to be unity.

Therefore, Eq. (3) was simplified to

$$A_{s_i} = \frac{\beta A_{0_i} \lambda_i \rho_i}{(\lambda_i + \alpha_i + \beta)} . \tag{4}$$

For cases of xenon and krypton, Eq. (4) was further simplified, because the purification system would not remove these nuclides, and the filter in the stack would not reduce the activity. Thus for xenon and krypton, Eq. (4) becomes

$$A_s = \beta A_{0_i} \frac{\lambda_i}{(\lambda_i + \beta)} . \tag{5}$$

The maximum concentration of a particular nuclide downstream from a continuous point source is given by

$$X_{max} = \frac{2A_s}{e\pi \bar{u} b^2} , \tag{6}$$

where

$\bar{u}$ = wind speed, m/sec,

h = stack height, m,

X_{max} = maximum concentration, $\mu c/cm^3$,

A_s = continuous source, curies/sec.

Therefore, the maximum concentration of a given nuclide downstream from the plant is

$$(X_{max})_i = \frac{2\beta A_{0_i} \lambda_i \rho_i}{(\lambda_i + \alpha_i + \beta)\, e\pi\bar{u}h^2} \quad . \tag{7}$$

Since the activity release at the stack is made up of many fission products, the exposure to a person at the point of maximum concentration will not be excessive if

$$\sum_i \frac{(X_{max})_i}{(X_{allow})_i} \leqq 1 \quad . \tag{8}$$

The important nuclides for determining exposure are tabulated in Table F.1. These nuclides are not all of the nuclides of interest, but they include the nuclides investigated in Chap. 7, as well as a few of the more important beta-emitting nuclides which contribute significantly to the exposure.

It may be seen from Eqs. (4) and (5) and from the values in Table F.1 that the most important nuclides for obtaining large exposure levels to the total body are the inert gases. The inability of the purification system or the stack filter to reduce the krypton or xenon activity would result in large activity release from the stack of the xenon and krypton nuclides.

The values listed in Table F.1 are based on a purification rate of 5×10^{-6} sec^{-1} and a leakage rate of 0.1% per day (1.16×10^{-8} sec^{-1}). The values of A_{0_i} are from Table 5, and for the cases of Kr^{85} and Sr^{90}, which were not included in Table 5, these values were estimated by using the methods outlined in Apps. A, B, and C. A stack height of 60 m and a wind speed of 2 m/sec were used for the calculation.

With a leakage rate of 0.1% per day, the exposure to the total body and to the thyroid (Table F.2) is not excessive. Table F.1 indicates that the leakage from the primary system could increase to about 0.2% per day before the exposure to the total body would be excessive.

Table F.1. Calculation of Exposure to Total Body

Nuclide	λ_i	A_{0_i}	ρ_i	A_{s_i}	$(X_{max})_i$	$(X_{allow})_i$	$\left(\frac{X_{max}}{X_{allow}}\right)_i$
Kr^{85}	2.14×10^{-9}	2.82×10^{-6}	1.0	5.14×10^{-3}	1.67×10^{-7}	3×10^{-6}	0.0556
Kr^{87}	1.48×10^{-4}	1.28×10^{5}	1.0	1.48×10^{-3}	4.81×10^{-8}	2×10^{-7}	0.240
Y^{90}	2.98×10^{-6}	6.74×10^{5}	0.01	2.90×10^{-5}	9.43×10^{-10}	1×10^{-6}	0.00094
Y^{91m}	2.26×10^{-4}	2.17×10^{5}	0.01	2.46×10^{-5}	8.0×10^{-10}	8×10^{-5}	0.0001
Y^{91}	1.38×10^{-7}	7.97×10^{5}	0.01	2.48×10^{-6}	8.06×10^{-11}	8×10^{-8}	0.001
Y^{92}	5.35×10^{-5}	3.7×10^{5}	0.01	3.91×10^{-5}	1.27×10^{-9}	1×10^{-5}	0.00013
Y^{93}	1.93×10^{-5}	6.98×10^{4}	0.01	6.41×10^{-6}	2.08×10^{-10}	4×10^{-6}	0.00005
Sr^{90}	7.85×10^{-10}	6.5×10^{5}	0.01	1.18×10^{-8}	3.82×10^{-13}	3×10^{-10}	0.00127
Sr^{91}	1.99×10^{-5}	6.34×10^{5}	0.01	5.85×10^{-5}	1.9×10^{-9}	2×10^{-6}	0.00095
Zr^{95}	1.27×10^{-7}	3.2×10^{4}	0.01	9.18×10^{-8}	2.98×10^{-12}	4×10^{-8}	0.00008
Nb^{95}	2.29×10^{-7}	3.2×10^{4}	0.01	1.63×10^{-7}	5.28×10^{-12}	2×10^{-7}	0.00003
I^{131}	9.96×10^{-7}	3.8×10^{5}	0.01	7.30×10^{-6}	2.37×10^{-10}	3×10^{-7}	0.00079
I^{132}	8.02×10^{-5}	6.99×10^{4}	0.01	7.64×10^{-6}	2.48×10^{-10}	6×10^{-6}	0.00004
I^{133}	9.25×10^{-6}	2.96×10^{5}	0.01	2.22×10^{-5}	7.2×10^{-10}	1×10^{-6}	0.00072
I^{134}	2.2×10^{-4}	5.86×10^{5}	0.01	6.65×10^{-5}	2.16×10^{-9}	2×10^{-5}	0.00011
I^{135}	2.89×10^{-5}	1.33×10^{5}	0.01	1.32×10^{-5}	4.27×10^{-10}	3×10^{-6}	0.00014
Xe^{135}	2.11×10^{-5}	6.64×10^{5}	1.0	7.70×10^{-3}	2.5×10^{-7}	1×10^{-6}	0.025
La^{140}	4.79×10^{-6}	6.56×10^{5}	0.01	3.73×10^{-5}	1.21×10^{-9}	9×10^{-7}	0.0013
Ba^{140}	6.27×10^{-7}	6.56×10^{5}	0.01	8.47×10^{-6}	2.75×10^{-10}	1×10^{-7}	0.00275
Total							0.55

Table F.2. Calculation of Exposure to Thyroid

Nuclide	λ_i	A_{0_i}	ρ_i	A_{s_i}	$(X_{max})_i$	$(X_{allow})_i$	$\left(\frac{X_{max}}{X_{allow}}\right)_i$
I^{131}	9.96×10^{-7}	3.8×10^{5}	0.01	7.3×10^{-6}	2.37×10^{-10}	4×10^{-9}	0.059
I^{132}	8.02×10^{-5}	6.99×10^{4}	0.01	7.64×10^{-6}	2.48×10^{-10}	1×10^{-7}	0.0025
I^{133}	9.25×10^{-6}	2.96×10^{5}	0.01	2.22×10^{-5}	7.2×10^{-10}	2×10^{-8}	0.036
I^{134}	2.2×10^{-4}	5.86×10^{5}	0.01	6.65×10^{-5}	2.16×10^{-9}	3×10^{-7}	0.0072
I^{135}	2.89×10^{-5}	1.33×10^{5}	0.01	1.32×10^{-5}	4.27×10^{-10}	5×10^{-8}	0.00854
Total							0.113

INTERNAL DISTRIBUTION

1. W. A. Albrecht
2. E. D. Arnold
3. M. Bender
4. L. L. Bennett
5. D. S. Billington
6. E. P. Blizard
7. A. L. Boch
8. C. J. Borkowski
9. G. E. Boyd
10. E. J. Breeding
11. J. C. Bresee
12. R. B. Briggs
13. W. E. Browning
14. F. Carlsen
15. C. E. Center (K-25)
16. R. A. Charpie
17. J. A. Conlin
18. J. H. Coobs
19–30. W. B. Cottrell
31. F. L. Culler
32–35. H. N. Culver
36. T. K. DeBoer
37. J. H. DeVan
38. L. M. Doney
39. D. A. Douglas
40. J. C. Ebersole
41. L. B. Emlet (K-25)
42. L. G. Epel
43. E. P. Epler
44. R. B. Evans
45. H. L. Falkenberry
46–48. M. H. Fontana
49. J. Foster
50. A. P. Fraas
51. J. H. Frye, Jr.
52. G. A. Garrett (K-25)
53. D. R. Gilfillan
54. J. M. Googin (Y-12)
55. B. L. Greenstreet
56. W. R. Grimes
57. A. G. Grindell
58. E. E. Gross
59. R. F. Hibbs (Y-12)
60. H. W. Hoffman
61. A. Hollaender
62. A. S. Householder
63. S. Jaye
64. W. H. Jordan
65. P. R. Kasten
66. C. P. Keim
67. V. J. Kelleghan
68. M. T. Kelley
69. J. J. Keyes
70. L. J. King
71. J. A. Lane
72. S. A. Levin (K-25)
73. R. S. Livingston
74. H. G. MacPherson
75. W. D. Manly
76. E. R. Mann
77. L. A. Mann
78. H. C. McCurdy
79. W. B. McDonald
80. H. F. McDuffie
81. F. R. McQuilkin
82. A. J. Miller
83. K. Z. Morgan
84. J. P. Murray (Y-12)
85. F. H. Neill
86. M. L. Nelson
87. L. G. Overholser
88. A. M. Perry
89. C. A. Preskitt
90. M. E. Ramsey
91. P. M. Reyling
92. G. C. Robinson
93. A. F. Rupp
94. G. Samuels
95. J. P. Sanders
96. H. W. Savage
97. A. W. Savolainen
98. J. L. Scott
99. A. J. Shor
100. O. Sisman
101. M. J. Skinner
102. A. H. Snell
103. R. D. Stulting
104. J. C. Suddath
105. C. D. Susano
106. J. A. Swartout
107. E. H. Taylor
108. D. B. Trauger
109. J. W. Ullmann
110. W. E. Unger

111. E. Von Halle (K-25)
112. C. S. Walker
113. J. L. Wantland
114. A. M. Weinberg
115. J. C. White
116. E. A. Wick
117. G. C. Williams
118. C. E. Winters
119. M. M. Yarosh
120–123. ORNL – Y-12 Technical Library, Document Reference Section
124–163. Laboratory Records Department
164. Laboratory Records, ORNL R.C.
165–166. Central Research Library

EXTERNAL DISTRIBUTION

167. C. M. Copenhaver, Lincoln Laboratories, Mitre Corp., Lexington, Mass.
168. Division of Research and Development, AEC, ORO
169–750. Given distribution as shown in TID-4500 (14th ed.) under Reactors-Power category (75 copies – OTS)